THE GEOLOGY OF THE LOUGH GUITANE VOLCANIC COMPLEX AND ASSOCIATED SEDIMENTS COUNTY KERRY, IRELAND

by

Mark Avison

Thesis submitted to the University of Keele

for the degree of Doctor of Philosophy

Volume I Text.

February, 1982

IMAGING SERVICES NORTH
Boston Spa, Wetherby
West Yorkshire, LS23 7BQ
www.bl.uk

CONTAINS PULLOUTS

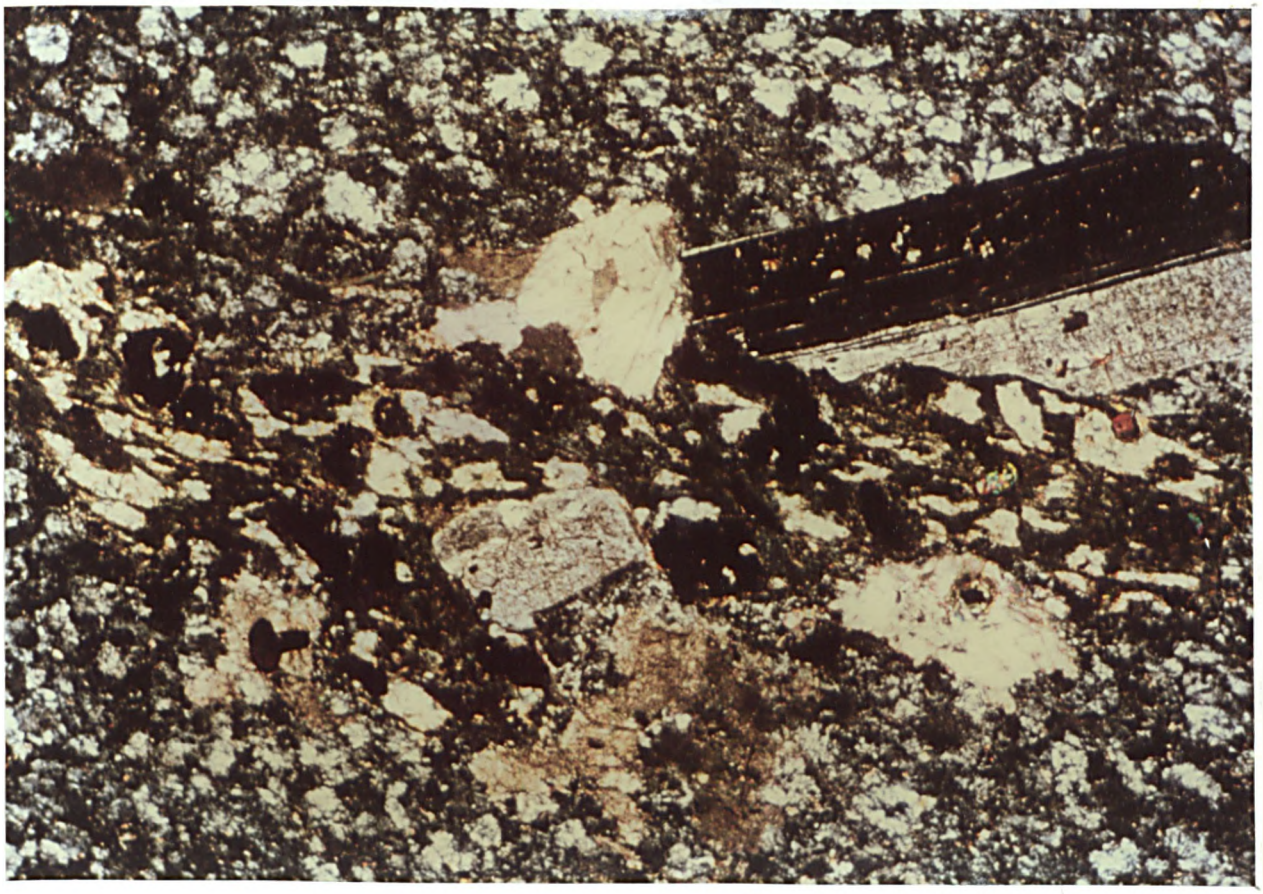

Frontispiece. Albitised plagioclase phenocryst nucleated on a pseudomorphed mafic phenocryst of restite origin, from the Bennaunmore Rhyolite Lava.

Abstract

The Lough Guitane volcanic rocks occur interbedded with the Upper Devonian fluviatile clastic sediments of the Munster Basin. Most of the volcanic rocks are shown to be associated with 3 separate volcanic centres, and consist exclusively of thick rhyolite lavas and acid volcaniclastics. Their distribution was strongly influenced in the Bennaunmore volcanic centre by complex faulting contemporaneous with the volcanism.

The volcaniclastics are always observed mixed with some terrigenous clastic sediment, and are believed to have been erupted in this mixed state as a result of rapid vent erosion, although some water reworking also occurred. There is a notable absence of evidence for explosive volcanic activity, and the lavas are virtually free of vesiculation.

The originally glassy lavas have been completely recrystallised to a quartz-albite-chlorite-phengite assemblage, with minor quantities of allanite, anatase and iron-ore. Despite this recrystallisation textural evidence remains for the incorporation of 1-2% of restite in the magma.

Geochemical analysis of the least altered specimens provides evidence for the derivation of the subalkaline rhyolitic magma by high degrees of partial melting of an anhydrous, acidic deep crustal rocks, controlled by the decomposition of amphibole at temperatures in excess of 950^{o}C.

Using mass-transfer computations, widely varying lava and dyke whole rock compositions are shown to have been probably derived from a common rhyolitic parental composition by varying degrees and types of metasomatism. Under severe metasomatic conditions only Zr, Ti, P and Al can be shown to be geochemically immobile.

The area was subjected to shallow, partially brittle deformation

during the Hercynian orogeny, leading to the development of E-W aligned structural features including a major anticlinorium lying south of a large reverse fault. Strong variations in the resistance to the compressive stresses due to the presence of thick lava flows and unexposed shallow intrusions led to the development of large oblique-slip cross faults which offset the major reverse fault in the north.

It is suggested that the orientation of volcanic features, and the geometry of the Munster Basin are cogenetically related by the same E-W oriented deep crustal fractures.

Acknowledgements

I wish to acknowledge a research studentship provided by the Natural Environment Research Council, without which this work could not have been undertaken. I also express my gratitide to the Department of Health and Social Security for its financial support during a further period of writing-up.

I wish to thank the Head of Department, Professor G. Kelling, for the provision of facilities in the Department of Geology at Keele.

Of the many academics to whom I owe so much for their help and guidance, I am especially grateful to Drs. P. A. Floyd and J. A. Winchester who supervised the research, and who both critically read a draft of this thesis. I am also grateful to Drs. G. Rowbotham, J. Collinson and R. G. Park for their critical assessment of particular chapters.

I thank Professor R. Oxburgh for the provision of his facilities in the Department of Earth Sciences, University of Cambridge, and Dr. P. Treloar forhelp and guidance in the use of the Energy-Dispersive Electron Microprobe System there.

Among the technicians at Keele, whose help was invaluable, I wish to thank in particular D. Emley for his considerable help with many aspects of geochemical analysis, P. Greatbach and his team for thin sections, Pat Douglass and D. Kelsall for photographic work, J. Pepper for useful advice concerning line drawings and maps, and M. W. Stead for raw materials. I am also grateful to G. Lees for his expert help with geochemical data processing.

In the field I was lucky enough to make the aquaintance of many of the inhabitants of Gortdromakiery, and I am particularly grateful to Rose and Owen Barnes for their warm hospitality and friendship.

I thank my fellow inhabitants of the Geology Research Facility

for many happy hours of non-geological diversion, especially those research students and demonstrators who shared with me so many pleasant evenings in the Keele Research Association bar, in particular, Tom Harland, Robin Dyer, Keith Sims and Jon Ineson.

Finally I thank Stephanie Cooper for her commendable tenacity in typing this thesis.

List of Contents

List of Figures

CHAPTER 1

Introduction

1.1 General - Geographical Location

Geological research has been undertaken into the Devonian volcanic rocks situated near to Lough Guitane, Co. Kerry, Ireland (fig. 1.1). The area lies about 9 Km south and east of Killarney, and covers an east-west elongate tract of ground about 17 Km long and 4-5 Km wide, dominated by mountains and bogs.

1.2 The Aims of the Research

The aim of the research was to interpret the petrogenesis of the volcanics in terms of the local sedimentological and regional tectonic environments. It was hoped that a detailed geochemical study of the volcanic rocks would lead to an understanding of their petrogenesis as well as any effects of secondary alteration.

It was also hoped that the work would assist in the general understanding of both ancient and modern volcanic environments, in particular, those interpreted as being in an intracontinental setting, and having undergone low-grade metamorphism and tectonism.

1.3 Physical Geography

The area under study covers the range of peaks from Mangerton Mountain (840 m in height) in the west to The Paps (696 m) in the east, and is dominantly mountainous and rugged. Passing from west to east, other major peaks include Stoompa (695 m) and Crohane (659 m).

A series of deep, mostly north-south orientated, glacially scoured valleys separate the highest peaks. These include the Cappagh river valley (Plate 4.2) and the Horses Glen. Except for

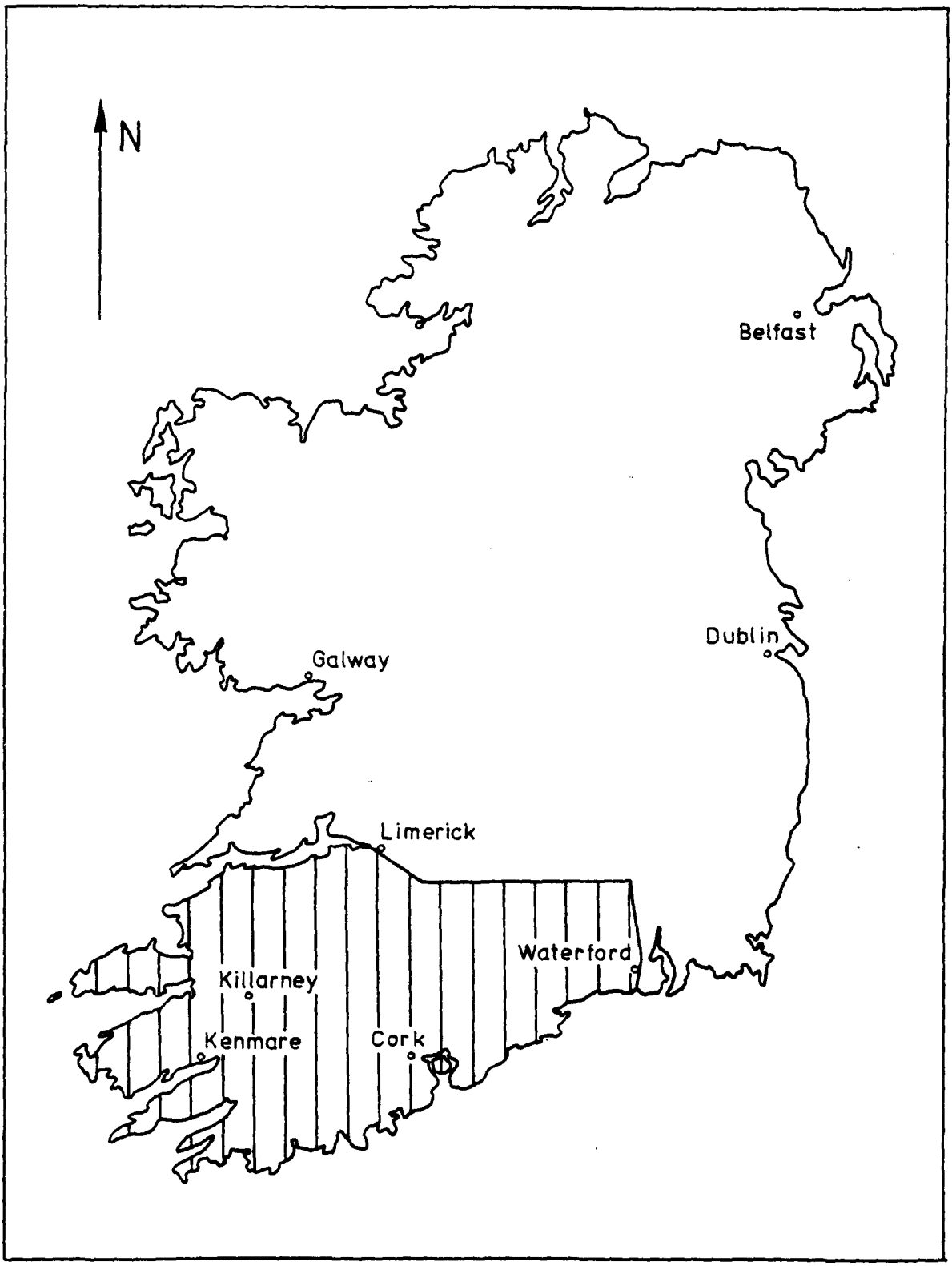

Fig. 1.1 Map of Ireland - cross hatch indicates area covered by Fig. 2.1

Glen FleSK, with its kilometre-wide alluvial plain bisecting the study area, the valleys fail to penetrate through to the south of the mountain chain, the valley heads being marked by corrie-like features.

Thus, the northern slopes of the mountains are dominated by steep-sided, glacially cut valleys, while the southern slopes are gentle and relatively unaffected by glacial erosion. The summits of the highest peaks, with the exception of Crohane which possesses a rocky pinnacle, are characterised by peat covered plateaus. In fact, large areas along the summit ridges and the southern slopes are covered by thick peat deposits, and by bounder clay on the northern slopes. The poor acid soils support only coarse grasses and heather with scattered mountain oak woodland.

1.4 Field and Laboratory Techniques

Approximately 25 weeks fieldwork was undertaken during the period October 1977 - May 1980. A set of aerial photographs were obtained from the Geological Survey of Ireland (Frames: V363-364, W136-138, W359-363). The original stereo pairs are printed on an approximate scale of 1:31,500. These prints were rephotographed and reprinted on 10 inch by 8 inch paper to a scale of 1:10560 and used with a transparent overlay for detailed field mapping. Ordnance survey maps on a 1:10560 scale were not used owing to the absence of topographic contours and reliable marker features such as field boundaries. Structural and palaeocurrent measurements were made using a Silva 15TD-CL compass/clinometer. Most ofthe field photographs were taken using a Pentax MV1 camera.

Field data was then transferred from the overlays to the ordnance survey maps from which were drawn the three geological maps presented in fig. 1.2 (the Horses Glen Volcanic Centre), fig. 1.3 (the

Bennaunmore Volcanic Centre) and fig. 1.4 (the Killeen Volcanic Centre).

No attempt was made to subdivide the dominant terrigenous sediments into mapping units beyond the regional formation names of Green Sandstone and Purple Sandstone.

All locations described in the text, and all sampling sites can be found in fig. 1.5.

In the laboratory, over 250 thin sections were examined using a Leitz Wetzlar binocular microscope with a range of magnifications up to 1250X. Modal analyses were made on this microscope with a Swift point counter using a 0.1 mm spacing for whole section analysis, and a 0.01 mm spacing for analysis of inclusion content of pseudomorphed ferromagnesian minerals. The photomicrographs were taken using a Vickers binocular microscope with a camera attachment. Details of techniques relating to X-ray fluorescence spectrometry and electron microprobe analysis are given in Appendix A.

CHAPTER 2

Previous Research in Southern Ireland

2.1 General

The first surveys undertaken in Southern Ireland were by J. B. Jukes and G. V. Du Noyer (1859, 1861). They published their work in the form of "Explanations to Accompany" sheets 184, 185 and 186 of the Geological Survey of Ireland - sheets 184 and 185 covering the area now under study. The map Jukes and Du Noyer produced is still the only comprehensive published version of the geology of the area to the south of Lough Guitane.

They recognised two types of igneous rock; "Felstone" and "Felstone Ash". The former they described only from Bennaunmore where they noted a discontinuous columnar structure, a fine "beautiful wavy texture", and a porphyritic character. The "Felstone Ash" is described as having bedding similar to "... that of an ordinary sandstone ... frequently characterised by oblique lamination". They inferred that the Felstone Ash was a "true aqueous deposited rock".

Jukes and Du Noyer also noted at least 10,000 feet (3050 metres) of The Old Red Sandstone which they divided into the Glengriff Grits, The Old Red Sandstone and The Upper Old Red Sandstone. They noted the dominant green nature of the lower strata, passing upward into a dominantly purple sequence, the rarity of both green and purple slates, the presence of "cornstones" and mud flake breccias, and the extreme rarity of conglomeratic horizons.

Between the work of Jukes and Du Noyer and the onset of modern interest in the region in the mid 1950s only Wright (1927) published a review paper on the geology of Killarney and Kenmare.

Modern research falls into two categories; localised detailed

mapping and papers concerning the stratigraphic correlation of the whole of The Old Red Sandstone of Southern Ireland and adjoining regions.

For example, in the first category, Shah (1958) produced an unpublished Ph.D. thesis entitled "The Rocks and Structure of the Country South-East of Killarney". He made some improvement on the one inch to a mile scale maps, and on the understanding of the structure of the region, but made no correct divisions within the volcanogenic deposits of the Lough Guitane region. In adjacent areas surveys have also been made: Husain (1957) in the Kenmore valley to the South and South-West, Walsh (1968) in the area centred on the Macgillycuddy's Reeks West of Killarney, and Wingfield (1968) who covered the Carboniferous strata of Killarney and Kenmore. Capewell has published work covering parts of the Dingle peninsula (1951, 1965) and the southern (1957) and the western (1975) parts of the Iveragh peninsula.

As diagnostic fossils have only been found very recently in the Old Red Sandstone of Southern Ireland (Russel, 1978), earlier attempts to correlate these areas within the Iveragh peninsula with each other and with adjacent regions have been based entirely upon lithological similarities and structural relationships.

2.2 The Nature of the Hercynian Front in Ireland

Fig. 2.1 shows the accepted trend of the Hercynian Front in Southern Ireland. Many authors have described it as a major boundary between differing styles of deformation. Its nature is variable (Naylor & Sevastopulo, 1979) and this will be discussed below in more detail. According to the published geological maps, in the Lough Guitane region the Hercynian Front takes the form of a high angle

Fig. 2.1 Geological Map of S.W. Ireland

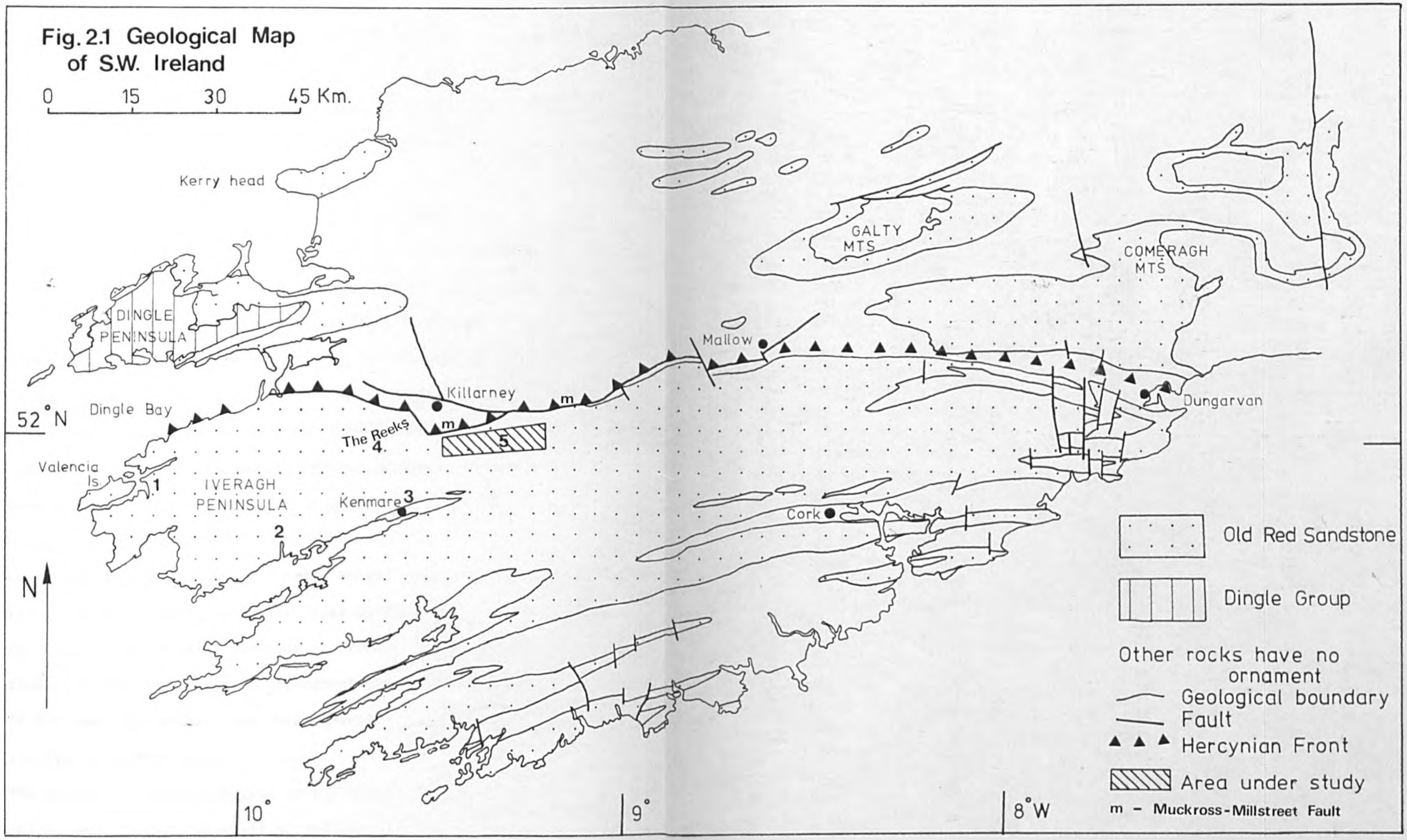

reverse fault inclined to the south, and lying approximately 0.5 Km north of Lough Guitane, with a roughly east-west course.

2.3 Stratigraphy South of the Hercynian Front

A summary of the published stratigraphy can be found in fig. 2.2.

The oldest rocks recorded belong to a fine grained slaty lithofacies variously named the Valencia Slate Formation (Capewell, 1957; 1975) and the Lower Slate Group (Husain, 1957; Walsh, 1968). The base of this lithofacies is not seen.

In some areas, for example, The Reeks (Walsh, 1968) and the Lough Guitane area this fine-grained lithofacies is not exposed, and the oldest strata are those of a dominantly coarse or medium grained sequence of green sandstones approximately 2000-2500 metres thick. These are succeeded by purple sandstones in all but The Reeks area where Walsh (1968) distinguished the 1000 metre sequence of the Grey Sandstone Formation underlying his Lower Purple Sandstone Formation. These dominantly pale purple coloured, medium grained sandstones are then overlain by variously named thin sequences totalling between 200 and 300 metres before basal Carboniferous strata, ascribed to the Lower Limestone Shales (Husain, 1957; Walsh, 1968) are encountered. Deposition was continuous through the Upper Devonian-Lower Carboniferous boundary, and no unconformity has been observed. No intraformational unconformities have been observed throughout the entire sequence of the Old Red Sandstone either, and this indicates continuous deposition in a steadily subsiding basin.

The absence of unconformities, or any other reliable marker horizons in such a great thickness of sediments has kept the need for the above correlation based upon colour changes which in the writers experience and that of others (Gardiner & Home, 1972) is at

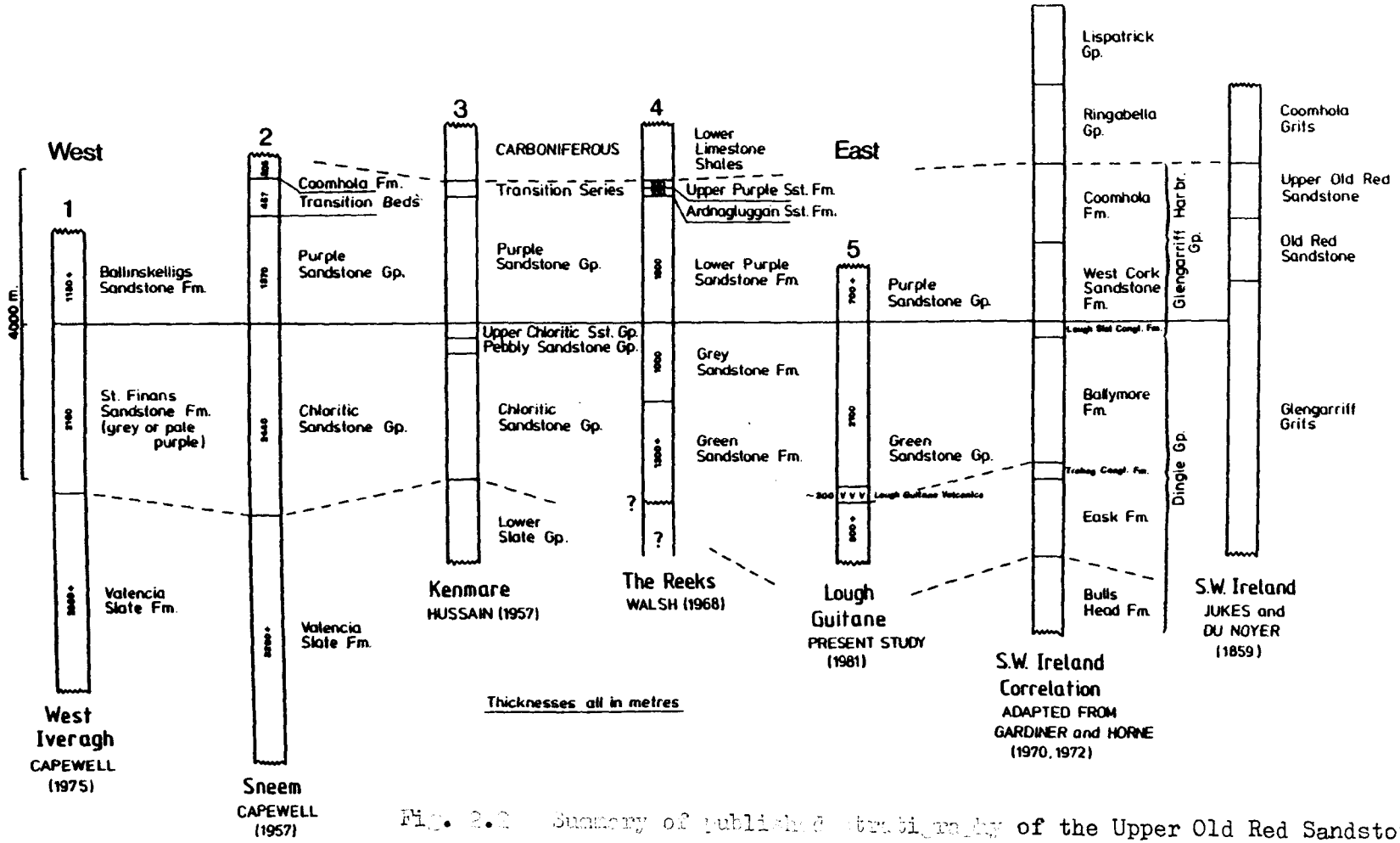

Fig. 2.2 Summary of published stratigraphy of the Upper Old Red Sandstone used in S.W. Ireland.

best rather unreliable. However, while individual horizons bearing particular colours are notably laterally discontinuous, on the scale of thousands of metres of sediments, a regular pattern emerges over the Iveragh peninsula.

2.4 Correlation of the Iveragh Peninsula Stratigraphy with Adjacent Regions and the Age of the Old Red Sandstone in South West Ireland

Much recent work has been devoted to the correlation of Devonian and Dinantian stratigraphy throughout South and South-West Ireland, in particular, the relationship between the rocks of the Dingle peninsula and those south of the Hercynian Front.

Much of the argument has centred upon the proposed correlation between the "Dingle Beds" of Jukes and Du Noyer (1863) and the lower part of the Old Red Sandstone succession south of the Hercynian Front. This proposal was originated by Kinahan (1879) and Hull (1879) on the grounds that the "Glengarriff Grits" of Jukes and Du Noyer were lithologically similar to the "Dingle Beds". An alternative correlation of the "Glengarriff Grits" with the lower part of the Old Red Sandstone on the Dingle peninsula was considered unlikely as it implied an unreasonably rapid thickening of these continental facies rocks over a very short distance.

Wright (1927) rejected the views of Kinahan and Hull in favour of Jukes' original assertion that the "Dingle Beds" were peculiar to the Dingle peninsula and could not be correlated with sequences further south primarily on the grounds that the strongly angular unconformity between the "Dingle Beds" and proven Old Red Sandstone facies rocks on the Dingle Peninsula is absent in the succession further south.

Shackleton (1940) identified the "Dingle Beds" as Downtonian.

Naylor and Jones (1967) again rejected correlation of these lowermost Devonian rocks with the lower sequences of the Iveragh Peninsula believing the latter to belong entirely to the Upper Old Red Sandstone of Britain because of the conformable relation of these rocks with the Irish Carboniferous.

Horne (1970), Gardiner and Horne (1972, 1976) and Gardiner (1975) resurrected the idea of correlating the "Dingle Beds" with the lower part of the succession on the Iveragh Peninsula, again using the lithological similarity of the two units as a criteria, and ignoring the strong arguments (stated above) against such a correlation. They further used conglomerate horizons (their Trabeg Conglomerate Formation) to subdivide the "Dingle Beds", (their Dingle Group of the whole of South West Ireland). This seems as unreliable as using localised thinly developed colour variations for regional correlations when Capewell (1957, 1975), Walsh (1968), Shah (1958) and Husain (1957) mapping in detail south of the Hercynian Front have emphasised the lenticular and laterally discontinuous nature of these rudaceous deposits. Gardiner and Horne (1972) also mention the Lough Guitane volcanics (page 343), stating that they occur immediately above the Trabeg Conglomerate Formation. In the course of detailed mapping the writer encountered no such conglomeratic horizon other than as localised developments which have been observed with equal rarity throughout the entire succession of the Lough Guitane region.

Capewell (1957, 1975) reviewed the history of attempts at regional correlation and dismissed as "highly unlikely", the correlation of the "Dingle Beds" with the lower part of the Iveragh peninsula succession.

More recently Russel (1978) identified fish remains in the Valencia Slate Formation down to 240 metres above the oldest strata

exposed at the western end of the Iveragh peninsula. Palaeontological analysis revealed these remains to represent fauna of Upper Devonian or possibly uppermost Givetian age. He concludes that "stratigraphical correlation of the Dingle Group with any part of the Iveragh peninsula succession is no longer tenable and a rapid northward thinning of the Old Red Sandstone succession is proven".

2.5 Structural Data and Tectonic Interpretation

The structure of the Hercynian Front itself and adjacent regions is fairly well understood. It is not within the scope of this work to review structural and tectonic interpretations of the Hercynian orogen outside the Lough Guitane area and its immediately neighbouring areas. Good reviews can be found in Walsh (1968), Capewell (1975) and Naylor and Sevastopulo (1979).

The concept of a Hercynian Front is well accepted. Deformation in general is a result of North/South directed compressive stress with the "front" marking the boundary between the foreland to the north, comprising comparatively undeformed and unmetamorphosed rocks with vertical fold axial planes, and to the south, mildly sheared and metamorphosed rocks of greenschist facies with fold axial planes inclined southwards. The "front" itself varies in character, but is usually placed immediately to the north of a zone of maximum change in structural elevation. The strongest deformation is always therefore to be found immediately to the south of the presumed course of the "front".

The style of deformation is typical of shallow tectonic effects in low grade metamorphic rocks, with brittle fracture the dominant type. Shah (1958) noted the importance of lithology in controlling the style of folding and faulting, and pointed out the comparatively

high resistance to deformation of the volcanogenic deposits. He made a detailed analysis of fold style zones, and presented maps of the major structural elements in the Lough Guitane region. He recognised the Mangerton anticlinorium as the major structural feature, its crest lying between 3.5 and 5 Km south of the supposed line of the "front". This major anticlinal structure can be traced as far as the west coast of the Iveragh peninsula where it bears the local name of the Kilcrohane anticline (Capewell, 1975).

As stated above, the Hercynian Front in the Lough Guitane area and to the east, is marked by a large reverse fracture, the Muckross-Millstreet fault (Wright, 1927). The fault is however never exposed. At its western end at the south-eastern corner of Muckross Lake, Walsh (1968) considers the downthrow to the north to be at least 2900 metres. Gill (1962) states that the Muckross-Millstreet fault at its western termination "... ends abruptly against a major north-west wrench fault near Killarney". Walsh (1968), mapping the area, could find no such termination or a fault with the trend Gill described. Walsh described the Hercynian front west of Killarney as being "not at all well defined". Here the "front" swings northwest, and takes the form of a zone in which the structural elevation to the south is taken up by a succession of faults and the steep northern limbs of asymmetrical folds. Walsh could find no particular reason for the heterogeneous nature of this part of the Hercynian front, or its change of strike, and only suggested that the Lower Slate Formation (Valencia Slate Formation of Capewell, 1975), must wedge out completely somewhere close to the line of the front, thereby producing a change in the competence of the Old Red Sandstone. However, he failed to explain his assertion that the Lower Slate Formation must wedge out, or its control over the course and nature

of the "front".

Towards the west coast Capewell (1975) implied basement control of the fold styles and the course of the front. He placed the front along the northern boundary of his "zone of tilted folds", with a narrow zone of vertical folds along the Dingle Bay coast belonging structurally to the foreland to the north.

Naylor (1978) produced a good review of Hercynian structures in southern Ireland based upon a structural section drawn from north to south, passing through Killarney. He also argued that lithology controls fold style throughout southern Ireland. He further demonstrated the basement control of the Glandore High (Naylor *et al.*, 1974), a north/south positive block in south County Cork, over both sedimentation and subsequent Hercynian tectonism.

Gardiner (1978), on an even broader scale, suggested that the Hercynian front in Ireland is a local feature whose course and style along with the fold and fault styles to its south, are controlled by Lower Palaeozoic deep structural features. He argued that no link can be made with the Hercynian front of South Wales because of the intervening positive block of the Celtic Sea-Wales platform.

Ziegler (1978) in a review of the tectonics and basin development in north-western Europe restricted the Welsh High to Wales, the southern half of the Irish Sea and the south-eastern corner of Ireland. He correlated Devonian rifting events in south-west England and north Germany with the Munster basin. Both Ziegler (1978) and Zwart and Dornsiepen (1978) considered the "front" in south-west Ireland to represent the true Hercynian front, and not to represent a local feature only.

Naylor and Sevastopulo (1979) reviewed the current state of knowledge of southern Irish, Upper Palaeozoic stratigraphy along with

a short discussion of the tectonic history of the area, and Clayton *et al.* (1980) published a general review of the Devonian rocks of the whole of Ireland.

2.6 Contemporaneous Volcanism in S. W. Ireland

Capewell (1975) briefly reported the occurrence of basic volcanics in the vicinity of Valencia Harbour, including a laccolithic dolerite intrusion, pyroclastics and a dyke. The only detailed descriptions can be found in the original memoir (Jukes *et al.*, 1861). These volcanics occur within the Valencia Slate Formation, and are thus older, by an unknown period, than those of Lough Guitane, but can still be ascribed to the Upper Devonian.

Penney (1978) made a detailed report of mugearitic, vesicular lavas from the Coumshingaun Conglomerate Formation (Upper Devonian) at Carrigduff in the Comeragh Mountains. He states that these volcanics occur about 3500 metres below strata of known early Tournasian age. He also presented a comprehensive list of the isolated occurrences of intrusive tuff, dykes and reworked tuffs found in the Devonian and Dinantian of southern Ireland.

Coe (1966) ascribed some of the intrusive tuffs of West Cork to the Lower Carboniferous, but correlation between the Lough Guitane volcanics and any of the examples cited in Penney (1978) is highly problematical.

2.7 Miscellaneous Research Data

Murphy (1974) published a gravity anomaly map for the whole of Ireland on a scale of 1:750,000, and on a larger scale (1:250,000) of the south-west of Ireland (Murphy, 1960). These maps show the Lough Guitane area to fall within a large negative anomaly centred

upon The Reeks. In the Dingle Bay area, this negative anomaly has a steep northern margin with the Dingle Peninsula exhibiting a positive anomaly. To the east the negative anomaly appears to be loosely connected to the large negative anomaly associated with the Leinster Batholith. This connection, along with The Reeks anomaly itself may be related to deep crustal lithology (Murphy, 1960). The Reeks anomaly, however may be related to the presence of the thick sedimentary deposits of the Munster Basin (Naylor, 1967; Clayton *et al.*, 1980).

Inamdar (1974) published a total field magnetic survey of Co. Kerry. This map showed no features which could be related to the geology of the Lough Guitane area.

2.8 Brief Summary of Local Stratigraphy

About 3800 metres of strata are exposed in the Lough Guitane area of which the upper 700 m belong to the Purple Sandstone Formation, with all underlying strata belonging to the Green Sandstone Formation. All the volcanogenic deposits are found within the Green Sandstone Formation.

The volcanics have been subdivided into three sequences based upon three separate source areas or volcanic centres, away from which their respective deposits thin rapidly. From west to east, the volcanic centres are named the Horses Glen Volcanic Centre, the Bennaunmore Volcanic Centre, and the Killeen Volcanic Centre.

Stratigraphic correlation of individual lava flows or volcaniclastic sequences within each volcanic centre has been fairly straightforward. Most problems have arisen in elucidating the relationships between centres due to large drift-covered gaps in exposure. On structural grounds the base of the Killeen Volcanic

Centre deposits occur at approximately the same horizon as the base of the Bennaunmore Volcanic Centre deposits. At the northern end of the Horses Glen a thin tuffaceous sequence is correlated with the main sequence of the Bennaunmore Volcanic Centre to the east and lies about 200 m above the top of the deposits of Horses Glen Volcanic Centre. The Devils Punch Bowl lava may be of the same age as the Horses Glen volcanics, and may be correlated with an agglomerate observed at the far western end of the Horses Glen, north of Lough Erhogh.

The volcanics were therefore erupted in two phases of activity; an early phase responsible for the Horses Glen Volcanic Centre lying about 2300 m below the base of the Purple Sandstone Formation, and a late phase which produced the Bennaunmore and Killeen volcanics lying about 2100 m below.

The stratigraphy of individual volcanic centres is complicated by rapid thickness variations of many of the units, in particular the lava flows. A schematic east-west section through the Lough Guitane area is presented in fig. 5.20. The detailed stratigraphy is described in the Volcanology chapter.

CHAPTER 3

Sedimentology

3.1 Introduction

Throughout southwest Ireland, the Devonian was dominated by sandstone and siltstone deposition, and within this setting, the Lough Guitane volcanism can be regarded as a localised and limited event. Mapping of the Lough Guitane region showed that bedded sandstones of fine to coarse grade were the dominant lithology. Thus non-volcanogenic sediments and processes play an important role in shaping the overall palaeoenvironment.

As sedimentological factors played an important role in influencing the volcanology (Chapter 5), it is necessary to characterise the sedimentological environment into which the volcanic rocks were erupted.

3.2 Previous Research on the Sedimentology of the Old Red Sandstone of the Munster Basin and its environs, S. Ireland

The general work done in south Ireland has been outlined in Chapter 2. Here it is necessary to expand upon the sedimentological data.

In much of the literature, the basin or cuvette which occupied south-west Ireland is referred to as the Munster Basin (Capewell, 1965). Above the unconformity at the base of the Old Red Sandstone no significant depositional breaks within the Old Red Sandstone have been observed in the Munster Basin. Most authors have either treated the Munster Basin as a simple wedge of molasse-type sediments (Naylor & Jones, 1967; Walsh, 1968; Doran *et al.*, 1973; Capewell, 1975), or avoided discussion of the detailed geometry of the basin through lack of data.

The former treatment describes a wedge of clastic sediments derived

from a northern uplifted area. The northern limit of the basin is controlled by large normal faults with an east-west orientation, and to the south by progressive distal thinning and fining of the units. MacDermot & Sevastopulo (1972) suggested that the northern marginal faults propagated northwards, progressively widening the depositional basin. This led to the base of the Old Red Sandstone being diachronous, becoming younger to the north. Such an effect might also be produced by the retreat northwards of the upland source area of the sediments (Doran *et al.*, 1973). Both processes may have played a role in determining the geometry and stratigraphy of the basin fill.

Naylor & Jones (1967) state that the axis of maximum subsidence lay near the northern margin of the basin. This resulted in a highly asymmetrical body of sediments when viewed in cross section.

However, even the coarsest stratigraphic correlations within the Old Red Sandstone are problematical. Regional isopach maps for the basin must be treated with suspicion as south of a line drawn from Dingle Bay in the west to Dungarvan in the east, the base of the Old Red Sandstone is never exposed.

Horne (1970) and Gardiner (1975) have both drawn attention to the potential complexity of the Munster Basin when detailed syntheses are attempted. These authors observed both southerly and northerly directed sediment transport. They drew the conclusion that from time to time uplifted horsts, probably shortlived, existed within an otherwise generally subsiding basin. They suggested that one such horst existed aligned roughly east-west along what is now Dingle Bay, and divided the Munster Basin from what has been called the Dingle Basin (Horne, 1970). Gardiner (1975), has also observed northerly directed transport in the Caherbla Group of the Galty Mountains, although no specific interpretation of this anomaly is made.

The first of these two complications is founded on northerly directed sediment transport in the Inch Conglomerates which outcrop on the south side of the Dingle Peninsula (Horne, 1970, 1975). However, Capewell(1951, 1965) suggests, also on the basis of sedimentary structures, and thickness variations, southerly or southwesterly directed sediment transport. These coarse deposits are widely thought to represent a coarse proximal alluvial fan facies. While Horne (1970) would have a source area for the Inch Conglomerates to the south on his uplifted horst, Doran *et al.* (1973) found " .... the introduction of an additional narrow, and yet much demanded source area between the Munster Basin and a "Dingle Basin" out of place ....".

It is not clear in the literature whether the southern margin of the Minster Basin was tectonically passive or active. The suggestion that the coarse continental clastic deposits passed southwards into the marine geosyncline presently off the south coast (Naylor & Jones, 1967) seems to be based largely upon the later Tournasian marine transgression which crossed most of Ireland.

Any attempt at a regional synthesis is fraught with problems, the most important of which is the total absence of reliable, regional marker horizons. When attempting to draw north-south sections through the basin, stratigraphic units of over 2000 metres apparently wedge out completely within a distance of only some 10-12 kilometres (Naylor & Jones, 1967). For example 2440 metres of the Chloritic Sandstone Group at Sneem (Capewell, 1957) is absent on the Beara Peninsula to the south (Coe & Selwood, 1963).

Another point on which there appears to be a general consensus is the continental, and dominantly fluvial nature of the deposition (Naylor & Jones, 1967; Gardiner, 1975; Walsh, 1968; Shah, 1958). The variations in dominant grainsize from region to region, and from stratigraphic unit

to stratigraphic unit was due largely to the varying proximity of the source area, and to differential rates of subsidence along the inferred northern boundary fault zone.

The only previous work on sediment derivation in the Lough Guitane area was included in the unpublished thesis of Shah (1958) who claimed that palaeocurrent directions derived from sedimentary structures in the sandstones indicated an exclusively southerly directed current system. Walsh (1968) studying the area of Macgillycuddy's Reeks, immediately to the west did not discuss palaeocurrent directions, but implied that the sediments were derived from the north.

Thus, according to published information it would be reasonable to predict that the Lough Guitane sedimentary rocks were deposited some 20-25 Km south of the northern, fault-controlled basin margin, on an alluvial plain at the distal end of an alluvial fan complex.

3.3 Latitude and Climate of Southwest Ireland during the Devonian

Recent palaeogeographic reconstructions in the Middle and Upper Palaeozoic in Atlantic-bordering continents have focussed on the timing of large sinistral displacements between Europe and North America (Van der Voo *et al.*, 1979, 1980 and Harland, 1980 among others). The general consensus places the southwest British Isles to the south of the major sinistral displacement zones at a latitude of between 0^{o} and $5^{o}S$.

In the Devonian the development of land plants was minimal and thus the high rainfall implied by the equitorial location would have led to high rates of erosion in mountainous areas coupled with rapid runoff and deposition in basinal environments. The rainfall, and therefore the deposition would have been fairly evenly distributed throughout the year preventing the extensive development of palaeosols.

Even if seasonal rains had been prevalent, the few months dry season would have been unlikely to be long enough for soils to develop.

3.4 General Observations on the Palaeoenvironment

General observations suggest that the conclusions drawn from the previous work on the Old Red Sandstone of southern Ireland are applicable to the Lough Guitane sedimentary rocks.

The following points support a continental depositional environment in the Lough Guitane area:

1. Marine fossils are totally absent

2. Desiccation cracks occur commonly in fine sandstones or finer lithologies

3. The sandstones are immature, containing common broken feldspar minerals, rock fragments, and angular to subangular quartz grains.

Further general observations can be made:

1. Strong intraformational erosion in the form of channelling over 50 cm deep is very rare.

2. Epsilon cross bedding (Allen, 1963) is absent.

3. The dominant grain size is medium or coarse sand.

4. Many of the individual cross, or parallel laminated sandstone units are sheet-like in geometry, often being traceable for over 100 metres along strike.

5. Within short sequences of the order of 10 metres, the palaeocurrent directions are strongly unimodal.

These observations lead to a working hypothesis on which the following detailed analysis of the sedimentology is based, namely that the sedimentary rocks of the Lough Guitane region were deposited by braided streams of low sinuosity.

3.5 Sedimentary Structures Present and Their Interpretation

The descriptions given below refer specifically to observations made within the Old Red Sandstone of the Lough Guitane area. The accompanying interpretations are based on work by Allen (1963a, 1963b), McKee *et al.* (1967), Harms *et al.* (1975), Walker (1976), Miall (1977, 1978), Collinson (1978), Rust (1978), Long (1978) and Friend (1978). Table 3.1 presents a summary of the data, including the frequency of occurrence of each lithofacies, both regionally, and in the Cappagh Measured Section (indicated on fig. 1.5). The "Cappagh Measured Section" will subsequently be abbreviated to "CMS".

Trough-crossbedded sandstone (St)

Description : (Plate 3.1)

Usually found in cosets of mutually cross-cutting troughs (festoon cross-bedding, pi cross-stratification of Allen (1963)). Set thickness is usually between 5 and 20 cm. Plan sections are very rare, and trough widths range up to 30 cm, being traceable downcurrent for up to 2 m (location 9179). Grain size varies from medium to coarse sand with quartzite pebbles present as rare clasts up to 1 cm in size. Sequences comprising this lithofacies exclusively may be up to 4 or 5 m in thickness (location 9102, Plate 3.1).

Interpretation :

This lithofacies has been deposited by migrating asymmetrical dunes with pronounced curved crests. While a minimum average flow depth of about twice the thickness of individual sets can be inferred (Harms, 1975), no maximum depth is implied.

Planar cross-bedded sandstone (Sp)

Description : (Plate 3.2)

These are found as either solitary sets (Alpha cross-beds of Allen

(1963)) or grouped sets (Omicron cross-beds of Allen (1963)), but more commonly they have flat or slightly scoured bases and tops. The grain size may be medium to very coarse sand with pebbles present up to 2 cm. Silt or mudstone intraclasts are commonly present in small amounts, and this lithofacies grades into the lithofacies of erosional scours described below. Individual cross laminae lie at between 15 and 35 degrees to the base. Set thickness varies from 5 cm to approximately 2 m, with groups of sets commonly occurring in cosets over 5 m thick in the CMS, and over 4 m elsewhere (e.g. location 81020). Individual sets may be traceable transversely to the palaeocurrent direction for at least 20 m (locations 9107 and 9107 and 9169), and downstream for up to 30 m (location 9169). Reactivation surfaces have only rarely been observed (location 9129).

At the south end of the Horses Glen (locations 9107 and 9169, plate 3.3) a series of planar tabular sets were observed, each averaging 50 cm in thickness, and which could be traced laterally for over 100 m. The large expanses of flat rock exposed on the north facing wall of the glen represent bedding planes between each tabular set.

Interpretation :

Tabular sets of cross-strata are deposited by migrating sand waves with straight crests. A lower flow strength is interpreted than for dunes as described above (Harms, 1975). The depth of water must exceed the maximum thickness of a set, but they may have very shallow flows on the upstream side of the sand wave crest. Again, sand waves imply no maximum depth of flow. Very thick tabular sets may represent deposition on oblique or longitudinal bars. A study of relative palaeocurrent directions might resolve this problem (Harms, 1975).

Horizontally bedded sandstone (Sh)

Description : (Plate 3.4)

This lithofacies exhibits a wide range of unit thickness and grain size. The latter varies from fine to very coarse sand with quartzite pebbles and mud/siltstone intraclasts. The former shows variation between unbroken sequences of a few centimetres to over 3 m in the CMS. The thicker sequences often contain gently undulating, low amplitude erosion surfaces every few metres.

Parting lineation is absent although this is almost certainly due to the low grade metamorphism which has affected all these rocks. The bases of units may be planar or scoured (plate 3.5).

Interpretation :

Miall (1977) observed that horizontal bedding can occur in two quite different flow regimes and environments; an upper and a lower flow regime. During strong flow, a plane-bed condition develops during an upper flow regime (Harms & Fahnestock, 1965) with virtually continuous particle movement. Poor sorting (the presence of numerous intraclasts and quartzite pebbles) is characteristic of this environment, as is a gently to strongly scoured base. However, it must be stressed that rapid deposition may damp out the development of other bedforms more appropriate for the current velocity in operation, so the above interpretation must be modified to include such situations of rapid deposition.

In contrast, a viable alternative lies in a low flow regime in sand coarser than 0.6 mm (Harms *et al.*, 1975). However, in the CMS a number of fining-upward sequences between 50 cm and 3 m thick occur which require further consideration. These sequences are characterised by generally finer grain size (medium grade sand or finer) and the total absence of the intraclasts and pebbles found in those horizontally laminated sequences positively ascribed to an upper flow regime. They

usually have planar or gently scoured bases.

Interpretation of these sequences is difficult. Those with gently scoured bases may represent the distal equivalent of the coarser, intraclast-rich deposits attributed to an upper flow regime. High sediment loads, and rapid percolation in these terminal parts of the depositional fan may completely suppress the formation of low flow regime structures such as ripple marks, thus rendering the fine grained part of the fining-up sequence indistinguishable from facies Fm and Fl (Miall, 1977 and see below) attributed to overback or floodplain environments well away from the main channel.

Ripple cross-laminated sand (Sr)

Description :

This lithofacies comprises only 11 percent of the CMS. Grain size varies from medium to very fine sand. Sets range up to 5 cm in thickness, and are rarely traceable transversely or downcurrent for more than a metre. In the CMS, an unbroken sequence of at least 5 m of ripple cross-bedding, and some small-scale planar tabular cross-bedding occurs in medium and fine grained sandstones. Sets vary from 1-10 cm in thickness, and are usually highly lenticular. Bases are usually gently scoured with relief up to 5 cm.

Small-scale rippled surfaces are also occasionally exposed on individual bedding planes (e.g. location 9035). At this outcrop the current ripples have an amplitude of 0.5 cm, and a wavelength of between 2 and 3 cm.

Interpretation :

These current ripples represent the bed form for low flow strengths. The morphology of the ripples varies according to the flow velocity, grain size, and aggradation rate. The importance of this lithofacies in terms of environmental interpretation is limited. Current ripples

can exist as the dominant bed form under quite shallow or very deep flows. Their rarity in the Lough Guitane area would seem to suggest either that low flow regimes were not the dominant depositional mode, or that the sediment was often too coarse for ripples to develop, so that the deposits were preferentially removed.

Compound cross-stratified sandstone (No Code)

Description :

The internal organisation of this lithofacies is illustrated in fig. 3.1. These sets range between 70 cm and 2.8 m in total thickness, and comprise 'larger-scale' cross-strata up to 8 cm thick which are themselves cross-stratified by 'fine-scale' planar tabular subsets. The grain size is usually poorly sorted coarse sand, containing numerous silt or mud intraclasts and occasional quartzite pebbles, although the 'large-scale' cross strata may be separated by thick fine sand partings.

The 'large-scale' cross strata lie at angles of about 20-25^{o} to the base of the unit, which is usually gently eroded or planar. The 'finer-scale' subsets lie at angles between 0^{o} and 10^{o} to the surfaces of the 'large-scale' cross strata. The two systems of cross-stratification have the same orientation, i.e. they both indicate the same direction of sediment transport.

These compound cross-sets are usually found as solitary units, but no useful data is available on their lateral extent. Within the sets, some of the large-scale cross-sets cannot be traced continuously from the top of the unit to its base suggesting that some mild erosion and reactivation has occurred.

Interpretation :

Harms *et al.* (1975) considers this type of cross-stratification to be produced by delta fronts, the large scale cross-bedding representing the slope of the delta front, the small scale subsets

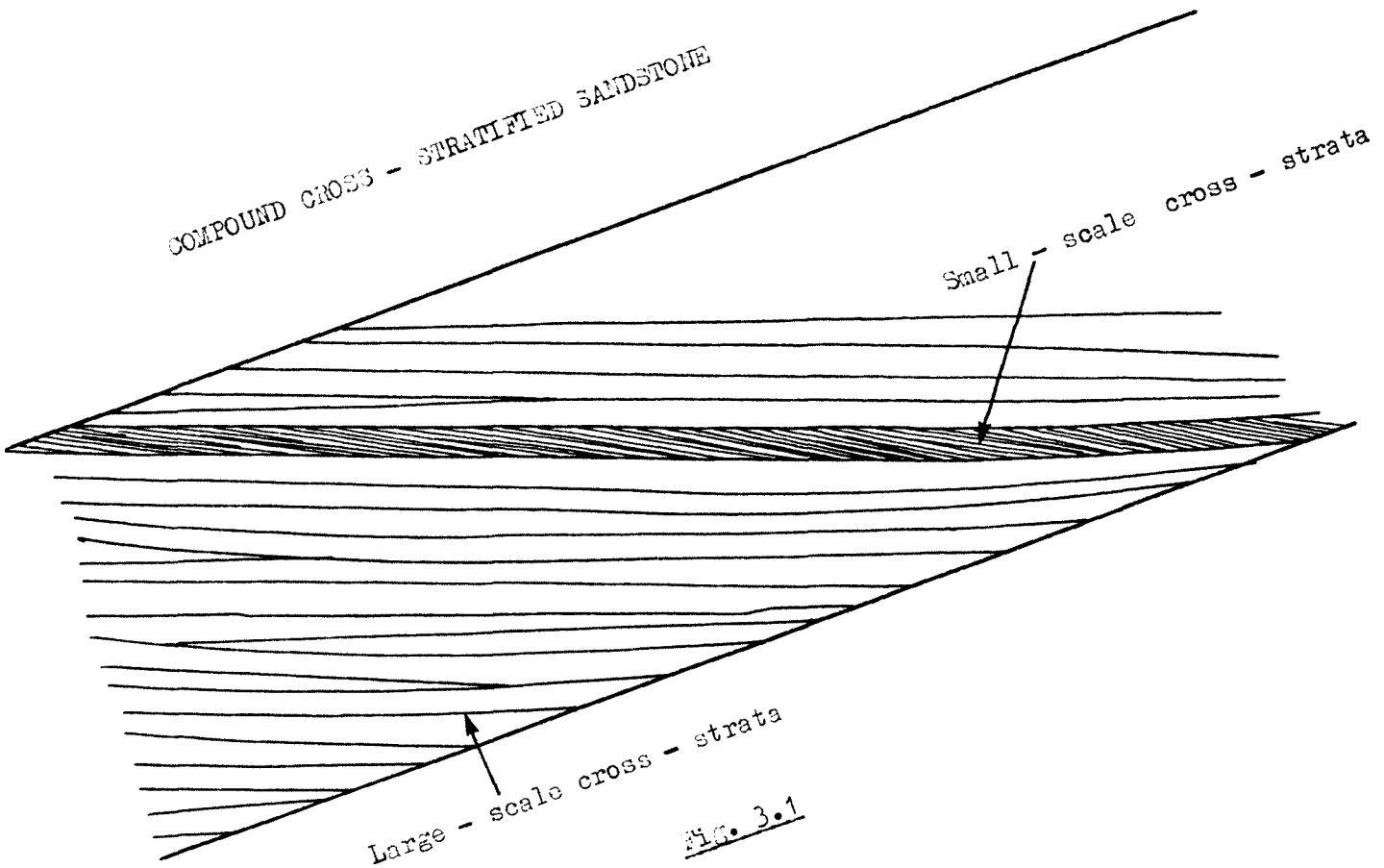
COMPOUND CROSS - STRATIFIED SANDSTONE
Small - scale cross - strata
Large - scale cross - strata

Fig. 3.1

being produced by migrating ripples as described above, deposited in currents flowing down the inclined surface of the delta front. The thin, fine sand partings are indicative of some low flow stage modification (McCabe & Jones, 1977). However, the example cited by Harms is about 10 m thick, and found in an intertidal environment (Howard, 1966). While not directly applicable, the above interpretation is probably broadly correct. This type of composite cross-stratification has however been poorly documented in fluvial systems, and the circumstances leading to the initiation of such bedforms is little understood.

Intraformational conglomerates ("Erosional scours with intraclasts", Miall, 1978) (Se)

Description :

This lithofacies is characterised by strongly eroded bases with scours up to 50 cm deep. The whole unit contains abundant siltstone and mudstone intraclasts supported by a matrix of massive or faintly cross-bedded coarse or very coarse sand. The greatest concentration of intraclasts occurs at the base of the unit, where some may be up to 30 cm in size. (Such a very coarse member occurs some 27 meters from the base of the CMS.) Rarely, a vestige of the fine grained sediments are still to be found in situ at the base of the unit. In the CMS, this lithofacies is found in solitary units up to 1 m thick.

This lithofacies grades into planar - tabular cross-stratified sandstone with progressively fewer intraclasts and with less marked basal erosion.

Interpretation :

The interpretation is not significantly different from that for planar cross-stratified sandstone. The highly erosive nature of the base of each unit, and the presence of numerous intraclasts is probably

related to:

a) the availability of easily erodable fine-grained sediments.

b) the proximity of that erosion to the point of deposition.

c) the volume of flow involved, i.e. flood events of relatively large volume, with high sediment loads will tend to dilute the content of intraclasts, travel further from the point of erosion, and produce deposits with more gently eroded bases and more sheet-like geometry.

Scour-fill sandstone (Ss)

Description :

This type of deposit is extremely rare in the Old Red Sandstone of the Lough Guitane area. The scours occur as elongate subparallel runnels, 5-10 cm deep and up to 80 cm wide (plate 3.6), and which may exceptionally be traceable downcurrent for 15 m (location 9395). They are infilled with medium to coarse, low-angle cross-stratified sandstone, (eta cross-stratification of Allen, 1963) indicating a current direction parallel to the long axes of the scours.

Interpretation :

It is envisaged that the scours were produced by a high velocity, probably short-lived laminar flow regime. Deposition would have followed under a much lower flow regime.

Low-angle cross-stratified sandstone (Sl)

Description :

As a separate lithofacies, low-angle cross-stratified sandstones are difficult to distinguish from horizontally laminated sandstone in which shallow scoured surfaces are common. It has only been positively identified, along with horizontally stratified sequences in the tuffaceous sediments (Chapter 5.1.6), and its lateral relationship with other lithofacies was not observed.

Interpretation :

Rust (1977) interpreted this lithofacies as being deposited by shallow, high velocity flow into low relief scours, citing an example of low angle cross-strata in the Malbaie formation, Gaspe, Quebec, which was laterally transitional into horizontally stratified sandstone.

Massive structureless sandstone (No code)

Description :

Sequences occur, many metres thick, which are apparently devoid of internal structure and organisation. These deposits vary from medium to very coarse sandstone with silt or mudstone intraclasts, and quartzite pebbles.

Interpretation :

The coarser sequences were probably deposited by similar flow conditions to those responsible for deposition lithofacies Sh and Sl (see above). The absence of internal organisation in the coarse textured rocks may be related to very high rates of aggradation damping the development of sedimentary structures. However, poorly developed structures present in the finer grained rocks may have been locally obliterated by the regional metamorphic/tectonic event.

Wave-rippled sandstone (No code)

Description :

This lithofacies is very rare, but well displayed in medium grade sandstones on the northern slopes of Stoompa (plate 3.7, location 8461). In this example the ripples are symmetrical, with an amplitude of between 0.5 and 1.0 cm, and a crest to crest wavelength of usually 2-3 cm, ranging up to 5 cm.

Interpretation :

Symmetrical ripples are produced by an oscillating current related to wave action. However, it is not possible to infer a unique

combination of wave size and water depth to produce a given ripple spacing for a given grain size. Such deposits must have occurred under standing water, but when localised, the environment could equally be lacustrine or fluviatile. The extreme rarity of such deposits is significant in terms of an overall environmental interpretation.

Fine-grained facies (No code)

Description :

The two lithofacies present (facies Fl and Fm) which belong to the fine grained group, will be described together, and treated as one facies. As such it includes all varieties of massive or laminated very fine sandstones, siltstones and mudstones. Individual laminations are on a scale of millimetres or rarely 1-2 cm.

Internal organisation includes normal grading in horizontally laminated units, climbing ripple cross-lamination and other small scale current ripples. Climbing ripples in particular are common. They have no erosive base and are interpreted as being deposited by the migration of trains of asymmetrical ripple marks with active deposition. Small scale flame structures are also present.

Desiccation cracks are common (location 9087, plate 3.8), and may be on an unusually large scale. At location 8644 on the northern slopes of Stoompa desiccation cracks in fine sandstone were observed infilled with medium to coarse grade sandstone. Each polygon has dimensions between 30 and 80 cm, and is usually four or five sided. Each crack varies between 1.5 and 7 cm in width. In dominantly fine-grained sequences, desiccation cracks have often been strongly tectonically distorted.

Bioturbation and plant rootlets are absent, but carbonate nodules occur rarely along particular horizons within a fine grained sequence. The nodules are usually between 1 and 5 cm in size, and in outcrop

weather out preferentially producing a pock-marked appearance

Interpretation :

In the Lough Guitane area these rocks comprise a significant proportion of the sediments. They are interpreted as having been deposited under very low flow velocity regimes, or in standing water. A floodplain environment is supported by the frequent occurrence of desiccation cracks which implies frequent subaerial exposure. The carbonate nodules may also be related to early diagenesis involved in such desiccation.

However, Miall (1977) points out that braided streams are not characterised by large floodplain areas, and in ancient deposits older than Carboniferous (i.e. including those under study), the absence or rarity of land vegetation to stabilise flood plain areas should inhibit the survival of fine-grained deposits. The presence of numerous intraclasts of mud and silt in coarser, high flow regime deposits, is strong evidence that many fine grained deposits were eroded. The overall environmental interpretation of the fine-grained deposits will be dealt with in the discussion section.

Miscellaneous sedimentary features

In addition to the above sedimentary structures, a number of other features have been observed, which deserve mention.

Flame structures

These loading features are observed quite commonly between sedimentary units of contrasting grain size. They vary in scale from a few millimetres (fig. 3.2) to many tens of centimetres.

Unusual cross-bedding (plate 3.9)

An interesting 50 cm thick, cross-stratified unit occurs at location 9586. The migrating dune responsible for this feature must have possessed a lee surface with an upper low-angle slope, and a lower,

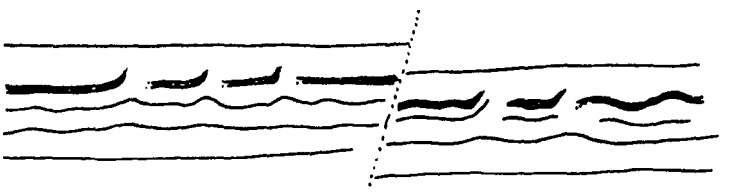

Fig. 3.2 Flame structures in very fine - grained laminated sediments (mudstones). (Real size).

high-angle slope. There is no erosional relationship between the two surfaces in plate 3.9, although upstream the upper low-angle surface passes transionally into a reactivation surface. Individual cross-laminations can be traced from one lee surface to the other although the laminations tend to thicken on passing through the junction into the higher angle slope. Deposition was therefore occurring simultaneously on both lee slopes. Although strongly eroded surfaces are absent, this structure is interpreted as a type of reactivation probably under high aggradation conditions.

Reactivation Surfaces

Other more normal types of reactivation surface are common in large scale tabular cross-beds (facies Sp). In general, these surfaces are interpreted as being caused by changes or interruptions in flow conditions (McCabe & Jones, 1977).

Sandstone dykes and contemporaneous microfaulting

These features are discussed in some detail under volcanology (Chapter 5) because of their intimate association with volcanic processes.

3.6 The Logged Sections - General

The choice of location of the logged sections in particular the longest of these, was controlled purely by outcrop availability. Although exposure is very good in much ofthe study area, it is usually of a broken, discontinuous nature. Tight folding and faulting contribute to a general difficulty in finding long continuous sequences.

The Cappagh measured section (CMS) occurs immediately west of, and parallel to the Cappagh fault in near-vertical strata, on the northern limb of the Mangerton Anticlinorium (fig. 1.5).

According to the stratigraphic synthesis presented in chapter 2, the section occurs in the Green Sandstone Formation. The top of the

section lies approximately 80 metres below the base of the Bennaunmore Centre volcanic sequence.

The section is physically composed of a low crag, exposing on average a lateral width of 3-4 meters of rock above the flood plain of the River Cappagh. The crag is ideal for the construction of a logged section because

1. The strata are near vertical and without minor folds,

2. The fault controlled nature of the section has produced a very long, almost perfectly straight outcrop pattern adjacent to the Cappagh fault zone,

3. The section is cut almost perpendicular to the strike of the strata,

4. Only 28.4 meters of strata are missing from a total section thickness of 142.9 meters.

The log of the section is presented in fig. 3.3. A detailed discussion of the sequence appears in the discussion section at the end of this chapter.

Two other, comparatively short sections were measured. They both occur at high altitude on the eastern side of the Horses Glen at locations 9129 and 9068 in the Green Sandstone Formation.

Detailed descriptions of these, and the sedimentological interpretation appears together with the CMS in section 3.8 of this chapter.

3.7 Palaeocurrent Analyses

3.7.1 Introduction

The interpretive importance of palaeocurrent measurements has been discussed in general terms by many authors, e.g. Long (1978); Potter & Pettijohn (1977). An extensive programme of palaeocurrent data collection was undertaken regionally, in addition to the thorough coverage

of the logged sections.

Two hundred and ninety two measurements were made on planar tabular cosets; 25 on ripple cross-laminated sandstones; and only 2 measurements were made on trough cross-bedded sandstones. Where possible, measurements were made on cross-strata exposed in three dimensions, although this was not always possible in the CMS, where the orientation of the cross-beds sometimes had to be interpolated in the field from two adjacent joint planes or weathering surfaces.

Regionally, the field location of each palaeocurrent determination was largely determined by the requirements of the mapping programme which was geared to the outcrop of the volcanics. However, some excursions, both north and south of the central axis of the study area, were made to extend the coverage of palaeocurrent data. While the collection of data is not claimed to have been random, measurements were made at regular intervals wherever crossbeds were well exposed in three dimensions irrespective of stratigraphic position, or crossbed orientation.

Cross-beds have been commonly tectonically distorted (Plate so that they lie almost at right angles to the coset bedding planes. These deformed cross-beds were never used for taking current directions, except in the CMS, where some slightly distorted examples were used.

Miall (1976) discusses the preservation potential of various current produced structures, and their reliability as indicators of prevailing current directions in a braided stream deposit. He concluded that preservation over the whole sedimentary record was random. In sequences of stable deposition and little scour, planar cosets could create palaeocurrent patterns with very low directional variance, although in general, sequences of trough cross-bedded sandstone showed the lowest directional variance. In an environment typical of deposition of the

Lough Guitane sediments, where strong erosion is very rare, measurement on planar cosets are reliable indicators of the prevailing drainage pattern.

3.7.2 Correction of Palaeocurrent Data for Tectonic Dip and Plunge

A computer program was used to reorientate the field data for tectonic plunge and dip. The program is entitled "Bristol University Palaeocurrent Analysis System" and was written by M. A. Cooper (1977).

The program consists of two packages, one entitled "Orient", responsible for the data correction, and one called "Palaeo", which draws palaeocurrent roses, and derives statistical information including an analysis of variance. The present study only employed the "Orient" package.

Briefly, the "Orient" program has the following facilities:

1. To remove from a palaeocurrent measurement the effect of tectonic plunge, the value of which may be supplied individually for each measurement or as one plunge value for a group of measurements.

2. To restore a palaeocurrent measurement to its pre-tilt orientation by rotating the bedding to horizontal.

3. The palaeocurrent measurement can be supplied as a direct measurement or as two measurements of pitch on oriented joint planes.

4. After processing and reorientation of the data, the reoriented measurements are printed out on a line printer and if required, punched out as a deck of cards in a format suitable for input to program "Palaeo".

3.7.3 Regional Data Analysis

The overall regional palaeocurrent rose for the Green Sandstone Formation is presented in fig. 3.4, and its weighted equivalent in fig. 3.5. Data from the younger Purple Sandstone Formation is dealt with separately (fig. 3.6).

The CMS palaeocurrent rose (fig. 3.6) resembles that of the regional

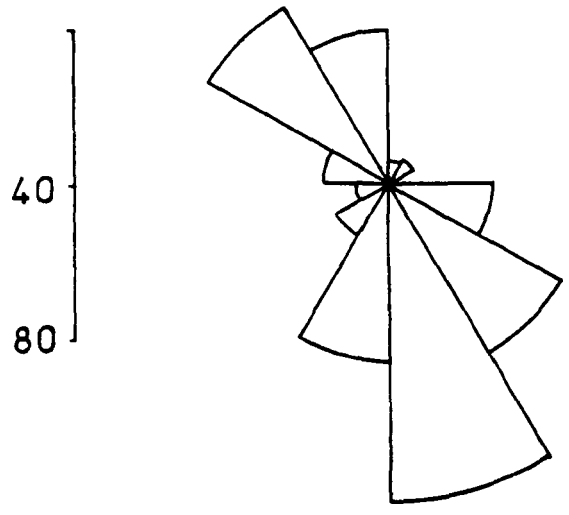

Regional

n = 319

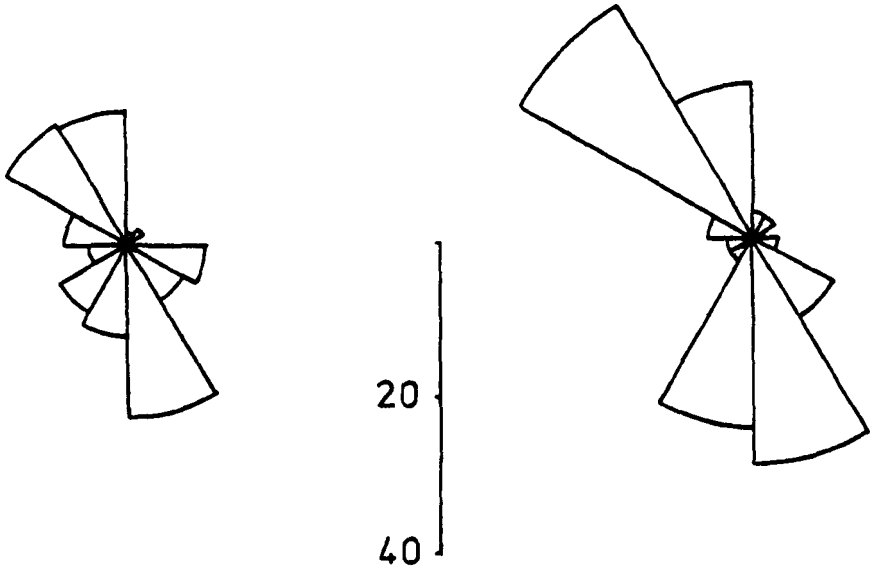

Regional North

n = 112

Regional South

n = 141

Fig. 3.4 Regional palaeocurrent rose diagrams.

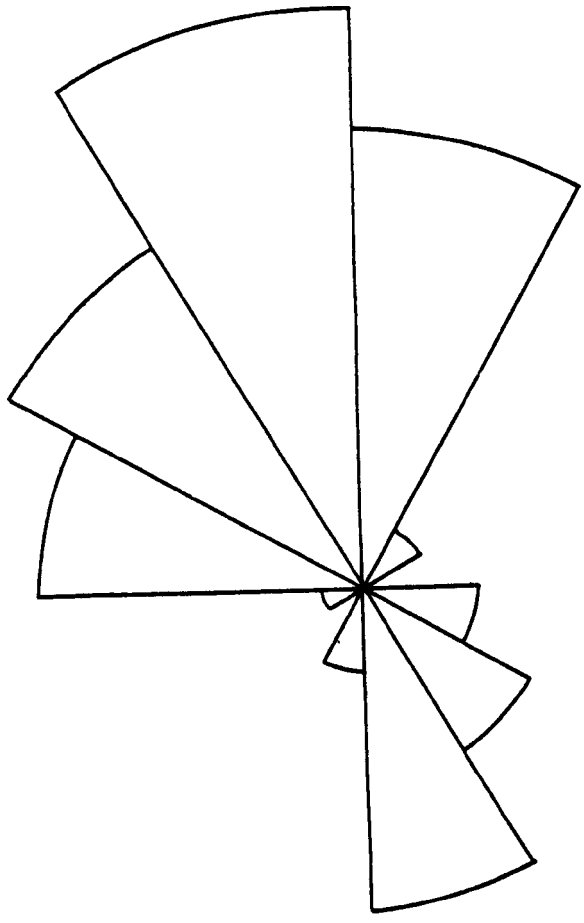

Regional
Weighted Palaeocurrent Rose

Fig. 3.5

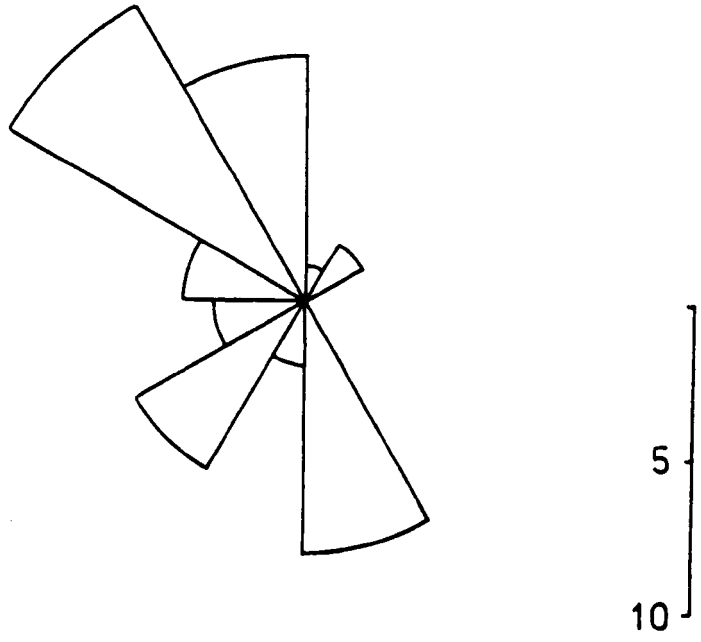

Cappagh Measured Section (Strat. E)

n = 45

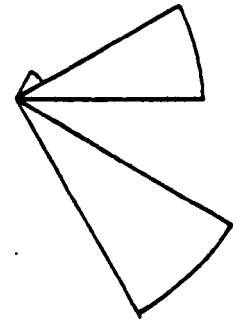

Purple Sandstone Group - Strat. A

n = 15

Fig. 3.6

data (fig. 3.4) in being strongly bimodal with NW and SSE-directed modes. The dominant mode is however directed to the south in the regional analysis, while it is to the NW in the CMS analysis. It must be stressed that the regional data is taken from a thickness of 4000 meters of fluvial sediments entirely within the Green Sandstone Formation.

In an attempt to understand the bimodal distribution of the data, the regional data has been presented in a form weighted in proportion to the thickness of the cross-stratified unit on which each individual palaeocurrent measurement was made (fig. 3.5). The data has also been subdivided in accordance with two other parameters:

1. Figs. 3.7 and 3.8 show the data subdivided according to the stratigraphic position within the Green Sandstone Formation. Each subdivision has been labelled according to the system outlined in fig. 3.9. While conforming generally to the overall bimodal pattern, each palaeocurrent rose displays a wide variation in the dominance of the two modes. Units B, C east and G exhibit virtually unimodal distributions directed towards the SE and SSE. Unit F exhibits a virtually unimodal distribution directed towards the NW. Units B, C east and E are bimodal with the dominance of the two modes variable.

2. In fig. 3.4 the data has been divided into two groups - those measurements made north of the crest of the Mangerton Anticlinorium and those to the south. The Mangerton Anticlinorium has been used because of its east-west orientation, and its central position in the study area. Data derived from sediments on the crest of the anticlinorium or in its immediate vicinity have been omitted. No statistically significant difference in palaeocurrent distribution is noted between the regional-north group, and the regional-south group.

Many authors (including Miall, 1974) describe techniques for weighting palaeocurrent measurements according to individual set thickness.

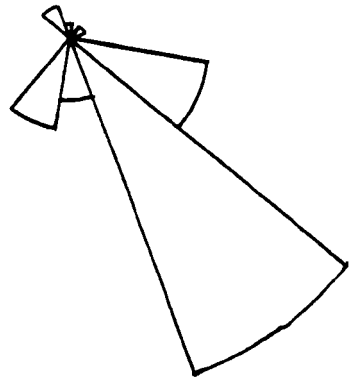

Strat. G n = 46

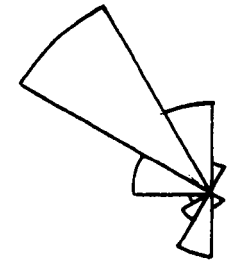

Strat. F n = 35

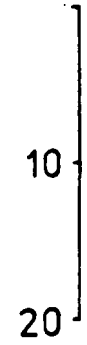

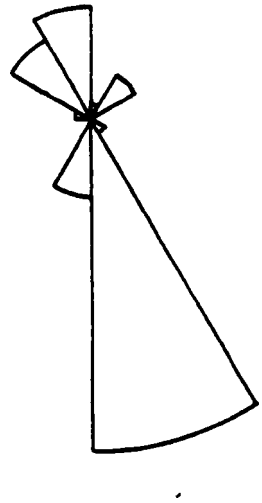

Strat. E West n = 45

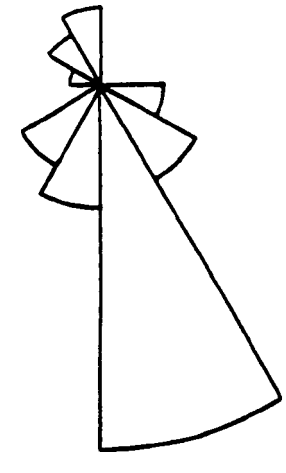

Strat. E n = 60

Fig. 3.7

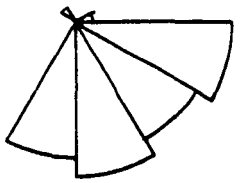

Strat. B East n=40

Strat. D n = 16

10

20

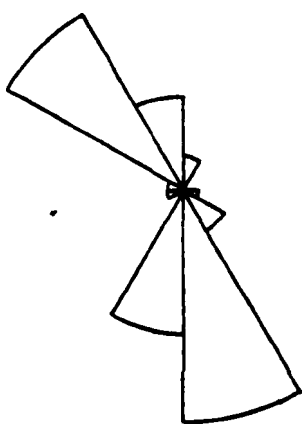

Strat. B n = 50

Strat. C n = 9

Fig. 3.8

Key to Stratigraphic Divisions Used in Figs. 3.6 - 3.8

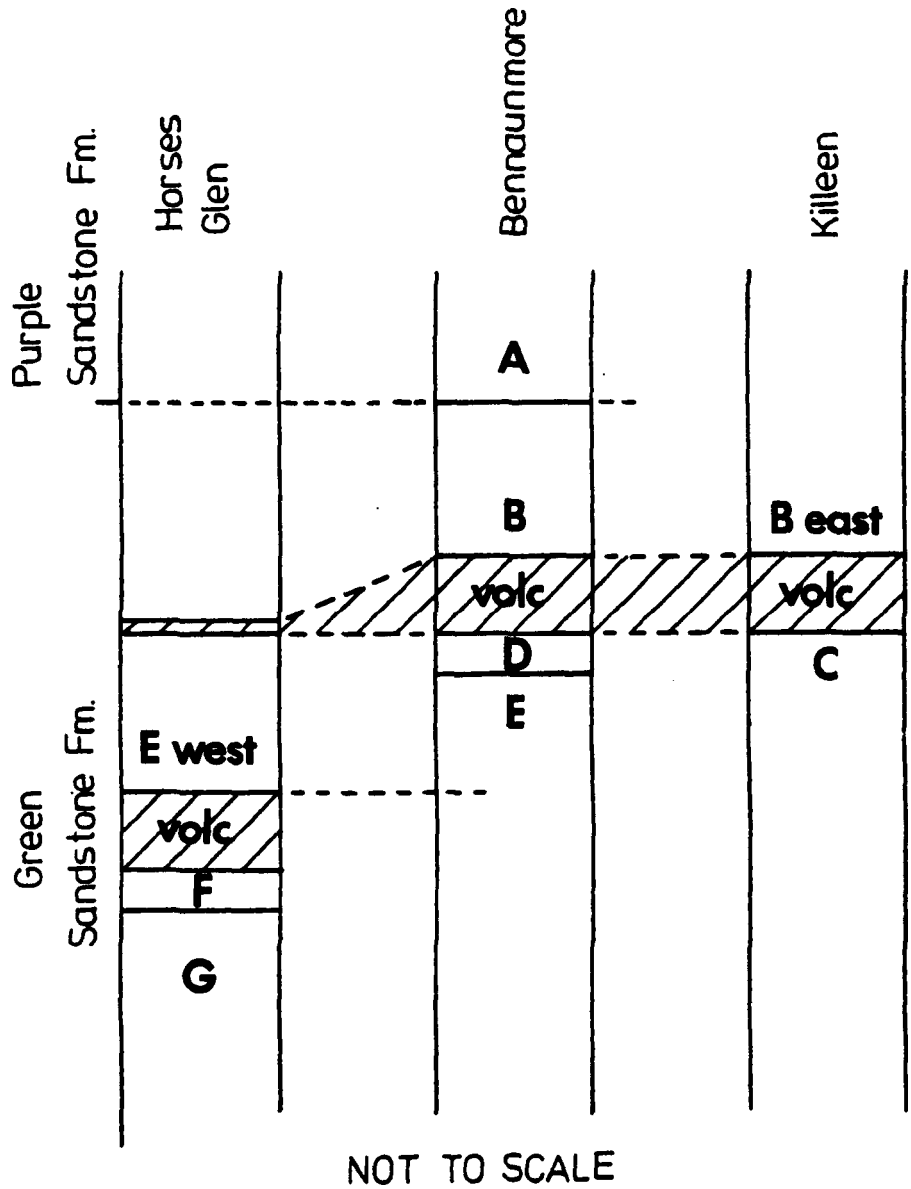

Fig. 3.9

This procedure gives a better estimate of the amount of sediment deposited by each current direction segment, and therefore the true importance of each palaeocurrent measurement.

Palaeocurrent data from the Cappagh measured section (45 measurements), were given the same treatment as the regional data with the exclusion of the north-south subdivision applied to the latter. The data have also been subdivided according to set thickness (fig. 3.10). The results are discussed in section 3.8.3.

3.8 Sedimentological Interpretation of the Lough Guitane Sediments

3.8.1 Introduction

Many authors have pointed out the problems involved in distinguishing low sinuosity, braided environments from those of higher sinuosity, or meandering fluvial systems. Similar or identical structures are known in deposits attributed to radically different sedimentary environments (Long, 1978). Interpretation must therefore be based on the relative abundance, scale, assemblage and sequence of lithologies, sedimentary structures and their directional properties. Characterisation of the Lough Guitane deposits by width to depth ratio of channels, and the slope against discharge considerations advocated by Leopold and Wolman (1957) are not possible when dealing with ancient deposits and outcrops of limited lateral extent.

It is possible, however, to consider the factors important in determining what lithologies and types of sedimentary structures are likely to occur. The absence of prolific land vegetation in the Devonian will have profound effects on the runoff characteristics (Long, 1978). The lack of vegetation will decrease channel bank cohesion and discourage channel incision (Friend, 1978), while there will also be a serious lack of water and sediment storage capacity

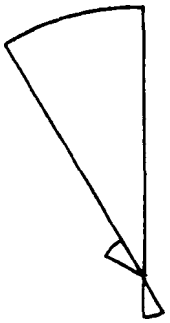

Unit Thickness 100 cm.+
n = 9

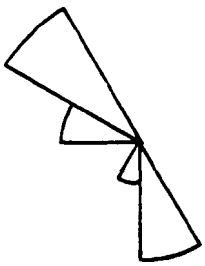

Unit Thickness 51-99 cm.
n = 10

CAPPAGH MEASURED SECTION

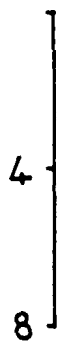

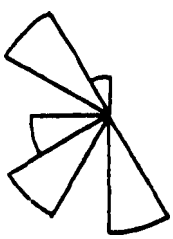

Unit Thickness 16-50 cm.
n = 12

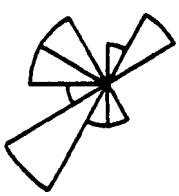

Unit Thickness 1-15 cm.
n = 12

Fig. 3.10 Cappagh Measured Section palaeocurrent roses subdivided according to set thickness.

resulting in strongly fluctuating discharges (Miall, 1977).

With regard to alluvial fans, one must also consider the documented differences between proximal and distal depositional environments. There are no absolute indicators (Miall, 1977), but several parameters can be used to infer downstream changes in channel morphology and discharge characteristics. Friend (1978) summarises features observed in the sediments (Oligocene and Miocene) of the Ebro Basin, Spain. The northern flank of the basin, in contrast to the southern flank, exhibits a lack of evidence for channel incision similar to that observed in the Lough Guitane sediments. It contains sandstone bodies which are dominantly sheet-like, with large-scale cross stratification and local basal scours indicating lateral channel movement. More distally sheet sandstones are still the commonest bed type, but they are usually thinner, and have planar bases.

In Spitzbergen (Friend & Moody-Stuart, 1972) the Old Red Sandstone of the Wood Bay formation contains sandstone bodies which lack basal irregularities of relief greater than a few tens of centimeters. Again these were interpreted as being deposited by sheet floods.

The series of papers published by Rust (1978) and Miall (1977, 1978) produced a set of models for braided alluvium. Given the general observations made in section 3.4 of this chapter, and the relative abundance of the various sedimentary structures described in section 3.5 (see table 3.1 for summary), it seems reasonable to assume a braided environment for the Lough Guitane sediments, and adopt such a modelling system. Each lithofacies is given a symbol according to the definitions given by the above workers.

The models are based upon the relative abundance of the lithofacies described, each being ascribed major or minor importance. The main facies of the CMS are Sp (28.0% of the exposed log) and Sh (29.9%).

Massive structureless sandstone, possibly attributable to facies Sh comprises a further 15.0%. Minor facies present are the fine grained group and then facies Se, Sl and Ss in order of abundance. Table 3.1 shows this subdivision of lithofacies alongside those of the facies assemblages of Miall (1978) subdivided in the same fashion.

Overall, the CMS appears to fall between the Platte and Bijou Creek types. The Platte type is defined as being deposited by very shallow rivers, or those without marked topographic differentiation. Linguoid, transverse and other sand bars are the dominant depositional structures in an environment dominated by sand grade sediments. This river type will occur on a broad flood plain perhaps equivalent to the distal parts of a large alluvial fan.

The Bijou Creek type is based upon observations made of the river of that name by McKee *et al.* (1967). This environment is dominated by ephemeral streams or catastrophic flash floods which affect extensive areas of the flood plain. Such floods would disrupt the Fm, Fl and Sr facies associated with the flood plain environment, producing numerous intraclasts of mud and silt flakes. In the Lough Guitane deposits, at one of a series of localities on the eastern flank of Crohane (e.g. location 9431), mudstone clasts, and volcanogenic fragments of up to 1 meter in size are commonly observed in an intraformational conglomerate up to 2 meters thick. The large size of the intraclasts provides evidence for the power of the currents involved. This coarse intraformational conglomerate lies at least 300 meters away from the margin of the Bennaunmore lava, and so the large lava clasts must have been carried at least as far, and cannot simply have fallen into place from the channel banks.

The comparative rarity of deep channelling (over a few tens of centimeters deep) is perhaps surprising in view of the ubiquitous

Table 3.1

Classification and Frequency of Sedimentary Lithofacies

	Facies Name		Regional Frequency	CMS[1] Frequency (percent)
	Allen (1963)	Miall (1978)		
Horizontally bedded sandstone		Sh	Common	29.9
Planar cross-bedded sandstone	Alpha	Sp	Common	28.0
Massive structureless sandstone		(Sh?)	Common	15.0
Trough-cross bedded sandstone	Theta	St	Rare	0
Ripple cross laminated sandstone		Sr	Rare	11.0
Scour fill sandstone	Eta	Ss	Virtually Absent	0
Low angle cross-stratified sandstone		Sl	Rare	0
Intraformational Conglomerates		Se	Rare	2.1
Compound cross-bedded sandstone			Rare	3.0
Laminated or massive fine sand, silt & mud		(Fl, Fm)	Fairly Common	14.0
Wave ripple cross-bedded sandstone			Very Rare	0
Epsilon cross-bedding	Epsilon		Absent	0

[1] Cappagh measured section

presence of intraclasts. However, this might in part be explained by the relatively soft, unconsolidated nature of most of the sediments. Miall (1978) also points out that the floods involved in such erosion might completely reorganise the drainage arrangement of the floodplain.

It is not suggested that the Lough Guitane sediments, and the CMS in particular, represent a transitional facies assemblage, but that there were temporal variations in discharge type. Parts of the CMS can be more easily ascribed to a Platte type of environment, while other parts to the Bijou Creek type.

A detailed study of the lithofacies of the CMS and their directional attributes in the following section is seen to support the above hypothesis.

3.8.2 The Cappagh Measured Section (CMS) - Lithofacies (see fig. 3.3)

The basal 38 m is rather incomplete, but the dominance of planar tabular cross bedding suggests a Platte-type of deposition. Palaeocurrents are strongly unimodal from the south or south-east and the cosets may be interpreted as being deposited on the downstream slopes of transverse or linguoid bars. The ill-defined base of a flood deposit occurs at 38.2 m. The deposit itself is apparently structureless, containing large numbers of mud and siltstone intraclasts. It is 4.6 m thick and overlain by 0.5 m of even coarser flood deposit. Two medium sand grade Sh units occur above this with an intervening pebbly Sp unit. The poorly exposed bases of these units makes definitive interpretation impossible, but the Sh units probably represent more distal flood deposits. Thus there are 8.5 m of dominantly Bijou Creek type deposition. The palaeocurrent direction derived from the Sp unit is still from the south-east.

About 8 m of sediments were then deposited by currents of dominantly lower velocity, including 4.7 m of small-scale ripple cross-laminated,

medium grade sandstone with a northward derivation. This is overlain by 5 m of flood deposits including two coarse Sh units and one Se unit. This is followed by a return to Platte type deposition with a series of Sp units and thin fining upward Sh units. The palaeocurrents show a wide dispersal between derivation from the south-east and the north.

There follow three separate flood deposits comprising 5.4 m of coarse horizontally laminated sandstones with pebbles or intraclasts and scoured bases. The uppermost unit is only 20 cm thick, but is rich in mudstone intraclasts.

These are overlain by 15.6 m of rather problematical sediments. They are dominated by horizontally laminated sandstone sequences, usually fining upwards, and sometimes having a scoured base. The base of one typical example occurs at 79.5 m in the CMS. It is scoured, but grades evenly up into 1.2 m of silt and then mudstone without any apparent break in deposition. As discussed before, the basal part of this unit could be interpreted as a sheet flood deposit, while the finer upper part resembles deposition from standing water. Three thin sequences of massive or laminated siltstone with sharply defined planar bases do occur, and these were almost certainly deposited by repeated influxes of fine sediment into standing water or from very low stream velocities. This general sequence of 15.6 m probably represents a slack period of deposition when the main channel was a considerable distance away, and only the terminal parts of flood events affected the area.

Between 88.9 m and 91.5 m occur two Sp units with well developed reactivation surfaces. Palaeocurrent directions are again from the SSE (Plate 3.10).

The following 9 m is again deposited in much quieter flow conditions. Deposition is dominated by horizontally laminated medium grade sandstone

ranging down to massive or laminated siltstone (Plate 3.11). Numerous thin fining upward sequences occur, the thinnest below 5 cm, and therefore not represented in the log. The siltstones also present strong evidence for subaerial exposure, with common dessication cracks. A few thin Sp units occur, some with scoured bases, but most are planar. Palaeocurrent measurements reveal currents directed towards the north-east (three measurements), unique for the CMS, and one to the north-west. The finer grain size, the thinness of the units, and the palaeo-currents displaced well away from the modal directions of north-west and south-east all suggest deposition well away from the main channel with occasional floods causing small scale dunes to migrate across a broad flood plain.

Between 100.4 m and 108.9 m, a series of Sp units outcrop, with some Sr lithofacies in the upper part of the sequence. The first of these sets is 2.8 m thick, coarse grained with intraclasts fairly common, and is clearly complexly cross-bedded as defined in section 3.5 above. The second of these Sp units also displays compound cross-bedding, but is thinner and intraclasts are more common. This sequence is interpreted as a relocation of a major depositional channel across the flood plain whose sediment is derived from the south-east. The thinner Sp and Sr units of the upper portion of the sequence, and ripples in the overlying fine grained facies yield palaeocurrent directions from the east or north-east. These cosets probably represent deposition on the lee slopes of laterally migrating bars in the newly established river system. Again the Platte-type of deposition appears to have taken over.

The following 16.5 m is incomplete, but the dominant exposed lithofacies are fine grained with rare structureless coarser sandstones. This part of the CMS is again interpreted as being deposited well away

from the main locus of deposition on the broad flood plain.

The remaining 17.7 m is initiated by 3.15 m of dominantly planar tabular cross-bedded medium sandstones with southerly directed palaeocurrents. These probably represent an influx of sediment from the north on the most distal parts of an alluvial system, as probably occurs on other previous occasions in the CMS. The top of the CMS is then composed mainly of fine grained silt sequences and rippl ed medium or fine grained sandstones with common dissication cracks. The two palaeocurrent measurements were derived from a pair of Sp sets, and are again from the north or north-west.

3.8.3 The Cappagh Measured Section - Palaeocurrents

The unweighted palaeocurrent rose derived from the 45 measurements made in the CMS can be seen in fig. 3.6. It shows quite a wide dispersal with a possible bimodal tendency. Miall (1973, 1974 and 1976) described techniques for the analysis of palaeocurrent measurements made in logged sections, including the calculation of a moving average azimuth and the moving average variance of the azimuth. It is felt however that the incomplete nature of the CMS, and the unavailability of some current data from poorly exposed cosets makes such a detailed quantitative analysis unwarranted.

The CMS palaeocurrents have been weighted according to set thickness. The resultant rose is presented in fig. 3.5. This treatment exphasises the bimodality of the currents, and also the dominance of N or NNW directed currents over S, or SW directed currents. This conclusion can also be inferred when the palaeocurrent data is treated in groups according to set thickness (fig. 3.10). It is found that the bimodality is entirely due to the thicker cosets, those over 50 centimeters.

Thus the CMS reveals an organised and systematic variation of

lithofacies and their directional attributes. If the overall bimodality was due to a meandering system, not only would a different lithofacies assemblage be expected, but the temporal variation of palaeocurrent direction would be expected to be more random. Published discussions of typical palaeocurrent distributions found associated with low sinuosity stream deposits have indicated that most are characterised by unimodal roses (Potter & Pettijohn, 1977; Long, 1978), therefore a special interpretation of the CMS palaeocurrents is required.

During the deposition ofthe CMS, the area may have been subjected to alternately northerly-directed and then southerly-directed river systems. Each system was quite separate and related to the morphology of the basin which would have been controlled by normal faulting along roughly east-west axes.

3.8.4 Other Logged Sections

The two shorter logged sections can be interpreted in similar terms. Log 9068 is clearly comparable to a Platte type of environment with Sp the dominant lithofacies (fig. 3.11), and rare erosional scours. The twelve palaeocurrent measurements are very strongly unimodal, varying within a segment of only 9^{o}.

Log 9129 represents the migration of sand bars inside a channel, followed by quieter deposition similar to parts of the CMS, on a flood plain well away from the main depositional activity.

3.9 General Summary and Discussion

The analysis of the regional palaeocurrents reveals a bimodal distribution, with currents from the N dominant (fig. 3.4). The weighted palaeocurrent rose (fig. 3.5) is not significantly different except to slightly accentuate the bimodality, and the dominance of southerly directed currents. The regional subdivision according to

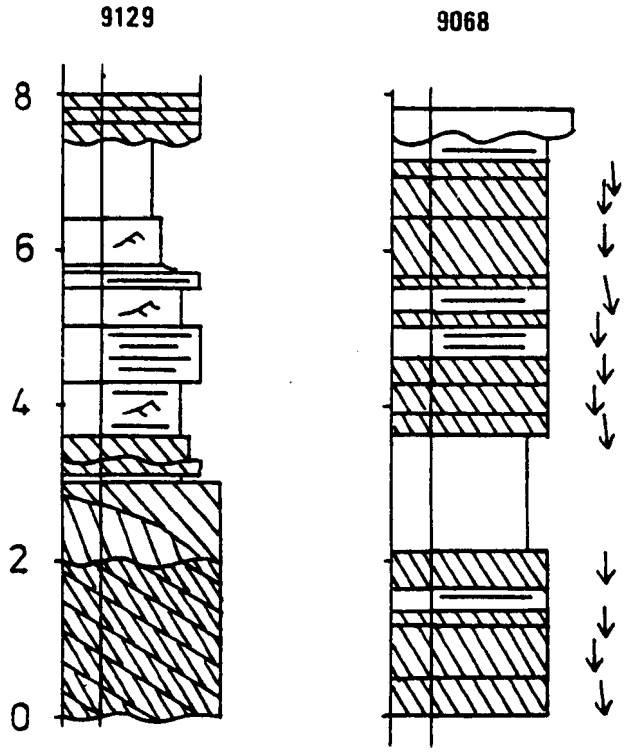

Short logged sections

fig 3.11

stratigraphic position as described above, (fig. 3.4) also seems to suggest a temporal alternation between northerly-derived sediment, and southerly-derived sediment, as two alluvial fans repeatedly overlapped in their distal portions.

However, no significant differences are detected between the two regional data groups subdivided into northerly outcrops and southerly outcrops. In view of the model suggested above, a bias for northward directed currents in the south, and southward directed currents in the north might be expected. The sampling was only undertaken in a narrow zone parallel to the axis ofthe basin, probably near to its centre. Such bias might only be detected if sampling had been possible in a much broader zone. Unfortunately the sediments of the Lough Guitane region under study outcrop along the axis of the Mangerton Anticlinorium which is also aligned east-west, and therefore are overlain by younger sediments both to the north and the south. To illustrate the probable total width of the depositional basin, the nearest conglomeratic deposits attributable to a proximal fan environment are found some 20-25 Km away (without pallinspastic correction) from the axis of the mapping area in the Inch conglomerates of the Dingle Peninsula. Furthermore, the rarity of deeply eroded features, and the sheet-like nature of many of the sandstone bodies lends support to the model of deposition in a distal part of a large alluvial fan similar to that found in the Ebro Basin described above (Friend, 1978).

The provenance of the Old Red Sandstone sediments has been discussed briefly by a few authors (Naylor & Jones, 1967; Shah, 1958; Clayton *et al.*, 1979). Most advocate derivation from upland areas to the north and possibly St. Georges Land in the east. It is suggested that the sources to the north were Precambrian rocks exposed by erosion in the provenance area.

In hand specimen, sandstones deposited by currents from the south appear identical to those deposited by currents from the north. However, the petrographic survey of these rocks is not extensive enough to support this view. It is possible however, in view of their similarity of appearance, that the southerly-derived sediments have been reworked from deposits originally derived from the north.

To summarise, Horne (1970) and Gardiner (1975) have suggested that a simple wedge model (Walsh, 1975) for deposition in the Devonian Old Red Sandstone basin of southern Ireland is untenable. While this study does not seek to support their specific conclusions on the palaeogeography of the basin, it does lend considerable weight to a more complex model. Deposition may well have been controlled dominantly by normal faulting with a throw to the south, along east-west axes roughly aligned with the present southern coast of the Dingle peninsula. However, from time to time downfaulting with throws to the north must have existed some distance to the south of the study area. This would have produced the reworking of sediments suggested above, and the palaeocurrent patterns observed in the Lough Guitane sediments.

CHAPTER 4

Structural Geology

4.1 Folding

Folding in the Lough Guitane area is dominated by the Mangerton anticlinorium (Jukes & Du Noyer, 1861), along the axis of which occurs the highest structural elevation in the area (fig. 4.1). It can be traced through the area south of the Reeks (fig. 2.1) as the Black Valley anticline (Walsh, 1968, p. 20), and further west to the coast of the western end of the Iveragh peninsula as the Kilcrohane anticline (Capewell, 1975). The Mangerton anticlinorium is not a simple anticline, but rather a composite fold of en echelon anticlines and synclines (Capewell, 1975).

In general, the major elements of the anticlinorium are symmetrical, with their axial planes dipping south at about 60° - 70°. However, the enormous variation of resistance to deformation between the terrigenous sediments and the thick lava flows has produced local areas of strong asymmetry, often bounded by cross-faults. The northern limb is near vertical, with numerous small-amplitude asymmetrical "zig-zag" folds whose axial planes dip south at between 60° and 40° (fig. 4.1 and Plate 4.1). The northern limbs of these parasitic folds may be overturned to give southerly dips of 70° or 80°, or rarely even up to 60°.

The southern limb of the Mangerton anticlinorium has an average southerly dip of about 45°. Small-amplitude parasitic folds occur with axial planes generally dipping south at about 70°, and with near-vertical northern limbs (fig. 4.2). This limb of the anticlinorium is locally homoclinal although minor parasitic folds of wavelengths between 20 m and 200 m sometimes occur at the southern edge of thick,

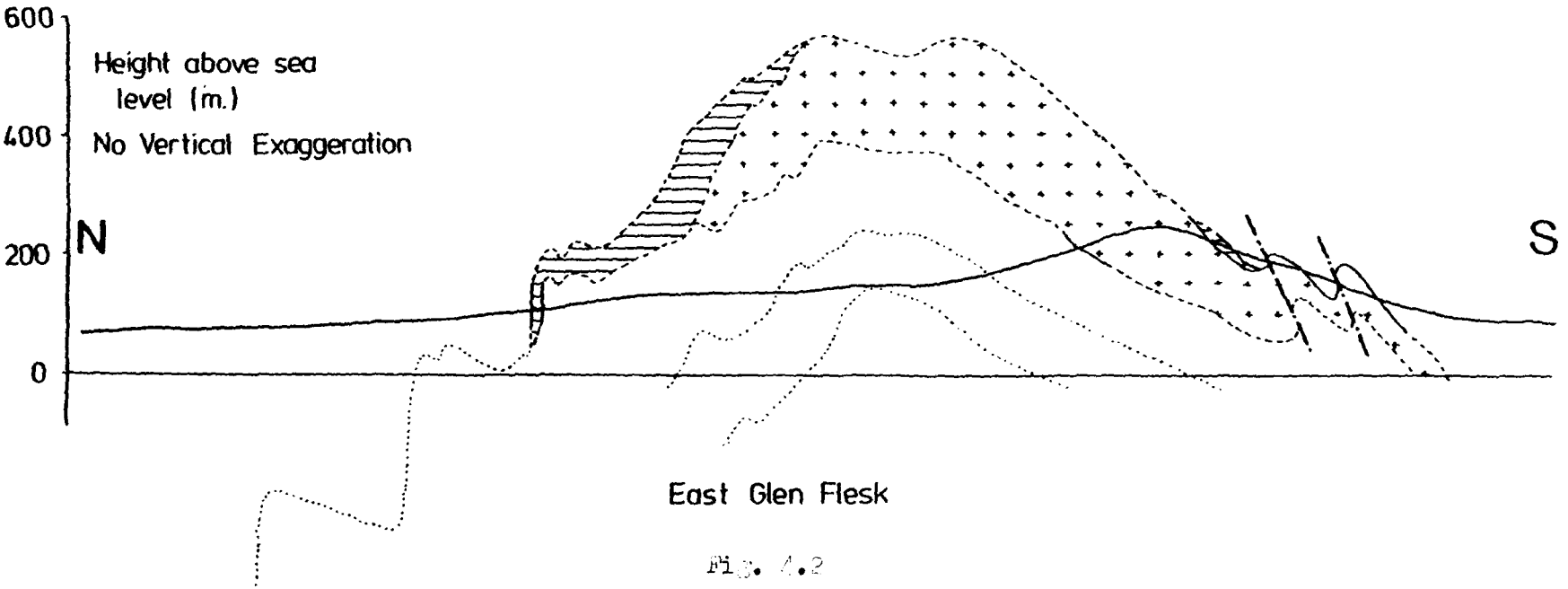

Fig. 4.2

N/S section along the east side of Glen Flesk (see fig. 1.4).

Key to ornamentation: Crosses - Killeen Rhyolite, Horizontal rule - Killeen Tuffs.

resistant units lava flows.

The influence of lithology over fold style can be seen in the upright, almost-isoclinal anticline of at least 100 m amplitude occurring on the east side of the Bare Island fault, near Lough Nabroda (fig. 5.1). This fold occurs where the Bennaunmore lava thins rapidly towards the south. The resistance to folding of the lava appears to have:

a) tightened the anticline to an almost isoclinal symmetry

b) modified the local tilt of the axial plane.

This fold can be traced westwards for about 1.5 Km, over which distance it displays the same fold style.

Folding in areas with a thick volcanic pile, and in particular with the thick Bennaunmore lava, appears to be of lower amplitude, and more subdued.

A traverse across strike from the summit of Bennaunmore southwards to the axis of the Kenmare syncline has revealed a fold amplitude of 4000-4500 m. This is comparable with estimates of the amplitude of the Kilcrohane/Mangerton anticlinorium further west of 2750 m in the area south of the Reeks (Walsh, 1968), and in excess of 3650 m on the west coast (Capewell, 1975). The structural elevation of the crest of the Mangerton anticlinorium above the Carboniferous strata north of the Hercynian "front" in the Lough Guitane area must include the considerable displacements inferred for the reverse faults marking the course of the Hercynian "front" itself, and must be in excess of 5000 m.

Fold axes in the west of the mapping area plunge consistently at about 20^{o} towards the east, although in the Horses Glen they are reduced to approximately 10^{o}. East of the River Flesk (fig. 4.1, in back pocket of thesis Volume 2) fold axes plunge eastwards at between

3^{o} and 5^{o}.

Fold plunges of this magnitude would lead to a structural elevation at the western end of the mapping area of between 4000 and 5000 m relative to the eastern end. This elevation is not observed, and much of it must be eliminated by downfaulting on the major cross-fault system prevalent in the Lough Guitane area. As will be discussed below, most of these faults are oblique-slip faults with both dip-slip and strike-slip elements of motion, the former downthrowing to the west.

The crest of the anticlinorium is broad, often comprising a number of low-amplitude open folds. In the central and western areas the main axis, or crest, is paralleled by another major anticline whose axis lies about 1 Km to the north. West of Bennaunmore the southern limb of this subsidiary anticline is marked by gentle southerly dips of around 10^{o} or 20^{o} corresponding to a zone where the volcanics are most thickly developed (over 300 m). East of Bennaunmore, the southern limb of this subsidiary northern anticline becomes steeper and is affected by parasitic folding. It cannot be traced east of Glen Flesk.

Fold amplitudes and wavelengths sometimes appear to change abruptly across major cross-faults. The best example of this is the Bare Island fault (fig. 4.1), a major oblique-slip dislocation. Such lateral discontinuity in fold style implies that folding and cross-faulting were, at least in part, coeval. This will be discussed below.

The parasitic folds are occasionally observed to change amplitude and die out laterally; e.g. to the west of Foiladuane Lake a short wavelength asymmetrical "S" fold emerges, and increases in amplitude eastwards. The northern syncline has a plunge eastwards of 18^{o}, while the southern complementary anticline has a plunge eastwards of only 5^{o}.

Asymmetrical "drag" folds related to large reverse strike faults have also been observed. One is well exposed on the western wall of the Lough Erlogh corrie to the south of the Lough Erlogh fault. Another smaller "drag" fold occurs to the south of the Fineen fault east of Lough Managh.

Neither Capewell (1975) nor Walsh (1968), in reference to the folding and faulting in their respective areas, could find evidence for more than one compressive phase of deformation. Likewise in the Lough Guitane area no unequivocal evidence for more than one stage of folding can be found. The major long-wavelength structures were probably coeval with the shorter-wavelength parasitic folds.

Other structural sections are presented in figs. 4.3-4.7.

4.2 Faulting

4.2.1 Introduction

Faults in the Lough Guitane area fall into four main categories:

a) Faulting contemporaneous with the volcanism

b) Strike faults

c) Oblique cross faults

d) Transverse cross faults

In general, the transverse cross faults have linear valleys marking their courses, often deepened considerably by glacial erosion, for example, the deep valleys marking the Cappagh fault and the Bare Island fault (Plate 4.2), and the Horses Glen fault. These topographic features have made mapping the transverse cross faults relatively easy. By contrast, since the gross topography, and consequently the outcrop patterns, are strongly aligned parallel to the strike, strike faults are difficult to recognise on the basis of linear topographic features. Their courses must be carefully mapped on the basis of lithology.

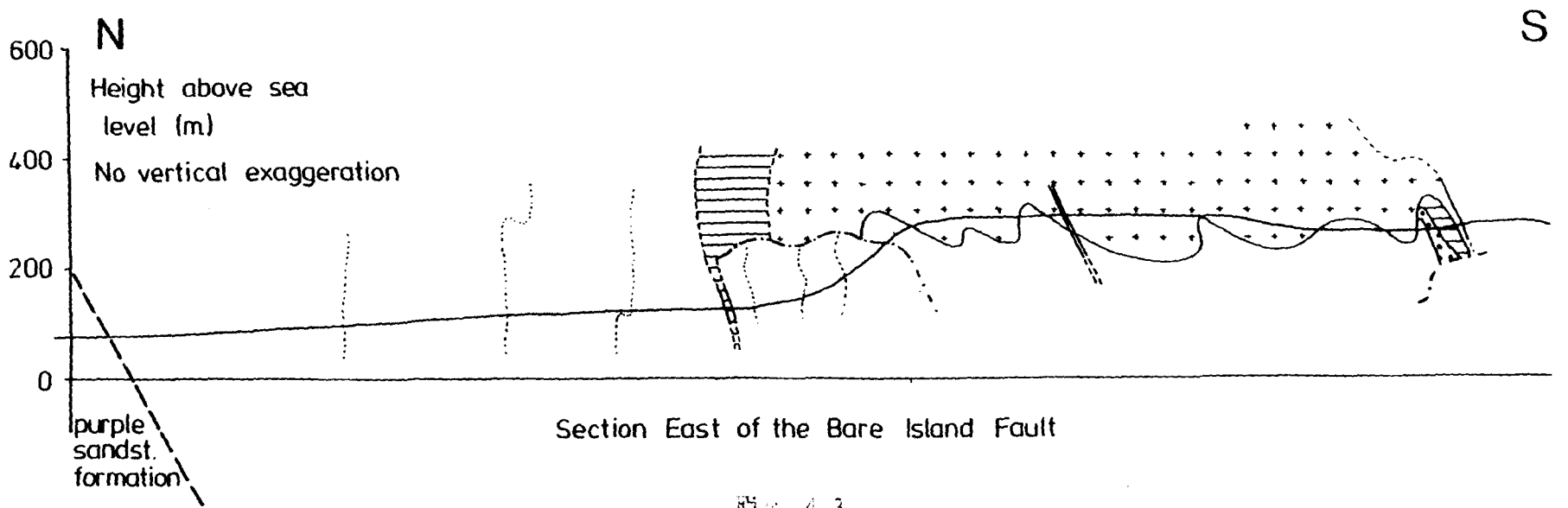

Fig. 4.3

Key to ornamentation: Dots - Lower Boulder Tuff, Horizontal rule - Tuffs, Crosses - Bennaunmore Rhyolite, Dash/Dot lines represent contemporaneous faults.

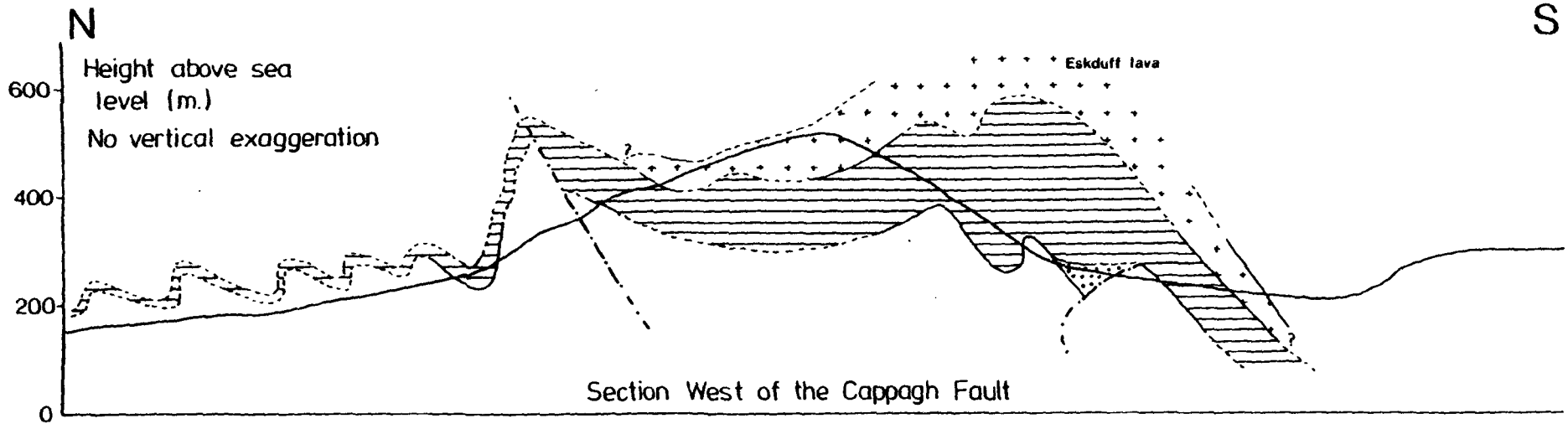

Fig. 4.4

Key to ornamentation: Dots – Upper Boulder Tuff, Horizontal rule – Upper Tuffs, Crosses – Eskduff Rhyolite, Dash/Dot lines represent contemporaneous faults.

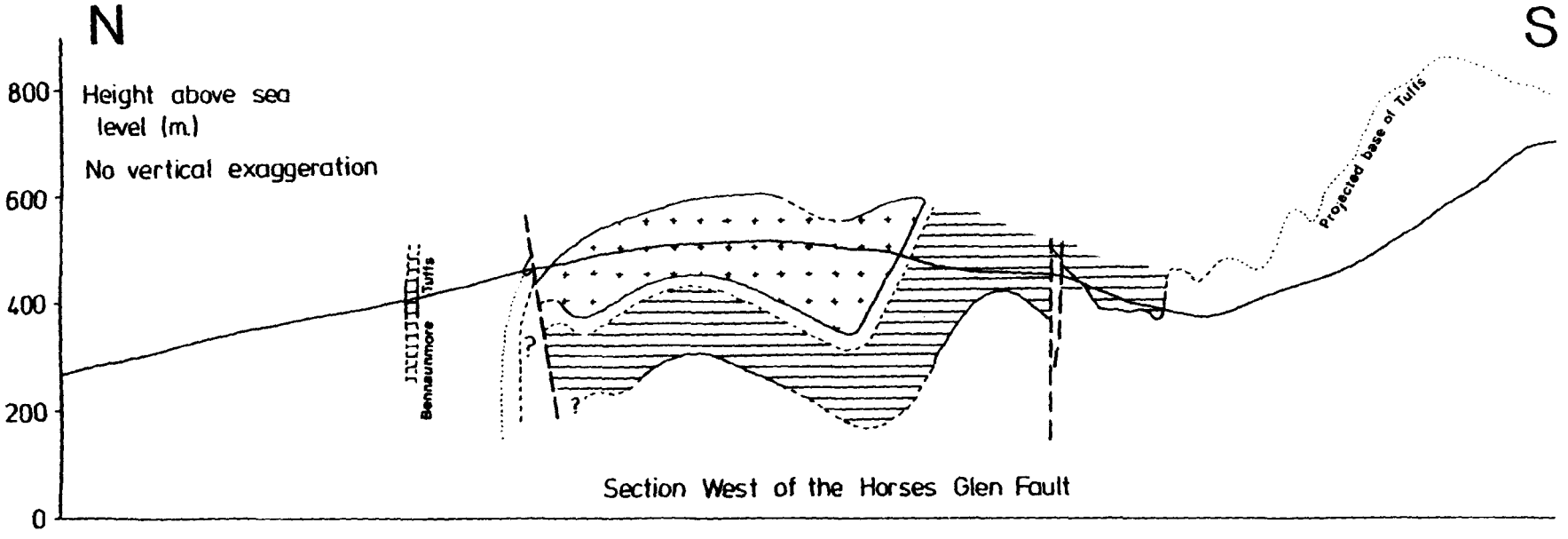

Fig. 4.5

Key to ornamentation: Horizontal rule - Tuffs, Crosses - Horses Glen Rhyolite.

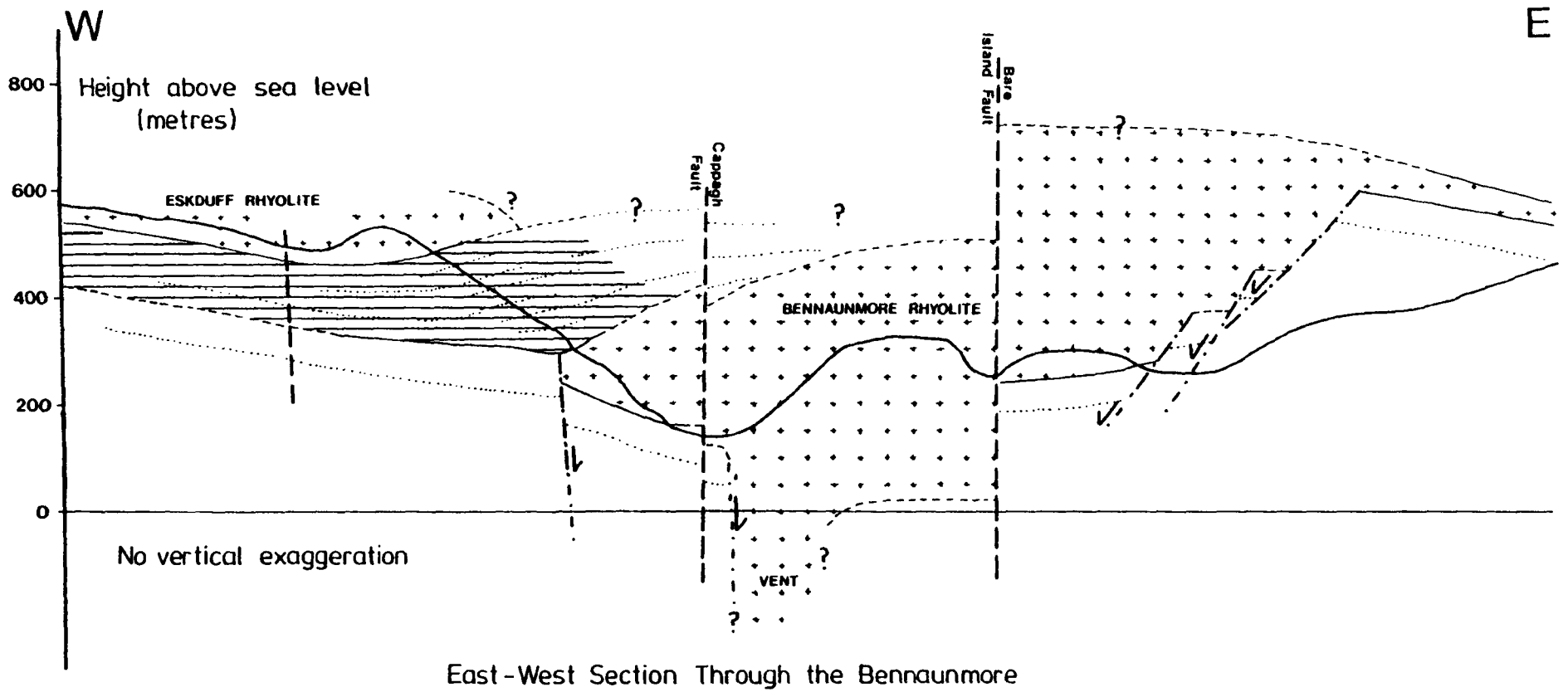

East-West Section Through the Bennaunmore Volcanic Centre

Fig. 4.5

Key to ornamentation: Crosses - Rhyolite lavas, Horizontal rule - Upper Tuffs (dots indicate bedding), Dash/Dot lines represent contemporaneous faults.

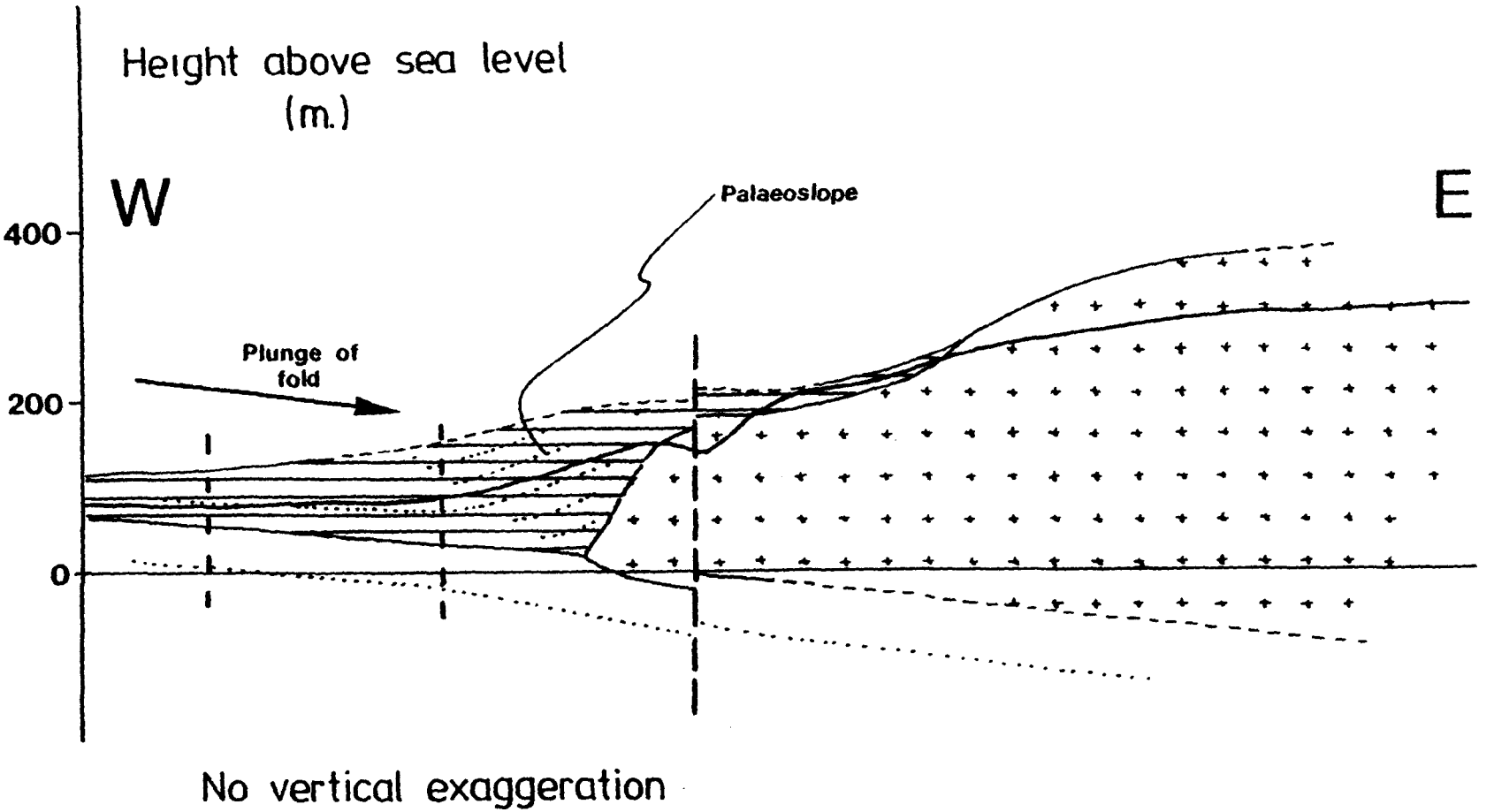

Fig. 4.7 E-W structural section through the SW. corner of the Killeen volcanic centre.

Key to ornamentation: Crosses - Killeen Rhyolite, Horizontal rule - Killeen Tuffs.

Reference should be made to fig. 4.1 (in pocket at the back of Vol. 2) and table 4.1 throughout the detailed descriptions of the faults.

4.2.2 Contemporaneous Faulting

The oldest faulting observed in the Lough Guitane area is contemporaneous with the volcanism. These faults have been deformed by folds of Hercynian age. The nature and significance of this early phase of faulting is discussed in detail in Chapter 5 (Volcanology).

4.2.3 Strike Faults

These faults fall into two categories, strike faults with a reverse sense of motion (compressional), and those with a normal sense of motion (tensional).

4.2.3.1 Reverse Faults

a) Lough Guitane Boundary Fault

This is the largest of this group of faults, and constitutes a major structural dislocation. It is a high-angle reverse fault with a maximum throw of about 2500 metres at its western end, where strata approximately 700 metres above the base of the Purple Sandstone Formation outcrop adjacent to strata of the Green Sandstone Formation about 350 metres above the base of the Lough Guitane volcanics.

The plane ofthe fault dips southwards at between 60^{o} and 70^{o}. The Purple Sandstone Formation rocks to the north of the fault are strongly discordant, with a N/S strike in contrast to the regional Hercynian strike of ENE/WSW. At its western end the Lough Guitane Boundary fault terminates abruptly against a major transverse cross fault, the Bare Island fault, and with which it defines the edge of a major structural block lying to the northeast. (The nature and significance of this block, named the Northeast Fault Block, will be discussed separately later in this chapter.)

Table 4.1

List of faults and their throws

Name	Abbrev.	Orientation	Type	Dip	Maximum Throw (m)*
Bare Island F.	BI	Cross	Obl.-slip (Dex.W)	Vert.	2500 m (north) 200-300m(south)
Cappagh F.	Ca	Cross	Obl.-slip (Sin.E)	Vert.	100/200+
Carrigawaddra F.	Cw	Cross	Obl.-slip? (Dex.W)	Vert.	? /20-60
Central Crohane F.	CC	Oblique	Dip (W)	Vert.	140
Clydagh F.	Cy	Cross	Dip (W)	Vert?	10
Coolcurtoga F.	Co	Cross	?	Vert?	small
Curreal F.	Cu	Cross	Dip? (W)	Vert?	small
Dog Rock F.	DR	Cross	Dip? (W)	Vert?	small
Drominaharee F.	Dr	Cross	Dip? (E)	Vert?	small
Eskduff F.	ES	Cross	Dip? (E)	E80°?	small
Fineen F.	Fi	Strike	Dip-Reversed	Vert.	400+
Foiladuane F.	Fo	Cross	Obl.-slip (Sin.E)	Vert.	100/120?
Garries F.	Ga	Strike	Dip-Normal	S steep	100
Glen Flesk F.	GF	Cross	?	Vert?	?
Horses Glen F.	HG	Cross	Obl.-slip (Dex.W)	Vert.	100/40
Killeen F.	Ki	Cross	Obl.-slip (Dex.W)	Vert.	40/30
Kirrisk Bridge F.	KB	Cross	?	Vert.	?
Loo Bridge F.	LB	Cross	Str-slip? (Dex?)	Vert?	?small
Lough Athooynastooka F.	LA	Strike	Dip-Normal	Vert.	< 50
Lough Erlogh F.	LE	Strike	Dip-Reversed	S70°	350+
Lough Guitane Boundary F.	LGB	Strike	Dip-Reversed	S60-70°	2500
Lough Managh F.	LM	Strike	Dip-Reversed	Vert.	100
North Crohane F.	NC	Strike?	Dip-Reversed	S45°?	small
Rose F.	Ro	Oblique	Str.-slip (Dex.)	Vert.	60
Rusheenmore F.	Ru	Cross	Dip? (E)	Vert?	?
East Sheep Fold F.	SFe	Cross	Dip (E)	Vert?	small
West Sheep Fold F.	Sfw	Cross	Dip (E)	Vert.	100, var.
Stoompa F.	St	Cross	Obl.-slip? (Dex.W?)	Vert.	< 200/?
Rodgers Rock F.	RR	Oblique	Dip (W)	Vert.	30

* For oblique-slip faults, throw of strike-slip component is quoted first

Eastwards, the Lough Guitane Boundary fault is defined by the discordance of the strikes to the north and to the south of the fault, and can be traced on this basis for about 5 Km. The strike to the north gradually becomes aligned with the regional Hercynian strike as the downthrow steadily diminishes until 500 metres east of the River Flesk the two strikes are concordant, and the eastward continuation of the fault cannot be conclusively proved.

The throw of the Lough Guitane Boundary fault is comparable with that estimated for the Muckross-Millstreet fault, (the previously accepted course of the Hercynian "front") at the southeast corner of Muckross Lake to the west, where Walsh (1968) quotes a downthrow to the north of at least 2750 metres.

b) The Fineen fault/Lough Managh fault

These faults occur to the east and west respectively of the dextral strike-slip Horses Glen fault. It seems possible that initially the two faults were continuous before development of the Horses Glen fault displaced them. Thereafter movement probably continued, producing the differing throws now observed in each fault.

The Lough Managh fault has a throw of about 100 metres on the western shore of Lough Managh. Moving westwards it can be followed clearly, in some instances with a visible fault zone about 2 metres wide, as the course of the fault bends west-northwestwards, until it disappears into the poorly exposed drift covered ground to the north.

The Fineen fault can be traced for a short distance from its western termination against the Horses Glen fault eastwards through the eastern slope of the Horses Glen before it disappears under drift covering the summit ridge of Stoompa. The downthrow to the north must be at least 400 metres taking into account the local fold axial plunge of 10° east, and the absence of tuffs outcropping along the ridge south

of the summit of Stoompa. An asymmetrical "drag" fold with a near vertical northern limb about 30 metres wide occurs immediately to the south of the fault.

c) The Lough Erhogh fault

This reversed fault, dipping at approximately 70° to the south, is only clearly demonstrable on the west slope of the Lough Erhogh corrie at the southwestern end of the Horses Glen. Its surface trend suggests that it is obliquely oriented to the regional strike by about 25°, and may have a dextral strike-slip element of displacement. The northward downthrow of the fault is estimated to be at least 350 metres.

To the east the fault passes under the waters of Lough Erlogh and does not reappear on the eastern shores of the lake. No cross-faults have been observed which could have been responsible for the absence of the Lough Erlogh fault here, and therefore it is assumed that the fault passes laterally into, and its displacement taken up by, the anticline observed in the bottom of the valley between Loughs Erlogh and Managh. This assumption is partly supported by the observation that to the west of Lough Managh, folding to the south of the Lough Managh Fault is of shallow amplitude while to the east of the lake, the folding becomes of progressively larger amplitude suggesting a lateral change in the style of deformation.

The steeply-dipping beds immediately to the south of the fault in the west wall of the Lough Erhogh corrie probably represent the near-vertical northern limb of an asymmetrical "drag" fold.

d) Other Minor Reversed Faults

The Bennaunmore, and North Crohane faults are poorly defined reverse faults with small throws. Both may represent dislocations related to the margin of the Bennaunmore lava flow.

4.2.3.2 Normal Faults

a) The Garries Fault

The Garries fault can be traced from Glen Flesk to its termination in the complex of fractures west of Lough Athooynastooka. For much of its course, the strike of this fault is parallel to the regional strike, although at the western end it curves northwestwards until its strike is almost normal to the regional strike. In this western part the downthrow to the south is about 100 metres, where it displaces the transverse cross fault, the Foiladuane fault. In the east the Garries fault is itself displaced by a series of small cross-faults.

b) Other Minor Normal Fractures

These include the Lough Athooynastooka fault, and others at the northern end of the Horses Glen and immediately west of Lough Managh.

4.2.4 Obique Cross Faults

a) The Central Crohane Fault

This fault trends northwest/southeast with a maximum downthrow to the west of about 140 metres where the fault outcrops on the western side of the Carrigawaddra fault, a cross fault which displaces it. To the east of the Carrigawaddra fault the downthrow is only about 20 metres.

b) The Rose Fault

This fault has a dextral displacement of 60 metres. The strike of the fault, where it is observed displacing Bennaunmore Volcanic Centre tuffs, is roughly NE/SW, although further south, feature mapping suggests it may swing round to a more N/S orientation.

c) The Rodgers Rock Fault

This fault is a persistent feature in the Killeen Volcanic Centre,

being traceable by feature mapping for at least 3 Km. It has a NE/SW strike with a near-vertical fault plane. In the south, displacement of the top of the Killeen lava flow suggests a downthrow to the west of 30 metres.

4.2.5 Transverse Cross Faults

These faults fall into two categories.

i) An early set, probably coeval with the large reverse faults described above, with relatively large downthrows to the west, and with a dextral strike-slip component of motion, i.e. they are oblique-slip faults. Their trend is normal to the regional strike.

ii) A late set, possibly related to the tensional normal fault system, with small throws either to the west or the east.

4.2.5.1 Early Cross Faults

a) The Horses Glen Fault

This fault follows the bottom of the Horses Glen for much of its length. It is essentially an oblique-slip fault with a dextral strike-slip component corresponding to a displacement of about 100 metres seen in the displacement of fold axes. The dip-slip component has a downthrow to the west of about 40 metres.

The cross-sections on either side of the fault afforded by the deep valley of the Horses Glen, reveal evidence for the coeval nature of the development of the Horses Glen Fault and the local folding in that both major and minor folds cannot be perfectly matched on either side of the Glen.

b) The Killeen Fault

This fault is best observed where it cuts the lavas and tuffs in the southwest corner of the Killeen Volcanic Centre. Here its surface topographic expression is a deep, sheer sided gully. Exposure on either side of this gully indicates a dextral strike-slip displacement

of roughly 40 metres, and a dip-slip component of about 30 metres downthrowing to the west.. The nature of the fault changes over quite short distances, and the folding on either side is not perfectly matched, suggesting a coeval nature for the two types of deformation. At the northern termination, the fault appears to splay into at least three small fractures

c) The Clydagh Fault

This fault is only observed near its southern termination against the Rodgers Rock Fault, where it throws down to the west the upper contact between lava and sediment by about 10 metres. Despite this small throw, the fault has a marked linear surface gully, which can be traced north across the Clydagh river valley and into the lava outcropping on the ridge to the north.

d) Other Minor Cross Faults

These include a large number of transverse cross faults with uncertain senses of displacement including the Stoompa, Carrigawaddra, Foiladuane, Loo Bridge, Glen Flesk and Kirrisk Bridge faults (see table 4.1).

A large number of minor dip-slip faults also occur in the Lough Guitane area, often with slightly sinuous courses, but with strikes generally normal to the regional strike.

The fault planes are all near-vertical with downthrows both to the west and the east. The throw is usually small, between 5 and 50 metres. West of Glen Flesk however, the West Sheep Fold fault has a maximum downthrow to the east of over 100 metres. Many of these faults, where they can be traced for over a few hundred metres exhibit variable throw, often, as in the case of the West Sheep Fold fault, apparently related to their coeval development with the late normal faults.

Other named faults in this category are: the Eskduff fault, the Dog Rock fault, the Curreal fault, the East Sheep Fold fault, the Drominaharee fault and the Coolartoga fault. Other unnamed groups of faults occur to the east of Lough Nabroda, and to the east of Foiladuane Lake.

4.2.5.2 The Bennaunmore Fault Complex - The Cappagh and Bare Island Faults

The two deep glens on either side of Bennaunmore (Plate 4.2) are the surface features representing two major oblique-slip cross faults, the Cappagh fault, and the Bare Island fault. These two faults define an apparently resistant body which will be called the Bennaunmore Fault Block. The two faults converge to the north, and they meet in a region of complex fracturing about 0.5 Km south of the shore of Lough Guitane.

The Cappagh Fault is sinistral with a dip-slip component downthrowing to the east. The magnitude of throw increases northwards. In the south, where the fault appears to splay into 3 separate fractures, the resultant northward surface displacement of the Bennaunmore Fault Block is about 150 metres. One kilometre north of this, the dip-slip component is at least 200 metres, and the strike-slip component at least 100 metres. Displacement probably reaches a maximum upon merging with the Bare Island fault.

The Bare Island Fault defines the eastern boundary of the Bennaunmore Fault Block. Essentially it has a dextral strike-slip component, and a dip-slip component downthrowing to the west. The throw increases steadily towards the north. In the south, on the shores of Lough Nabroda, the resultant northward surface outcrop displacement of the Bennaunmore Fault Block is about 100 metres. The dip slip component 1 Km north of this is between 200 and 300 metres.

The Bennaunmore Fault Block has effectively acted as a wedge, resisting the structural elevation of the rocks to the west and east. The strike-slip elements of its bounding faults cannot accurately be assessed, and the displacement is probably variable due to the coeval nature of the folding and faulting, where the two faults meet in the north, a "crush zone" complex of faults is observed. Displacements here are impossible to assess, and folds cannot be traced from one "crush fragment" to another from east to west.

North of this "crush zone", the Bare Island fault is inferred to continue to the junction with the Lough Guitane Boundary fault, where the throw of the former increases abruptly. The maximum downthrow to the north of the latter has been estimated to be about 2500 metres at the junction with the Bare Island fault. All of this displacement must be taken up by the Bare Island fault north of the junction because strata of basal Bennaunmore Volcanics age outcrop on the western shore of Lough Guitane. The course of the Bare Island fault north of the junction, is based on the rapid and linear deepening of Lough Guitane immediately east of Bare Island.

Thus the Bare Island fault and the Lough Guitane Boundary fault define a fault block, (to be called the North East Fault Block) structurally depressed relative to adjacent strata by a maximum of about 2.5 Km in the west. The significance of the Bennaunmore Fault Block and the North East Fault Block, and their relation to other geological aspects of the Lough Guitane region will be discussed in section 4.7.1 of this chapter below.

4.3 Cleavage

4.3.1 Introduction

Cleavage is widely developed in the Lough Guitane area, as it is elsewhere in southern Ireland (Walsh, 1968; Capewell, 1975). Slaty

cleavage is common in siltstones and finer sediments (Plates 4.3 and 4.4), but rare in coarser grained sediments, where fracture cleavage is common. Cleavage dips vary greatly according to the grain size of the host rock, but generally range between 40°S and 80°S, with a strike parallel to the regional fold trends.

4.3.2 Cleavage Fanning and Refraction

Both convergent and divergent cleavage fans have been locally observed in the mapping area. Convergent fans are common e.g. the fan illustrated in fig. 4.8a.

Cleavage refraction between beds of different grain size is very commonly observed. For example, in sediments dipping at 85° north, southwest of Lough Garagarry in the Horses Glen, a cleavage developed in a sequence of siltstones dips 80° south, while the weaker, fracture cleavage present in the interbedded medium grade sandstones dips at 43° south.

4.3.3 Stereographic Projections

An equal area stereographic projection of poles to cleavage planes for all the data collected in the course of mapping the Lough Guitane area is presented in fig. 4.8, illustrating the dominance of steeply dipping, southwards directed cleavages.

4.4 Jointing

An extensive system of dilational joints appear to have developed at the end of the late tensional phase of deformation. Some of the master joints appear to be related to the late minor cross faults. Two major groups of joints are present, those parallel to the regional strike, and those normal to that strike.

The columnar jointing observed in the Bennaunmore lava will be described in the Volcanology Chapter because it does not relate to the

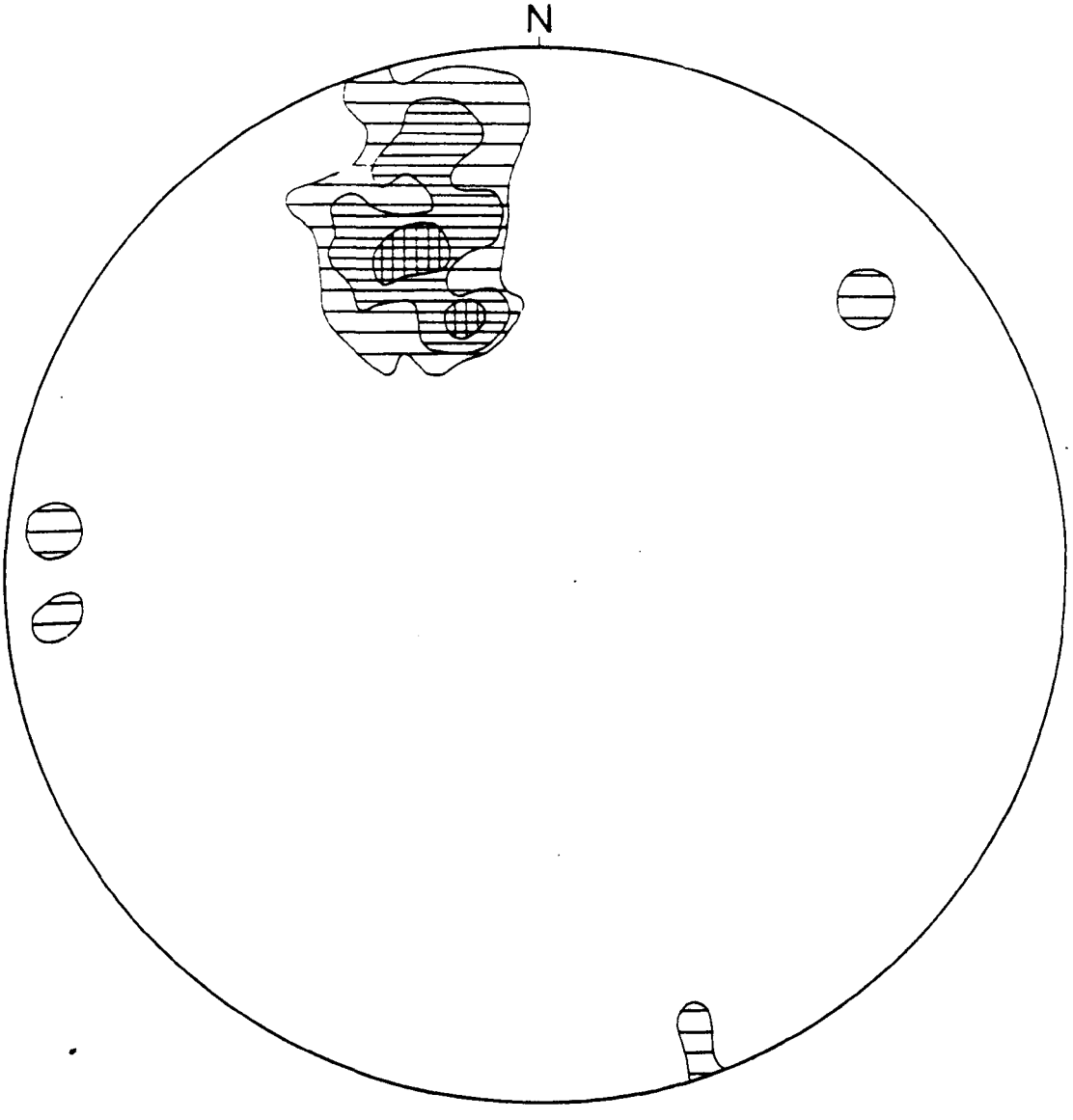

CONTOURED EQUAL AREA STEREOGRAPHIC PROJECTIONS OF POLES TO CLEAVAGE PLANES

1 Measurements per unit area
2 Measurements per unit area
4 Measurements per unit area

Fig. 4.8

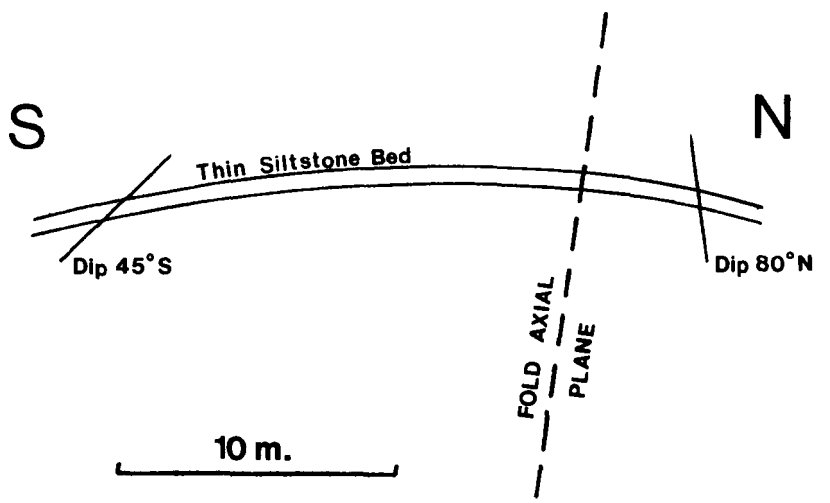

Fig. 4.8a Convergent cleavage fan in folded siltstone bed.

stress fields responsible for the deformation previously described, but to those resulting from cooling of the igneous body.

4.5 Slickensides

Slickensides were rarely observed in the Lough Guitane area, although locally they may be quite common. For example, immediately south of the western end of the Lough Guitane Boundary fault, slickensides occur along fractures dipping south at about 15^{o}. Striations and linear quartz veining indicate a sense of motion aligned north-northwest/south-southeast. Given the local tectonic environment, this implies overriding towards the north-northwest related to the Lough Guitane Boundary fault.

4.6 Tectonic Distortion of Sedimentary Structures

This is commonly observed in sediments of all grain sizes, especially on the northern vertical limbs of folds. Two examples have been chosen to illustrate the internal strain which the sedimentary strata have undergone during folding.

1) Distorted desiccation cracks have been observed near the eastern shore of Lough Managh in strata older than the Horses Glen volcanics at location 9087 (fig. 1.5). Plate 3.8 illustrates the polygonal fracture pattern. Fig. 4.9 illustrates a cross-section of one of the infilled cracks which occurs parallel to the bedding strike, and has a cross-section in the plane of maximum strain.

2) Planar cross-bedded sandstones have been observed on the north-east side of Glen Flesk at location 9671 (fig. 1.5) where the cosets have been tectonically steepened until they intersect the bedding plane at up to 90^{o} (Plate 4.5).

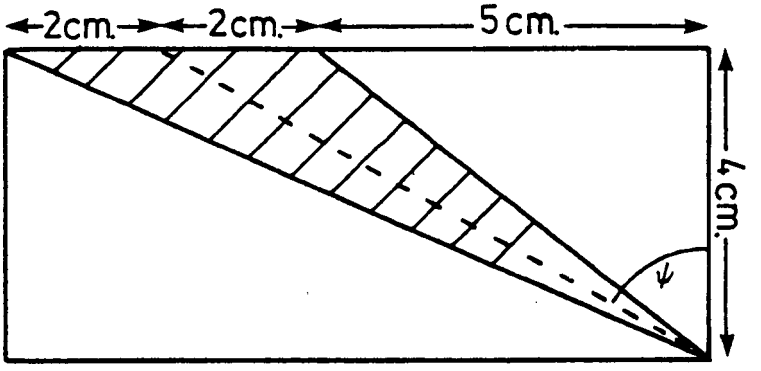

$$\text{Shear strain} \quad \gamma = \tan \psi$$
$$= \frac{7}{4}$$
$$= 1.75$$

Fig. 4.9

Cross-section through a tectonically distorted mud crack. Diagram is in a plane perpendicular to both the bedding plane and the strike.

4.7 Discussion

4.7.1 Local Tectonic Interpretation

Deformation in the Lough Guitane area is influenced by the close proximity of the region to the supposed Hercynian Front lying to the north. Deformation can be subdivided into an early dominant phase of roughly N/S directed compression leading to the structural elevation and overfolding of strata to the south of the Hercynian Front, followed by a late phase of tension, again directed N/S, producing only minor normal faulting. The relative age of events in the Lough Guitane area is schematically summarised in fig.4.10.

After initiation of the major E/W fold structures at the onset of the early compressional phase, reversed strike faulting and oblique-slip cross faulting developed.

Previous research in the Lough Guitane area (see Chapter 2) has placed the Hercynian Front along the course of the Muckross-Millstreet Boundary fault, a large reverse strike-slip fracture, which lies about 0.5 Km north of Lough Guitane. As stressed above, the bounding faults of the North East Fault Block are of a magnitude comparable to that estimated for the Muckross-Millstreet fault to the west (Walsh, 1968). Thus, the west and south margins of the North East Fault Block represent a major discontinuity of structural elevation within the narrow zone immediately south of the presumed course of the "front" through the Lough Guitane area.

Using the criteria submitted by Walsh (1968) for defining the course of the "front" ("... a zone of maximum change in elevation."), the "front" itself might be considered to be offset by the Bare Island fault, and lie, for a short distance, along the western end of the Lough Guitane Boundary fault where the latter exhibits a maximum downthrow to the north. Furthermore, the dips and strikes of strata to either side

Fig. 4.10 Summary of Tectonic Events in the Lough Guitane Area.

(Based on field observations)

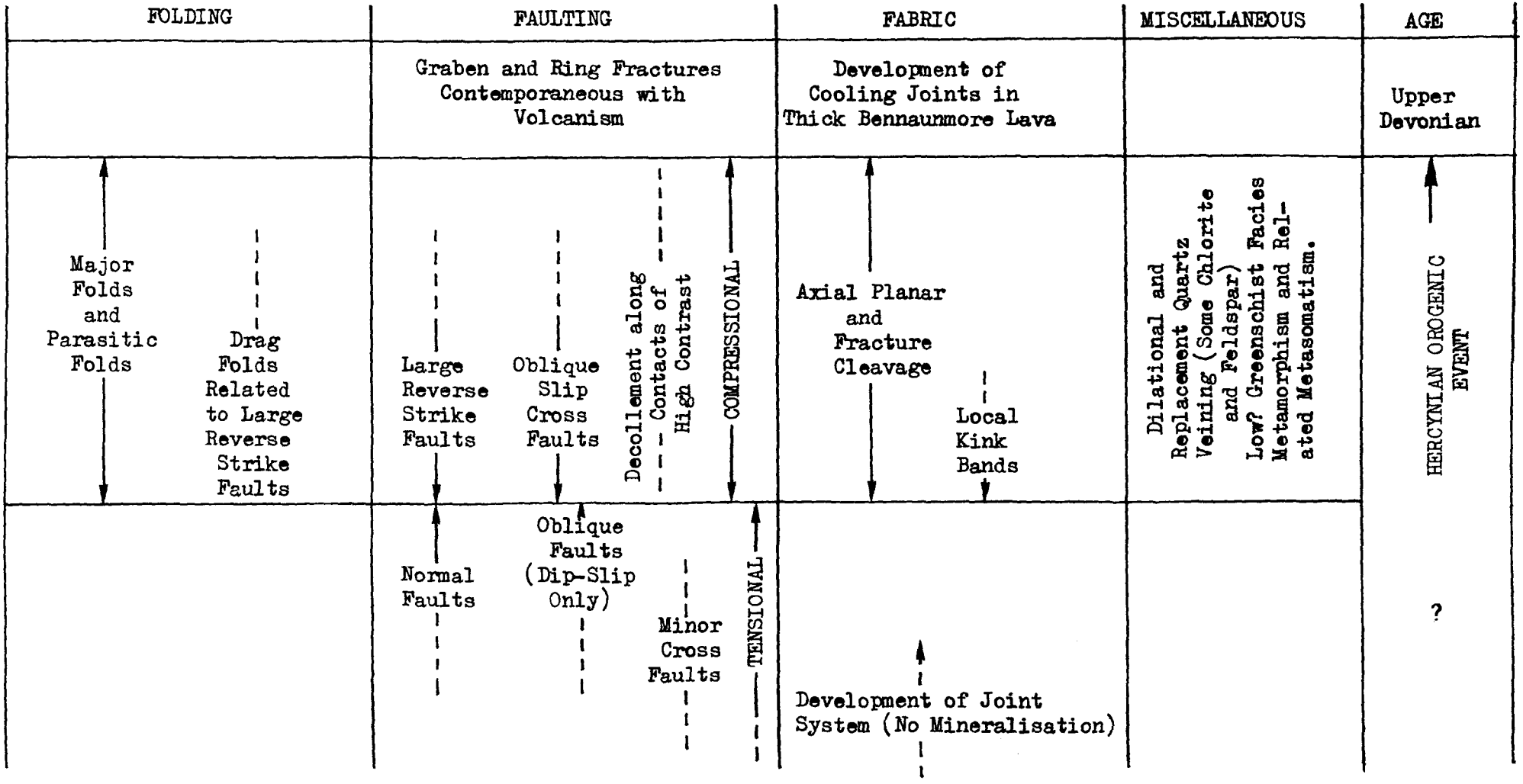

of the Bare Island fault suggest that the throw of this fault increases northwards. It is therefore unlikely that another fault (i.e. the Muckross-Millstreet fault) lying to the north has a throw of a magnitude approaching that of the Lough Guitane Boundary fault.

It is suggested that the major structural discontinuity described above is probably related to the presence of a body, highly resistant to deformation by the N/S compressive stresses, lying beneath the Bennaunmore Volcanic Centre. Detailed mapping has revealed the presence of at least one vent in the southwest corner of the Bennaunmore Fault Block, and most of the volcanic activity appears to have been centred upon this small area of Bennaunmore (see Volcanology Chapter). Thus, it seems possible that an intrusive igneous body lying beneath Bennaunmore is responsible for this structural resistance.

If the Lough Guitane Boundary fault is assumed to dip south at between 60^{o} and 70^{o}, it would lie at between 4.0 and 5.5 Km beneath the vent observed in the southwest corner of Bennaunmore. It is tentatively suggested that the top ofthe intrusive body which fed the Bennaunmore volcanics lies at a comparable depth beneath the present level of erosion.

4.7.2 Regional Tectonic Interpretation

Inspection of the geological map of southwest Ireland (fig. 2.1) reveals that the position of the Hercynian Front in the Lough Guitane area lies anomalously far to the south. In the far west, the front is taken to lie along the north coast of the Iveragh Peninsula (Capewell, 1975). Passing east into the area mapped by Walsh (1968) the front turns south in the form of an oblique fault or faults abruptly cutting off major fold structures with a Hercynian trend of east northeast/ west southwest. This change of course of the "front" is illustrated by the fact that Kilcrohane/Mangerton anticlinorium lies about 4-5 Km

south of the "front" in the Lough Guitane area, but between 15 and 25 Km south of the "front" in the western part of the Iveragh peninsula.

To the east of the Lough Guitane area this folding trend continues as far as Mallow where it becomes more nearly east/west, and thence west-northwest/east-southeast towards Dungarvan on the east coast. A line can be extended east from the north coast of the Iveragh peninsula, with a trend parallel to the fold trends described above until it rejoins the course of the "front" between Mallow and Dungarvan. In the Lough Guitane area the "front" lies about 15 Km south of this line.

The Hercynian front is only marked by reversed faulting where its course swings anomalously southwards. Elsewhere, to the west, and to the east, the change in structural elevation south of the "front" is less intense, and taken up largely by folding.

It is tentatively suggested that a large intrusive igneous body, related to the body postulated in the preceding section, lies at depth beneath much of the Lough Guitane area, influencing the course of the Hercynian "front" on a regional scale. This concept is further supported by the demonstrable need for a large magma chamber beneath the three volcanic centres of the area (Chapters 5 and 6). The E/W lateral extent of this batholith may therefore correspond approximately to the lateral extent ofthe anomalous "front" described above.

CHAPTER 5

Volcanology

5.1 The Bennaunmore Volcanic Centre

5.1.1 Introduction

The following field descriptions will attempt to illustrate the volcanology of the Bennaunmore Volcanic Centre, and in particular, the control over the pattern of eruption and deposition exerted by faulting contemporaneous with the volcanism. The initial descriptions are concerned with two volcaniclastic agglomerate bodies termed the Lower and Upper Boulder Tuffs, and their often complex and noncomformable relationships with the underlying terrigenous sediments and the overlying bedded volcaniclastics and lavas.

5.1.2 Boulder Tuff - A General Description

The Boulder Tuffs consist of rounded to highly irregular sandstone clasts up to 4 metres in diameter, set in a massive tuffaceous matrix composed of varying proportions of unsorted epiclastic and volcaniclastic material. The variations in character of these deposits are determined by the number, size and morphology of the sandstone boulders, together with the presence or absence of angular blocks of acid lava and the ratio of epiclastic to volcaniclastic material in the matrix. Plates 5.1 - 5.6 illustrate 6 types, the detailed descriptions of which appear in their accompanying captions.

5.1.3 The Lower Boulder Tuff

5.1.3.1 The Section East of Lough Nabroda

This, the most easterly outcrop of boulder tuff, can, because of the relative simplicity of the field relations, be used as an introduction. A schematic north-south section through this area shows the outcrops forming the core of a tight upright fold (fig. 5.1). The

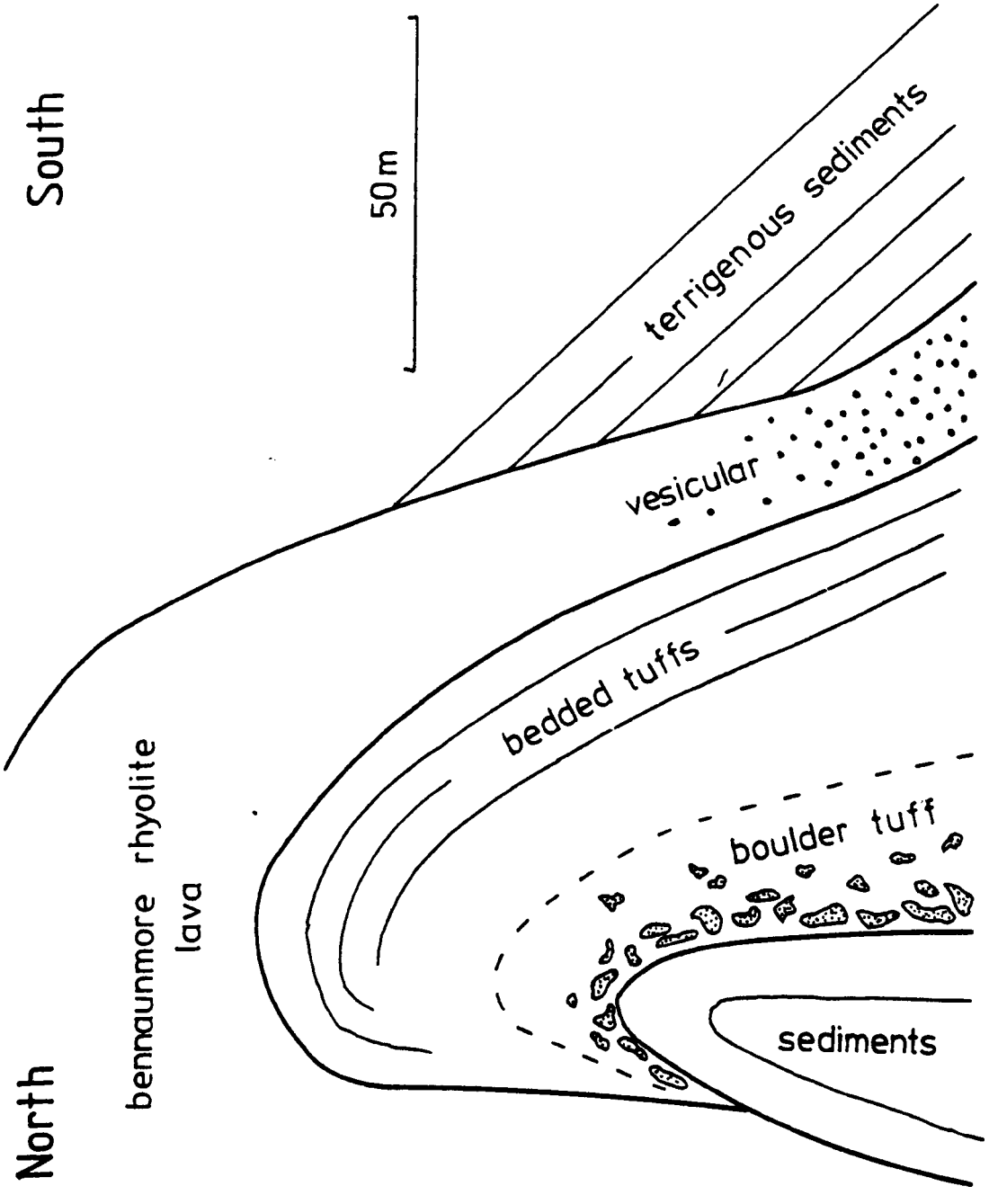

Fig. 5.1 Schematic N/S section through area east of Lough Nabroda.

volcaniclastic sequence underlying the Bennaunmore Rhyolite reaches a maximum thickness of about 60 metres on the southern limb of this fold, and wedges out completely on the northern limb.

The Lower Boulder Tuff is found at the base of the volcanogenic sequence and consists of rounded or sub-rounded sandstone boulders up to 1.5 metres in size, set in a homogeneous matrix of both volcanogenic and epiclastic material - a mixed matrix. The volcanogenic component includes euhedral and broken feldspar crystals, ash, lapilli and some small angular blocks of recrystallised acid lava. The epiclastic component consists of angular quartz sand grains and silt or mud intraclasts up to 1 cm in size. The lowest deposits exhibit a volumetric sandstone boulder to matrix ratio of approximately 1:1. This grades up into very poorly bedded deposits containing progressively fewer and smaller sandstone fragments (5 - 10 cm in size), and finally into well bedded mixed tuffs with low amplitude and low angle scours typical of those found elsewhere in the Lough Guitane area. (The term "mixed tuff" describes a sediment comprised of a mixture of volcaniclastic and epiclastic material. See section 5.1.6.3 for a fuller description.)

5.1.3.2 The South West Bennaunmore Section

The structure of the strata exposed on the western side of Bennaunmore can only be inferred from the structure of adjacent areas along the strike because bedding structures here are usually contorted, and rarely reliable as structural indicators. The geology of this area is shown in fig. 5.2 and a schematic section has been drawn in fig. 5.3. The field relations can be best described by a series of traverses.

Traverse 1 :

The oldest strata are found in a small area adjacent to the Cappagh fault at 'G', and are composed of bedded sandstones and

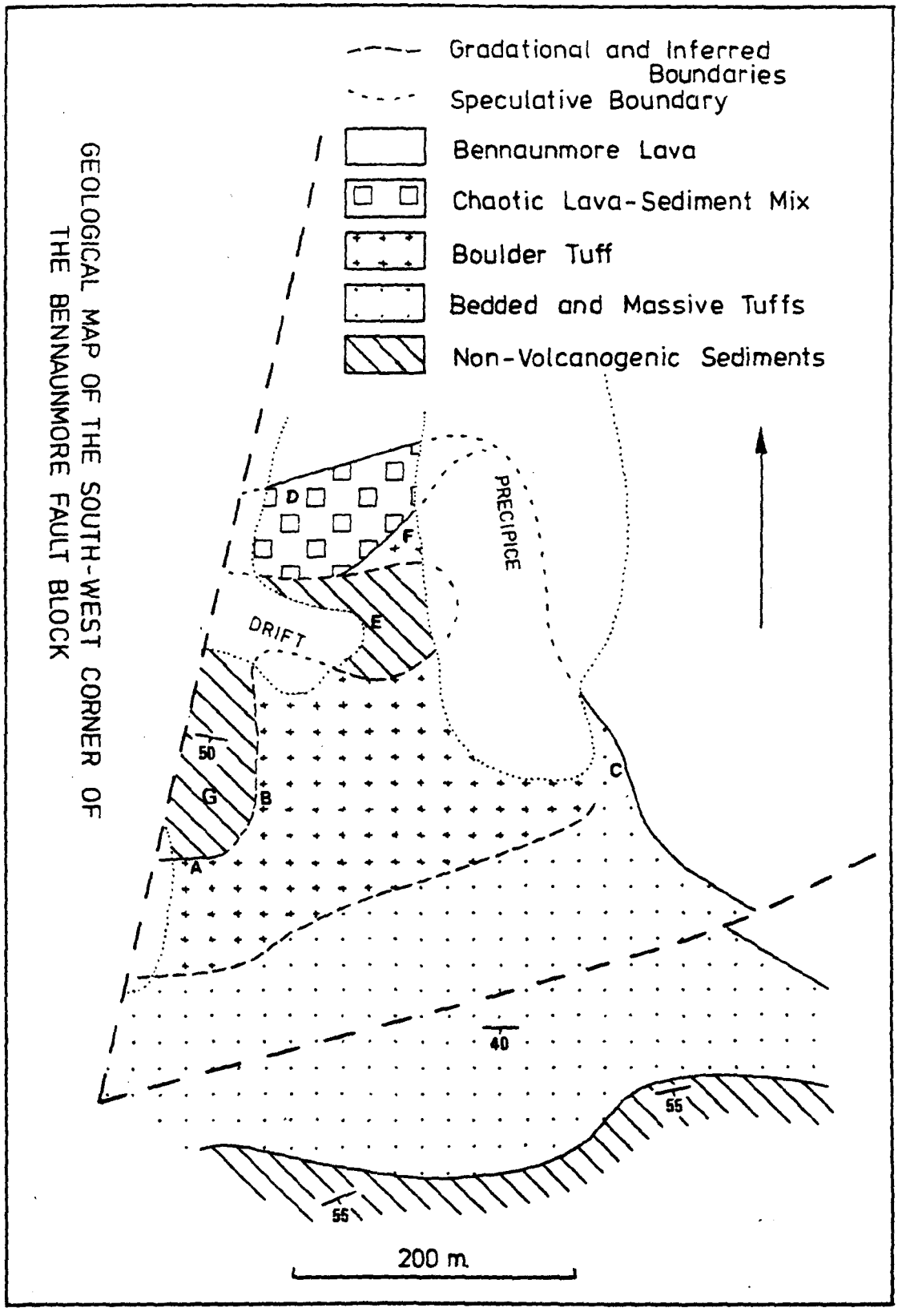
Gradational and Inferred Boundaries
Speculative Boundary
Bennaunmore Lava
Chaotic Lava-Sediment Mix
Boulder Tuff
Bedded and Massive Tuffs
Non-Volcanogenic Sediments
GEOLOGICAL MAP OF THE SOUTH-WEST CORNER OF THE BENNAUNMORE FAULT BLOCK
PRECIPICE
DRIFT
D
F
E
C
B
G
A
50
40
55
55
200 m

Fig. 5.2

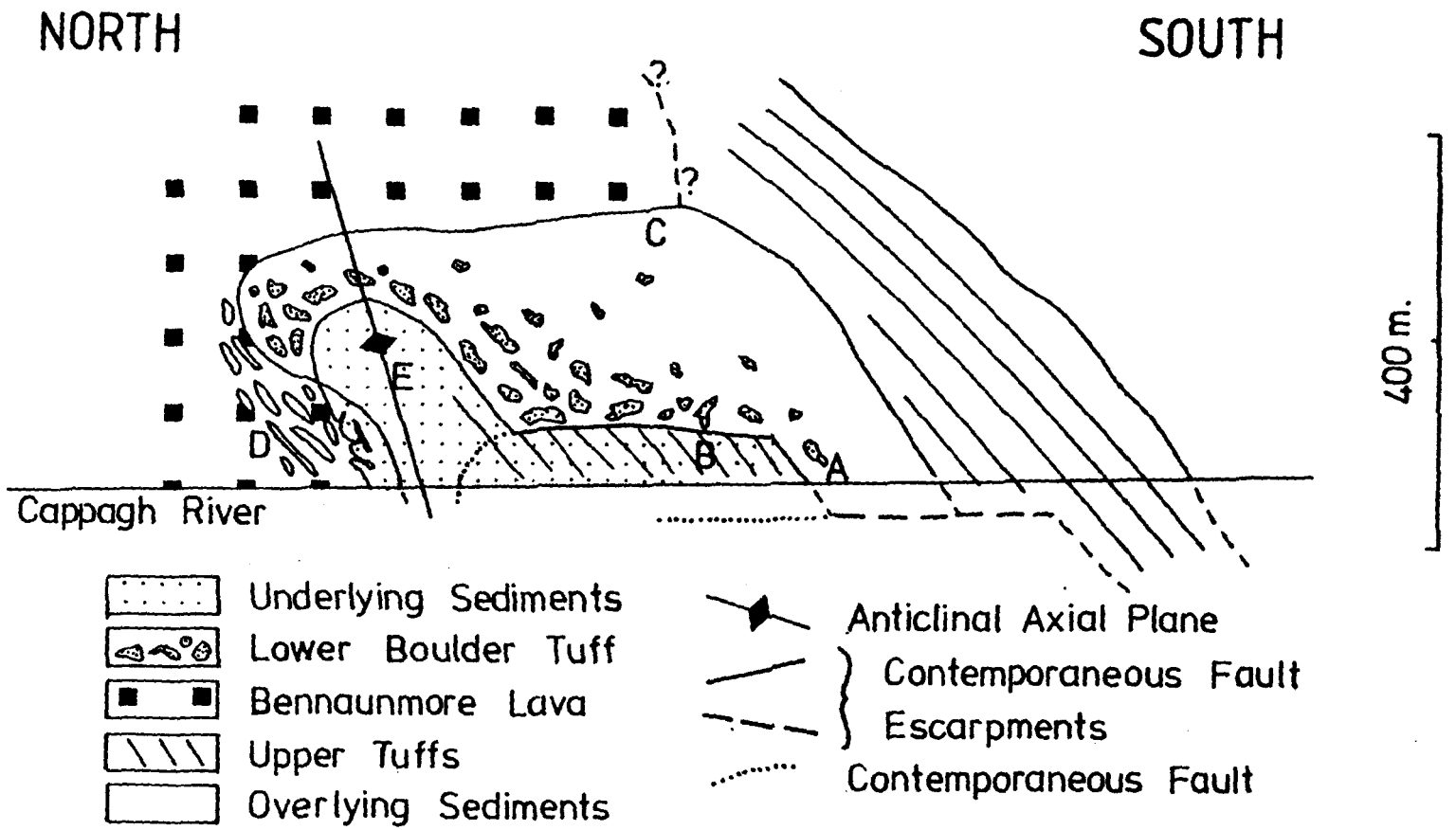

Fig. 5.3 Schematic section through the area shown in fig. 5.2.

siltstones which dip south at about 50°. At the southern extremity of this terrigenous sequence at 'A', they are overlain conformably by massive coarse mixed tuffs with rare sandstone boulders. These are overlain by bedded mixed tuffs which in turn are overlain by terrigenous sediments further south. Assuming a continued dip of about 50°, the bedded tuffs must be approximately 150 metres thick.

The conformable basal contact between terrigenous sediments and tuffs at 'A' cannot be followed east along the strike up the slope of Bennaunmore. Instead, a poorly defined, subhorizontal contact between underlying, south-dipping sandstones and overlying volcanics is traceable northwards from 'B'. These volcanics are chaotic boulder tuffs similar to those found east of Lough Nabroda. The upper part of this area of the Lower Boulder Tuff is transitional to, and passes up into well bedded mixed tuffs dipping south, in a similar manner to the gradational change noted east of Lough Nabroda. These bedded tuffs are also overlain conformably by terrigenous sediments dipping south at about 50°.

Traverse 2 :

A traverse east from 'B' to 'C' (fig. 5.2), a vertical distance of nearly 200 metres, passes through chaotic boulder tuffs. The 30 metres of volcaniclastics immediately underlying the Bennaunmore Lava at 'C' show some internal organisation with a marked upward decrease in sandstone boulder size and frequency. Massive and poorly bedded mixed tuffs are encountered dipping north, subparallel to the base of the Bennaunmore Lava, at approximately 20°.

The contact of the volcaniclastics with the Bennaunmore Lava can be traced southeastwards until just south of the Bennaunmore Fault it swings parallel with the strike. Here the lava is clearly overlain by south dipping bedded mixed tuffs.

The whole area covered by the Lower Boulder Tuff in Fig. 5.2 passes northwards into highly contorted sandstones with generally steep southerly dips. Some outcrops near 'E' show irregular, narrow, apparently intrusive veins of tuff.

Traverse 3 :

At locality 9405 (fig. 1.5) the Bennaunmore Lava is exposed showing columnar jointing and flow laminations. About 200 metres to the south a 2 metre wide zone is encountered dipping steeply south, in which the flow laminations become discontinuous and brecciated. This passes southwards into a zone 50 to 60 metres wide, ('D' in fig. 5.2) which has been interpreted as exhibiting evidence for mechanical mixing between the rhyolite lava and the adjacent sediments. Here, large masses of sandstone appear as elongate rafts up to 20 metres long and 3 metres thick within the lava, and aligned parallel to the margin of the undisturbed lava, their long axes dipping south at between 30^{o} and 60^{o}.

Plates 5.7 and 5.8 illustrate cut sections of specimens taken from near 'D' (fig. 5.2), adjacent to the 2 metre wide brecciated zone of the lava. Here, numerous lensoid and irregular chloritic patches between 0.5 and 4 cm in size were observed set in a sandstone matrix. The patches are often rimmed by a thin (1-2 mm) zone of calcite and contain subhedral feldspar crystals identical to the phenocrysts found in the Bennaunmore Lava.

Plate 5.9a illustrates fine scale intermixing between lava and sediment in which fine ribbons of sand are present in an irregular patch of rhyolite which itself appears to be embedded in sandstone.

Despite this mixing, no field evidence for thermal metamorphism was found in the

terrigenous sediments of this zone.

All these exposures occur on the western steep slope of Bennaunmore, whereas in the valley bottom they are obscured by talus. However, the margin of the Bennaunmore Lava is apparently in contact with a 50-60 metre wide zone composed of a mixture of lava and sediment. A small area of boulder tuff was found around 'F' (fig. 5.2).

5.1.3.3 Summary of the Key Features of the Southwest Bennaunmore Area

a) The concordant relationship between terrigenous sediments and overlying volcaniclastics at 'A' (fig. 5.2).

b) The discordant relationship between the same units at 'B'.

c) The contact between the volcaniclastics and the overlying Bennaunmore Lava at 'C' dips steadily north at about 20^{o}.

d) The Bennaunmore Lava has a thickness of at least 300 metres in the north of the Bennaunmore Fault Block, but wedges out completely in the space of less than 0.5 Km southwards.

e) In the north, at 'D', considerable disruption of the sediments by the lava has occurred in the form of rafting of sandstone and intimate mixing between lava and sediment. Apart from in a small area immediately west across the Cappagh fault (fig. 5.4), this type of feature is unique in the Bennaunmore Volcanic Centre.

5.1.3.4 The Geometry and Interpretation of the Lower Boulder Tuff

The interpretation of the southwest Bennaunmore area is problematical not only because reliable structural data are rare, and few relationships between the lithological units appear to be concordant, but because a critical part is inaccessible.

However, a schematic section from north to south is presented in fig. 5.3 and represents the best interpretation on the data available. These relations can be compared with those along strike already

LAVA FLOWS OF THE BENNAUNMORE VOLCANIC CENTRE

Fig. 5.7

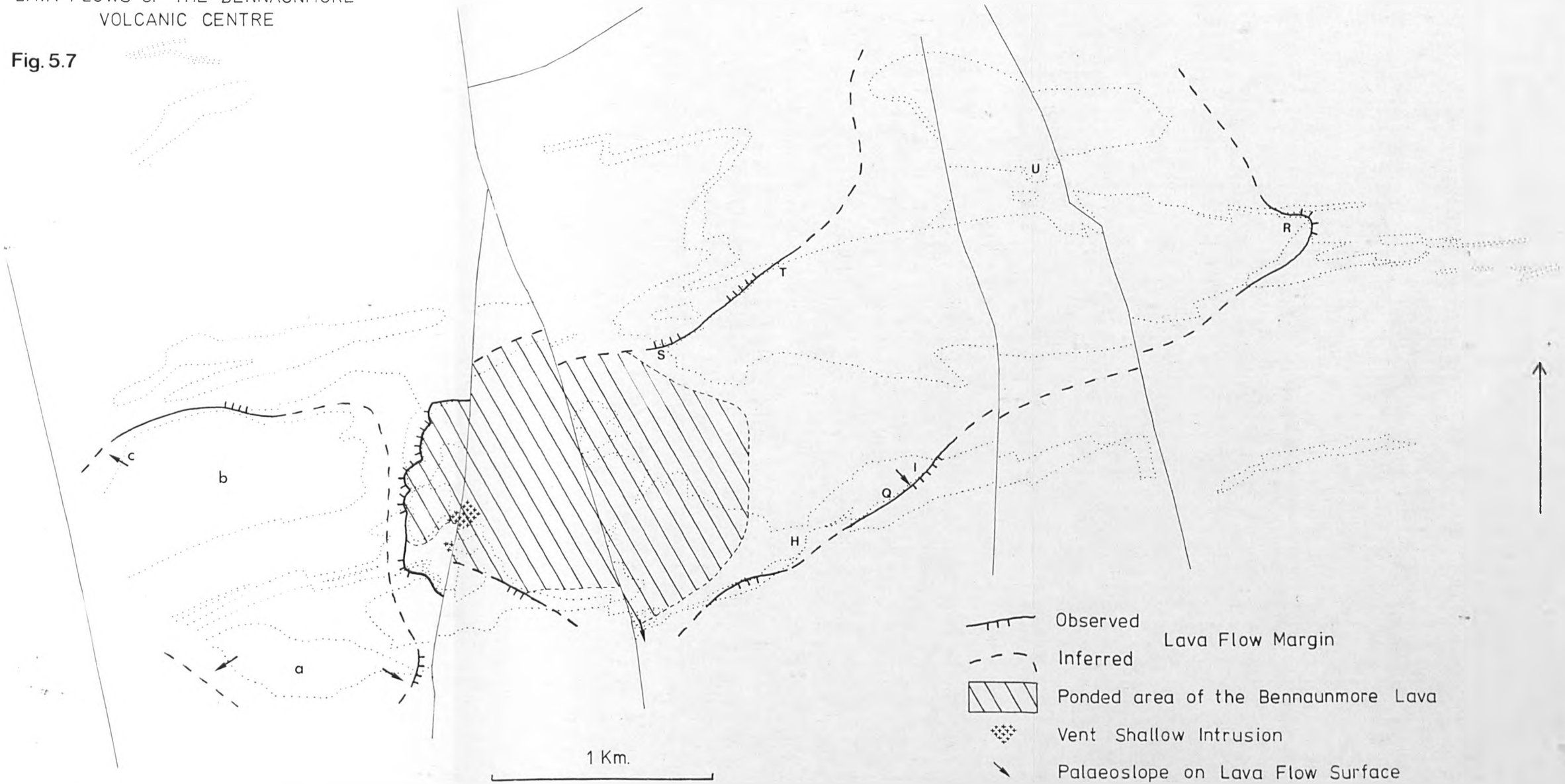

described from east of Lough Nabroda (fig. 5.1) on the assumption that the geological structure of the two areas is similar.

The section afforded by the southwest Bennaunmore area is cut to a structurally deeper level than that of the area east of Lough Nabroda. If only the upper 100 metres of the southwest Bennaunmore section is considered, broad similarities emerge, with the northward thinning unit of the Lower Boulder Tuff overlying terrigenous sediments in the core of a tight anticline, itself overlain by the southward thinning Bennaunmore Lava.

The extra depth of exposure in the southwest Bennaunmore complex reveals a possible vent for the Bennaunmore Lava around 'D', and evidence for faulting contemporaneous with the volcanism. The features at 'A' and 'B' in fig. 5.2 can be interpreted in two ways;

i) that the tuffs at 'B' are intruding the sediments

ii) that the two units are faulted, with a sub-horizontal fault plane.

The gentle northerly dip at 'C' is discordant with those along strike at 'B' and 'A', but is however clearly not intrusive, and is interpreted as the north directed palaeoslope of the top of the Lower Boulder Tuff. This throws considerable doubt on interpretation (i) above. The second interpretation (ii) invokes a faulted contact, the subhorizontal nature of which is highly atypical of the high angle, often vertical faults associated with the Hercynian phase of deformation. Furthermore, it appears that the fault could be responsible, at least in part, for the rapid variations in the thickness of the Lower Boulder Tuff, and as such would be contemporaneous with its eruption. Such a fault might be traceable along strike to the area east of Lough Nabroda, although it probably lies beneath the present level of erosion.

Thus, the Lower Boulder Tuff is revealed to be a wedge shaped body, the geometry of which is controlled by contemporaneous faulting, and a steeply sloping upper surface onto which the Bennaunmore rhyolite lava flowed. Further discussion occurs on page 131.

5.1.4 The Upper Boulder Tuff

West of the Cappagh fault, the order of events presented by the field relations appears to have been different. The base of the Bennaunmore Lava is found at the base of the volcanic sequence, and is overlain by a boulder tuff unit - the Upper Boulder Tuff. This implies both a rapid westward thinning of the Lower Boulder Tuff observed east of the Cappagh fault, and at least two phases of deposition of boulder tuff.

The structure west of the Cappagh fault is similar to that observed to the east, and is dominated by a large, tight, upright anticline which conveniently subdivides the area. In a small valley following the axis of the anticline terrigenous sediments outcrop. To the south the volcanics outcrop along a ridge which runs roughly parallel to the strike through 'D' (fig. 5.4). Here, the Bennaunmore lava, only some 1.5 to 3.0 metres thick, lies conformably on terrigenous sediments in a linear east-west outcrop. It wedges out completely 200 metres west of the Cappagh fault (at 'D' in fig. 5.4) suggesting that its flow margin lies a short distance, perhaps only a few metres, south of the linear outcrop. It is overlain by boulder tuff which passes laterally into massive structureless mixed tuff along the strike to the west.

In the lowest part of this, the Upper Boulder Tuff, rounded or subrounded boulders of sandstone up to 2 metres in diameter lie in a predominantly terrigenous sandstone matrix containing rare angular lapilli or small blocks of acid lava up to 15 cm in diameter. This grades up into boulder tuffs with matrices exhibiting progressively

greater proportions of volcanogenic sediment containing subhedral feldspar crystals up to 2 mm across and angular acidic lapilli. At 'D', the boulder tuff is overlain by bedded mixed tuffs, but erosion has removed them completely nearer the Cappagh fault, such that the top of the Upper Boulder Tuff is not seen.

The structural section (fig. 4.4), and the schematic section (fig. 5.5) illustrate the interpretation of these critical relations south of the anticlinal axis. All along the south side of the ridge, and in the valley to the south, approximately 100 metres of undisturbed terrigenous sediments dip south at between 30^{o} and 40^{o}, overlain further south by bedded mixed tuffs. To the west however, these terrigenous sediments are absent.

Inspection of the ridge crest reveals that the sediments are apparently laterally replaced by the lava-boulder tuff-bedded tuff sequence described above, with an intervening zone of chaotic mixing of sediments and mixed tuffs. In this zone irregular "dykes" of mixed tuff, from 1 mm veins to 2 metres in thickness, were seen penetrating the sediments and vice versa. Blocks of sediments over 5 metres across are also present embedded in a structureless mixed tuff matrix in which the contacts are commonly perpendicular to the laminations in the sandstone.

This area is interpreted as a contemporaneous fault zone (see fig. 5.5). On the basis of thickness variations the fault must have had a downthrow to the north on a plane dipping north at about 60^{o} which has been subsequently tilted into its present orientation, dipping northeast at between 10^{o} and 30^{o}, by the Hercynian deformation. The valley north of the ridge exposes a window through the now subhorizontal contemporaneous fault (around 'C' fig. 5.5), revealing the older terrigenous sediments now folded so that they underlie the fault plane.

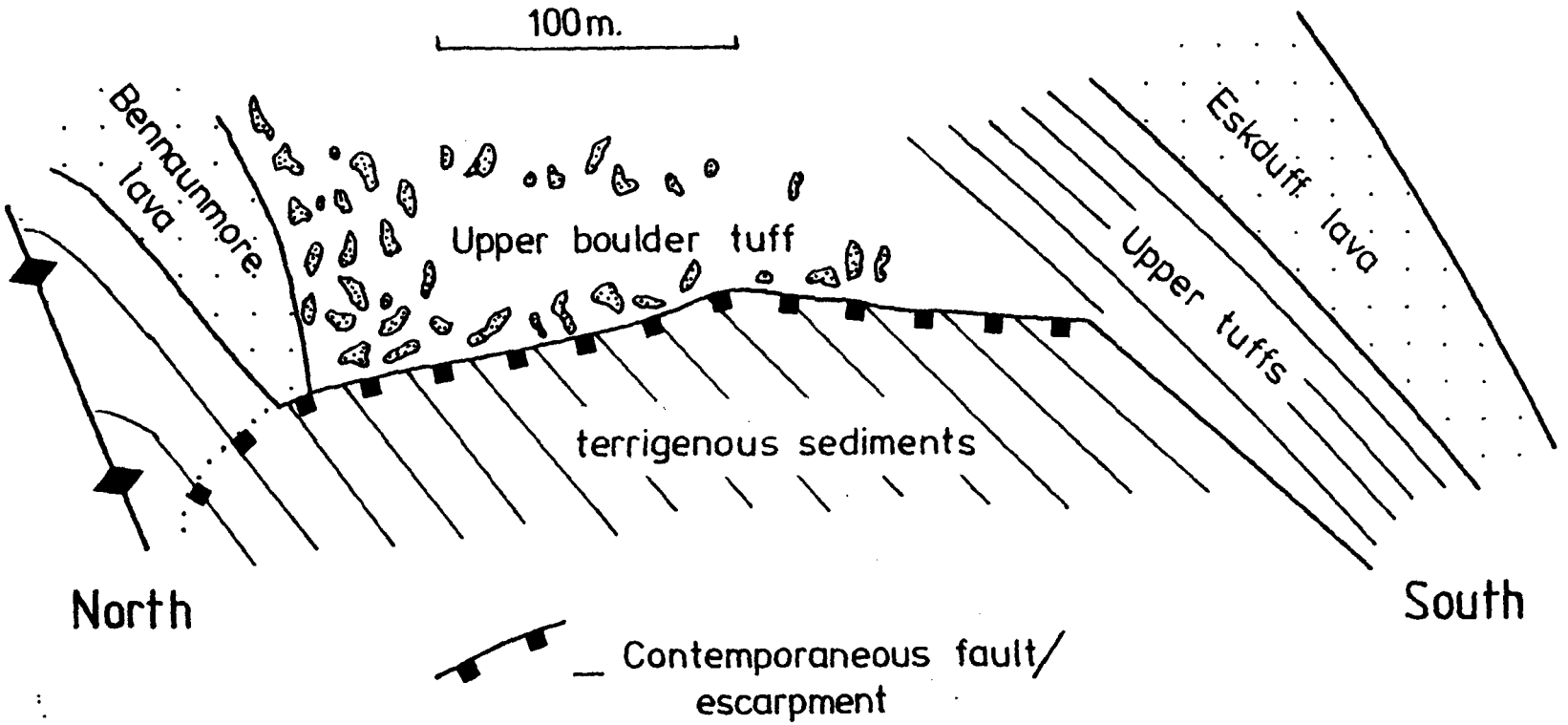

Fig. 5.5 Schematic N-S section through the area west of the southern end of the Cappagh Fault.

To the west the fault is "buried", and nowhere cuts the surface.

As in the southwest Bennaunmore area there appears to be an intimate relationship between contemporaneous faulting and the presence of wedges of boulder tuff.

5.1.5 The Bennaunmore Rhyolite Lava

5.1.5.1 Contemporaneous Fault Controlled Margin Phenomena

a) West of Bennaunmore

To the west of the Cappagh fault and north of the anticlinal axis described in the previous section, the Bennaunmore lava lies conformably on gently folded terrigenous sediments (Plates 5.10 and 5.11). The exceptions are two small areas of lava outcrop, 'X' and 'Y' in fig. 5.4 which will be discussed separately later.

In a narrow zone adjacent to the Cappagh fault the western margin of the Bennaunmore lava appears to coincide with a contemporaneous fault with a downthrow to the east of less than 50 metres. The trend of the fault lies normal to the trend of the Hercynian deformation in a zone of gentle folding. The fault plane is now nearly vertical, having been steepened from its likely original 60^{o} - 70^{o} eastward dip by the eastward plunge of the folds. In Plate 5.12 this plane can be seen as an irregular contact between randomly flow-laminated and partially brecciated lava and a chaotic mixture of varying grades of sandstone in irregular patches.

Bedded mixed tuffs are the only lithology observed to overlie the Bennaunmore lava, and terrigenous sediments the only lithology to underlie it. The outcrops where tuffs were observed to overlie both lava and adjacent sediments in some east-west vertical sections along the lava margin, and the absence of the Bennaunmore lava lying conformably on terrigenous sediments anywhere west of the contemporaneous fault might suggest that the lava filled to the brim the depression

produced by the faulting. However, this may equally be a spurious effect resulting from further and complete erosion of the remaining exposed fault escarpment before deposition of the later bedded volcaniclastics. The suggested sequence of events is presented in fig. 5.6.

The unusual cuspate course in plan view of the lava flow margin is interpreted as the result of slumping along the exposed fault escarpment prior to eruption of the rhyolite lava.

b) East of Bennaunmore

A traverse north from 'CC' (fig. 5.4) on the shores of Lough Nabroda, along the east side of the valley eroded along the Bare Island Fault to 'N', reveals a series of minor folds which repeatedly expose the base of the Bennaunmore lava lying conformably on terrigenous sediments as far as the northern limit of its outcrop. The lava is continuously exposed from its base at 'CC', east of Lough Nabroda to the top of the ridge 0.5 Km northeast, a vertical distance of about 200 metres. There is no evidence for any large faults in this traverse and it must be assumed that the thickness of the Bennaunmore lava exceeds 200 metres. This can be compared with a lava thickness exceeding 300 metres in the Bennaunmore area to the west, estimated from continuous exposure of the lava from the bottom of the Cappagh valley to the summit of Bennaunmore.

Two further important observations concerning the thickness of the Bennaunmore lava east of the Bare Island fault must be emphasised:

1) Immediately east of Lough Nabroda, where the lava is estimated to be in excess of 200 metres thick, the base of the lava lies between 250 and 280 metres above sea level.

2) At localities 'H' and 'I' to the east (figs. 5.4 and 5.7), the lava is estimated to be less than 50 metres thick, and its base lies at about 500 metres above sea level.

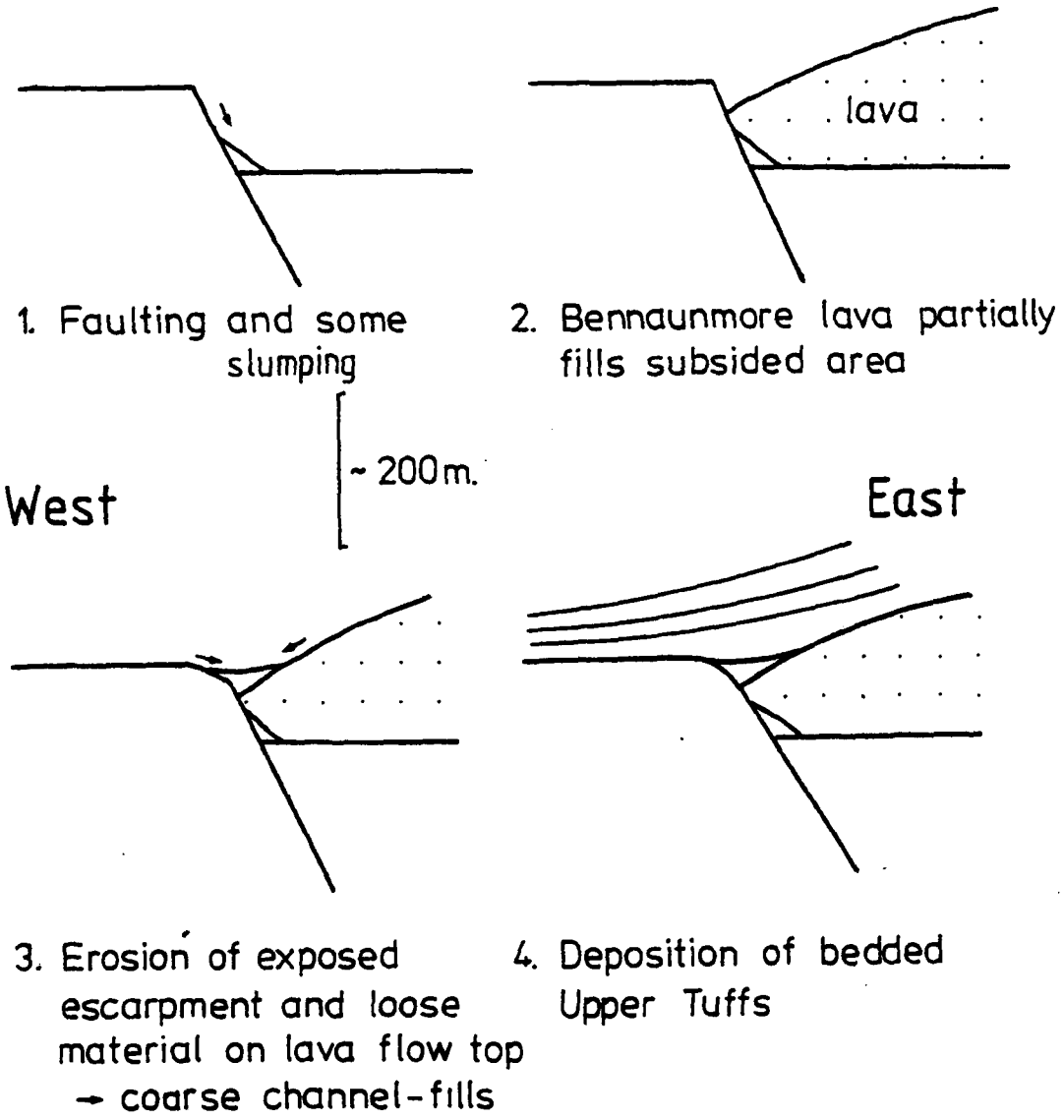

Fig. 5.6 Evolution of the western part of the circular ring fracture (Bennaunmore volcanic centre).

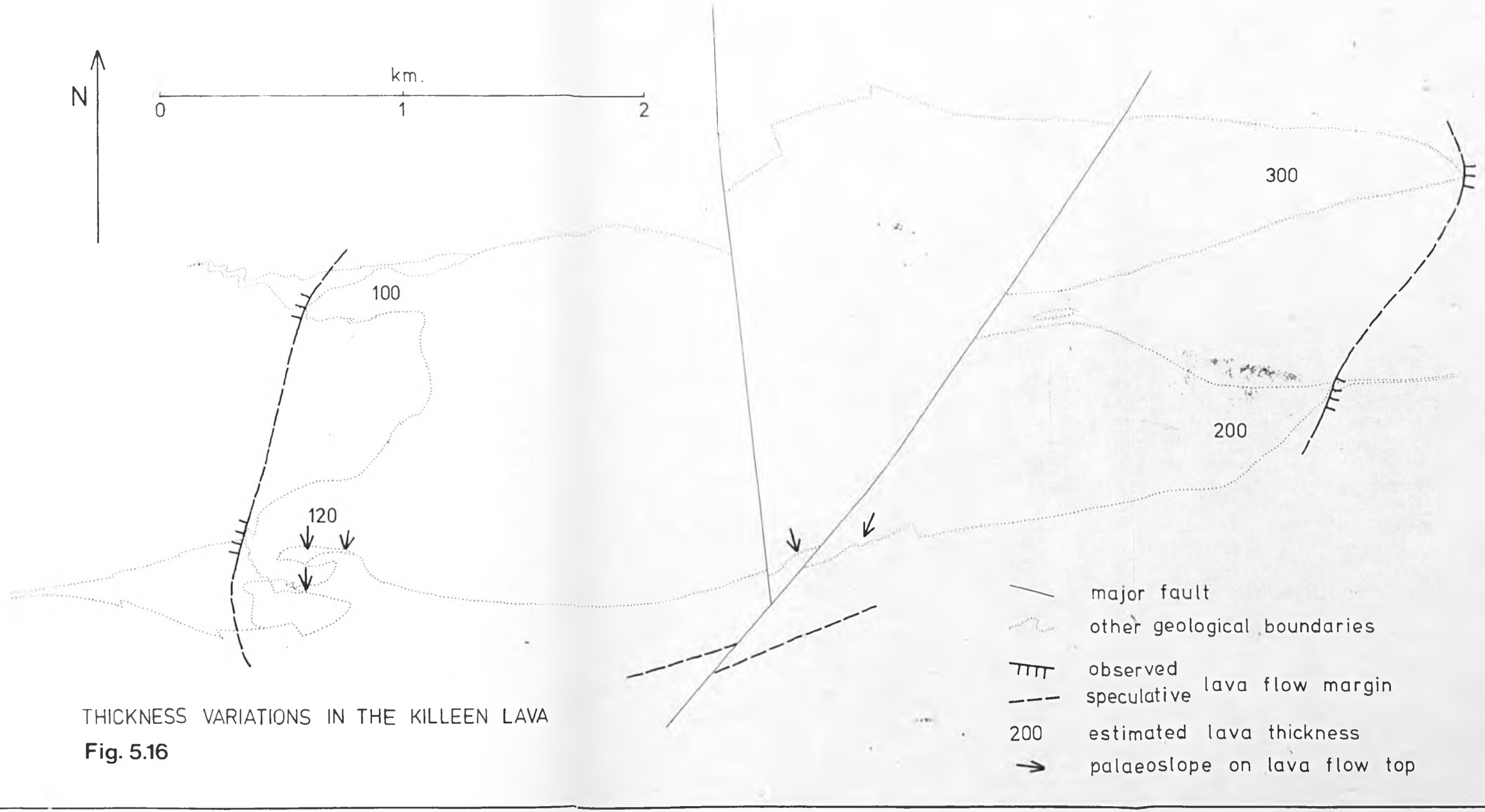

THICKNESS VARIATIONS IN THE KILLEEN LAVA

Fig. 5.16

The two feasible hypotheses to explain these observations are

a) A large fault or series of faults of Hercynian age, with downthrows to the west, displace the base of the lava. The rapid thickness variation is due to doming of a viscous rhyolitic lava near its source.

b) The relationships are controlled by faulting contemporaneous with the volcanism.

Examination of the area indicated a general continuity of structural features, and the presence of only one small fault with a downthrow to the west of under 5 metres. No evidence was found for a large displacement of over 100 metres.

At locations 'J', 'K' and 'L' (fig. 5.4) a series of roughly north-south vertical contacts between terrigenous sediments to the east and lava to the west are present (Plate 5.13). The base of the Bennaunmore lava between 'L' and 'J' is displaced up to the east in a series of 3 steps totalling about 100 metres. From 'L' eastwards the base of the lava continues to be discordant with the underlying sediments (Plate 5.14) resulting in a further elevation of the base of the lava above sea level of almost 100 metres.

The trends of the vertical contacts described from 'J', 'K', and 'L' can be traced into the sediments underlying the lava to the north, as zones of distortion and brecciation. Detailed descriptions of the characteristics of these zones occur alongside plates 5.15-5.18. The disturbance of the sediment seems to have occurred when they were soft or only semi-consolidated. The style of deformation is highly irregular and atypical of brecciated zones attributed to the much later Hercynian tectonism, in which quartz veining is ubiquitous.

Another linear zone of "soft brecciation" was also observed further east at 'M' (fig. 5.4). All of these linear zones converge towards the north, forming a single zone, and are interpreted, as in

areas further west (e.g. the western margin of the Bennaunmore lava) as being related to faulting contemporaneous with the volcanism. The vertical contacts are interpreted as surface fault escarpments existing prior to the eruption of the Bennaunmore lava, and the soft brecciation as near surface fault zones.

The trend of the contemporaneous faulting is inferred to swing westwards as the fault planes are folded to lie near horizontal in the steep northerly dipping beds north of 'N'. (Also see structural section in fig. 4.3). The base of the lava at N dips gently south at about 30^{o}, and about 30-40 metres north of this a major fold axis is encountered with a steep northern limb. Thereafter near vertical dips are present for over 500 metres. The only volcanogenic deposits are encountered at 'P' (fig. 5.4) where under 5 metres of mixed tuffs occur wedging out to the east. This compares with over 200 metres of mixed tuffs exposed in the adjacent Bennaunmore fault block, where the contemporaneous faulting is not exposed at the surface. Between 'N' and 'P' the fault zone has been removed by erosion.

5.1.5.2 Other Margin Phenomena

East of the area described in the preceding section the base of the lava lies conformably on terrigenous sediments, and is exposed on either side of the crest of the Mangerton anticlinorium. To the south, the upper surface of the lava lies parallel to the strike, and is overlain by thin mixed tuffs and then terrigenous sediments dipping south at about 50^{o}. On the southern limb of a small parasitic fold the lava is absent suggesting that its margin lies only a few tens of metres south of the present outcrop line.

From 'Q' (fig. 5.7) eastwards to where the lava wedges out, a highly brecciated facies is developed (Plate 5.18a). A 10 to 15 metre high south-facing outcrop surface (location 'I') sloping southwards at

70^{o}-80^{o} is thought to represent the exhumed sloping margin of the Bennaunmore lava in which terrigenous sandstone is seen infilling spaces between the lava blocks. The overlying mixed tuffs and sediments, which dip south at only 50^{o}, are effectively banked up against the autobrecciated flow margin. East of this locality the Bennaunmore lava does not outcrop on the southern limb of the anticlinonium, and the margin of the lava is assumed to continue with an eastnortheast trend until it is again encountered at 'R' (fig. 5.7) on the northern limb where the field relations suggest that it turns northwards.

The northern flow margin of the lava is clearly traceable between 'S' and 'T' (fig. 5.7), but further east its coarse can only be inferred.

5.1.5.3 The Source Vent for the Bennaunmore lava

The Bennaunmore lava has been observed outcropping in two small areas on the west side of the Cappagh fault, well below the stratigraphic base of the main lava outcrop (locations 'X' and 'Y' in fig. 5.4). The single outcrop at 'X' lies approximately 10 metres below the projected base of the lava, but has an uncertain relationship with the adjacent outcrops of terrigenous sediments. The group of outcrops around 'Y' occur in a small gorge out by the Cappagh River and lie between 40 and 50 metres below the base of the lava flow.

In contrast with the steep faulted margins of the Bennaunmore lava described in section 5.1.5.1, in which lava and sediment are only slightly mixed along the contact, the boundaries between lava and sediment at 'Y' are gradational and show abundant evidence for intimate mixing. The zone of mixing is between 2 and 10 metres across and exhibits a variety of textures, some of which are similar to those described from the lava-sediment contact on the eastern side of the Cappagh fault ('D' in fig. 5.2). Narrow laminations of sandstone

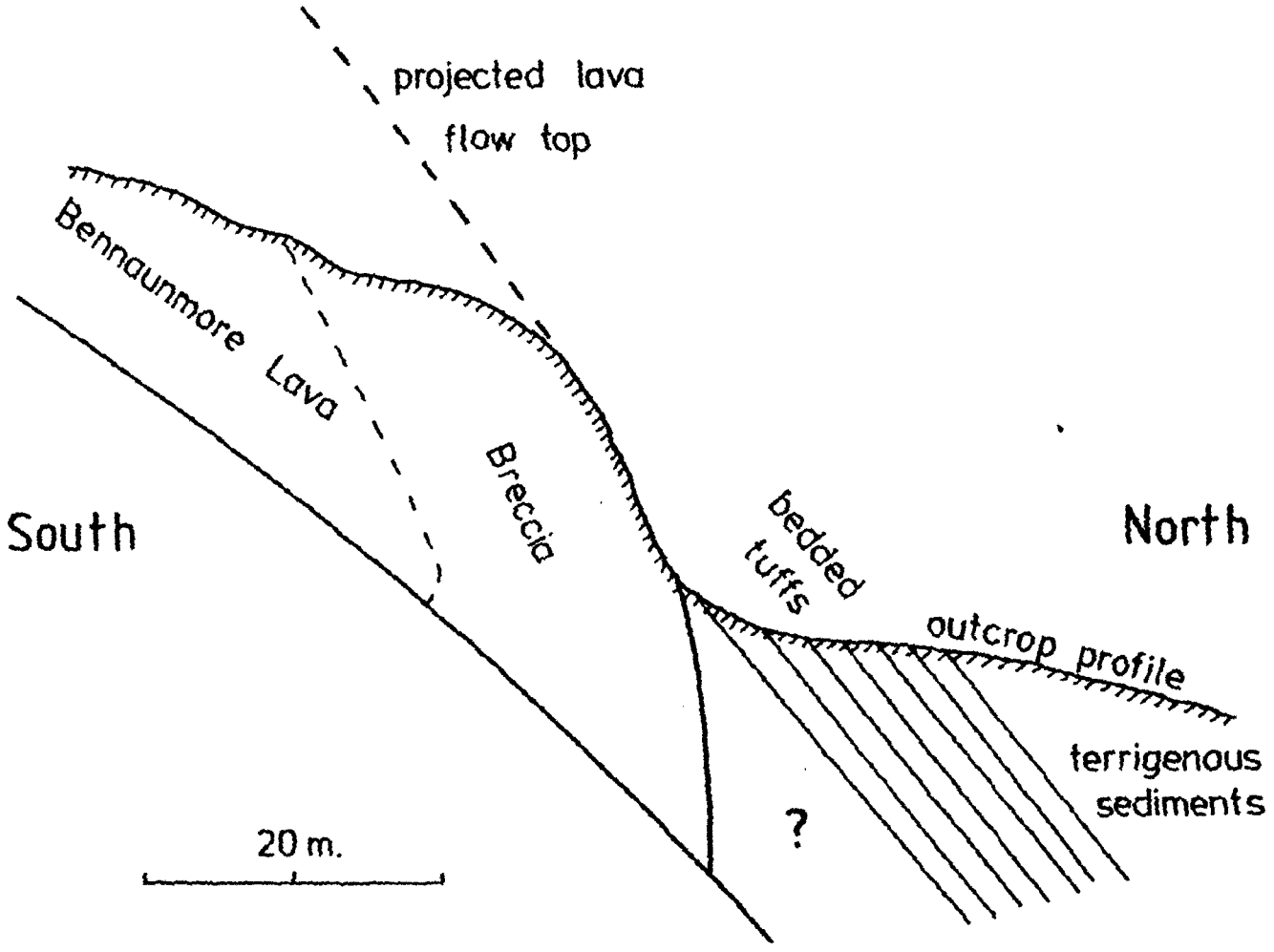

Fig. 5.8 N-S section through the southern margin of the Bennaunmore rhyolite lava at 'I' (fig. 5.7).

between 2 and 20 cm in thickness are present in the margin of the lava and lie parallel to the flow laminations of the lava. The sandstone laminations may extend for over 2 metres and have an irregular or wavy outline.

Close inspection of the area around 'Z' (fig. 5.4), 100 metres north of 'Y' suggests that the lava outcropping immediately adjacent to the Cappagh fault is intrusive. Fig. 5.9 illustrates schematically a north-south section through the area. Quartz veining is a common feature especially in the sediments lying in the contact zone (Plate 5.19) while there is some evidence for gradational contact zones between lava and sediment, sharp contacts were also observed (Plate 5.19). However, the sediments south of 'Z' are devoid of sedimentary structures and sometimes possess a peperitic texture with large numbers of angular and irregular fragments of lava from 1-2 mm up to 2 or 3 cm in size (fig. 5.10A). They have been almost entirely silicified, and remnant feldspar phenocrysts are usually only observed in thin section.

To the north of 'Z', the near-vertical contact passes northwards into a perfectly conformable relationship between undisturbed sediments overlain by the lava. It seems likely that the intrusive relationships described from the area immediately east of the Cappagh fault (section 5.1.3.2) are related to the similar lava-sediment relationships described above. It is further concluded that all these relationships, both west and east of the fault, represent the near surface margins of the vent which fed the Bennaunmore Lava. Only the uppermost 50 metres of the vent, which in plan view appears to have been irregular in shape, is exposed. Evidence for offshoots or tongues of lava intruding the margins of the vent occur at 'X' (fig. 5.4). Such complexity, and the variability of the physical properties of the near-surface sediments probably accounts for the varied types of lava-sediment interaction observed.

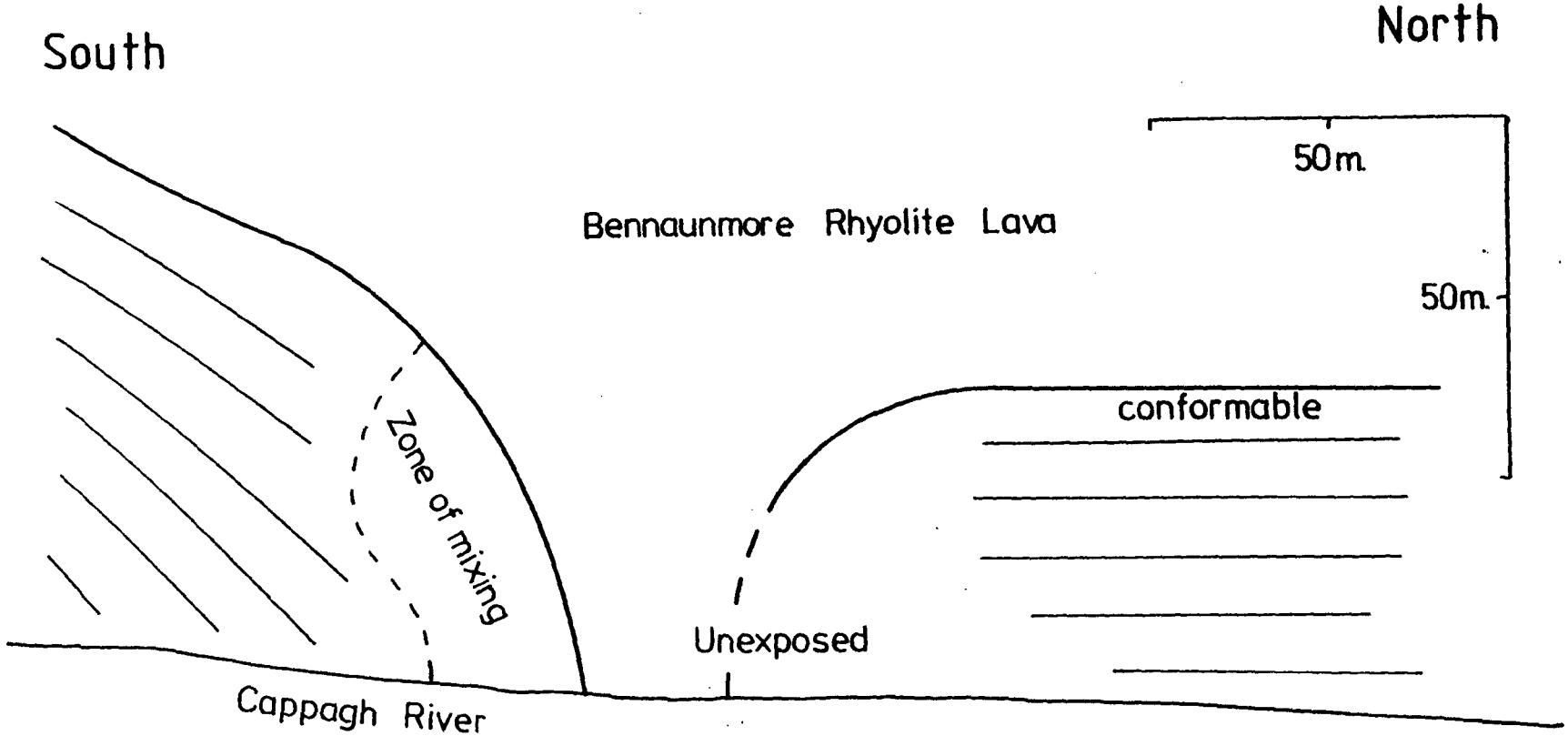

Fig. 5.9 Schematic N-S section through the area around 'Z' (fig. 5.4).

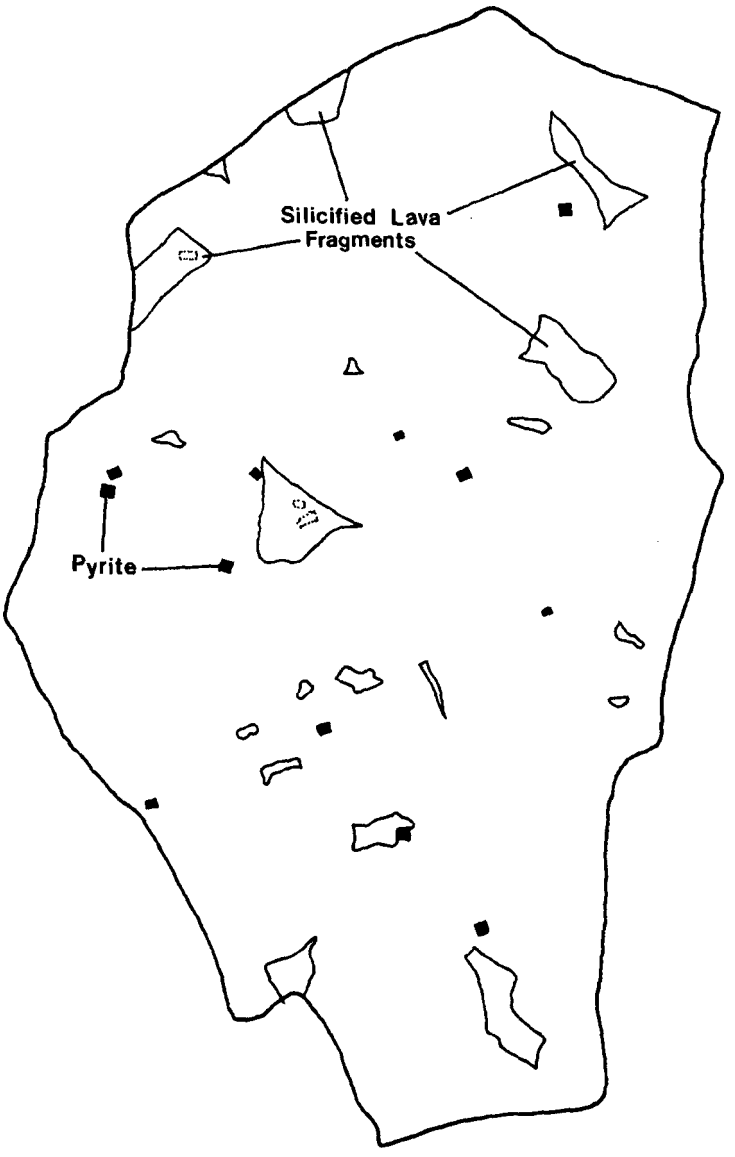

Fig. 5.10a

Drawing of hand specimen posessing a peperitic texture from near 'Z' in fig. 5.4 (Real size).

5.1.5.4 Internal Characteristics of the Bennaunmore Rhyolite lava

(a) Introduction

The lava always weathers to various shades of cream or light brown to rust colour, the latter indicative of secondary ferric iron staining. The flow laminations are usually clearly visible as either slight colour variations or by variations in the depth of weathering. White or pink subhedral to rounded feldspar phenocrysts up to 0.5 cm in size are always visible on the weathered surfaces with rounded quartz phenocrysts and nearly black chlorite clots replacing a primary mafic also present up to 1 mm.

In freshly exposed surfaces the Bennaunmore lava consists of a grey-green, flow laminated, microcrystalline matrix containing varying numbers of cloudy white subhedral to rounded feldspar phenocrysts (Plate 5.27) along with glassy quartz microphenocrysts and very dark green or black irregular shaped spots of chlorite pseudomorphing a former ferromagnesian mineral.

(b) Columnar Jointing

A system of columnar joints is well developed in the thicker parts of the lava flow away from its upper, lower, and faulted marginal surfaces, especially on Bennaunmore, where nearly all the exposures are columnar jointed. The jointing produces irregular polygonal columns, 25 to 50 cm across, with between four and seven faces, and may in well exposed sections be vertically traceable for up to 20 metres (Plate 5.20). The columns are commonly slightly curved or sinuous and single columns may vary in thickness along their length. In addition they may be cut by cross joints which do not pass into neighbouring columns. All these features are typical of the jointing pattern produced by the contraction of cooling near-surface or surface igneous bodies (Francis, 1976; Williams & McBirney, 1979).

Away from the base or margin of the Bennaunmore lava the columnar joints become progressively better developed. Fig. 5.11 illustrates this, and also the variation in orientation of the long axes of the columns. The columns mostly dip at between 70° and 90° (Plate 5.21, around the summit of Bennaunmore) in a generally southeasterly direction, although in the north the dip may be as little as 48° (Plate 5.21). The continuous presence of columnar joints through the 300 metres of exposed Bennaunmore lava, and the total absence of brecciated horizons within this thickness suggests that the Bennaunmore lava is the product of one phase of eruption.

It is considered that columnar structure develops in response to stresses induced by the cooling of an igneous body (Francis, 1976; Williams & McBirney, 1979). The orientation of the joints is related to the temperature gradients within the igneous body, and they form perpendicular to the outer cooling surfaces. The Bennaunmore lava has an outer zone or skin up to 50 metres thick in which columnar jointing is absent or poorly developed; also, strong curving of the columns in response to irregularities in the outer surface are absent. This is in contrast with the joint patterns in basic magmas described by Williams & McBirney (1979), in which the jointing persists to within approximately one metre of the outer edge of the lava.

It is not clear whether the pattern of orientation of the columns is caused by Hercynian folding or tilting or whether the Bennaunmore fault block has acted as a tectonically competent unit and that the orientations are of primary origin in response to the domed surface of the lava.

(c) Flow Structures and Autobrecciation

Much of the exposed Bennaunmore lava possesses a strongly developed flow lamination. Plates 5.22-26 illustrate some varieties

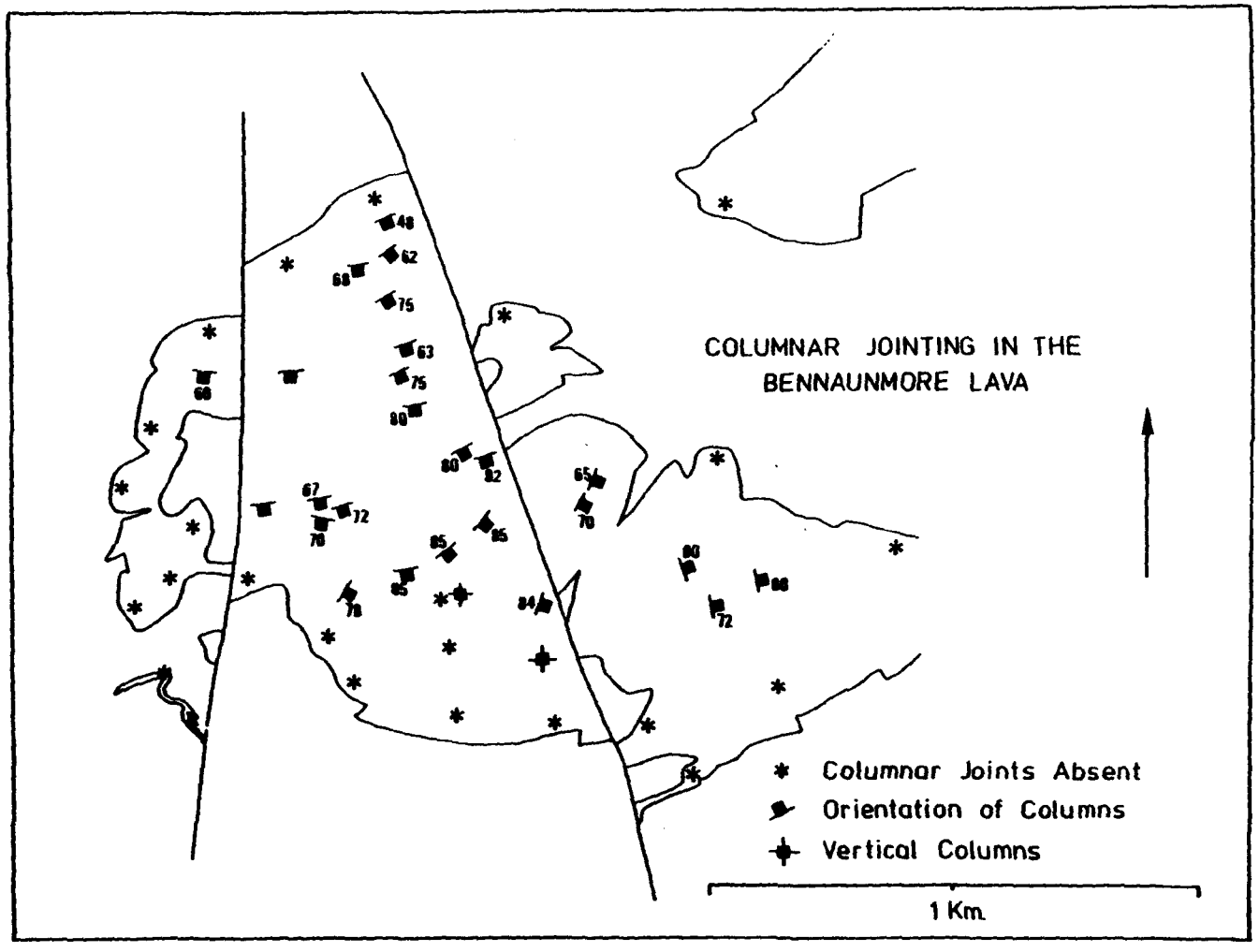
COLUMNAR JOINTING IN THE
BENNAUNMORE LAVA
Columnar Joints Absent
Orientation of Columns
Vertical Columns
1 Km

Fig 5.11

of flow structure within the lava. The laminations vary in thickness between 1 and 50 mm, and are related to variations in the crystalline texture of the lava. The lighter, more weather resistant laminations are coarser grained and poorer in the microscopic sericite and chlorite groundmass components than the darker, less resistant bands, which are finer grained and poorer in quartz and feldspar. In glassy lavas like the Bennaunmore rhyolite (Chapter 6, page 166) flow lamination reflects small differences in primary composition and viscosity which have been destroyed here by recrystallisation.

In some outcrops the flow laminations are remarkably even and unfolded. Plate 5.11 illustrates an example where over 10 metres of lavas is laminated parallel to the exposed base of the flow. However, more commonly the laminations are distorted, producing a suite of features related to tensional or compressional stresses within the lava caused by differential flow. Compressional features include flow folding with wavelengths ranging from a few millimetres and over 10 metres. Flow folds of different wavelength are frequently superimposed, and appear to relate to successive phases of development, with the shortest wavelength folds forming last in the cores of the larger folds (Plates 5.24 and 5.25).

Tensional features are less common and are usually characterised by the boudinage of groups of laminations between 2 and 10 cm thick (Plates 5.22 and 5.23). Other flow distortions occur as a result of the incorporation of solid, irregular shaped blocks of lava within the flow (Plate 5.26).

A survey of the dips and strikes of the flow laminations in the Bennaunmore lava (fig. 5.10) reveals that dip angles exceeding 45^{o} are scarce, and most measured less than 30^{o}. Christiansen and Lipman (1966) observed that within the upper parts of flow laminated rhyolite lavas,

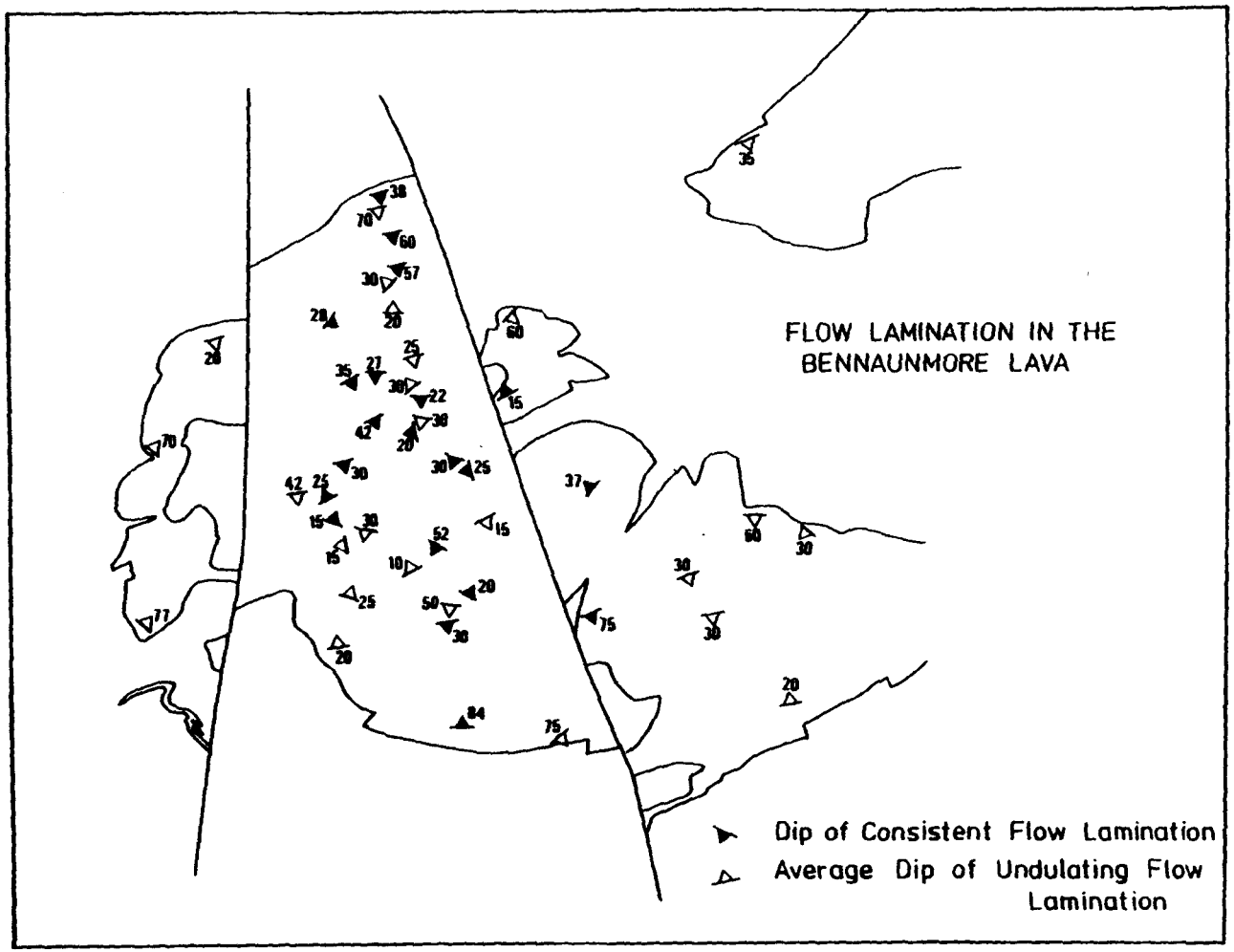
FLOW LAMINATION IN THE
BENNAUNMORE LAVA
Dip of Consistent Flow Lamination
Average Dip of Undulating Flow Lamination

Fig 5.10

ramp structures develop with steep internal structures. The absence of steeply dipping flow laminations in the Bennaunmore lava supports the concept of it being a single flow unit.

Fig. 5.7 indicates where the lava is partially or wholly brecciated and blocky in appearance. Such autobrecciation is restricted to the distal extremities of the flow. There is no evidence for brecciation at the base of the flow within the subsided area around Bennaunmore, while elsewhere only scattered evidence exists. Furthermore, in most localities the lava appears to have scarcely disturbed the underlying sediments.

At location 'U' (fig. 5.7), west of Lough Athooynastooka, the top of the lava flow is clearly exposed, overlain by terrigenous sandstones. The flow top is blocky, but remarkably smooth with no evidence for the infill of fissures in its surface by sediment perhaps suggesting that all loose material was removed by erosion before burial. Sometimes angular blocks of lava between 2 cm and 2 metres in size, are present in the lowest few metres of sediments overlying the lava, but which are not in contact with the flow surface. These detached blocks are embedded in silts to fine sands and are unlikely to have been transported there by the current which deposited the sediment. It is possible that they have rolled, fallen, or been otherwise eroded from the sloping surface of the lava flow nearby.

Vesiculation in the Bennaunmore lava has only been observed in a small area south-east of Lough Nabroda (fig. 5.1) where the lava is thin. The vesicles are mostly around 1 cm in size and quartz filled. Vague sub-vertical laminations in the basal 2 metres of the flow immediately southwest of 'X' (fig. 5.4) are suggestive of pipe vesicles. The upper parts of many are slightly curved in consistently the same direction.

5.1.5.5 Summary and Discussion

Analysis of the gross morphology and internal structure of the Bennaunmore lava must involve consideration of the viscosity of the magma. Lava viscosity is controlled primarily by composition and temperature, and to a lesser extent by volatile content, crystallinity and vesicularity (Williams & McBirney, 1979). Petrographic and Geochemical studies (Chapters 6 and 8) have confirmed a rhyolitic composition for this lava, and the presence of small numbers of phenocrysts. The likely range of erupted magma temperatures for such a lava are unlikely to have significantly influenced the high viscosity. The rarity of vesicles suggests a low volatile content, which in turn suggests that volatiles would not have markedly lowered the viscosity, and the mechanical effects of vesicles and crystals would have been minimal.

While viscosity is the most important factor governing the nature of fluid motion in lavas and their internal features, the general morphology of acid flows is probably controlled largely by the rate of effusion. For example, low rates of effusion promote the formation of a thick, cool, blocky surface, and the dome-like morphology of a tholoid. Field observations have shown little evidence for autobrecciation except of a limited extent on the upper surface of the distal parts of the flow. The bulk of the lava is flow laminated and columnar jointed. It has been suggested that the presence of a blocky base indicates that the flow front advanced slowly enough for loose blocks from the autobrecciated flow top to fall down the slope of the flow front and be overriden (Macdonald, 1972). The absence of blocks at the base of the Bennaunmore lava, and the presence of flow laminations to within a metre of, and parallel to the base of the lava suggests that the Bennaunmore lava flow front advanced comparatively rapidly except at its

distal extremity.

In the absence of any independent evidence for an unusually low viscosity for this lava it must be concluded that the rate of effusion was particularly rapid. The observations in sections 5.1.5.1-5.1.5.4 present a clear picture of the development and resulting morphology of the Bennaunmore lava. Its source vent lay in the southwest corner of a roughly circular downfaulted "cauldron" about 1.5 Km across with a maximum subsidence of about 300 metres. Once the floor of the central area had been covered, further effusion filled the depression, producing a viscous lava lake with a volume approaching 0.5 Km^3. The absence of brecciated horizons within the thickness of 300 metres suggests that effusion was continuous, and that the thickening within the subsided area was an endogenic process. An unjointed domed upper surface probably further increased the overall lava thickness.

Subsequently the lava flowed eastwards for at least 2.5 Km being between 50 and 100 metres thick, and about 1.3 Km wide with a thin blocky surface. This considerable thickness observed to within a few tens of metres of the distal margin of the flow is further evidence of the high viscosity of the magma. The dimensions quoted above lead to a minimum estimate of the total volume of the Bennaunmore lava of 0.8 Km^3

5.1.6 The Upper Tuffs

5.1.6.1 Introduction

The Bennaunmore lava is overlain in the west by a thick sequence of volcaniclastic sediments. They have their greatest development west of the Cappagh fault (over 200 metres thick), although they thin rapidly away from this area. To the east, the Bennaunmore lava is often directly overlain by wholly epiclastic sediments, although thin tuffs can be traced discontinuously as far as Glen Flesk both to the north and the south of the crest of the Mangerton Anticlinorium.

Fig. 5.12 illustrates the thickness variations of the Upper Tuff sequence and the control of contemporaneous faulting, previously mentioned, can be clearly demonstrated.

5.1.6.2 The Upper Tuffs west of the Cappagh Fault

The sequence immediately west of the Cappagh fault and south of the axis of the Mangerton anticlinorium has been described under section 5.1.4 above, and the control exercised by contemporaneous faulting over the variable thickness of the Upper Boulder Tuff and the overlying volcaniclastic sediments was demonstrated (see Fig. 5.12). The tuffs can be traced westward from location 'W' (fig. 5.12), outcropping both to the north and south of the eastward plunging Mangerton anticlinorium until, with a reduced thickness of about 50 metres they disappear under glacial drift southeast of the summit of Stoompa (fig. 5.12 and 1.3). No mixed tuffs attributable to the Bennaunmore volcanic complex reappear further along the strike.

The discordant westward-plunging dips observed west of 'V' (fig. 5.12 and 1.3) are interpreted as a primary feature related to deposition of the Upper Tuffs onto a westward-sloping surface corresponding to the western margin of the Bennaunmore lava.

The base of the tuffs can be followed north and then west from location 'V' around the east ridge of Stoompa. North of this ridge a narrow strip of the underlying terrigenous sediments outcrop in the core of a major subsidiary anticline the axis of which marks the southern boundary of the near vertical northern limb of the Mangerton anticlinorium (location 'AA' fig. 5.12). Plate 5.28 shows a panormic view of the ground on the northwestern slope of this ridge. A large structural discordance occurs between the sequence to the south of the axial plane of the anticline, and that found to the north. The discordances can be summarised.

THICKNESS VARIATIONS IN THE UPPER TUFFS
OF THE BENNAUNMOR VOLCANIC CENTRE

Fig. 5.12

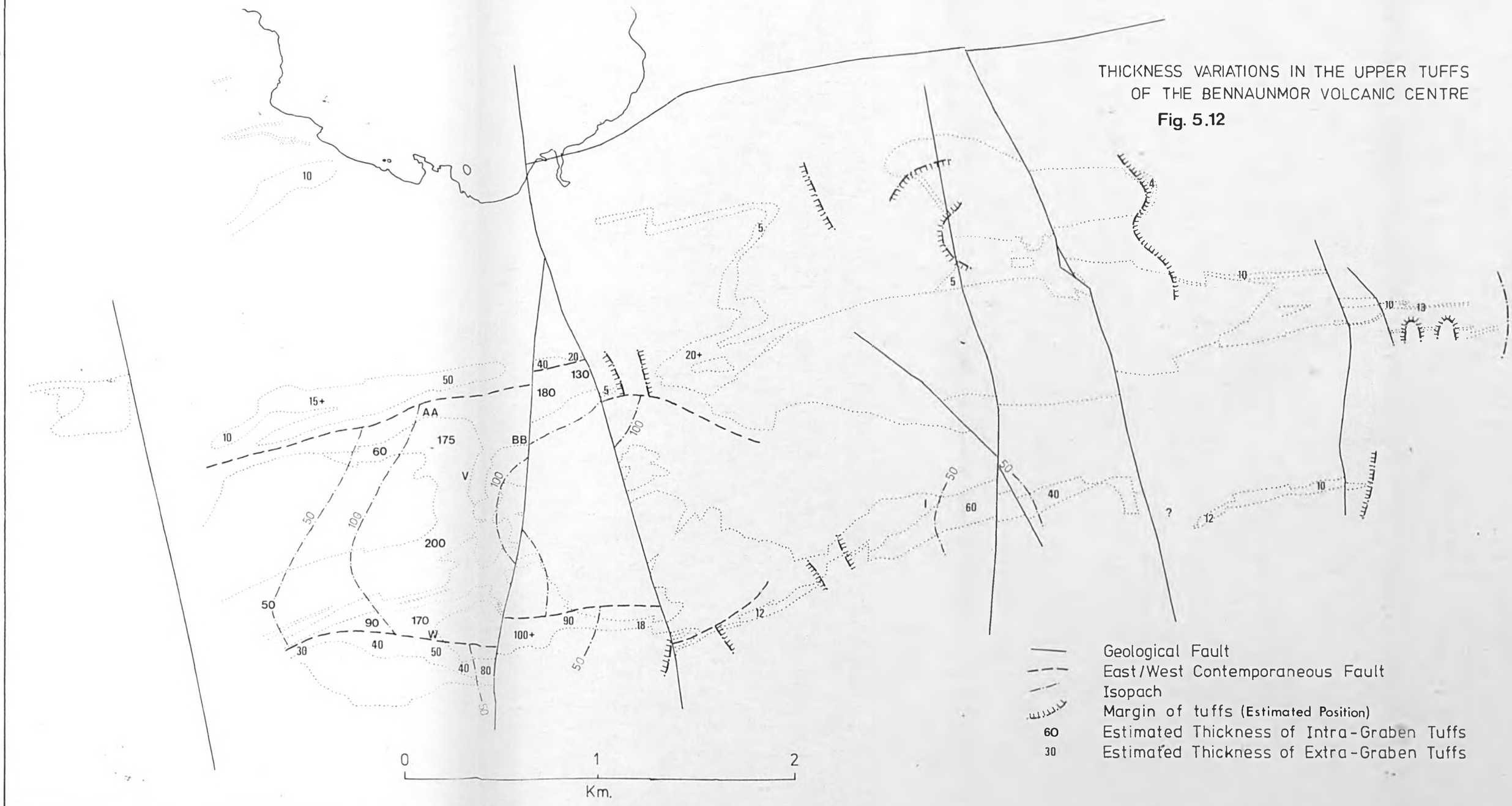

1. South of 'AA' - the position of the axial plane of the anticline on the skyline in Plate 5.28 (see also fig. 5.12) - a 175 metre thick sequence of bedded mixed tuffs dip gently south. North of 'AA', about 100 metres of northward younging, vertically dipping, terrigenous sediments are overlain by 50 metres of tuffs.

2. Immediately west of the Cappagh fault, in the valley bottom, the margin of the Bennaunmore lava is in contact with approximately 10 metres of structureless sediments (location 'BB' in fig. 5.12), separated by at least 300 metres of northward younging, near-vertically dipping terrigenous sediments from a thin development of the upper tuffs.

A large normal fault with a plane coinciding approximately with the axial plane of the anticline may be responsible for the relationships, and if so, the rapid changes in thickness of the upper tuffs suggests that the faulting may again have been contemporaneous with the volcanism. A study of the base of the mixed tuffs southeast of 'AA' reveals evidence for such faulting. The fault zone can be subdivided into a series of subparallel subzones which all dip steeply south (fig. 5.13).

Subzone A : Undisturbed, bedded mixed tuffs which grade into

Subzone B : Structureless mixed tuff containing distorted areas or blocks of terrigenous sandstone (1 metre wide approx.)

Subzone C : A 3 to 5 metre wide zone of chaotically disturbed terrigenous sediment which grades into

Subzone D : a broad zone of microfaulted sandstones about 10 metres wide in which the intensity of microfaulting diminishes away from subzone C into

Subzone E : Undisturbed terrigenous sediments.

Fig. 5.29 shows an oblique section cut through part of the contemporaneous fault zone, and Plate 5.30 shows how the microfaulting is

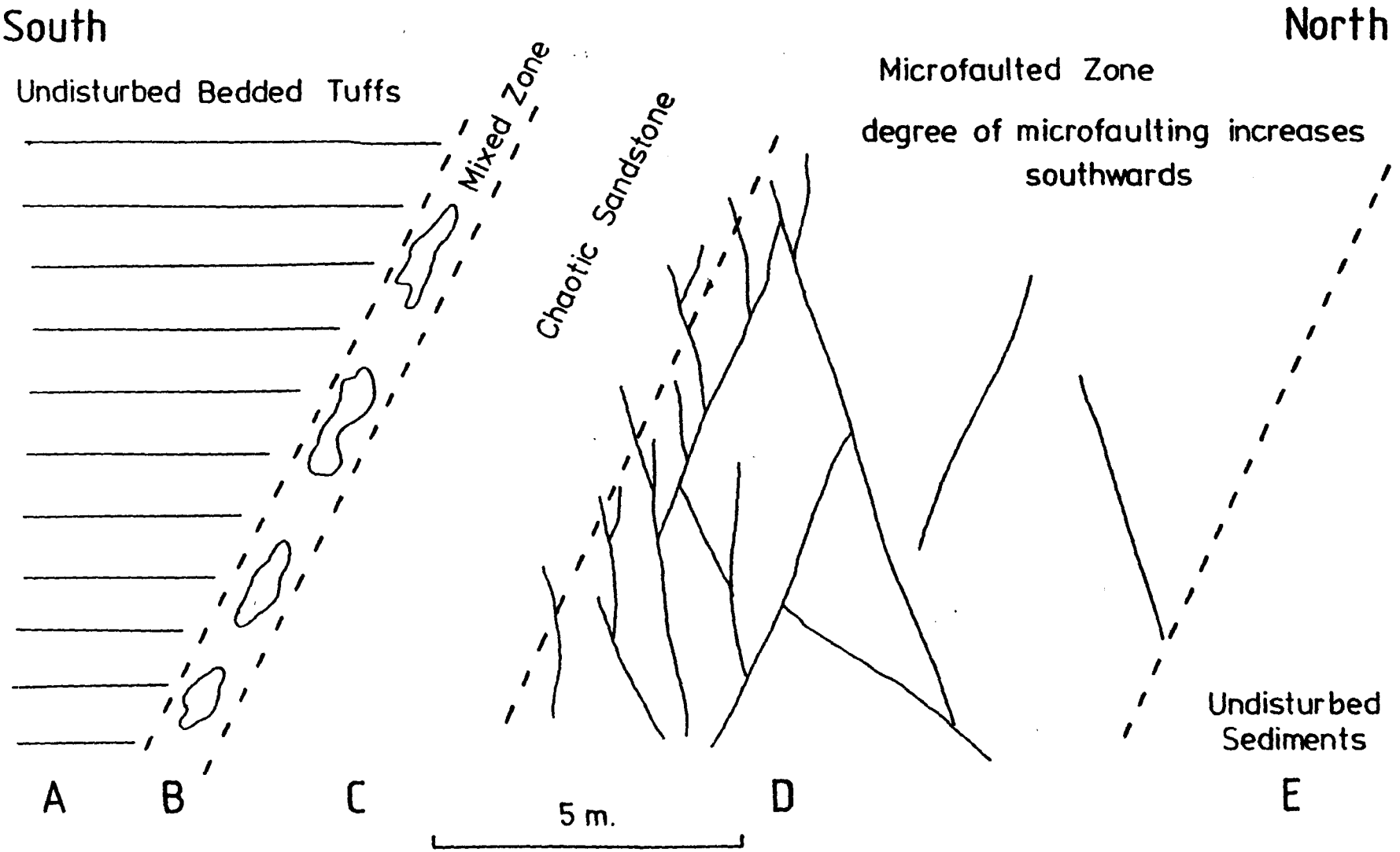

Fig. 5.13 Schematic N-S section through the northern contemporaneous graben fault around 'AA' (fig. 5.12).

older than both the folding and the quartz veining of Hercynian age. The microfaulting is folded (not clearly shown in this plate) and displaced by the quartz veins.

At 'AA', the fault plane dips south at between 50° and 70°, parallel to the axial plane of the anticline. Further south, although not exposed, the fault plane must dip at a much lower angle before it returns to a steep southerly dip of about 70° in the zone immediately north of the margin of the Bennaunmore lava flow near 'BB' (fig. 5.12, and Plate 5.28).

Fig. 5.4 shows the course of the fault in plan view, and how it intersects with the cuspate contemporaneous fault controlling the western margin of the Bennaunmore lava. On the basis of the same structural discordances outlined at location 'AA', although not exposed, the fault is inferred to continue for at least a Km west of 'AA'. South of the fault the upper tuffs thin rapidly westwards. North of the fault they only thin very slowly northwards and westwards, and can be recognised over 2 Km to the north on the western shores of Lough Guitane.

The original strike of the fault was probably nearly due east-west. However, subsequent folding and topographic effects have combined to distort this. Two east-west striking contemporaneous faults have thus been identified in addition to the subcircular subsided area around Bennaunmore. Together, the east-west faults characterise an east-west orientated graben which developed during the eruption of the volcanics.

5.1.6.3 Internal Characteristics of the Upper Tuffs West of the Cappagh Fault

The most striking feature of the tuffs is that none of them are wholly volcaniclastic, being composed of various admixtures of

volcaniclastic and epiclastic sediment. Locally derived volcanogenic material includes angular or irregular lapilli and subhedral or broken feldspar phenocrysts. Epiclastic material includes angular quartz grains and mud or siltstone clasts up to 5 cm in size. In thin section the tuffs are shown to contain a variable, but usually high content of finely crystallised quartz and feldspar (probably albite) which has probably replaced and recrystallised the ash grade fraction of the volcanogenic component.

The tuffs are parallel bedded with rare shallow scours and low angle cross bedding or massive and unbedded. Rare agglomeratic, shallow channel deposits occur near the base of the succession adjacent to the margins of the Bennaunmore lava. The best examples of agglomerate are found along the western margin of lava where they appear to lie in shallow channels up to 2 metres deep (Plates 5.31 and 5.32), all within the basal 10 or 15 metres of the Upper Tuffs. The total unsorted contents include angular to subrounded blocks of rhyolite and siltstone or sandstone up to 50 cm across, embedded in a mixed tuff matrix. These deposits are overlain by a progressive fining upwards sequence. Some of these channels may be related to erosion of the exposed surface of the Bennaunmore lava and influenced by the remaining exposed contemporaneous fault escarpment described previously under section 5.1.5.1. Channelling of this nature is absent above the basal 10 or 15 metres of the Upper Tuffs suggesting that once the adjacent prexisting topography had been smoothed out by a combination of erosion and the mantling effect of the tuffs the conditions to promote channelling ceased to exist. The large blocks of rhyolitic lava are petrographically identical to, and were probably derived from the Bennaunmore rhyolite lava flow, while the larger epiclastic blocks were probably eroded from the contemporaneous fault escarpment.

The bulk of the overlying mixed tuffs are parallel bedded or massive (Plate 5.34), with some low angle scours and rare cross lamination (Plate 5.33). General rules can be applied to their field appearance when estimating the proportions of the various components described above:

1. High contents of silt or mud clasts result in a pock-marked appearance due to preferential weathering of these less resistant components.

2. High contents of silt or mud clasts may be accompanied by high contents of irregular or angular, cream or yellow weathering rhyolite lapilli which stand proud from the outcrop surface.

3. Subhedral or broken volcanogenic feldspars (up to 2 mm in size) are ubiquitous and weather to a pale cream or whitish colour.

4. High epiclastic sand contents result in an overall darker weathering, often purplish in colour.

5. Low sand contents, and a high content of fine recrystallised volcanic ash result in a paler overall colouration.

It must be stressed however, that sediments composed of only one of the above components are never observed; the tuffs are always mixed.

Bed thicknesses vary from fine laminations only mm thick, to units over 10 m thick for which neither a base nor a top can be found within an individual outcrop. Normal grading is sometimes observed along with low angle erosion features, (Plate 5.33). It is likely that this erosion was produced by water, but the channels are never deeper than approximately 50 cm.

Sandstone dykes have been observed at a number of locations in close proximity to the contemporaneous faults. One set of dykes occurs in the lowest 20 m of tuffs adjacent to the western margin of the Bennaunmore lava (Plate 5.35) at 'V' in fig. 5.12. Another set occurs

further south at 'W' in fig. 5.12. The dykes consist of structureless medium grained sandstone with no volcanogenic component, and may pass into thin sills of limited lateral extent (Plate 5.35). They are usually between 20 and 40 cm across with minor offshoots which may be up to 1 cm thick. The flame-like, upward tapering nature of many of these dykes, and their passage into sills suggests that they have been injected from below, and are probably related to disturbances and fracturing caused by motion along the contemporaneous faults.

North of the northern graben contemporaneous fault the upper tuffs are the only representatives of the Bennaunmore Centre volcanics. The thickness variations suggest they were deposited in the form of a low fan, the thickest part of which occurred near to 'AA' in figs. 5.4 and 5.12, corresponding to the thickest development of intragraben tuffs. Their field apperaance is very similar to those described from within the graben except for the absence of thick massive units. The grain size and volcaniclastic content decreases away from location 'AA', and interdeposition of wholly epiclastic sediments becomes increasingly prevalent as the volcaniclastics are progressively diluted by epiclastic sediment. Sedimentary structures including shallow scours and ripple cross-stratification clearly indicate that these distal tuffs were deposited by water.

5.1.6.4 The Upper Tuffs east of the Cappagh Fault

In the north of the Bennaunmore fault block, the lava is overlain by approximately 200 metres of bedded and occasionally massive mixed tuffs identical in character to those described from west of the Cappagh fault. They dip consistently and steeply northwards. The contemporaneous fault bounding the northern side of the central cauldron subsidence is inferred to lie sub-horizontally beneath the present level of erosion.

To the south of the axis of the Mangerton anticlinorium the Upper Tuffs are only 30 to 40 metres thick, and overlie the Bennaunmore lava on the east side of the Bennaunmore fault block. In the west of the fault block, the lava wedges out, and the Upper Tuffs directly overlie the Lower Boulder Tuff, and attain a thickness of up to 150 metres.

East of the Bare Island fault the Upper Tuff never exceeds 60 metres in thickness, and rarely 10 metres. The coarsest deposits and those containing the highest volcaniclastic component occur in the lower parts, grading up into progressively volcaniclastic-poor deposits with interbedded terrigenous sediments. The tuffs are thinly bedded, often graded and may exhibit shallow erosion features and cross lamination. Sorting and grading has rarely produced beds composed of 80 percent lapilli sized lava fragments, highly irregular in shape, with a tendency to be rather elongate in cross-section (Plate 5.36).

The field appearance is characterised by a pale cream weathering colour, while those mixed tuffs in the upper parts of the sequence may only be identifiable by the presence of a few broken feldspar crystals weathering white in contrast to their darker host epiclastic matrix.

In general, the development of these reworked aqueous tuffs overlying the Bennaunmore lava is patchy, but extends as far east as Glen Flesk (fig. 5.12). The base of the tuff is often very uneven, especially in the northeast of the area where the pre-existing surface appears to have been extensively channelled and frequently infilled with very coarse debris. At location 9431 (fig. 5.12 and 1.5) blocks of Bennaunmore lava up to 2 metres across occur with siltstone and mudstone boulders up to 1 metre across in the basal 2 or 3 metres of the tuffs.

In the south, adjacent to the margin of the Bennaunmore lava near 'I' (figs. 5.7 and 5.12) the tuffs exceed 60 metres in thickness, but

thin rapidly eastwards to only 1 metre thickness over a distance of 0.5 Km. Further along strike the tuffs thicken, wedge out, reappear and thicken to 20 metres, and finally wedge out a short distance from the alluvial plain of Glen Flesk. A 1-2 metre thick unit of red sandstone, a very distinctive and unusual lithology, overlies the Upper Tuffs conformably throughout this area. Its continuity suggests that the thickness variations are entirely due to basal irregularities, and that the upper surface of the tuffs was flat or near-horizontal.

Northwest of Crohane a fan shaped deposit of the Upper Tuffs appears to be derived from between 'S' and 'T' (figs. 5.7 and 5.12) where they attain a thickness of over 50 metres. They thin in all directions being only 5 metres thick 0.5 Km to the north. Further east on the northern limb of the anticlinorium only localised and very thin developments of tuff overlie the lava flow.

5.1.7 The Eskduff Rhyolite Lava Flow

The final phase of volcanic activity was marked by the extrusion of the Eskduff lava. It outcrops in only two areas, both west of the Cappagh fault.

1. On the southern limb of the Mangerton anticlinorium around location 'a' (fig. 5.7).

2. On the crest of the east ridge of Stoompa around 'b'.

The lava conformably overlies the Upper Tuffs and can be seen in plate 5.28 as the highest unit at the top of the steep slope on the western side of the Cappagh fault valley.

In area (1) the lava is seen to thin rapidly from a maximum thickness of about 150 metres in the centre of a lateral extent of only 1 Km. The overlying terrigenous sediments dip towards the lava at angles up to 30^{o} implying that its surface possessed a marked palaeoslope. In area (2) the top of the lava is only seen at 'c'

(fig. 5.7) where the overlying sediments have a similar relationship indicating a northwesterly directed palaeoslope. Here, a minimum thickness of 100 metres has been estimated.

Only a rough picture of the morphology of the lava flow can be deduced from the limited exposure. It probably formed a tholoid of subcircular plan with a maximum length of 2 Km and thickness of over 150 metres with margins sloping at approximately 30^{o} or more.

In the southern area (1) the lava is often blocky, especially in its upper parts, almost certainly as a result of autobrecciation. Individual blocks are usually under 30 cm in size, although some as large as 1 m have been observed. Outcrops of unbrecciated, flow-laminated lava occur near the base of the thicker parts of the flow. Highly nodular facies are present, with lithophysae up to 10 cm in size and filled with coarse grained quartz and earthy haematite. In area (2) blocky facies are rare and the lava is usually flow laminated with patchy occurrences of nodules, often developed preferentially within particular flow laminations (Plate 5.38).

In general the lava is deeply weathered and fresh specimens difficult to obtain despite the absence of well-developed jointing. The fresher specimens appear pale brown in colour with cloudy feldspar phenocrysts. In cases of more extreme alteration large irregular patches up to 10 cm across are replaced by quartz and haematite with the feldspar phenocrysts entirely altered to sericite.

5.1.8 Magmatic Dykes in the Bennaunmore Volcanic Complex

A number of dykes intrude the Bennaunmore lava and have been grouped into three categories according to their field and petrographic characteristics.

5.1.8.1 The Green Dyke

Only one such dyke has been observed northwest of the summit

of Bennaunmore (Plate 5.37) at location 8742A in fig. 15 . (For chemical and petrographic analyses see under sections 8.4.2 , 6.4.2). It varies between 10 and 20 cm in thickness and has a north-northeasterly trend which can be followed for 10 metres. The dyke is dark green in colour (due to the high matrix chlorite content) and porphyritic, with a phenocryst assemblage of milky white plagioclase feldspars (up to 3mm in size), rounded quartz microphenocrysts and chlorite pseudomorphs after unidentified ferromagnesian crystals.

The dyke margins are sharply defined although rare small angular inclusions of pale coloured Bennaunmore lava up to 1 cm in size are present. No evidence for marginal chilling has been observed, and the columnar jointing of the Bennaunmore lava passes unaffected through the dyke implying that the intrusion occurred when the lava flow was still hot and before the cooling joints developed.

5.1.8.2 The Pale Dykes

Three of these strikingly pale coloured dykes are present north-northeast of the summit of Bennaunmore (Plate 5.21). They are approximately 2 metres thick and have a northeasterly trend, some being traceable for up to 100 metres. The most northerly dyke dips south at 40^{o}, the others are subvertical.

The outcrop appears pale pink in colour, and freshly broken specimens vary from very pale grey to various shades of pinkish grey. The weathered skin is only a few millimetres thick, flaky, and nearly white in colour. The dykes are resistant to weathering and erosion relative to the Bennaunmore lava. The dyke margins are poorly defined and appear to grade into the Bennaunmore lava over a distance of approx. 50 cm. The columnar jointing fades into these margins, and is absent in the central parts of the dykes.

Subhedral laths and rounded phenocrysts of milky white to clear

plagioclase up to 3 mm in size occur along with 2 mm sized aggregates of magnetite often in association with rounded feldspars. Quartz phenocrysts are absent, and the matrix is composed of very fine grained microscopic albite.

5.1.8.3 The Rhyolite Dyke

A subvertical dyke, 1 metre thick, trending east-northeast outcrops 400 metres north of Lough Nabroda. Its location makes this dyke unique in that it isthe only intrusive body observed outside the confines of the Bennaunmore fault block. It is very similar in appearance to the Bennaunmore lava, but possesses a well-developed platy fracture cleavage in contrast to the columnar joints of the host lava. The cleavage occurs along subparallel planes related to segregation of the secondary dark minerals (largely chlorite) which separate 0.2 to 2 mm thick lenticular or planar leucocratic areas composed of fine grained quartz and feldspar. The phenocryst content is essentially the same as that of the Bennaunmore lava.

5.1.9 Summary and Discussion

Any general discussion of the volcanic rocks of the Bennaunmore volcanic centre must focus on the relationship between contemporaneous faulting and the volcanism. It has been shown that such faulting occurred in two orientations

i) a set of east-west faults which bound a graben about 1.5 Km wide, and

ii) a second set related to a roughly circular depressed area centred upon Bennaunmore.

Table 5.1 illustrates the proposed relative timing of the various eruptive and faulting phases and figs. 5.14 and 5.14a show a proposed stratigraphic correlation through the Bennaunmore volcanic complex. Not only did these faults control the thickness variations of the various

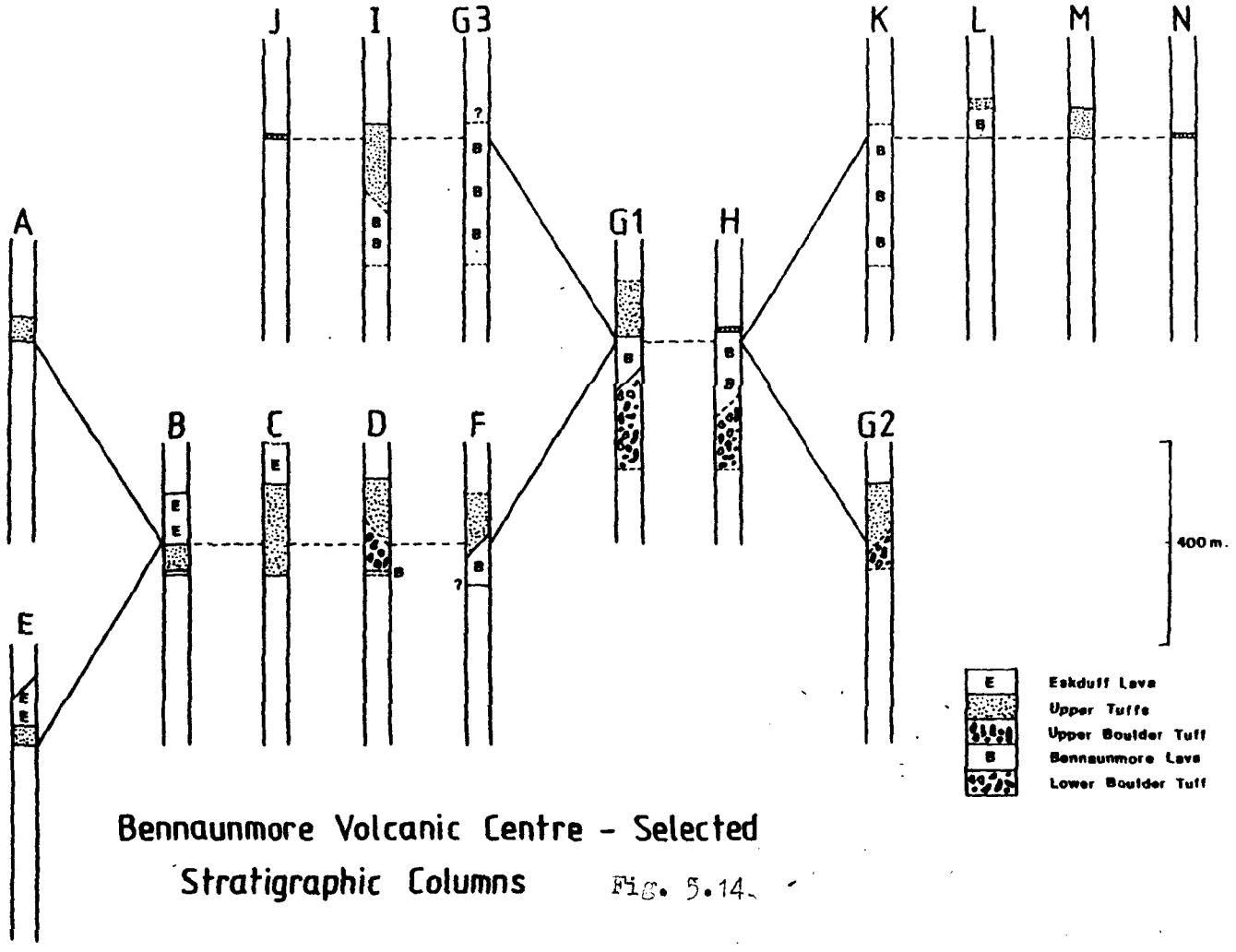

Bennaunmore Volcanic Centre - Selected Stratigraphic Columns Fig. 5.14.

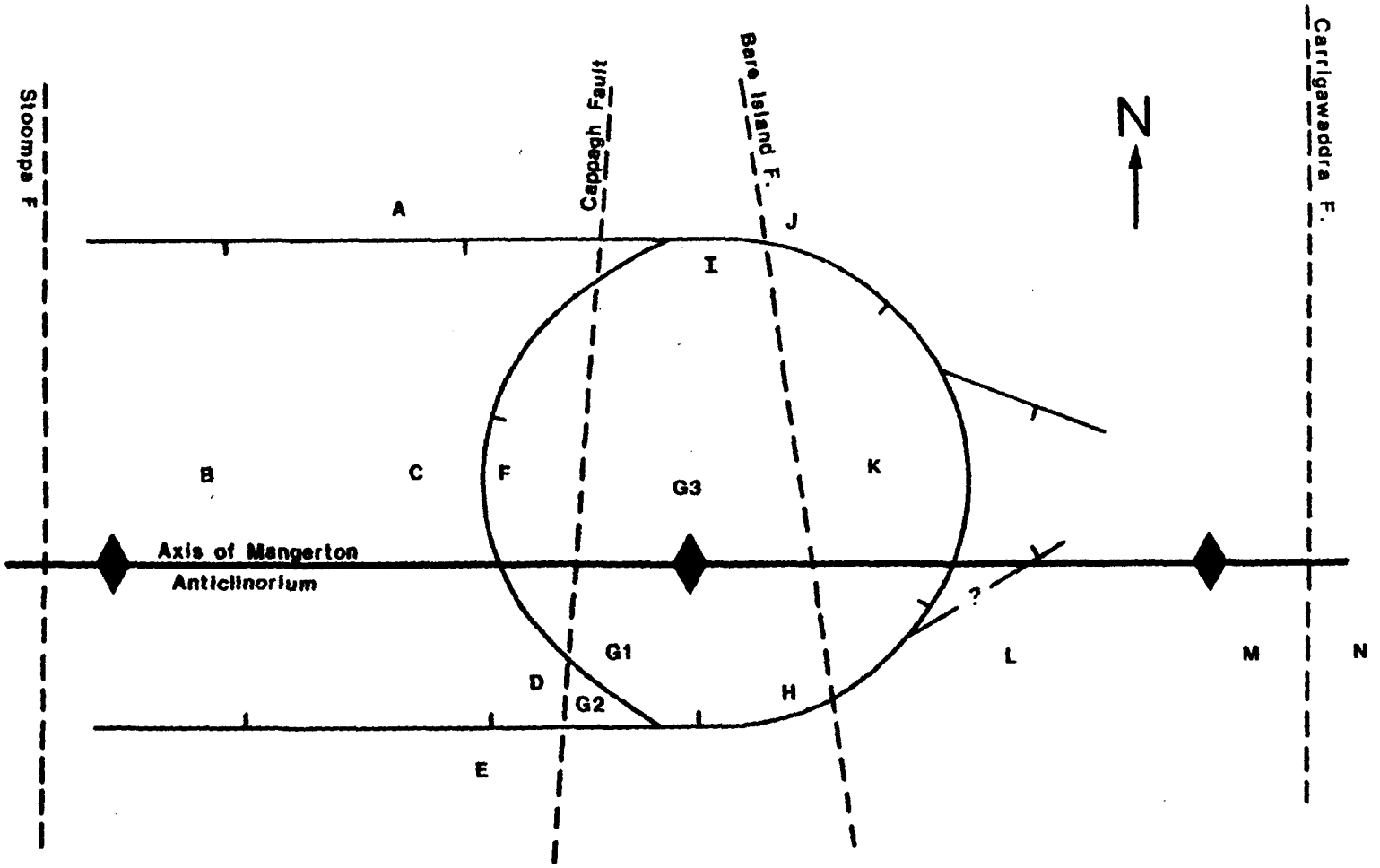

Fig. 5.14a Key to the location of the syratigraphic columns drawn in fig. 5.14 relative to the contemporaneous faults.

stratigraphic units, but in some cases it will be shown that they themselves appear to have functioned as conduits for the volcanic rocks.

The geometry of the Lower Boulder Tuff is that of a wedge elongated east-west parallel to the central part of the southern graben fault with a pronounced northerly directed palaeoslope, suggesting that the two features are intimately related and possibly cogenetic. The highly unsorted, mixed nature of the boulder tuff, and its disordered internal texture is reminiscent of laharic deposits described by many authors, although the matrix is somewhat coarser. However, the rapid northward thinning suggests a low mobility, and it seems more feasible that the deposit was produced by slumping away from the contemporaneous fault scarps.

However, there is strong evidence that the Lower Boulder Tuff cannot have been generated exclusively by gravitational downslope movement. The absence of volcanics older than the Bennaunmore lava anywhere else in the region leads to the conclusion that the volcanogenic component of the Lower Boulder Tuff was the first volcaniclastic material to be erupted, i.e. it was not reworked from any older deposit recognised in the area. The possibility that older deposits might have been entirely removed by erosion before eruption of the Bennaunmore lava is highly unlikely given that the whole area was undergoing rapid subsidence, and would therefore have been a site for deposition, not erosion. The absence of erosion is further supported by the presence of a distinctive sequence of a few metres of fine purple siltstones which outcrops at the base of the lava flow throughout the region. Thus, it is possible that the volcanogenic component of the Lower Boulder Tuff was erupted from a fracture or fractures very closely related to the southern graben fault.

There are two alternative mechanisms by which the volcaniclastic and epiclastic components of the Lower Boulder Tuff came to be mixed.

i) Eruptive mixing in the vent

ii) Mechanical mixing during slumping.

The total absence of what might be termed "normal" tuffs, unmixed with epiclastic material, anywhere in the Bennaunmore volcanic complex, or elsewhere in the Lough Guitane region hints that many of these deposits were erupted in a mixed state. The absence of air fall, or any other type of pyroclastic deposit from the base of the succession, elsewhere in the area implies that all of the juvenile volcaniclastic material erupted was incorporated in the Lower Boulder Tuff. Furthermore, this would have been highly unlikely if the volcanogenic component had been erupted wholly unmixed, and some vestige of normal air fall tuffs would be preserved elsewhere at the base of the succession. It is likely therefore that the volcanogenic component of the Lower Boulder Tuff was erupted mixed with epiclastic material.

Mixing must have occurred near the surface where the sandstones and siltstones were only semi-consolidated or wholly unconsolidated (see Macdonald, 1972, p. 382). Many sandstone boulders show evidence betraying their semi-consolidated state at that time; for example, the various states of disintegration and abrasion of the boulders illustrated in figs. 5.1 to 5.6. These probably relate to the varying lengths of time they were exposed to the disruptive effects of the matrix. However, the relative proportions of sandstone boulders derived from the vent walls and the surface fault escarpment is not known. The tendency for larger, less disturbed boulders to occur near the base of the unit, especially in the section exposed on the eastern side of Lough Nabroda (fig. 5.1) can be explained by both subsurface and surface phenomena: Respectively

i) initial eruption of a boulder rich agglomerate as the vent was cleared, and

ii) derivation of a high proportion of boulders from the fault scarp surface as slumping was initiated.

The limited northward extent of the Lower Boulder Tuff, and its strongly wedge-shaped geometry imply a low eruptive energy, and low eruptive dispersal, and that deposition was dominated by low energy gravitational processes. While eruption and faulting were almost certainly coeval, the importance of mixing of volcaniclastic and epiclastic material by eruptive processes relative to the mechanical action of gravity down the palaeoslope cannot be ascertained. However, it seems likely that both processes were active.

Having established that some mixing must have occurred in the vent, the precise nature of this process can now be discussed. While the partly consolidated sediments into which the magma was intruded contained pore water, the eruption is unusual for a phreatic eruption in that it was not explosive. However, explosive phreatic eruptions rely on a high confining pressure while water is vaporised and stored. The sequence of fluviatile sediments present probably did not provide sufficient confinement, and hence the vapour phase produced would have found its way to the surface rapidly, mixing the brecciated capping to the magma body with the surrounding cold wet sediments. The brecciation of the magma must have been very efficient because angular lava fragments over 2 or 3 cm in size are very rare.

The material was probably transported to the surface in a fluidised state, and once a route had been found, erosion of the walls of the vent would have been rapid. The eruption column could not have attained any great altitude, and as discussed above, the resulting areal dispersal very limited. The temperature of the eruptive products would have been considerably below the solidus temperature of the magma owing to the cooling effect of the sediments.

While the Lower Boulder Tuff was erupted along east-west fractures related to the southern contemporaneous graben fault, the thickest

development of this unit occurs in the southwest corner of the Bennaunmore fault block. It was from this vicinity that the Bennaunmore lava was subsequently erupted. It is probable that the continued rise of the head of the magma led to its eruption from a vent northwards from the southern edge of the circular subsided area (fig. 5.7). The dry siliceous magma was erupted with minimal autobrecciation, first filling the 300 metre deep subsided area (figs. 5.4 and 5.7) before flowing out northeastwards as a thick lava flow with a thinly developed autobrecciated surface.

Eruption of the Upper Boulder Tuff was again cogenetic with movement on the southern graben fault. The most interesting feature of this unit is the grading of matrix composition from wholly epiclastic at its base, to mixed tuff near the top. This implies a number of phases of deposition, each with differing sources of material. It is assumed that the same processes were in operation in the production of the Upper Boulder Tuff as were for the Lower Boulder Tuff, although early slumping must have occurred before any volcanogenic material was available.

Further eruption produced the thick sequence of bedded Upper Tuffs. While these mixed tuffs commonly show evidence of deposition in water (Plate 5.33), many thick, massive, apparently homogenous beds have also been observed showing no signs of water reworking. These are tentatively interpreted as laharic deposits poor in large clasts. Reworking alone is not an adequate explanation for the total absence of unmixed, "normal" airfall tuffs. The above discussion of the petrogenesis of the Lower Boulder Tuff is of fundamental importance, providing a possible explanation for such absence. Eruption of these tuffs was probably always accompanied by mixing with epiclastic material from the walls of the vent.

Throughout the Upper Tuffs, large volcaniclasts are very rare, as they are also rare in the boulder tuffs. Evidence for the existence of pumiceous material is also scanty and inconclusive. A high proportion, possibly in excess of 50 percent, of the volcanogenic component of the mixed tuffs appears to have been very fine ash which has since been totally recrystallised. These observations suggest that the brecciation process operating at the magma-sediment interface in the vent was very efficient.

The final event in the Bennaunmore Volcanic Complex was the eruption of the Eskduff lava. The source vent for this lava has not been identified. The lava flow is only present west of the Cappagh fault, and it is likely that the Bennaunmore lava, and the overlying tuffs produced a topographic barrier to its flow eastwards. The northern margin coincides with the northern graben fault, while in the south, the southern graben fault did not provide a barrier. The Eskduff lava may have acted as a stabilising capping to the thick intra-graben tuff deposits preventing further erosion and redistribution of these mixed sediments.

To summarise, there is strong evidence that contemporaneous faulting operated throughout the Bennaunmore volcanic episode in a number of phases (see table 5.1). Examples of slumping along the exposed fault escarpments have been observed in addition to many near-surface fault breccias. It must be stressed that the temporal and structural models of contemporaneous faulting presented are probably gross simplifications of what must have been a very complex system (fig. 5.14b).

5.2 The North Stoompa Rhyolite Lava and Associated Tuffs

An isolated group of exposures of mixed bedded tuffs and blocky lava occur on the north side of Stoompa, and form a prominent bluff

Table 5.1

Summary of Phases of Volcanic Activity in the Bennaunmore Volcanic Centre

Reworking Phases	Eruptive Phases	Faulting Phases	Notes
	Lower Boulder tuff	Ring fracture initiated	Some slumping along western ring escarpment
	Benn. Lava flow/lake	Continued movement on ring fractures Initiation of graben fractures?	
	Upper Boulder tuff	Continued movement on graben fractures	
	Upper Bedded tuffs	? Some movement on west ring fracture	Sandstone dykes in base of upper bedded tuffs
Reworking of upper tuffs		Large movement on Graben fractures	
	Eskduff lava	? Limited motion on northern graben fracture	
Limited reworking of exposed margins of upper tuffs			
Burial by Non-volc. seds.			

SCHEMATIC BLOCK DIAGRAM OF THE BENNAUNMORE VOLCANIC CENTRE

Illustrating the system of contemporaneous faults

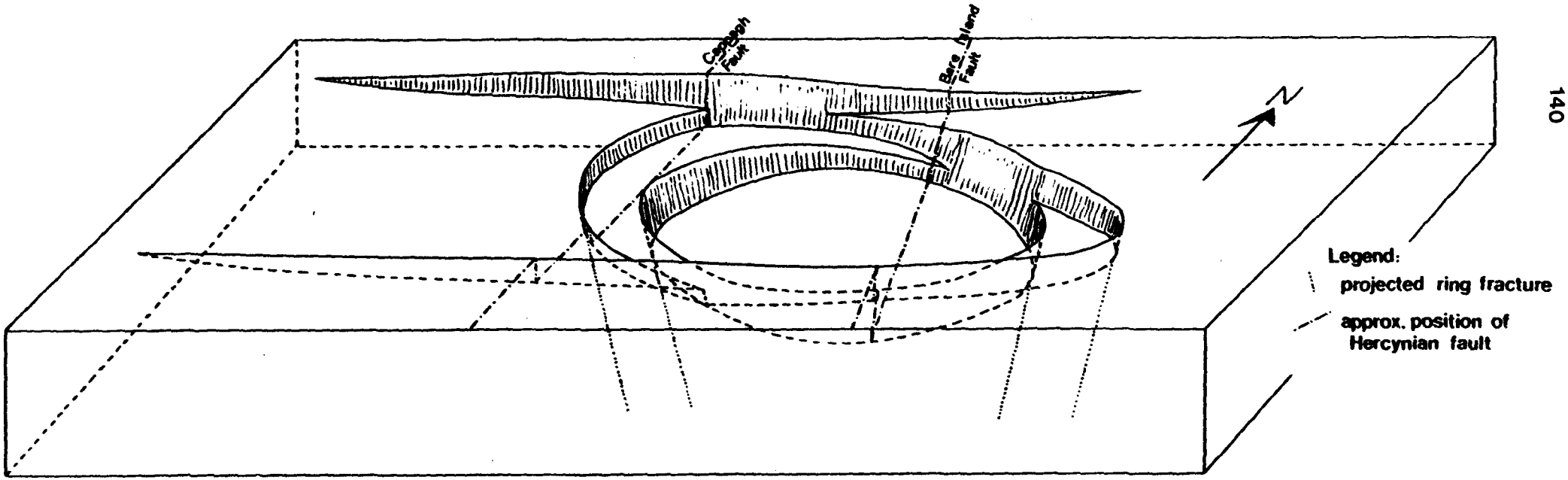

All sub-horizontal surfaces lie at the base of the volcanic sequence.

Fig. 5.14b

about 400 metres wide (locations 9746 and 9747 on fig. 1.5). The lava, which wedges out southeastwards, conformably overlies terrigenous sediments, and is overlain by the tuffs. The lava flow is blocky throughout, has a maximum thickness of 20 metres (fig. 5.15), and probably represents a distal portion of a more extensive flow lying to the north, which is not exposed. It is the only lava in the Lough Guitane complex that has a source which lies outside the main axial trend of the region.

As with other blocky lavas in the Lough Guitane area, the field appearance of this flow is highly variable in both texture and colour, but no systematic variation attributable to separate flow units was found. Four examples are illustrated in Plates 5.39 to 5.42. The various colours are all due to differing recrystallisation textures, and do not represent primary compositional variations. Thin section studies show that the darker fragments possess a much finer grained quartzofeldspathic matrix containing abundant finely disseminated opaque ore grains. The green type is relatively rich in chlorite, while the pale, often pink coloured type is coarser grained, quartzofeldspathic, and very poor in both chlorite and ore minerals. All of these recrystallisation textures possess the same phenocryst assemblage of small numbers of plagioclase laths and anhedral rounded crystals up to 5 mm in size with rare rounded quartz microphenocrysts, and chlorite or magnetite pseudomorphs after an unknown ferromagnesian mineral.

The tuffs cannot be traced along strike, but are structurally correlated with the thin distal reworked tuffs of the eastern extremities of the Bennaunmore volcanic centre, and the thin tuffs exposed at the northern end of the Horses Glen (fig. 5.15). Less than 10 metres thick, they are well bedded, with grading and common cross-stratification

major fault with lateral displacement

other geological boundaries

observed
inferred
speculative
} lava flow margin

lava flow isopach

150 estimated lava flow thickness (m.)

pyroclastics isopach

120 estimated thickness of pyroclastics (m.)

□□□ agglomerate

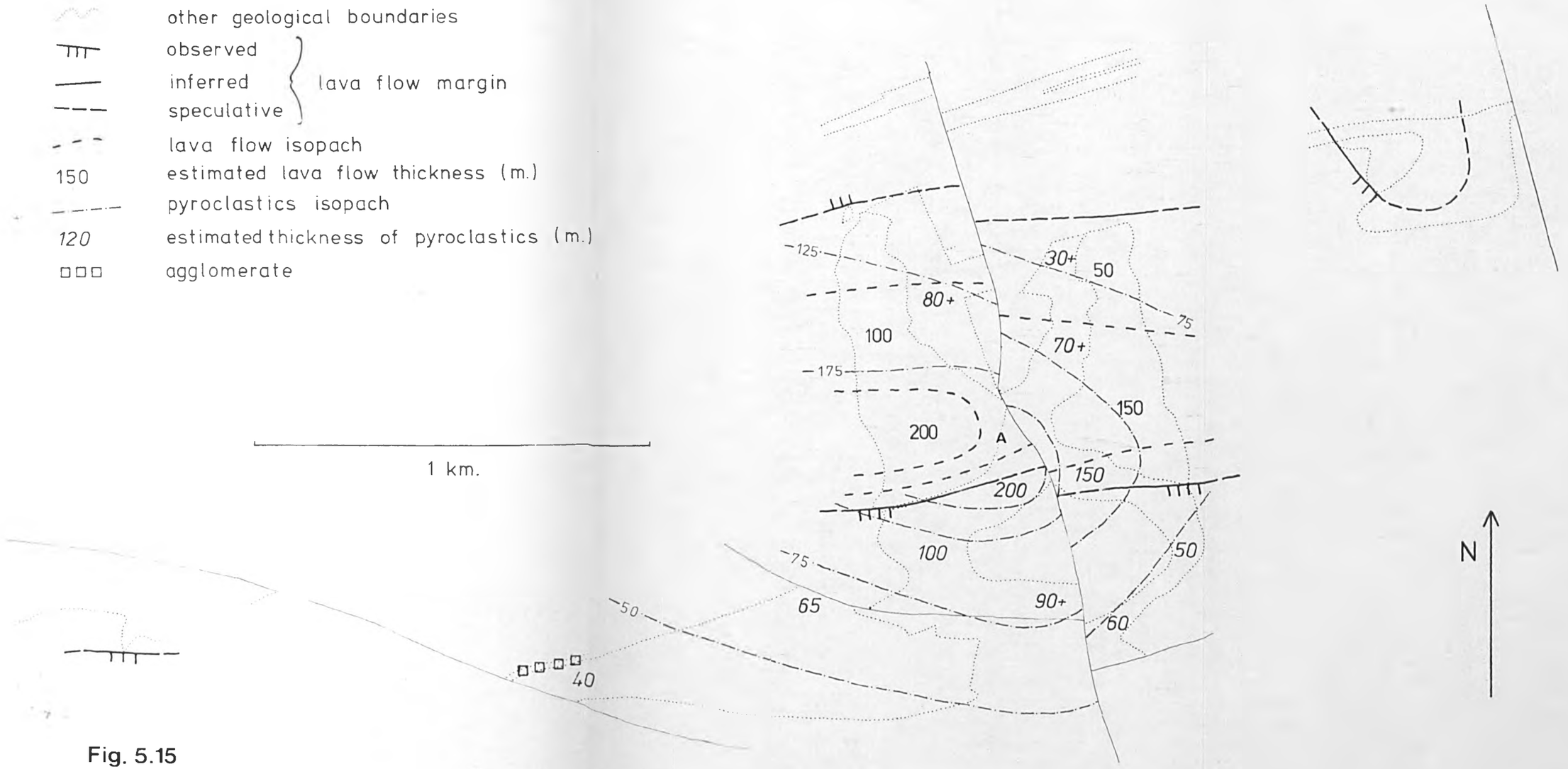

Fig. 5.15

Thickness Variations in the Lava and Pyroclastic Deposits of the Horses Glen Volcanic Centre

typical of the distal reworked tuffs from all the Lough Guitane volcanic centres. The lava which underlies these tuffs must therefore have an age similar to that of the Bennaunmore lava.

5.3 The Horses Glen Volcanic Centre

5.3.1 Introduction

Structural correlations suggest that the volcanics representing the Horses Glen volcanic centre are older than those of the Bennaunmore centre. Volcanic activity falls into two phases;

i) pyroclastic eruptions leading to the deposition of a sequence of tuffaceous sediments or mixed tuffs - the Lower Tuffs, and

ii) eruption of a thick rhyolite lava flow - the Horses Glen Lava.

5.3.2 The Lower Tuffs

Fig. 5.15 possesses isopachs for the Lower Tuffs which reach a maximum thickness of about 200 metres in the centre of the area, and thin rapidly in all directions. They lie conformably on terrigenous sediments of the Green Sandstone Formation into which some basal channelling up to 1 metre deep has occurred.

Evidence for the reworking of these deposits by water is very common. Plate 5.43 shows an example of shallow channelling in well bedded mixed tuffs. Plate 5.44 shows a rarer example of ripple cross stratification in fine sand grade mixed tuffs or tuffaceous sediments. Sorting and normal grading is also common. With one exception described on page 144 , the Lower Tuffs are very poor in volcanogenic clasts exceeding 1 cm in size.

The field appearance of these tuffs is governed by the same factors outlined for the Upper Tuffs of the Bennaunmore Centre (see section 5.1.6.2). The volcanogenic component of the Lower Tuffs is wholly rhyolitic, and mineralogically similar to the Horses Glen Lava.

Usually the volcaniclastic component is relatively small, and the Lower Tuffs show a marked decrease in the proportion of volcanogenic material towards the top of the sequence. The upper parts are characterised by beds of purely epiclastic sediment interbedded with thin laminations, the only identifiable volcaniclastic component of which is a small number of broken, white feldspar crystals between 1 and 5 mm in size.

The controls governing the genesis of the Bennaunmore Centre tuffs cannot be applied to the Lower Tuffs of the Horses Glen volcanic centre. There is no direct evidence that the latter tuffs were erupted in a "mixed" state. The fact that the Horses Glen Lava always overlies water lain sediments with a very small volcanogenic component suggests that a time interval elapsed between eruption of the bulk of the pyroclastics, and the later eruption of the Horses Glen lava during which little or no further pyroclastic eruptions took place and the tuffs were redistributed and mixed with epiclastic sediment.

The only coarse volcaniclastic material identified is found in the extreme west of the area, south of Lough Erlogh, at location 9148 (figs. 1.5 , and 5.15). In an outcrop 50-60 metres across, the top of the Lower Tuffs is characterised by a 3.5 metre thick unsorted agglomerate containing abundant subangular blocks of rhyolite lava commonly approximately 50 cm across but ranging up to 1 metre in size.

The base of the agglomerate is gently scoured, with a maximum relief of about 50 cm, and characterised by a particularly block-rich facies. This passes up into the central parts of the unit containing fewer blocks, and finally the top of the agglomerate where coarse blocks are again particularly common. All these internal variations are gradational, and no sharply defined boundaries were found. Throughout the matrix consists of a poorly sorted sand grade mixed tuff. These features are very similar to those exhibited by lahars described by

Williams and McBirney (1979, pages 171-178). Such a lahar might be related to the western margin of the Horses Glen lava. The coarsening of the base of the lahar is probably a result of a limited degree of gravitational settling of the larger blocks, while the coarsening of the top of the unit may have been due to later, preferential removal of some of the matrix by subsequent water currents. The upper surface of the agglomerate is irregular with large blocks protruding into the terrigenous siltstones that overlie it.

5.3.3 The Horses Glen Rhyolite Lava

The Horses Glen lava outcrops in high cliffs on both the east and west slopes of the Horses Glen. It conformably overlies the largely epiclastic sediments at the top of the Lower Tuffs. The thickness variations illustrated in fig. 5.15 suggest that the lava flow may have taken the form of a rather lop-sided dome or tholoid, being some 600-700 metres wide and with its thickest development of about 200 metres lying within 250 metres of its southern margin. The northern and southern margins of the lava flow are well defined, but its east-west lateral extent is not known.

The base of the flow is often irregular, with evidence for loading and disruption of the underlying sediments (see fig. 5.15position 'A'). The base of the lava possesses a maximum relief of 3 metres and may have irregular fragments of sediment incorporated into the 2-3 metre thick basal breccia (Plate 5.45) which passes up into flow laminated lava. The laminations are usually sub-parallel to the base of the flow. However, within the central parts of the flow, laterally discontinuous brecciated horizons have been observed, especially in the northwestern part of the outcrop. However, no overall systematic development has been observed which could lead to the distinction of more than one flow unit. The top of the lava is always brecciated

(Plate 5.46) and its surface irregular. Plate 5.47 is taken from the eastern side of the Horses Glen, and illustrates where the lava flow top has been overlain by laminated fine sandstones. The maximum relief on the surface of the lava is about 1 metre.

Unbrecciated, flow-laminated lava is usually pale green to pale grey in colour. Lath shaped or rounded plagioclase feldspar phenocrysts up to 5 mm in size are always present. Sporadic, glassy, rounded quartz microphenocrysts are widely distributed and irregular, dark ferromagnesian rich patches up to 5 mm in size, composed of chlorite or iron oxide are sometimes observed. The matrix sometimes exhibits a fine lace-like colour variation (Plate 5.48), especially in pale green examples, where millimetre size, irregularly shaped, paler areas are set in a darker matrix. Brecciated lava facies are characterised by an uneven surface due to the blocks being less resistant to weathering, and colour variations between incorporated blocks and the host lava matrix, including contrasting shades of green,grey, pink and brown (Plate 5.49).

In contrast with the Bennaunmore Volcanic Centre, evidence for large-scale contemporaneous faulting is absent, and therefore the rapid variations in lava flow thickness must have produced a marked and steep flow margin, which in the south must have approached 45°. This is a clear indication of the high viscosity and slow effusive rate of the lava. The blocky surface of the lava was almost certainly produced by autobrecciation, and the basal breccia by blocks rolling down, and being overidden by the slowly advancing flow front.

The eruption of the Horses Glen lava flow was the final volcanic activity of the Horses Glen Volcanic Centre.

5.3.4 The Devils Punch Bowl Rhyolite Lava

This lava outcrops in a small area northwest of the Devils Punch Bowl lake, and is structurally separated from the main sequence of the Horses Glen volcanic centre by the Lough Erlogh fault (see fig. 5.15 and 1.2). North of the fault the ground is drift covered, concealing the stratigraphic position of the lava relative to the Horses Glen volcanics.

From its exposed southern margin the lava thickens rapidly northwards (fig. 5.15). Neither the upper nor the lower contacts between lava and sediment are exposed, although these boundaries can be defined with confidence using closely adjacent exposures. The lava is always flow laminated, but never brecciated. Outcrops on the shore of the lake, near the base of the lava have a spherulitic texture, with numerous 2-3 mm wide, subcircular areas weathering out preferentially.

The lava is usually very deeply weathered due to well developed platy jointing. In the fresher broken specimens the matrix is a variety of shades of brownish, yellowish or pinkish grey. Small altered plagioclase phenocrysts are rare in comparison to the lavas so far described from other areas. They are often pale yellow and accompanied by irregular dark patches up to 2 mm in size. Quartz microphenocrysts were also observed.

This lava can be equally interpreted as an extrusive lava flow or a shallow intrusive body owing to the poor exposure, and absence of brecciation.

5.4 The Killeen Volcanic Centre

5.4.1 Introduction

Volcanic rocks derived from the Killeen volcanic centre outcrop along the hinge zone of the Mangerton anticlinorium in an elongate, east-west area, about 6 Km long and 1.5 Km wide situated east of Glen

Flesk. The deposits consist of a thick rhyolite lava flow termed the Killeen rhyolite lava which is overlain in the west by the Killeen tuffs, a sequence of mixed tuffs.

5.4.2 The Killeen Rhyolite Lava

Volcanic activity in the Killeen volcanic centre started with eruption of a thick rhyolite lava. The eastern and western margins of this lava flow are well defined (fig. 5.16). In its thickest part the lava exceeds 300 metres in thickness, and in the south and southwest the flow top exhibits a marked palaeoslope.

The base of the lava is nowhere brecciated, but is well flow laminated to within a couple of metres of, and usually subparallel to, the basal contact. The sediments immediately underlying the lava have been only slightly disturbed except near locality A (fig. 5.17) which provided the only evidence for contemporaneous faulting. Here the contact between lava and sediment is discordant and displays an irregular pseudointrusive relationship very similar to that described from contemporaneous fault zones in the Bennaunmore volcanic centre (section 5.1.5.1). The base of the volcanics is downthrown about 30 metres to the east.

Most of the lava is flow laminated and devoid of brecciation, however the flow top usually exhibits a thinly developed breccia about 2 metres thick, containing angular to subrounded blocks up to 50 cm in size. Only in the southwest corner of the area (fig. 5.17) was a breccia horizon observed within the body of the lava (location 'B') traceable for less than 100 metres. Some localised primary variation in phenocryst content has been observed, but no marker horizons were encountered which could have been used to subdivide the considerable thickness of lava exposed.

Near location 'C' (fig. 5.17) and around localities 8374/5 and 9586 (fig. 1.4) a strongly nodular facies was observed. In specimen

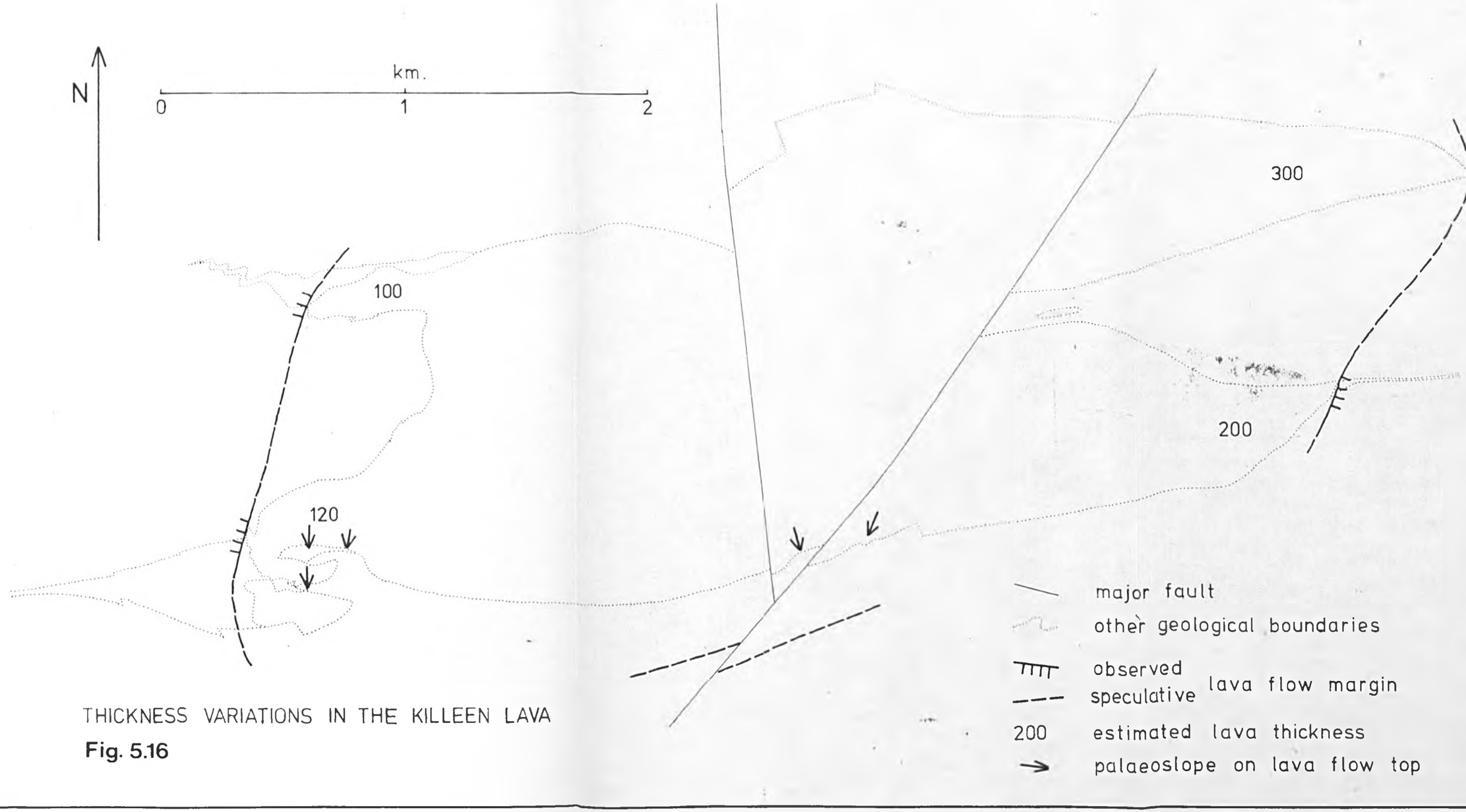

THICKNESS VARIATIONS IN THE KILLEEN LAVA

Fig. 5.16

Southwest Killeen
Volcanic Centre
Fig. 5.17

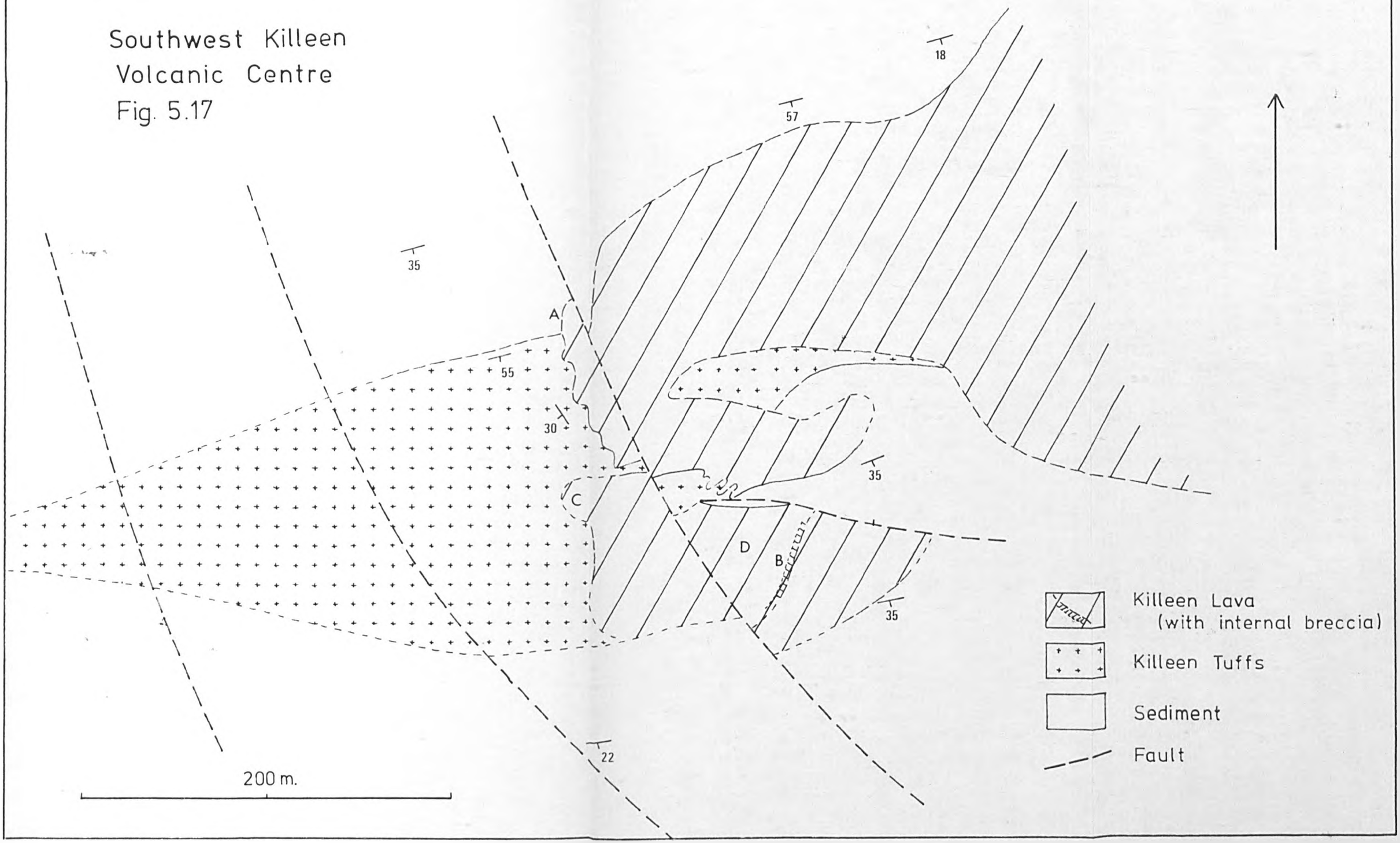

8374 (plate 5.50) the nodules, which are randomly arranged, usually 2-3 mm across and quartz filled, are considered to be relict vesicles, as they always exclude the phenocrysts. However, petrographic evidence has clearly shown that the nodular development at 'C' and around 9586 in the central part of the lava is derived from relict spherulites which formed in the glassy lava before the main secondary phase of recrystallisation.

As with previously described rhyolites of the Lough Guitane area, the extreme variability of the appearance of the Killeen lava is largely a product of the variation in character of the secondary recrystallisation and alteration. With one exception the phenocryst assemblage consists of two distinct types of feldspar phenocryst up to 3 mm in size; a subhedral lath-shaped type and a rounded type often associated with chlorite replacing an unknown ferromagnesian phenocrysts. Both feldspar types are always clouded by sericitic alteration and may be white or pink. In some specimens only the rounded feldspars are stained pink, the laths remaining white. Rounded quartz microphenocrysts up to 1.5 mm are rarely visible, and chlorite or iron oxide replace the unknown ferromagnesian phenocryst phase.

The lava is usually poorly jointed and massive, although a penetrative cleavage is sometimes developed near the base of the flow. The overall colour varies between shades of pale brown, green or pink, to darker greys where the recrystallisation is particularly fine grained.

The Killeen lava is directly overlain by terrigenous sediments in all but the western part of the volcanic centre, and although poorly exposed, the flow top appears to be irregular and undulating on a scale of a few metres. South of 8374 (fig. 1.4), the lava is overlain by siltstones and mudstones. The contact is sharp, and

embedded in the sediments, especially in certain horizones, well dispersed angular blocks of Killeen rhyolite between 5 and 30 cm in size are observed. Although no structures were identified within the sediments which indicated any disturbance by the blocks, it seems unlikely that they were carried to their final positions by the same currents which deposited the siltstones, but rather that they rolled down the sloping margin of the lava flow.

5.4.3 The Killeen Tuffs

5.4.3.1 A General Description

A sequence of bedded and sometimes massive tuffs overlie the Killeen lava in the west of the area (fig. 5.18). A very thin development of reworked tuffaceous sediments were also found in the far southeast of the area.

The apparently thickest development (approximately 120 metres), occurs immediately west of the western margin of the Killeen lava. Westwards the tuffs thin steadily and wedge out within 1 Km. Eastwards from the lava margin the thinning is even more dramatic (fig. 5.18). The relationship between the tuffs and the lava and a proposed sequence of events in the deposition of the tuffs is presented in fig. 5.19. The bulk of the tuffs form a wedge banked up against the lava flow margin, with only a thin development actually lying on the upper surface of the lava. This model is substantiated by the discordant dips measured in the tuffs immediately to the west of the flow margin. The westerly directed palaeoslope onto which the tuffs were deposited may have been as steep as 45^{o}.

The Killeen tuffs are similar to those described from elsewhere in the Lough Guitane area in that they always contain an epiclastic component made up of angular sand grains, silt/mud flakes and rare rounded sandstone fragments up to 15 cm in size. However, they are

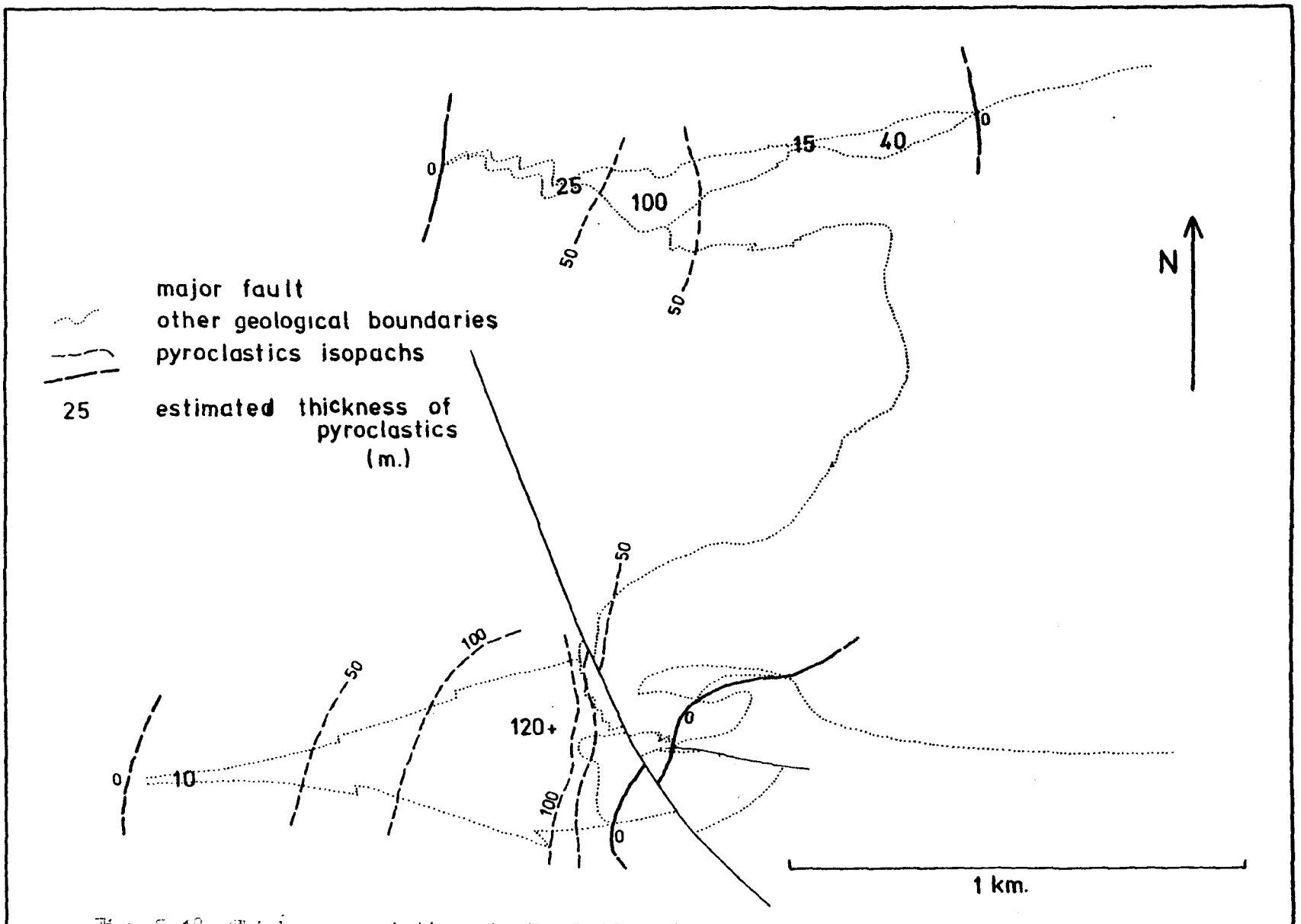

Fig. 5.18 Thickness variations in the Killeen Tuffs.

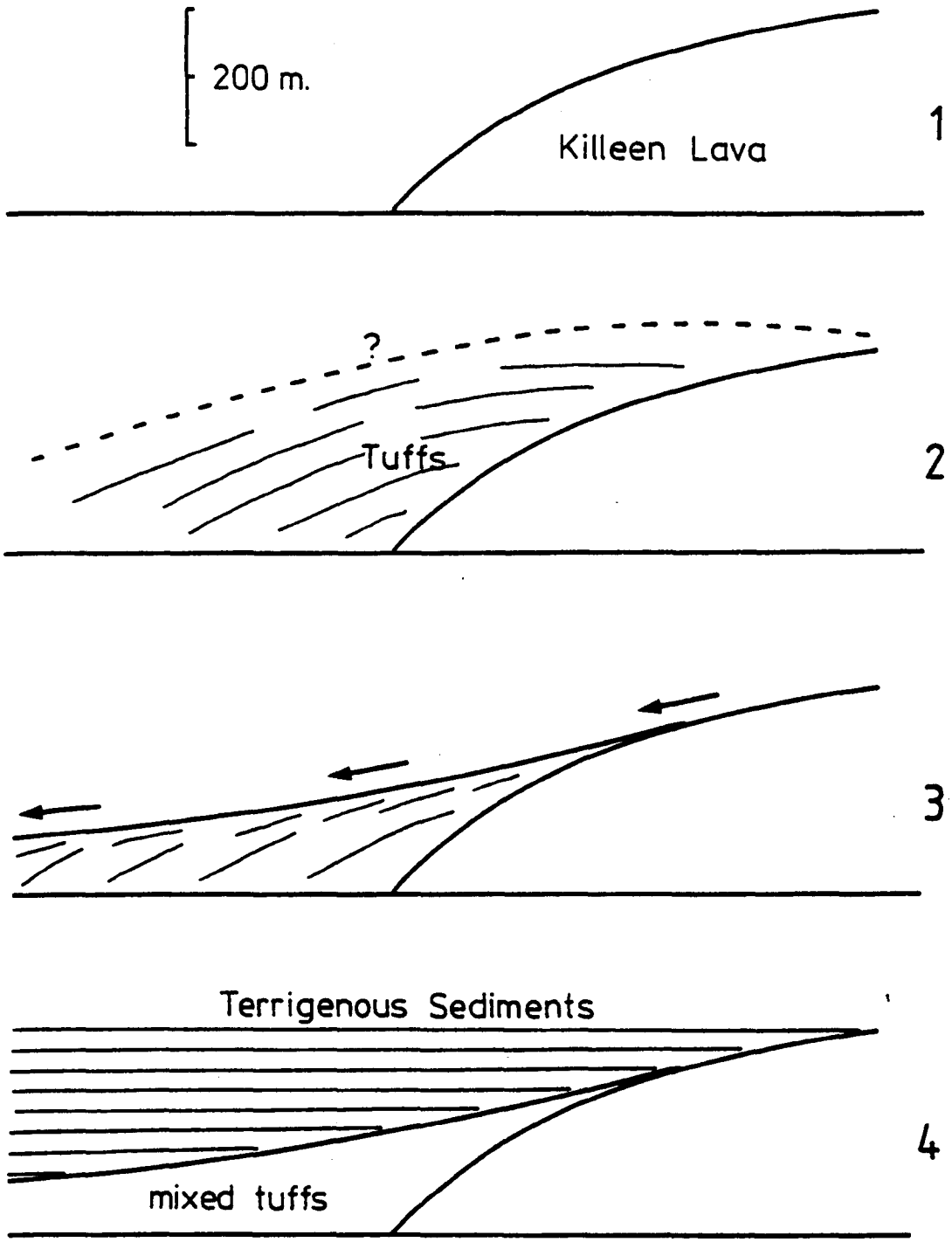

Fig. 5.19 Proposed evolution of the SW. part of the Killeen volcanic centre.

unique in containing three types of lava clast easily distinguishable in the field in addition to a third noted only in thin section. The tuffs also contain broken feldspar crystals and fine grained recrystallised ash.

The three types of clast, ranging in size from lapilli to small blocks, are distinguished primarily by colour. Previous studies of colour variations within the acid volcanics of the Lough Guitane area have proved them to be due to variable secondary recrystallisation processes. Closer examination of these tuffs was made in an attempt to find other features which might indicate primary and possibly petrogenetic differences.

Group A: The clasts have a pale colouration, and strongly resemble the Killeen lava. They are always angular, and range up to 20 cm in size although lapilli sized clasts are most common.

Group B: - have a dull slaty or soapy appearance with numerous small euhedral to rounded, white or pale brown feldspar laths and rare glassy quartz microphenocrysts. These clasts range in size from 2-3 mm, up to rarely 50 cm. Most are angular, or subangular in shape. The groundmass is dominated by sericite and may or may not contain broken spherulites.

Group C: - contains only one observed clast over 20 cm in size which appeared to be spindle shaped (specimen 9305). The phenocryst content is essentially the same as that of group B, but the feldspar laths are arranged subparallel to the margin of the clast. Plate 5.51 illustrates a cut section through this specimen. Thin section study of this very dark coloured clast has revealed a matrix dominated by chlorite and thus is unique among the volcaniclasts.

Group D: - are exclusively ash and lapilli sized clasts which are of a composition and texture radically different from any rocks exposed

in the Lough Guitane area. Thin section study reveals a doleritic texture (see section 6.5.2).

The hypothesis suggested is that groups A and B represent reworked accessory ejecta derived either from the vent or the overlying lava through which the eruption took place. Group C may represent juvenile material, originally of the same composition as groups A and B. The matrix has however been preferentially chloritised, a process probably related to its petrogenesis and subsequent rapid cooling. Group D must have been derived from the wall rocks of the vent at a depth greater than the oldest rocks exposed in the Lough Guitane complex i.e. below approximately 800 metres.

Near the margin of the lava the bedded tuffs sometimes exhibit poor grading, but elsewhere they show abundant evidence of reworking, cross lamination and sorting being common. Towards the distal parts of the deposits the tuffs are interbedded with wholly epiclastic sediments. The thin tuffs which overlie the Killeen lava can be classed as mixed agglomerates containing blocks of types A, B and C in a mixed tuff matrix.

In the northwest the tuffs are also banked up against the margin of the Killeen lava. The thickness variations (fig. 5.18) are very similar to those described from the southwest. Only type A volcaniclasts have been observed, and thick massive units are rare. Most of the tuffs are well-bedded and show evidence for reworking by water.

The thin tuffs observed in the far southeast of the area have a very low volcaniclastic component and may have been reworked from the brecciated surface of the Killeen lava to the north and west.

5.4.3.2 Petrogenesis of the Killeen Tuffs

The presence of agglomerates high on the sloping margin of the lava is very important when discussing the petrogenesis of the

Killeen tuffs. Of particular significance is the presence of an epiclastic component to the matrix. The two possible mechanisms by which epiclastic material can become mixed with these tuffs are:

i) Mixing in the vent during eruption

and, ii) Mixing during water reworking.

The agglomerate overlying the lava represents stratigraphically the highest pyroclastic deposit. The upper surface of the Killeen tuffs, in sympathy with the margin of the Killeen lava must have possessed a pronounced palaeoslope directed towards the west and the sediments which are observed dipping gently towards the lava margin are devoid of volcanogenic material. This indicates that the burial of the Killeen lava and the Killeen tuffs involves little or no reworking and that the present gross morphology of the volcanic pile in the southwest was not substantially modified by the currents depositing the terrigenous sediments involved in the burial.

Any reworking of the tuffs high on the margin of the lava must have been caused by water run-off from the surface of the flow and would have had no epiclastic sediment load. Hence, the epiclastic component of these agglomerates cannot have been carried there by any fluvial process operating in the adjacent alluvial plain.

The only alternative is option (ii) above, that these tuffs were erupted in a mixed state; the same conclusion as was reached for the petrogenesis of the Bennaunmore Centre volcaniclastics. The presence of the dolertic group D clasts in these tuffs implies that much older volcanic activity must have occurred in the region.

5.5 General Summary - The Relative ages of the Three Volcanic Centres

The Bennaunmore and Eastern Volcanic Centres have provided strong evidence for mixing of volcaniclastic and epiclastic material during

eruption. Nowhere in the Lough Guitane area have unmixed pyroclastics been seen. The considerable thickness of wet unconsolidated or partially consolidated sediments through which the volcanics passed must have had a powerful influence over the style of eruption.

Fig. 5.20 presents a schematic section through the whole of the area under study from east to west illustrating the probable age relationships between the three volcanic centres. The Bennaunmore and Eastern Volcanic centres were developed at roughly the same horizon on the grounds of structural correlation across Glen Flesk.

The tuffs at the extreme northern end of the Horses Glen are assumed to be the western distal developments of the Bennaunmore Centre tuffs, also on structural grounds. The Horses Glen Centre volcanics are thus stratigraphically separated from the Eastern and Bennaunmore Volcanics by about 200 metres of sediment. The relative age of the Devils Punch Bowl Lava is not accurately known.

Further discussion of the volcanism in relation to other features of the Lough Guitane area occurs in the final chapter.

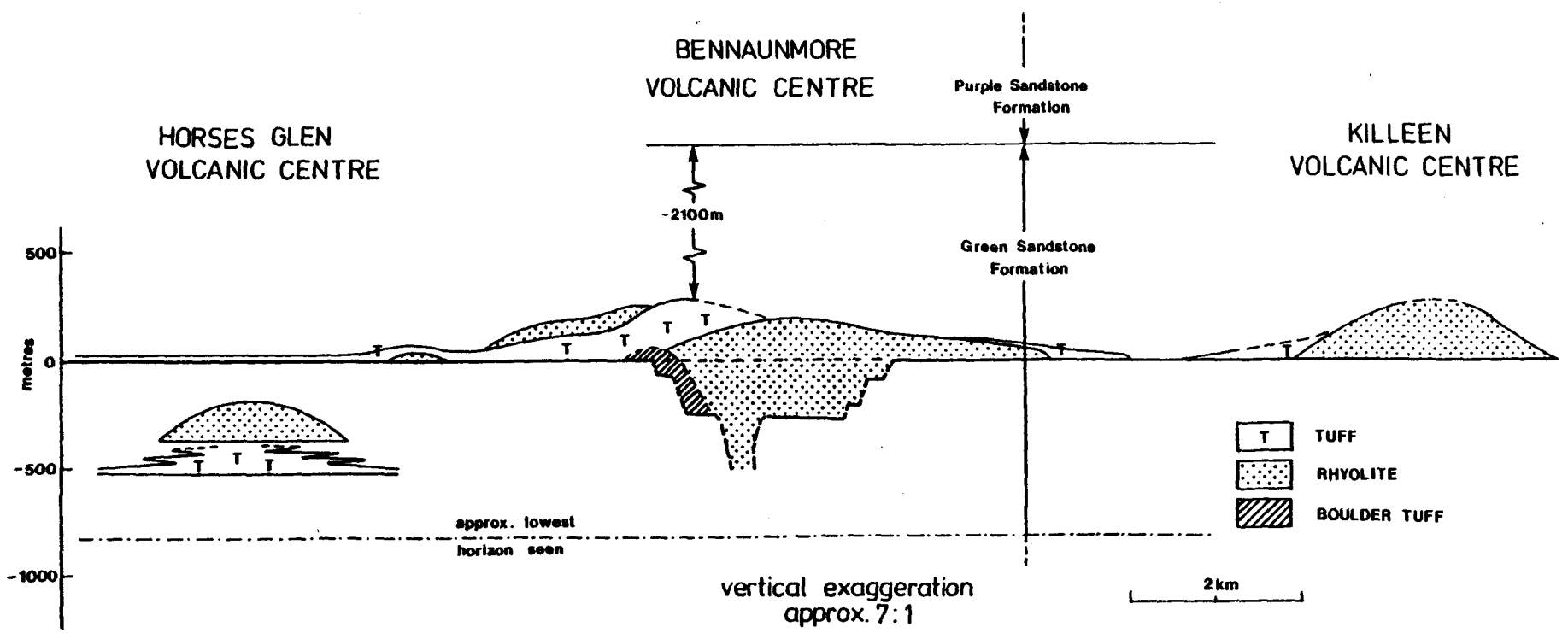
Schematic East-West Section
Through the Lough Guitane Volcanic Complex
BENNAUNMORE
VOLCANIC CENTRE
Purple Sandstone
Formation
HORSES GLEN
VOLCANIC CENTRE
KILLEEN
VOLCANIC CENTRE
~2100m
Green Sandstone
Formation
500
0
-500
-1000
metres
T
T
T
T
T
T
T
T
T
T
T
approx. lowest
horizon seen
T TUFF
RHYOLITE
BOULDER TUFF
vertical exaggeration
approx. 7:1
2km

Fig. 5.20

CHAPTER 6

Petrology

6.1 General Introduction

The Lough Guitane lavas can be divided on petrographic grounds into two groups, each of which is characterised by the mineralogical and textural uniformity of its members. Any small variations from flow to flow are dealt with separately.

In the Bennaunmore Lava Group are the Devils Punch Bowl lava, the Horses Glen lava, the North Stoompa lava, the Eskduff lava and the least altered member, the Bennaunmore rhyolite lava. The second group consists of all the examples of rhyolite lava collected from the Killeen volcanic centre, the Killeen Lava Group.

In general the petrographic descriptions refer to the least altered specimens available unless otherwise specified.

6.2 The Bennaunmore Lava Group

6.2.1 The Phenocryst Assemblage

Quartz, plagioclase and an unknown mafic mineral pseudomorphed by chlorite and sericite are ubiquitous phenocryst phases. Their modal percentages are presented in appendix **F** . Total phenocryst contents are usually about 3 modal percent, ranging up to 5 modal percent.

Quartz phenocrysts are rounded to subhedral, rarely embayed, and range between 0.2 and 1.5 mm in diameter, and always occur as discrete crystals. Subhedral varieties sometimes exhibit a rounded hexagonal form (Plate 6.1). They may also often exhibit fractures and deformation lamellae (Plate 6.2), and trains of bubbles (Plate 6.1).

Plagioclase phenocrysts occur as discrete, partially rounded laths up to 5 or 6 mm long, but also in crystal clusters which may be associated

with a chloritised mafic mineral. Apart from rarely identified xenocrysts, these clusters include all the remaining phenocryst phases. They exhibit a variety of morphologies and textures which can be classified as follows.

i) Irregular groups of laths sometimes apparently related by a common nucleation centre.

ii) Clusters of anhedral or irregular grains with broken or slightly rounded outlines, and possessing an allotriomorphic-granular texture which may include a pseudomorphed mafic phase (Plates 6.3 and 6.4).

iii) Type (ii) clusters grade into glomerocrysts dominated by the mafic phase which may have no associated plagioclase (Plate 6.5).

Both types (ii) and (iii) commonly act as nucleation sites for plagioclase laths often rendering the correct classification of some crystal clusters impossible. Hence no distinction is made between the three types of cluster in the modal analyses (appendix F).

In the plagioclase, albite twinning is ubiquitous and combined Albite-Carlsbad twins common. The extinction angles of the latter were used to determine a plagioclase composition of nearly pure albite (An_{0-5}). In all types partial replacement by fine-grained white mica or sericite is ubiquitous (Plate 6.3), and irregular patches of calcite are common. The sericite may occur as either randomly oriented flakes or aggregates or preferentially aligned along cleavages or other crystal planes, or along fractures. Sericitic replacement may be virtually absent in patches where large numbers of finely disseminated opaque iron ore inclusions occur. The concentration of the opaque inclusions is variable, but probably responsible for the pale brown or pink colour of the plagioclase in hand specimen.

In partially silicified specimens levels of sericitic alteration

and opaque ore clouding is generally reduced, while in strongly foliated types the plagioclase may be almost entirely replaced by sericite and calcite.

Anatase, zircon, apatite, magnetite, allanite, leucoxene and sphene (in order of abundance) have all been recorded as small inclusions in, or associated with plagioclase phenocrysts. However, the highest concentrations of such inclusions occur in the pseudomorphed mafic phenocrysts (or PMP.s).

PMP.s occur as discrete irregular patches of chlorite and/or sericite (Plate 6.5), or intergrown with clusters of irregular plagioclase crystals of types (i) and (ii) above (Plates 6.4 and 6.6). Chlorite is usually the dominant replacement, but some specimens contain pseudomorphs dominated by sericite with a little stilpnomelane and opaque ore in irregular aggregates or rimming the phenocryst. In these generally more altered specimens, amorphous opaque minerals may also cross the PMP.s in trains, possibly following original crystal fractures or cleavages.

The PMP.s range up to 4 mm in size, and when enclosed in a crystal cluster their morphology is controlled by the crystal faces of adjoining plagioclase crystals, i.e. infilling the interstices between feldspars (Plate 6.4). The chlorite occurs as parallel or radiate bundles of flakes, whereas the finer sericite is found as parallel bundles.

The most impressive feature of the PMP.s is their high content of accessory minerals (Plates 6.5, 6.6 and 6.7).

Zircon occurs as small, stumpy to elongate crystals commonly between 0.01 and 0.05 mm long (rarely up to 0.25 mm) are generally rounded (Plates 6.7 and 6.8) and corroded (Plate 6.9), although, rarely, almost euhedral examples have been found (Plate 6.8). Modal percentages of zircon included in PMP.s range between 0.0 and 10.0 percent (Plate

6.6) and when embedded in chlorite are always surrounded by dark pleochroic halos. The zircons may be well scattered or grouped in microglomerocrysts associated with anatase (Plates 6.8, 6.10, 6.11 and 6.12) in both the PMP.s and the plagioclase phenocrysts and sometimes in the groundmass.

Sphene has only rarely been identified, and electron microprobe analyses (Chapter 7) has demonstrated that anatase is the commonest titanium bearing mineral, occurring as anhedral grains up to 0.05 mm in size. It occurs as discrete crystals or irregular aggregates (Plate 6.10) or as elongate aggregates (Plates 6.11 and 6.12) perhaps as a pseudomorph after rutile. The anatase is commonly rimmed with an irregular and amorphous overgrowth of leucoxene (Plate 6.10).

Allanite occurs as discrete subhedral or rounded grains up to 0.5 mm in size, and also as intergrown aggregates (Plate 6.5). The mineral is moderately pleochroic from brick red to pale yellow or greenish-yellow and often exhibits both simple and multiple twinning. When enclosed in chlorite it is surrounded by a dark pleochroic halo. Although common in the PMP.s (approx. 9.0 modal percent), allanite is a rare inclusion in the plagioclase phenocrysts and in the groundmass.

Apatite is common in both the PMP.s and the plagioclase phenocrysts, occurring as euhedral to subhedral elongate crystals (Plates 6.5 and 6.6).

Opaque ore minerals occur as amorphous aggregates up to 0.03 mm across, often associated with leucoxene or anatase (Plates 6.7 and 6.8).

Calcite is a common replacement mineral in the PMP.s, and may be almost complete.

6.2.2 Microxenoliths and Other Unusual Minerals

a) In the Bennaunmore lava

Plate 6.13 illustrates a microxenolith almost entirely composed

of a microgranular aggregate of anhedral plagioclase crystals with a unique twinned plagioclase overgrowth. While all of the feldspar is now albite, such an overgrowth indicates a marked disequilibrium between the aggregate and magma.

Plate 6.14 shows a unique rounded microxenolith composed of quartz, allanite and an unidentified pale blue mineral with very high refractive index (> 1.9) which might possibly be anatase (in contrast with grains of yellow anatase elsewhere in the thin section). This blue mineral appears to rim the irregular quartz grains, separating them from the allanite.

Fluorite has been observed in 3 specimens (8371, 8418 and 8795) as discrete irregular patches up to 1.4 mm in length (Plate 6.15), and also apparently replacing PMP.s in the crystal clusters. Fluorite has been very rarely observed as a subhedral inclusion in a plagioclase phenocryst. Included minerals are commonly chlorite and sericite along with apatite, zircon, (Plate 6.16) anatase, magnetite and quartz. Zircon induces a strong purple coloured halo in the fluorite.

Chalcopyrite has been identified as small anhedral patches embedded in allanite in a number of sections cut from specimen 8392 (e.g. Plate 6.17). Chalcopyrite has also been observed in the Green Dyke (specimen 8742A). A zone immediately surrounding the chalcopyrite possesses a bright orange colouration which grades into normal allanite. Electron microprobe analyses revealed this zone to be identical in major element content to the normal allanite suggesting that a trace element may be causing the colour.

b) In the other lavas

Plate 6.18 illustrates a unique example of chessboard albite (Battey, 1955; Smith, 1974) from the Eskduff rhyolite lava, which exhibits apparent partial resorption by the groundmass along some of the

boundaries between the "tiles" or "grains". Similar types of chessboard albite have been recorded from the Horses Glen and Devils Punch Bowl lavas. The overall rounding of these aggregates is in contrast with the irregular outline of a chessboard albite from the North Stoompa lava (Plate 6.19) which also lacks the intergrain resorption described above.

Plate 6.20 illustrates a unique phenocryst pair consisting of an albite lath intergrown with a rather irregular, partially embayed quartz crystal.

Small muscovite books up to 0.2 mm in size have been identified from the Horses Glen and Devils Punch Bowl lavas. They always contain fine amorphous opaque iron ore which is strongly developed along cleavage traces.

6.2.3 Groundmass Mineralogy and Secondary Textures

The groundmass is completely recrystallised and felsitic, and is generally microcrystalline to submicrocrystalline. Chlorite, sericite and calcite are common minor constituents, but the groundmass is dominated by a very fine grained intergrowth of quartz and feldspar, sometimes arranged in a snowflake texture. The chlorite, sericite and rarely stilpnomelane are patchily distributed, sometimes in a lace-like pattern, or concentrated in phenocryst strain shadows (Plate 6.14).

Opaque ore minerals are common as minute subhedral to anhedral grains, or as amorphous aggregates up to 0.05 mm in size. Many specimens contain leucoxene in similar aggregates. Most sections contain calcite in irregular patches, often in strain shadows or zones of low strain, e.g. inside spherulites or phenocrysts. Allanite is present as rare, small irregular crystals often in association with chlorite. Anatase, zircon and apatite are rare accessories. In some more altered specimens stilpnomelane is more common along with haematite.

In partially silicified specimens coarser quartz occurs in irregular patches up to 1 mm across with chlorite less abundant (Plate 6.21). Some specimens, especially those from near the base of the lava, are foliated, with marked alignment of a sericite-rich groundmass.

Some sections from the Horses Glen lava possess a groundmass composed entirely of subparallel, intergrown and cloudy albite microlaths. Others show segregation textures (Plate 6.22) in which irregular areas of chlorite-free, sericite-poor coarser grained felsite are delimited from finer grained chlorite and sericite rich felsite by a discontinuous band of chlorite.

6.2.4 Relict Primary Groundmass Textures

a) Spherulites

Many sections possess spherulitic textures. In the Bennaunmore lava they are preserved by very fine grained cores of radiate feldspar rimmed with a coarser intergrowth of irregular grains of quartz and feldspar (Plate 6.23). They may occur discretely or in groups, and frequently occur centred upon a phenocryst or as an incomplete overgrowth presumably using the crystal as a nucleation agent. In the Eskduff lava the spherulites may be flattened (Plate 6.24) and do not possess an outer coarse quartzo-feldspathic overgrowth.

b) Flow lamination

In thin section the flow laminations observed in hand specimen are represented by subtle, but well-defined variations in the grainsize of the felsite, and the abundance and habit of the chlorite flakes. In more altered specimens particular lamellae are marked by highly silicified or sericitised zones (Plates 6.25 and 6.26). No significant systematic variation in phenocryst content between lamellae was detected.

c) Relict perlitic cracks

Perlitic cracks are rarely preserved in the Bennaunmore lava, but

well preserved in the Eskduff lava where they are defined either by circular or subcircular trains of chlorite or sericite (Plate 6.24), or by the circular pattern of grain boundaries within the felsite groundmass itself.

d) Vesicles

Only in the Eskduff lava are vesicles up to 1 mm across clearly preserved (Plate 6.24). They are filled with clear unaltered fibrous albite arranged in a radiating pattern which gives a cruciform extinction in crossed polars. Some are crossed by trains of chlorite flakes, and many are rimmed with chlorite. Phenocrysts are never observed included in these relict vesicles.

e) Autobrecciated textures

Specimen 7211 exhibits a fine example of the relict autobrecciated textures commonly encountered. In thin section they are characterised by the wide variety of recrystallisation textures within the discrete fragments (Plate 6.26). Some fragments in this section exhibit an unusual texture of aligned ore grains (Plate 6.27) suggestive of a primary texture similar to perlitic cracks.

6.2.5 Veins

Quartz, quartz-albite, and quartz-albite-chlorite veins occur commonly as dilational infills up to 1 mm across, but non-dilational replacement veins are also encountered. Plate 6.28 illustrates a rare quartz-albite-chlorite-allanite vein.

6.3 The Killeen Lava Group

6.3.1 The Phenocryst Assemblage

Quartz phenocrysts up to 1 mm in size are commonly rounded or embayed and only rarely subhedral. Feldspar phenocrysts are always albite in composition (An_{0-5}), but unlike those of previously described lavas can be divided into two quite distinct categories.

i) albitised and sericitised plagioclase crystals corresponding to all the feldspars of the Bennaunmore Lava Group and

ii) feldspars interpreted as albitised K-feldspars which possess radically different characteristics, and are never observed in association with pseudomorphed mafic phenocrysts (or PMP.s).

The features of types (i) and (ii) plagioclase phenocryst are summarised in table 6.1

i) In common with the feldspar phenocrysts of the Bennaunmore lava group these plagioclases may be either lath shaped, between 1 and 2 mm in length, or broken and anhedral as members of crystal clusters. Some of the broken crystals appear to have acted as nucleation centres for the subhedral laths. Albite twins are common, and pass uninterrupted through the entire phenocryst. Inclusions of apatite and zircon are common.

Alteration of the plagioclase is dominated by randomly oriented sheaves of sericite. Replacement may be complete in some instances (Plate 6.29). Calcite in association with amorphous opaque ore (possibly haematite due to the red colour of translucent grains) in aggregates may also replace large portions of a phenocryst. Chlorite and stilpnomelane are common minor alteration minerals and submicroscopic disseminated opaque ore is ubiquitous. The concentration of this fine dusting of opaque minerals may be higher in either one or the other type of phenocryst.

ii) The albitised K-feldspar phenocrysts are usually subhedral, rounded or embayed, up to 2 mm in size, or sometimes elongate/rounded and rather lath-like. They are almost always discrete crystals. Despite their nearly pure albitic composition, the most distinctive feature is the ubiquitous presence of apparent perthitic intergrowths including string or braid perthites on a very fine scale (Plate 6.30),

Table 6.1

	Type (i) Albitised Plagioclase	Type (ii) Albitised K-Feldspar
Gross Morphology	lath shaped, straight edged or broken as part of glomerocryst	rounded to oval
Twinning	albite law polysynthetic continuous	patchy discontinuous polysynthetic in disseminated ore-poor regions relict perthitic textures
Alteration	sericitization ubiquitous with some chlorite and calcite	sericite only occurs along fractures chlorite rare
Inclusions	non-abundant, but evenly distributed ore	patchily disseminated ore relatively high concentrations lead to pinkish colour in some hand specimens
Associated Minerals	occasionally crystal clusters commonly in groups of 2 or more which may include P.F.P.s	rarely in groups of 2 or more

and patch perthites. The latter type are characterized by albite twinning of patches relatively free of disseminated opaque ore grains demarcated by untwinned areas rich in ore grains (Plates 6.31 and 6.32). Those phenocrysts possessing the fine scale string/braid perthite occasionally exhibit zoning (Plate 6.33) defined by concentrations of opaque ore grains and breaks in the perthite.

Sericitic replacement is poorly developed in the K-feldspars, and occurs in discrete small patches or along crystal fractures together with chlorite and stilpnomelane in some sections. Inclusions of zircon, apatite and elongate aggregates of opaque ore granules are common.

Pseudomorphed mafic phenocrysts (PMP.) are common, rounded, up to 3 mm in size, and nearly always intergrown with albitised plagioclase in crystal clusters (Plate 6.34). The replacement minerals are usually opaque ore, possibly hematite, and white mica in various proportions and textures. In badly altered specimens amorphous opaque minerals dominate the replacement. The white mica occurs as randomly oriented sericitic flakes, but also as optically continuous patches up to 0.25 mm across. The $2V_{\alpha}$ of these white micas is about -10^{o}. Such a small optic axial angle is unusual for a muscovite sensu stricto, although phengites have been recorded with equally low optic axial angles (Deer *et al.*, Vol. 3, 1962). A phengitic composition is confirmed by electron microprobe analyses of white micas from other lavas (Chapter 7).

In well preserved examples, the PMP are crossed by relict fractures infilled by sericite and lined with opaque ore (Plate 6.34). The fractures are irregular and not crystallographically controlled. Inclusions of zircon, often in aggregates, are common.

Subhedral books of yellowish pleochroic white mica also occur as a rare phenocryst phase up to 0.8 mm in length. Opaque ore is

distributed along cleavage planes. These phenocrysts are only rarely included in PMP-plagioclase crystal clusters. Needle-like micro-phenocrysts up to 1 mm in length occur as discrete crystals and as inclusions in other phenocrysts. In fresher specimens they consist of strings of anatase crystals rimmed by amorphous opaque ore. This mineralogy coupled with the phenocryst morphology suggests that they may be pseudomorphs after rutile.

To briefly recap, the crystal clusters in the Killeen lava group consist of pseudomorphed mafic phenocrysts in roughly equal proportions with intergrown albitised plagioclase crystals which may be lath shaped or broken, and may be completely enclosed in the PMP.

6.3.2 Microxenoliths

Plate 6.35 illustrates a partially disaggregated microxenolith of fine sandstone characterised by a loosely associated group of angular quartz grains.

Plate 6.36 illustrates examples of a quartz-muscovite type of microxenolithic aggregates found in specimen 9446. The equigranular quartz grains range between 0.1 and 0.2 mm in length and possess both dimensionally preferred and partial lattice preferred orientations. The muscovite flakes are considerably larger than any observed elsewhere in the section, and range up to 0.5 mm in size. Although the preferred orientation of the quartz grains is suggestive of crystallisation under high stress, the orientation of the crystal long axes varies from aggregate to aggregate. Such granoblastic-elongate textures (Spry, 1979 p. 263) are incompatible with the metamorphic history of the lava, thus implying a xenolithic, deep crustal origin.

6.3.3 The Groundmass

The groundmass mineralogy of the Killeen Lava Group is essentially the same as that of the Bennaunmore Lava Group. The grain size of

recrystallisation is however very variable, often within a single thin section. The more altered specimens usually possess the coarser groundmasses (average grain-size approx. 0.3 mm) and indicate a degree of silicification (Plate 6.37) with irregular patches or bands of larger quartz crystals replacing the groundmass. Minor constituents include disseminated and aggregated amorphous opaque ore, leucoxene aggregates, zircon often attached to rutile pseudomorphs, rarely preserved anatase, and variable quantities of calcite and chlorite.

The Killeen Lava Group present abundant evidence for the original glassy state of these flows. Commonly relict perlitic cracks are preserved as trains of sericite flakes (Plate 6.38) or chlorite in a very fine grained felsitic matrix, or by organised patterns of the crystalline groundmass which may be replaced by calcite (Plate 6.39). The perlites are usually between 0.5 and 1.0 mm across.

In some sections relict spherulites reminiscent of those found in the Bennaunmore lava are present (Plates 6.23 and 6.40), but others in finer grained groundmasses may be more clearly defined by a sercitic rim surrounding a radiating quartz-feldspar-sericite interior (Plate 6.41). A phenocryst is often at the centre of a spherulite, and Plate 6.42 shows two interferring spherulites apparently nucleated on an albite phenocryst.

Another texture (Plate 6.40) illustrates quartz pseudomorphs after tridymide needles embedded in an albitic matrix.

6.4 The Minor Intrusions

6.4.1 The Felsite Dyke (Specimen 9787) and the Pale Dyke (Specimen 8859)

The plagioclase phenocrysts (An_{0-5}) are identical in habit and abundance to those of the Bennaunmore Lava Group, including laths, and

rounded crystal clusters associated with pseudomorphed mafic phenocrysts. Chloritic and sericitic replacement is not well advanced, but a fine dusting of disseminated opaque ore is ubiquitous. Quartz phenocrysts are absent.

In the Felsite dyke the groundmass is dominated by fine grained elongate quartz-feldspathic patches up to 4 mm long, and separated by narrow zones rich in matted chlorite and sericite. Fibrous albite in spherulites up to 1 mm across is common, and subhedral albite laths between 0.1 and 0.4 mm long are also present. Anatase and leucoxene occur rarely with zircon in microglomerocrysts.

In the Pale dyke the groundmass consists almost exclusively of fine grained fibrous albite exhibiting undulose, and sometimes cruxiform extinction. Individual mats of albite measure between 0.01 and 0.1 mm in size. Subhedral albite laths up to 0.2 mm in size occur rarely, and minute flakes of chlorite and sericite are very rare. Fine grained opaque ore occurs with leucoxene in small aggregates, and zircon, up to 0.2 mm occurs as discrete subhedral to anhedral crystals, or as aggregates sometimes associated with anatase, opaque minerals and chlorite. Some zircons exhibit evidence for two phases of growth with well defined cores which are optically continuous with the later overgrowth (Plate 6.43).

6.4.2 The Green Dyke

Subhedral to rounded quartz phenocrysts up to 1.2 mm in diameter may be often embayed, strained and sometimes fractured crystals. They may have a thin fibrous albite rim. Plagioclase phenocrysts present include all types observed in the Bennaunmore lava except the chequer albite. Alteration/replacement is ubiquitous, usually by patchy sericite or stilpnomelane. Finely disseminated ore is common, and small aggregates of zircon and anatase occur as inclusions along with

euhedral to subhedral apatite. Ferromagnesian pseudomorphs also strongly resemble those described from the Bennaunmore Lava with high contents of zircon and anatase.

The Groundmass (Plate 6.44) is dominated by fine grained chlorite with ill-defined irregular patches of quartz up to 0.2 mm and albite microlaths up to 0.2 mm. Small irregular patches of fibrous albite occur up to 0.5 mm which sometimes resemble the micropegmatitic spherulites described from the Bennaunmore Lava. A poorly developed foliation may be produced by the streaky development of sericite.

6.5 The Volcaniclastic Sediments

6.5.1 The Bennaunmore and Horses Glen Volcanic Centres

Without exception, all the tuffaceous deposits of the Lough Guitane volcanic complex consist of a mixture of (i) volcaniclastic, and (ii) epiclastic sediment in varying proportions, and have thus been referred to as "mixed tuffs". They should more correctly be termed tuffaceous sandstones (Le Bas & Sabine, 1980). Because of the fine-grained nature of some of the material, and its subsequent recrystallisation, it is impossible to determine the absolute proportions of fine volcanogenic ash and epiclastic mud (Plate 6.45).

(i) The petrographic evidence suggests that the same magma was involved in the genesis of the lavas and the volcaniclastic deposits. Lapilli of recrystallised lava possess an identical phenocryst assemblage, and similar felsitic groundmass to the rhyolite lava flows. Volcanogenic crystals also commonly occur separated from their matrix, including often broken plagioclase (albite) and highly rounded quartz crystals easily distinguishable from their highly angular detrital counterparts.

The lapilli of felsite are usually angular to irregular in shape with poorly defined margins due to recrystallisation. Pumice clasts

or shards have not been positively identified although despite recrystallisation some fragments possess vaguely vesicular textures (Plate 6.46). Some specimens are particularly rich in irregularly shaped fragments of felsite with no indication of vesiculation. Field evidence demonstrates that these lapilli-stones have been water sorted and angular detrital quartz sand, seen only in thin section, lies between the closely packed lapilli (Plate 5.36).

ii) The epiclastic or non-volcanogenic component of these mixed tuffs falls into three categories (Plate 6.45):

a) epiclastic quartz sand and silt with subordinate feldspar and other minerals

b) intraclastic silt and mud flakes

c) detrital rock fragments.

The quartz sand grains are angular to subangular, and 0.1-0.3 mm (rarely up to 0.7 mm) in size. In most sections they are randomly distributed, mostly as floating grains with rare point and long contacts (Pettijohn *et al.*, 1972 p. 90-91). In specimens richer in epiclastic sand, some sutured contacts are observed. Epiclastic microcline is encounted rarely as broken crystals free of the finely disseminated ore grains characteristic of locally derived volcanogenic feldspars. Among other detrital minerals muscovite flakes up to 0.25 mm are quite common and are often strongly distorted. Rounded zircons (approximately 0.02 mm in size) are occasionally present along with tourmaline, garnet, epidote and opaque ore.

The intraclastic silt and mud flakes range in size from 1 mm to 2 cm in thin section (but may be much larger in hand specimen). Recrystallisation is usually strong, especially in mud grade flakes where they may be almost entirely converted to schistose mats of sericite sometimes with an opaque mineral rich core. In sheared rocks the

intraclasts have been mechanically rotated to lie with their long axes parallel to the general foliation. Detrital rock fragments up to 1 mm in size are rarely encountered. One small clast of a crenulated muscovite-chlorite schist was observed.

Much of the tuffaceous sediment is composed of very fine grained quartz, feldspars and micas (sericite and chlorite) and variable quantities of stilpnomelane and opaque minerals. As previously stated, the original nature of this matrix is difficult to ascertain.

6.5.2 The Killeen Volcanic Centre

The mixed tuffs of the easternmost volcanic centre are identical to those described above, with the exception of the volcaniclasts which show some petrographic variation. They fall into two categories;

i) those which appear to have had a similar magmatic composition to the Killeen lava, and

ii) those which have a basaltic composition and texture.

Group (i), which includes lapilli and fine blocks of acidic composition, irregular to angular in shape, possess all the phenocryst types observed in the Killeen lava. They can be subdivided according to the nature of the secondary groundmass recrystallisation.

a) Normal felsitic or partially sericitised types possess a groundmass dominated by fine grained intergrown quartz and feldspar. They commonly contain large broken spherulites up to 4 mm in size (Plate 6.47) suggesting that solidification and partial devitrification had occurred prior to brecciation.

b) Sericitised clasts possess a strong foliation in which many of the feldspar lath phenocrysts have been rotated or broken so that their long axes lie parallel the cleavage. There are exceptions however, such as the albite crystals in Plate 6.48 which have not been rotated and which exhibit strain shadows where the white mica has become coarser

grained.

c) A smoothly outlined, chloritised clast, about 10 cm long and resembling a spindle bomb was observed in specimen 9305. The groundmass consists dominantly of matted chlorite with small irregular patches up to 0.5 mm in size which appear to be relics of the original felsitic groundmass (Plate 6.49). The phenocrysts, with the exception of some of the albite laths, are strongly embayed and rounded (Plate 6.50). The shape of the embayments or inclusions which have been observed in albite laths appears to be controlled by the radiate and sheaf-like habit of the chlorite aggregates while the embayments of the quartz crystals are smooth.

Opaque minerals are rare and usually present in aggregates of subhedral grains up to 2 mm across. Fine grained leucoxene, usually in aggregates of anhedral crystals are a very common accessory, usually with a faintly darker pleochroic hala in the host chlorite. They are often associated with small subhedral zircons. Apatite occurs as subhedral crystals and stilpnomelane is associated with fractures in the rock. White mica is very rare.

Group (ii) volcaniclasts have a texture and mineralogy quite different to the Killeen lava. They are usually subrounded to subangular or irregular, and distinguishable down to ash sized clasts 1 mm in size. Volumetrically they constitute only a minor part of the mixed tuffs. Specimen 9305 contains a single exceptionally large (16 mm) and texturally typical lapillus of this type.

They are characterised by a basaltic texture comprised of lath-shaped albite phenocrysts (An_{0-5}) between 0.5 and 2.0 mm in length, set in a finer grained matrix of interlocking plagioclase laths with interstitial chlorite (Plate 6.51). Euhedral to anhedral opaque ore minerals, probably magnetite, and aggregates of leucoxene are common

accessories (Plate 6.52). One untwinned, rounded albite phenocryst was observed with numerous inclusions of opaque ore and leucoxene arranged in concentric zones. Chlorite-sericite pseudomorphs after an unknown mafic mineral are also fairly common.

The lapillus described from specimen 9305 also possesses three distinct zones with a characteristic groundmass grain size and with well defined boundaries (Plate 6.53) which are terminated at the edge of the clast. This imples that these textural variations are primary features of the disrupted source rock. Other lapilli have groundmasses possessing fluxional textures.

One specimen of a small angular sericitised block revealed an additional mineralisation texture. Chlorite in association with calcite occurs in large irregular patches up to 1 cm in size. The chlorite occurs as intergrowths of randomly oriented sheaves, which progressively replace large areas of the foliated sericite groundmass. The chlorite encloses some fine examples of yellow subhedral sphene with dark haloes and in the vicinity of fractures in the rock, stilpnomelane is well developed replacing the chlorite (Plate 6.54).

The most interesting feature of this section is a fracture with which are associated large numbers of euhedral to subhedral allanite crystals. The fracture itself is marked by a zone, up to 0.8 mm wide, in which the sericite groundmass is partially obscured by a high content of fine grained opaque minerals (Plate 6.55). The crystals of allanite, which may be as long as 1.2 mm are most common in contact with the fracture zone (Plate 6.55), but they also occur within a one centimetre zone to either side. The allanite is pleochroic from brick red (α), to brownish yellow (β), to pale greenish yellow (γ) with a $2V_{\alpha}$ of between 85^{o} and 90^{o}. Most of the crystals show an early phase of growth producing the euhedral-subhedral shapes, followed by a later phase

of limited, more darkly coloured but irregular overgrowth (Plate 6.56). The overgrowths are in optical continuity with the initially formed crystal.

6.6 The Terrigenous Sediments

Specimen 9724: This is a clast-supported, medium grained sandstone. Sutured and long contacts are common. The grains are angular, but reasonably well sorted, and comprise over 75% quartz. Among the other detrital minerals, broken feldspars, muscovite flakes, tourmaline and opaque ores are present along with some, mostly volcanic, rock fragments. The interstices are recrystallised, and filled with a mixture of sericite, calcite, chlorite and a little leucoxene. This rock can be classified as a sublitharenite (Pettijohn *et al.*, 1972).

Specimen 7759: This is a fine grained micaceous sandstone classified as a lithic graywacke (Pettijohn *et al.*, 1972). The interstitial material consists of secondary calcite, chlorite, sericite and stilpnomelane.

Specimen 7758b: This fine-medium grained sandstone is classified as a sublitharenite (Pettijohn *et al.*, 1972). The grains are angular and comprise about 80% quartz. This rock is notable for heavy mineral-rich laminae containing abundant sphene, brown spinel, zircon, epidote/clinozoisite and tourmaline.

6.7 Discussion

Any discussion of the petrology of the Lough Guitane volcanics must focus upon distinguishing between primary and secondary features, and the interpretation of secondary mineralogies and textures in terms of their primary parentage. The authigenic mineral assemblage of albite-chlorite-sericite-quartz is characteristic of greenschist facies metamorphic terrains, and under such conditions very few primary minerals

will survive unaltered.

The lavas are notable for their textural and mineralogical uniformity. Among the six lavas observed, only the Killeen lava can be separated as being significantly different. All of these lavas should be strictly classified as quartz keratophyres (Streckeisen, 1980). Their original mineralogy was probably that of a rhyolite, and nearly all exhibit abundant evidence for an original glassy groundmass, now totally recrystallised to a fine grained intergrowth of quartz and plagioclase with subordinate sericite and chlorite.

The wide variation in the relative abundance of these minerals described from a thin section study can be better ascribed to small primary variations in the characteristics of the glass, rather than localised variations in the physicochemical conditions controlling secondary recrystallisation. This is illustrated by plate 6.26 in which the whole of a thin section of the autobrecciated top of the Bennaunmore lava flow is showed, revealing the wide variety of recrystallisation textures present. It must be noted that each texture is restricted to sharply defined, individual clasts. Subsequent to the lava flow coming to rest following extrusion, the clasts must have been subjected to the same physicochemical environment. Such radical diversity in groundmass texture must therefore relate to very small primary variations in composition or other unknown factors which have been grossly exaggerated by recrystallisation. Similar variations have been recorded from the acid lapilli of the Killeen Tuffs.

Among the phenocrysts, quartz is unquestionably of magmatic origin, showing partially resorbed euhedral-subhedral outlines. While the plagioclase phenocrysts are uniformly albitic in composition, there is wide textural variety suggesting at least two primary feldspar types. In the Killeen lava, they are characterised by differing morphologies

and styles of recrystallisation representing primary K-feldspar in addition to plagioclase phenocrysts. Other lavas exhibit two or more feldspar types, but the distinguishing features are less obvious, and the interpretation different.

Types (ii) and (iii) of the crystal clusters described in section 6.2.1 are found in all the lavas, and their origin requires careful consideration. Flood *et al.* (1977) proposes five alternative hypotheses for the origin of phenocrystic aggregates in extrusive igneous rocks.

1) Accidental microxenoliths

2) Synneusis clusters (Vance & Gilreath, 1967)

3) Anhydrous products formed by the breakdown of high pressure "megacrysts" of pargasitic amphibole (Stewart, 1975)

4) Disrupted cumulate material

5) Refractory residues or "restite".

Synneusis is an unlikely petrogenesis because of the anhedral shapes of the constituent grains, and the multimineralic nature of those grains (Vance & Gilreath, 1967). The attachment of plagioclase laths to some of the clusters is more likely to be due to the latter acting as a nucleation site rather than a process of synneusis (Dowty, 1980).

It is unlikely that low pressure breakdown of amphibole would produce the coarse grained textures observed, and replacement textures are absent (Garcia & Jacobson, 1979). The first, fourth and fifth mechanisms proposed by Flood *et al.* (1977) are more difficult to resolve. Many of the observations seem to be conflicting in their petrogenetic implications.

Unless a very short residence time is proposed, the lack of resorption implies that the crystal clusters were in equilibrium with

the melt. However, the remarkable uniformity of internal distribution within lava flows, and texture from flow to flow discriminate against a microxenolithic origin. Furthermore, a short residence time would prevent the cluster acting as a nucleation site for plagioclase crystallisation. The equidimensional grain shapes are possible in both refractory and deep-level slowly annealed cumulates (Vernon, 1970).

The high zircon content of the P.M.P.s is difficult to reconcile with a cumulate origin. A process of preferential incorporation might produce relatively high concentrations of included zircons - a sweeping-up mechanism - it is hard to envisage such a process operating to produce the textures and concentrations illustrated in plates 6.6 and 6.7. A restite origin for these crystal clusters seems likely. Only geochemical data discussed in chapter 8 can resolve whether the sum total of the crystal clusters and the lava liquid phase, not necessarily in the erupted proportions, could have melted to produce a liquid of the composition erupted.

Possible interpretations of the development of chessboard albite, and related granular albite aggregates include:

1) A metasomatic porphyroblastic paragenesis (Battey, 1955).

2) Soda metasomatism of K-feldspar (Smith, 1974, pp. 287-290).

3) Albitisation of microxenolithic plagioclase aggregates.

A number of varieties have been observed (including those in Plates 6.18 and 6.19). The presence of groundmass in irregular areas and "veins" between many of the albite laths or "tiles" comprising the chessboard texture in Plate 6.18 is either of primary magmatic origin due to partial resorption, or due to granoblastic growth similar to that described by Battey (1955). The latter seems unlikely in view of the regular rounded outline of the aggregate, and the observation that the crystals contain a finely disseminated distribution or dusting of fine

ore along with an amount of sericite equal to that of continuously twinned phenocrysts elsewhere in the section. Battey uses the absence of such inclusions and alteration in his porphyroblastic albite as a definitive criterion to be used in distinguishing them from ore rich, sericitised phenocrystic albite. Other similar examples exhibit textures in which they appear to have acted as nucleation sites for magmatic plagioclase crystallisation.

The choice between options 2 and 3 is more problematical. A possibly high pressure K-feldspar phenocryst phase in the process of resorption would surely be more commonly observed, and such a pattern of resorption highly unlikely for such a crystal type. It is likely therefore that the chessboard albites have a microxenolithic origin.

The muscovite microphenocrysts rarely observed in some sections are almost certainly a primary texture, but unlikely to be a primary mineralogy. The presence of numerous ore grains along cleavage traces in the crystal suggests the original crystal had a much higher iron content, and the subhedral, albeit rather ragged outline suggests a micaceous primary mineral. White mica could not have crystallised in magma erupted at the temperature of 950^{o}C suggested in Chapter 8. However, some biotites can crystallise under these conditions (Eugster, 1956) and may also be replaced by white mica under hydrothermal conditions (Schwartz, 1958).

Among the more unusual mineralogies, the fluorite recorded from 3 specimens of the Bennaunmore lava is thought to be of post-magmatic, pneumatolytic or hydrothermal origin. Its localised development, and association with apatite and calcite would imply the presence of a volatile phase permeating the lava probably while still glassy, leading to the preferential replacement of crystalline phases, in particular the mafics. The randomly distributed chalcopyrite aggregates may be of similar origin, the later regional metamorphic event having led to

the development of a rim of allanite.

The precise nature of the primary controls over the character of recrystallisation of the groundmass, as stated above, is unknown, and probably very complex. However, the resultant textures reflect the mobility of iron (chlorite and opaque iron ore), sodium (albite), potassium (muscovite/sericite), and silica (quartz). In general the coarser grained groundmasses are partially silicified. The mobility of these elements is further highlighted by the presence of dilational and non-dilational veins of all combinations of these minerals and allanite. The high concentration of allanite in the PMP may not therefore reflect any primary high rare earth element concentration but rather a secondary migration of these elements to, and incorporation in, a crystal lattice capable of accommodating them.

The phenocryst petrography of both the Green dyke and the Pale "dykes" suggests the possibility of a metasomatic origin for these rocks from original compositions close to that of the Bennaunmore lava. This hypothesis, among others, are discussed in detail in Chapter 8.

Without unduly stressing the point, the volcaniclastic deposits invariably occur intimately mixed with considerable quantities of epiclastic sediment. The petrogenesis of these rocks has already been discussed on the basis of field relations in Chapter 5. On a microscopic scale, recrystallisation has almost completely destroyed the original textures, leaving vaguely outlined felsite lapilli and ash, and angular quartz sand and mudstone/siltstone intraclasts set in a very fine grained felsitic matrix. The morphology of the lapilli is never preserved well enough to be used as a petrogenetic indicator in the fashion described by Honnorez & Kirst (1975). However, vesiculated clasts are rare, and many show evidence for solidication prior to the brecciation presumably associated with eruption.

On the other hand, some of the Killeen Tuffs contain lapilli within a single hand specimen or thin section showing widely varying styles of recrystallisation. As proposed for both unbrecciated and brecciated lavas above, some primary attribute must be in control. Along with reworked lava fragments, some juvenile ejecta must be present among which are probably some, if not all of the sericitised and chloritised lapilli, or those without prexisting solification textures (spherulites etc.).

Mineralogically and texturally, almost all of the volcaniclasts observed are directly comparable to local contemporary lavas. Only the "basic" or "basaltic" lapilli of the Killeen Tuffs are radically different. Their presence is a further indication of the erosion of vent walls composed of sequences older than the oldest Green Sandstone Group sediments in the area. Further discussion of the significance of the presence of fine grained basaltic rocks at depth will be discussed in the final chapter.

In summary, secondary recrystallisation has made interpretation difficult. However, all the rhyolitic lavas appear mineralogically very similar both in terms of the phenocryst and microxenolith contents. Such uniformity suggests a common magma chamber for all but the Killeen Lava.

CHAPTER 7

Mineral Chemistry

7.1 Introduction

One hundred and forty one mineral analyses were made using an energy-dispersive electron microprobe system (appendix A). The following elements were determined: Na, Mg, Al, Si, P, S, K, Ca, Ti, Cr, Mn, Fe and Cu. No analyses of volatile contents were possible leading to low totals for hydrous phases e.g. chlorite (< 90.00%), and white mica (< 95.00%). Rare earth analyses are also not possible using this particular energy-dispersive electron microprobe leading to totals below 70.00% for the allanites.

Selected and averaged analyses are present for each mineral in tables 7.1 to 7.5, together with calculated mineral formulae. For comparison, mineral analyses from other published sources are presented in table 7.6.

7.2 Plagioclase Feldspars

Eleven analyses of plagioclase feldspars are presented in table 7.1. All analyses represent plagioclase of albitic composition, confirming the conclusions made on optical grounds in Chapter 6. The highest anorthite content (anal. 3) is only $An_{5.1}$, while some fall below the instrumental detection limit of about $An_{0.2}$. The orthoclase content is also extremely low, only up to 2.5% in anal. 2, and often falling below the instrumental detection limit of about 0.2%. In fact, anals. 8 and 9 represent as near pure albite as the electron microprobe was capable of registering. Given the prevailing low greenschist metamorphic conditions (Chapter 6), these plagioclases probably possess the low albite structure which can take very little

Table 7.1

Albite Analyses

Analysis Number		1	2	3	4	5	6	7	8	9	10	11
Average of		4	2	4	3	4	1	1	2	3	3	2
Rock Number		8409	8409	8392	8392	8418	8418	8552	8742	8742	8613	8613
	SiO_2	67.19	68.61	67.64	68.93	69.47	69.57	70.54	69.05	69.06	69.31	68.84
	Al_2O_3	19.48	20.21	20.19	19.90	19.50	19.33	18.96	19.56	19.18	19.43	19.46
	FeO*	Tr	Tr	Tr	Tr	Tr	nd	nd	Tr	nd	nd	0.30
	CaO	0.32	0.50	1.06	0.46	0.19	0.08	nd	Tr	Tr	0.15	0.10
	Na_2O	11.28	10.32	10.88	11.03	11.09	11.35	11.17	12.01	12.18	10.78	11.20
	K_2O	0.09	0.38	0.10	0.16	0.13	0.07	0.07	Tr	Tr	Tr	Tr
	TOTAL	99.08	100.02	99.87	100.48	100.38	100.40	100.74	100.62	100.42	99.67	99.90
	Si	11.97	11.95	11.84	11.96	12.02	12.07	12.17	11.97	12.02	12.04	12.02
Numbers of	Al	4.04	4.15	4.17	4.07	3.99	3.95	3.86	4.00	3.93	4.00	4.00
ions on the	Fe											0.04
basis of	Na	3.85	3.48	3.69	3.70	3.73	3.82	3.74	4.04	4.11	3.64	3.79
32(O)	Ca	0.06	0.09	0.20	0.09	0.04	0.02	< 0.01	< 0.01	< 0.01	0.03	0.02
	K	0.02	0.09	0.02	0.03	0.03	0.02	0.02	< 0.01	< 0.01	< 0.01	0.01
	Ab	98.0	95.1	94.4	96.9	98.2	99.0	>99.2	>99.5	>99.5	>98.9	99.2
Mol. %	An	1.5	2.5	5.1	2.4	1.1	0.5	< 0.2	< 0.2	< 0.2	0.8	0.5
	Or	0.5	2.5	0.5	0.8	0.8	0.5	0.5	< 0.2	< 0.2	< 0.3	0.3

nd = not detected
Tr = trace

calcium into solid solution (to about An_3), (Deer *et al.*, Vol. 4, pp. 96). Iron contents are very low or below detection limits, in contrast with the high contents of fine grained ore inclusions. No zoning was present in accordance with the optical properties already noted. The feldspar analyses have been plotted on an Ab-An-Or triangular diagram (fig. 7.1).

Such near pure albites are the characteristic plagioclase feldspars of low grade metamorphic rocks (Deer *et al.*, Vol. 4, pp. 149), and its composition appears not to vary with the bulk rock composition (see anal. 6, table 7.2, from a chlorite schist). Battey (1955), Donnelly (1963) and others have suggested that albite phenocrysts will crystallise from especially hydrous magmas. This seems very unlikely to have been the case in view of the contention (Chapter 8), that the erupted magmas possessed a particularly low volatile content of under 1.5%.

7.3 Chlorites

Fourteen analyses of chlorites are presented in table 7.2, including two of darkened chlorite in the vicinity of zircon (anals. 23 and 25). The analyses have been plotted on a diagram recommended by Hey (1954) and Deer *et al.* (1966) which utilises the Si and total Fe ionic contents calculated in the mineral formulae (fig. 7.2). It is assumed that the chlorites are unoxidised (under 4.0 percent Fe_2O_3) on the grounds that the whole rock analyses of the specimens from which the mineral analyses were taken possess insufficient Fe_2O_3 for oxidised chlorite to be present when chlorite is the dominant Fe mineral. The bulk of the analyses straddle the boundary between aphrosiderite (a variety of ripidolite) and brunsvigite while the chlorite from the Green Dyke lies close to the junction between

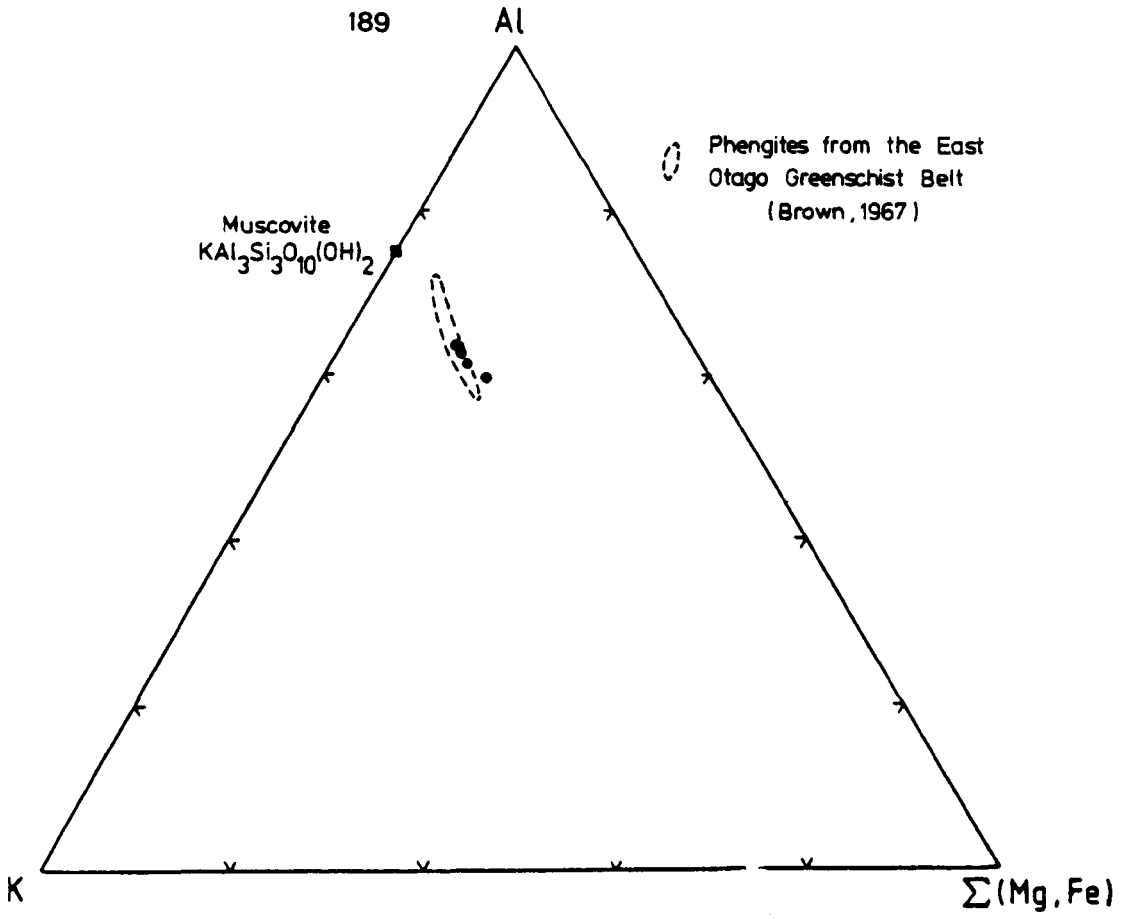

Fig. 7.5 Triangular Al–K–(Mg+Fe) plot of phengite compositions displayed in table 7.3.

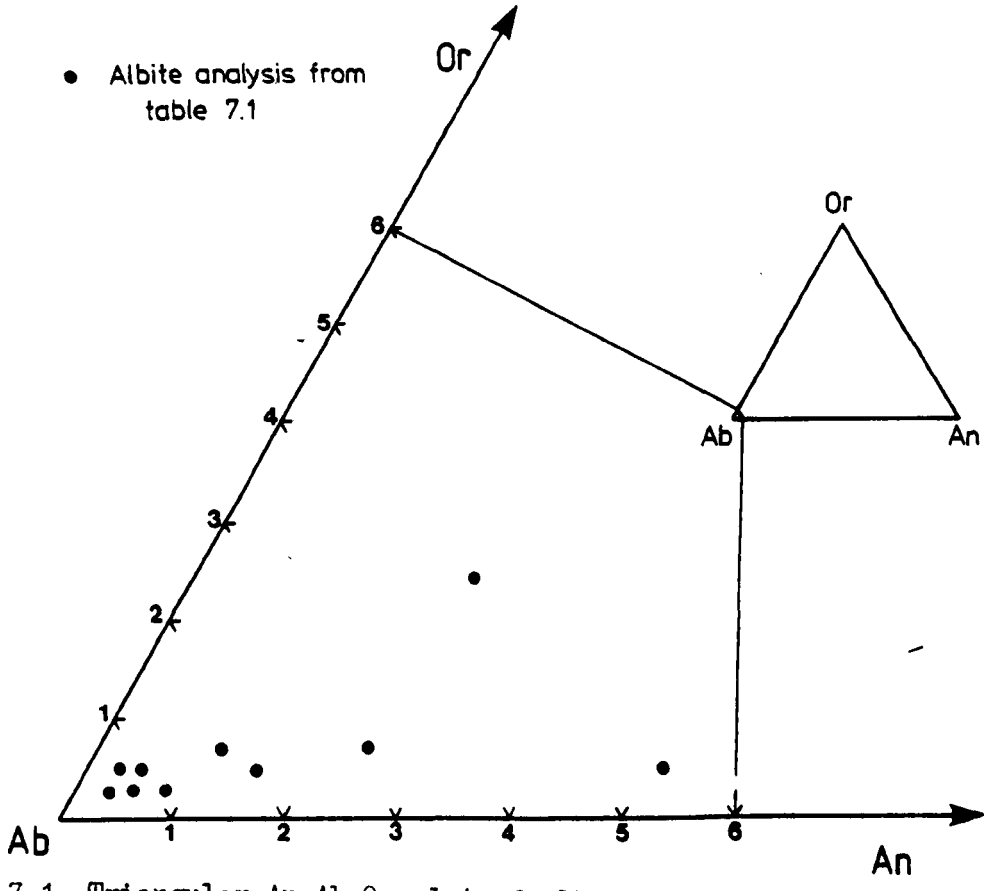

Fig. 7.1 Triangular An–Ab–Or plot of albite compositions displayed in table 7.1.

Table 7.2

Chlorite Analyses

Analysis Number		12	13	14	15	16	17	18	19	20	21	22	23	24	25
Average of		3	2	2	2	3	3	3	1	1	2	2	1	1	1
Rock Number		8392	8392	8392	8392	8392	8552	8742	8418	8418	8613	8613	8392	8552	8552
	SiO_2	24.84	24.80	24.83	25.30	25.68	23.20	26.16	24.57	24.32	27.23	25.65	28.21	24.84	36.71
	TiO_2													0.18	0.23
	Al_2O_3	20.17	19.87	19.77	19.79	20.29	18.62	20.11	19.79	19.43	19.38	19.29	20.80	19.53	23.80
	FeO*	35.59	36.51	36.32	36.13	35.29	35.17	28.93	37.10	36.70	34.56	35.73	31.41	34.92	22.12
	MnO	1.48	1.54	1.53	1.55	1.46	0.25	0.44	0.84	0.61	1.07	1.06	1.21	0.24	0.11
	MgO	5.32	5.28	5.32	5.21	5.04	6.41	12.33	5.79	5.27	5.90	6.28	4.49	6.86	4.57
	CaO	Tr	nd	nd	nd	nd	Tr	nd	0.19	0.10	nd	Tr	0.30	nd	nd
	Na_2O	nd	nd	nd	nd	nd	nd	nd	nd	nd	Tr	nd	nd	nd	nd
	K_2O	0.35	0.34	0.31	0.25	0.67	0.13	nd	nd	0.15	nd	Tr	1.80	0.25	4.85
	TOTAL	87.75	88.34	88.08	88.23	88.43	83.78	87.97	88.28	86.58	88.14	88.01	88.20	86.82	92.39
	Si	5.582	5.569	5.589	5.665	5.709	5.471	5.599	5.517	5.570	5.971	5.716	6.140	5.596	7.120
	Al	2.418	2.431	2.411	2.335	2.291	2.529	2.401	2.483	2.430	2.029	2.284	1.860	2.404	0.880
Number of	Al	2.928	2.829	2.834	2.890	3.027	2.649	2.672	2.755	2.815	2.982	2.794	3.477	2.783	4.562
ions calculated	Ti	-	-	-	-	-	-	-	-	-	-	-	-	0.031	0.033
on the basis	Fe	6.689	6.860	6.836	6.765	6.563	6.947	5.179	6.967	7.028	6.339	6.661	5.717	6.578	3.589
of 28 (O)	Mn	0.282	0.293	0.292	0.295	0.275	0.051	0.078	0.159	0.118	0.199	0.200	0.223	0.046	0.019
	Mg	1.781	1.766	1.783	1.738	1.671	2.255	3.934	1.937	1.799	1.929	2.086	1.455	2.303	1.322
	Ca	-	-	-	-	-	-	-	0.046	0.025	-	-	0.069	-	-
	K	0.101	0.097	0.090	0.072	0.189	0.039	-	-	0.044	-	0.025	0.500	0.073	1.200

nd = not detected
Tr = trace

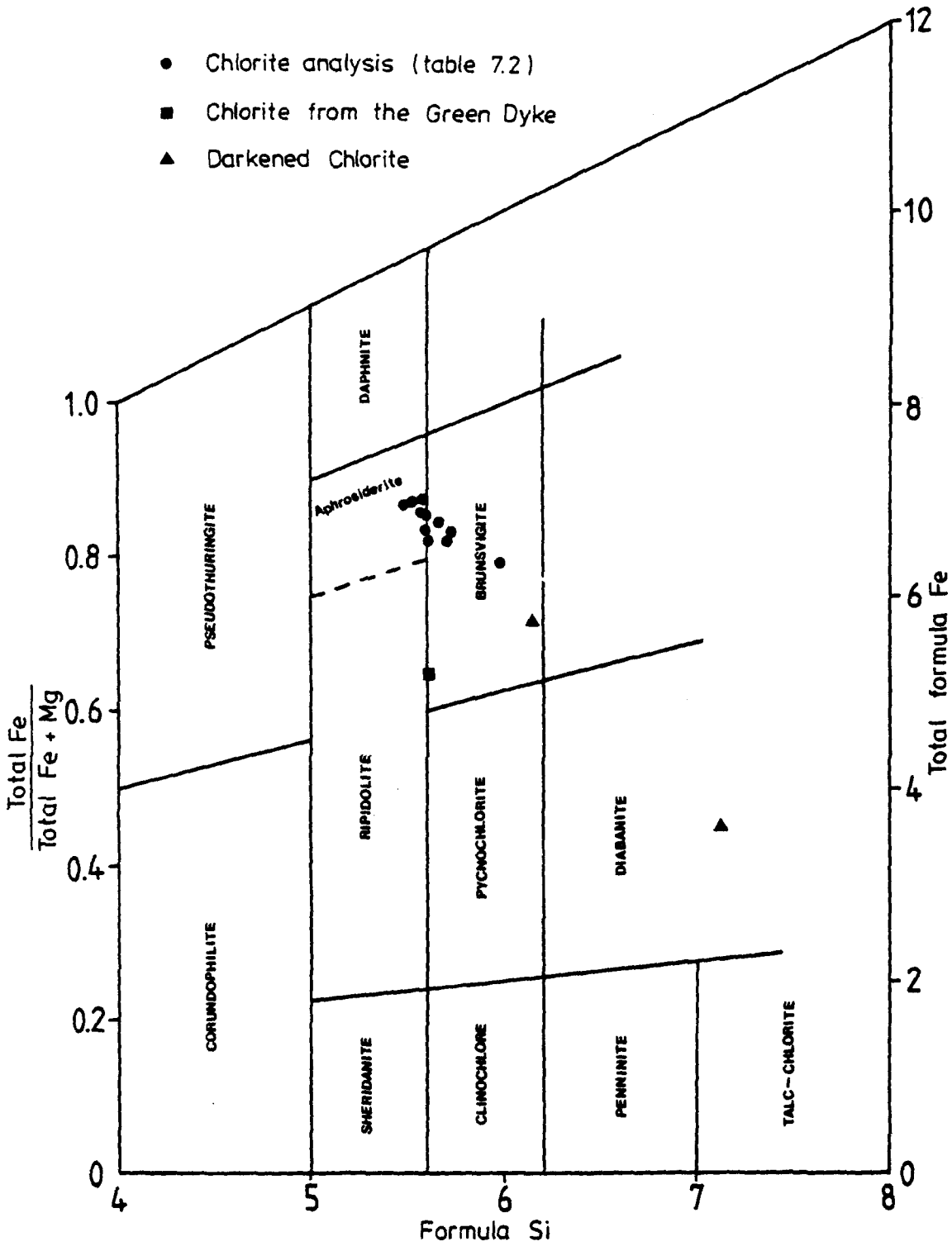

Fig. 7.2 Chlorite nomenclature (Hey, 1954).

the three fields of ripidolite, brunsvigite and pycnochlorite. The darkened chlorites are displaced towards the bottom right hand corner of the diagram by increased formula silica.

If all the iron is assumed to be ferrous an alternative classification suggested by Foster (1962) (fig. 7.3) places the bulk of the chlorite analyses in the chamosite field with only a few lying in the thuringite and brunsvigite fields. None can be termed ripidolite under these criteria, and the Green Dyke chlorite analysis lies well within the brunsvigite field.

While analyses of chlorites from individual specimens are very similar, no systematic relationship can be found among the rhyolites (specs. 8392, 8418, 8552 and 8613) between the whole-rock and chlorite MgO/MgO + MnO + FeO* ratios (fig. 7.4). If chlorite is accepted to be the dominant Fe, Mg mineral, then the ratios should be nearly equal, and lie near to the line drawn in fig. 7.4. The displacement to the right of this line of chlorite analyses from specimens 8418 and 8552 is problematical because it implies that these rocks contain significant quantities of magnesium in phases other than chlorite. No such magnesium-bearing mineral has been identified, and therefore this problem must remain unresolved.

The chlorite from the Green Dyke (spec. 8742A) contains over twice as much MgO as all the other chlorites in association with a whole rock geochemistry displaying a marked enrichment in MgO relative to the Bennaunmore rhyolite (Chapter 8.4.2). The dominance of chlorite in the groundmass of this rock (Cahpter 6.4.2) is reflected in the correspondence between the whole-rock and chlorite Mg/MgO + MnO + FeO* ratios (fig. 7.3).

The differences in the composition of the darkened chlorites (anals. 23 and 25, table 7.2) reflect the disruption of the chlorite

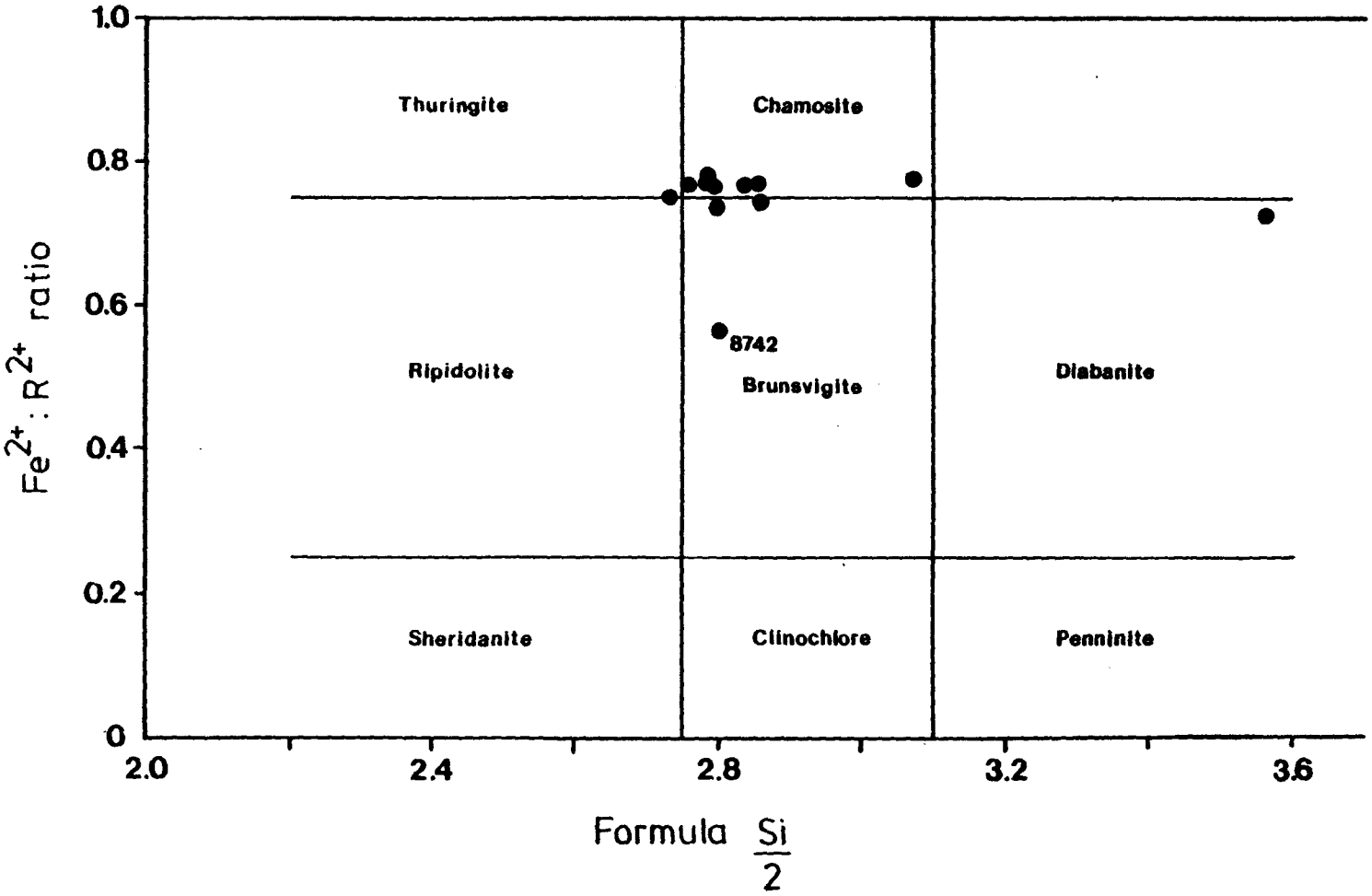

Fig. 7.3 Chlorite nomenclature (Foster, 1962).

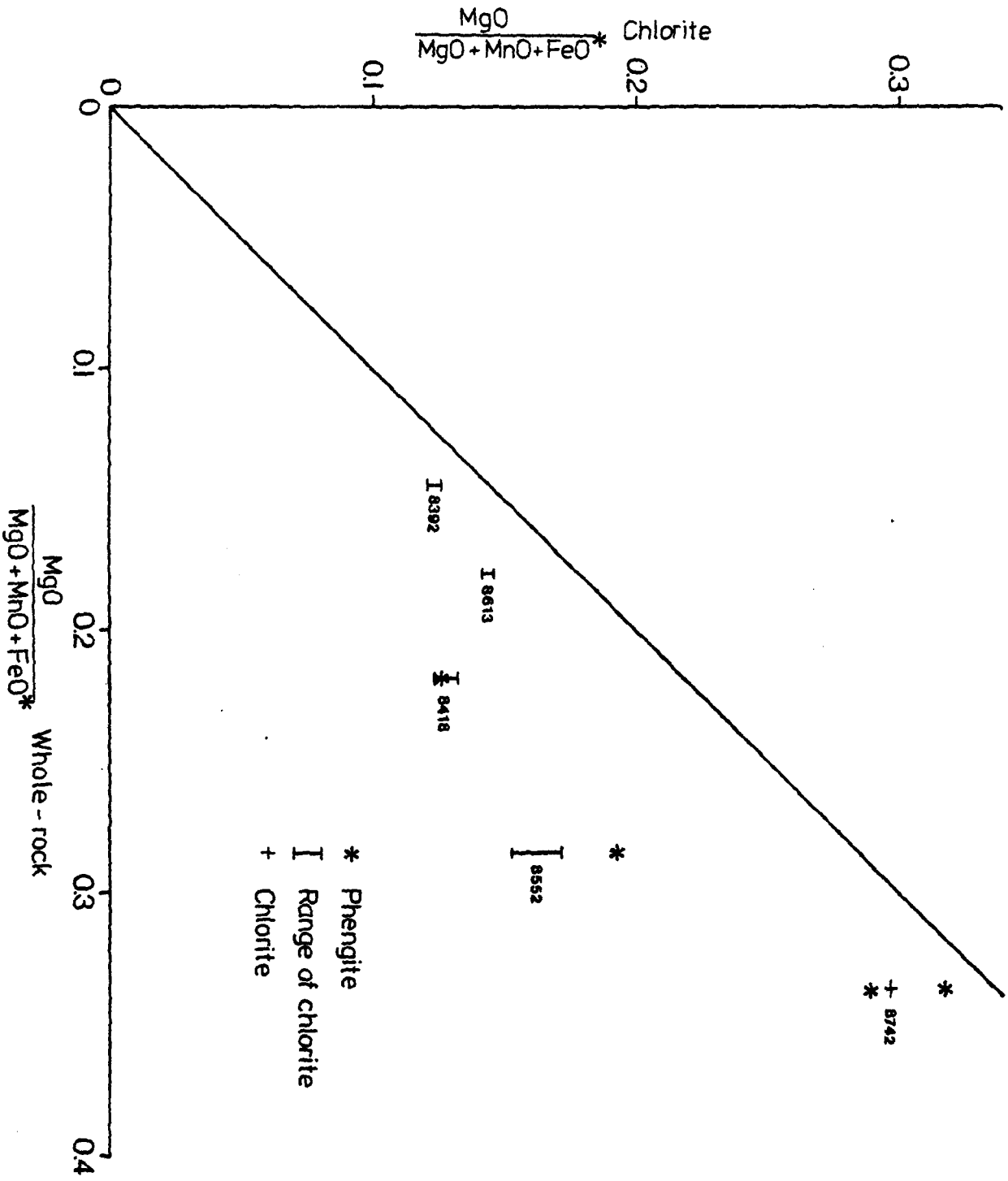

Fig. 7.4 Plot of chlorite and phengite MgO : MgO+MnO+FeO ratios against their corresponding whole rock ratios.

structure by the decay of radioactive isotopes present in the zircons. This disruption has led to increased silica and decreased total iron, and in anal. 25, loss of water reflected in the higher total.

7.4 White Mica (Phengite)

The high SiO_2, MgO and FeO, and low Al_2O_3 levels displayed by the white micas analysed (table 7.3) suggest that they can be classified as phengites (Deer *et al.*, 1966, Vol. 3, p. 15), and can be compared with the phengite analysis of Schaller (1950) and the pure muscovite of Hurlbut (1959). (Both analyses also appear in Deer *et al.*, 1966, vol. 3, tables 5 and 36 respectively.)

The authigenic nature of the phengite is not in doubt, however, sericitisation alone cannot be used as an indicator of pressure and temperature conditions because quartz-muscovite assemblages are stable through a wide range of conditions. It also seems unlikely that the Si^{4+} ionic content of the phengites, which Velde (1967) claimed could be used as an independent indication of metamorphic grade, can be applied outside strictly defined whole-rock compositions (Brown, 1968). However, the composition of the Lough Guitane phengites are very similar to those from other greenschist grade rocks, and in fig. 7.5 are compared with those from the East Otago greenschist belt (Brown, 1967).

Like the chlorites discussed in the previous section, only some of the phengites analysed, from the green dyke (spec. 8742A, anals. 3 and 5 in table 7.3) appear to be in chemical equilibrium with their host rocks. However, all the phengites do appear, perhaps surprisingly to be in equilibrium with chlorites from the same rocks (fig. 7.5).

7.5 Allanite

Table 7.4 provides analyses and ionic formulae for six allanites.

Table 7.3

Phengite Analyses

Analysis Number		26	27	28	29	30
Average of		3	2	2	3	1
Rock Number		8409	8552	8742	8418	8742
	SiO_2	48.97	49.42	49.82	48.72	48.99
	TiO_2	0.41	0.19	0.27	0.21	0.31
	Al_2O_3	26.43	28.01	27.49	28.58	27.81
	FeO*	5.95	5.22	4.38	5.27	5.21
	MgO	2.57	1.25	2.03	0.83	2.12
	CaO	nd	nd	nd	Tr	nd
	K_2O	9.68	10.02	9.96	10.12	10.34
	P_2O_5	nd	Tr	nd	nd	nd
	TOTAL	94.01	94.11	93.95	93.73	94.78
Number of ions calculated on the basis of 24 (O, OH, F)	Si	6.271 } 8	6.734 } 8	6.778 } 8	6.679 } 8	6.664 } 8
	Al	1.279 }	1.266 }	1.222 }	1.221 }	1.336 }
	Al	2.998 } 4.25	3.233 } 4.10	3.187 } 4.12	3.898 } 4.19	3.124 } 4.18
	Ti	0.042 }	0.020 }	0.027 }	0.022 }	0.032 }
	Fe	0.683 }	0.595 }	0.498 }	0.604 }	0.592 }
	Mg	0.526 }	0.253 }	0.412 }	0.169 }	0.430 }
	K	1.697	1.743	1.729	1.771	1.794

nd = not detected
Tr = trace

Table 7.4

Allanite Analyses

Analysis Number		31	32	33	34	35	36
Average of		3	1	2	1	3	1
Rock Number		8409	8409	8409	8392	8392	8392
	SiO_2	28½72	28.72	28.56	28.46	29.40	28.83
	Al_2O_3	14.37	14.59	14.35	14.72	14.72	15.09
	FeO*	12.73	13.16	12.70	14.68	13.54	14.44
	MgO	Tr	0.32	nd	nd	nd	nd
	CaO	10.32	10.42	10.48	10.12	11.87	10.14
	K_2O	Tr	nd	Tr	nd	nd	nd
	TOTAL	66.14	67.21	66.18	67.98	69.53	68.50
	Si	2.951	2.906	2.931	2.874	2.893	3.225
Number of ions	Al	0.049	0.094	0.069	0.126	0.107	-
calculated on	Al	1.972	1.936	1.956	1.819	1.855	2.322
the basis of	Fe	1.270	1.300	1.272	1.447	1.301	1.576
13 (O, OH)	Mg	-	0.056	-	-	-	-
	Ca	1.319	1.318	1.345	1.278	1.461	1.418
	†REE + Mn	0.681	0.682	0.655	0.722	0.539	0.582

nd = not detected
Tr = trace

†REE content estimated from calcium deficit

The low totals obtained from the energy dispersive microprobe are due to the non-determination of the REE which are not analysed by this system. The REE replace calcium in the crystal lattice, and on this basis their ionic substitution has been estimated at between 25 and 35 percent of the calcium sites. Such high total REE contents, and the ubiquitous presence of allanite as an accessory mineral, imply that it possesses the bulk of the whole-rock REE content. Little replacement of Si by Al is indicated, typical of most epidotes (Deer *et al.* Vol. 1, pp. 213, 1966).

7.6 Sphene

Only one averaged analysis of sphene was obtained (table 7.5). The high alumina and low titania contents suggest that it belongs to the grothite variety, (Deer *et al.*, Vol. 1, page 74, 1966) although some doubt must be thrown on the reliability of the analysis. The unusually high potash and silica contents suggest some analytical interference from the white mica in which the sphene grain was embedded.

7.7 Apatite and Anatase

The inability of the electron microprobe to detect either volatile elements (F, Cl or H_2O), or trace elements, renders the two apatite analyses, and the single anatase analysis relatively uninformative. The high totals (> 98.5%) obtained for the apatites do suggest however, that their volatile contents were low.

7.8 General Conclusions

In summary, the phengites and chlorites from the same rock appear to be in chemical equilibrium with each other, but only sometimes with the corresponding bulk rock analysis, despite their dominance as

Table 7.5

Miscellaneous Mineral Analyses

Analysis Number		37	38	39	40	41
Average of		3	1	3	2	5
Rock Number		8742	8742	8409	8552	8392
	SiO_2	nd	nd	32.74	nd	Al Tr
	TiO_2	nd	nd	33.29	98.51	Fe 31.08
	Al_2O_3	nd	nd	4.76	0.35	Ca Tr
	FeO*	Tr	0.90	1.24	0.34	S 34.57
	MgO	Tr	nd	Tr	nd	Cu 35.43
	CaO	55.16	54.09	24.24	Tr	
	K_2O	nd	nd	0.89	Tr	
	P_2O_5	43.35	44.26	nd	nd	
	TOTAL	98.51	99.25	97.16	99.20	101.08
		Apatite[1]	Apatite[1]	Sphene[2]	Anatase[3]	Chalcopyrite
Numbers of ions, calculated on the basis of: 1.26 (0, OH, F) 2.20 (0, OH, F) 3.2 (0)	P	10.106	9.795	Si 4.317	Al 0.007	(Elemental
	Ca	6.275	6.332	Al -	Ti 0.966	abundances)
	Fe	-	0.131	Al 0.739, Fe 0.137, Ti 3.303 = 4.18	Fe 0.003	
			6.46	K 0.149, Ca 3.426 = 3.57	0.98	

Fe, Mg phases. Little comparison can be made between the Lough Guitane chlorites and those from similar metamorphic environments because of the dependence of chlorite composition upon the whole-rock chemistry. However, the Lough Guitane phengites compare favourably from those from the East Otago greenschist belt (Brown, 1967) supporting the local grade of metamorphism suggested on petrological grounds in Chapter 6.

Table 7.6

Mineral Analyses from Other Sources

	1 Muscovite (Hurlbut, 1956)	2 Phengite (Schaller, 1950)	3 Chlorite (Ripidolite) (Hallimond, 1939)	4 Allanite	5 Sphene	6 Albite (Takubo, 1941)
SiO_2	45.87	49.16	24.35	30.54	30.59	66.84
TiO_2			0.04	1.10	35.16	
Al_2O_3	38.69	30.81	20.21	17.48	3.53	19.62
Fe_2O_3			38.19*	4.19	1.47*	0.57
FeO	tr	1.43		9.22		
MnO	tr		0.48	0.58	0.04	
MgO	0.10	2.22	5.57	0.85	0.11	
CaO	tr		0.10	11.00	28.10	0.58
Na_2O	0.64	0.48				11.53
K_2O	10.08	10.90				0.10
P_2O_5						
H_2O^+	4.67	4.73	10.46			0.73
H_2O^-		0.15				0.04
TOTAL	100.05	100.07	99.96	100.23†	99.34	100.01

* Total Fe as FeO

† includes: ThO_2 = 1.27%, SnO_2 = 0.41%, Y_2O_3 = 0.63%, Ce_2O_3 = 9.94%, La_2O_3 = 10.55%, total REE = 21.12%.

CHAPTER 8

Geochemistry

8.1 Introduction

Forty-nine whole-rock analyses are presented in table 8.1. Twelve major elements and eleven selected trace elements were determined. Of the six lava units identified, the Bennaunmore, North Stoompa, Devils Punch Bowl and Eskduff lavas are thought to represent single lava flows, while the Horses Glen and Killeen lavas may constitute more than one flow unit. In addition one analysis each of the Green Dyke (spec. 8742A), and a Pale Dyke (spec. 8859), a lava block from an agglomerate in the Horses Glen (spec. 9148), and a lava block from an agglomerate east of Crohane (spec. 9431) are presented. Eight analyses of tuffaceous sediments and three of terrigenous sediments are also tabulated.

Sampling sites (fig. 1.5) were selected primarily where relatively fresh specimens could be obtained, although the need for representative specimens from all parts of the lavas sometimes led to the collection of more altered rocks. A detailed description of specimen size and their preparation for analysis is presented in Appendix C.

In the low greenschist facies metamorphic environment, many elements are subject to some secondary redistribution. However, it was hoped that elements considered to be relatively immobile (e.g. Pearce and Cann, 1973; Floyd and Winchester, 1975, 1978; Winchester and Floyd, 1975, 1977; Smith and Smith, 1976) would provide clues to any primary magmatic variation among the lavas, and distinguish between any different flow units.

The lava analyses were further examined with the aim of quantifying the behaviour of the elements under the secondary environment, and a

Table 8.1

	Bennaunmore Lava							
Wt%	8365	8366	8392	8396	8396W	7750	8418	8552
SiO_2	75.27	75.62	75.26	81.26	80.41	75.51	75.69	75.54
TiO_2	0.252	0.259	0.258	0.225	0.225	0.264	0.267	0.269
Al_2O_3	12.10	12.11	11.86	10.08	10.07	12.56	12.34	12.09
Fe_2O_3	0.61	0.48	0.49	0.37	0.42	0.63	0.55	0.58
FeO	1.51	1.48	1.43	0.71	0.77	1.35	1.76	1.47
MnO	0.08	0.05	0.07	0.03	0.04	0.05	0.07	0.03
MgO	1.22	0.95	0.33	0.54	0.63	0.63	0.65	0.80
CaO	0.65	0.34	0.50	0.63	0.87	0.34	0.51	0.29
Na_2O	1.66	2.85	2.84	2.81	2.82	2.59	2.72	2.64
K_2O	5.26	3.47	4.73	2.41	2.34	4.96	4.64	4.66
P_2O_5	0.15	0.15	0.16	0.15	0.15	0.09	0.15	0.14
H_2O^+	1.03	0.93	0.54	0.91	0.92	0.79	0.60	0.63
CO_2	-	-	-	0.28	-	-	0.19	-
L.O.I.	1.49	1.26	1.24	-	1.37	1.14	1.11	0.97
TOTAL	100.25	99.02	99.17	100.59	100.12	100.12	100.46	99.46
ppm								
Ba	965	628	766	918	987	707	814	849
Rb	165	131	179	84	77	172	142	163
Sr	193	227	116	153	152	98	145	147
Y	63	57	62	45	50	63	68	56
Zr	214	214	224	182	184	231	228	226
Cu	36	31	54	27	29	-	32	-
Th	14	17	19	14	13	13	15	16
Nb	21	22	20	20	20	25	21	21
La	39	39	36	31	53	45	41	38
Ce	77	86	80	70	96	91	87	79
Nd	50	46	48	44	55	55	50	44
U	nd	nd	nd	7	5	4	7	nd
Pb	362	124	77	23	91	nd	46	58
F	-	-	-	-	-	-	860	-
Cl	-	-	-	-	-	-	98	-
Zn	92	81	128	58	63	-	75	-

Table 8.1 (cont)

	Bennaunmore Lava				Eskduff Lava				
Wt%	8824	8909	9281	9386	8461	8444	8613	8666	8674
SiO_2	75.11	74.16	77.16	77.65	77.92	75.59	79.00	75.71	77.79
TiO_2	0.263	0.276	0.263	0.256	0.259	0.262	0.240	0.267	0.260
Al_2O_3	12.47	13.43	11.86	11.55	11.80	12.50	10.80	11.73	11.94
Fe_2O_3	0.65	1.10	1.54	1.44	2.09	2.02	0.89	1.21	2.19
FeO	1.49	0.62	0.26	0.33	0.14	0.11	0.65	0.94	0.12
MnO	0.05	0.03	0.02	0.01	0.02	0.02	0.06	0.05	0.02
MgO	1.16	0.62	0.31	0.36	nd	0.18	0.83	0.50	0.20
CaO	0.46	0.26	0.27	0.25	0.18	0.40	1.21	0.51	0.19
Na_2O	2.80	2.97	3.08	1.35	7.29	3.16	3.48	2.71	6.99
K_2O	5.09	4.92	4.47	5.47	0.18	4.30	1.85	4.38	0.19
P_2O_5	0.17	0.17	0.16	0.16	0.14	0.14	0.21	0.15	0.18
H_2O^+	1.02	0.74	0.48	0.70	0.44	0.49	0.90	0.84	0.15
CO_2	-	-	-	-	-	-	-	0.31	0.04
L.O.I.	0.87	0.99	0.79	1.18	0.19	0.97	1.45	1.11	0.29
TOTAL	100.73	99.55	100.18	100.01	100.21	99.65	100.12	99.21	100.35
ppm									
Ba	780	914	645	1187	nd	616	957	1290	nd
Rb	193	172	137	203	nd	150	76	141	nd
Sr	87	161	108	75	87	159	232	223	93
Y	63	52	44	59	112	73	54	60	76
Zr	219	230	221	208	226	226	206	227	220
Cu	-	-	-	-	24	25	34	-	-
Th	16	19	20	21	22	17	17	15	18
Nb	20	21	25	19	25	22	22	19	24
La	50	36	19	46	68	27	42	43	84
Ce	100	71	42	79	147	67	83	82	215
Nd	60	47	32	52	70	42	50	51	131
U	nd	nd	5	nd	nd	nd	nd	nd	nd
Pb	14	19	nd	nd	242	92	63	nd	nd
F	-	-	-	-	-	-	-	212	-
Cl	-	-	-	-	-	-	-	27	-
Zn	-	-	-	-	18		38	51	-

Table 8.1 (cont)

	Bennaunmore Lava							
Wt%	8555	8742B	8755	8756	8850	7751	8775	8795
SiO_2	75.91	75.91	75.77	75.76	76.32	74.27	76.53	75.50
TiO_2	0.268	0.262	0.265	0.262	0.261	0.265	0.264	0.270
Al_2O_3	12.67	12.26	12.20	11.81	12.15	12.29	11.92	12.52
Fe_2O_3	0.50	0.88	0.71	0.63	0.63	0.68	0.54	0.62
FeO	1.44	1.37	1.50	1.26	1.35	1.41	1.40	1.43
MnO	0.07	0.03	0.04	0.03	0.05	0.05	0.06	0.05
MgO	1.18	1.42	1.22	0.73	0.65	0.40	0.48	0.51
CaO	0.38	0.22	0.32	0.27	0.31	0.58	0.54	0.40
Na_2O	2.75	2.77	2.55	3.08	2.60	2.56	3.20	2.83
K_2O	4.13	3.02	4.51	3.81	4.76	5.24	3.74	4.83
P_2O_5	0.16	0.16	0.14	0.15	0.16	0.09	0.15	0.15
H_2O^+	0.89	1.26	0.86	0.73	0.73	0.54	0.80	0.69
CO_2	0.14	-	-	-	0.11	-	0.23	-
L.O.I.	1.21	1.42	1.08	1.05	0.94	1.20	0.96	0.93
TOTAL	100.67	99.70	100.31	98.84	100.18	99.04	99.85	100.04
ppm								
Ba	900	720	963	745	928	778	646	707
Rb	145	144	167	130	172	191	128	177
Sr	203	109	161	129	167	112	170	100
Y	62	58	64	61	52	76	56	56
Zr	222	228	219	220	220	227	207	218
Cu	-	-	-	-	31	-	-	-
Th	17	11	18	16	15	14	20	16
Nb	22	22	21	22	21	22	21	21
La	33	42	39	36	27	43	31	40
Ce	70	86	83	79	52	87	68	88
Nd	42	52	48	43	38	55	39	50
U	nd	nd	nd	nd	4	nd	nd	7
Pb	12	nd	nd	nd	79	8	14	nd
F	-	-	-	-	453	-	-	-
Cl	-	-	-	-	193	-	-	-
Zn	-	-	-	-	62	-	-	-

Table 8.1 (cont)

	Devils Punch Bowl Lava		Horses Glen Lava				North Stoompa Lava	
Wt%	8390	9728	81108	81120	9070	9126	9746	9747
SiO_2	78.47	75.20	75.83	75.58	80.62	71.66	85.74	75.47
TiO_2	0.246	0.287	0.242	0.262	0.229	0.284	0.233	0.279
Al_2O_3	11.55	13.55	11.22	11.96	10.20	13.24	6.94	12.30
Fe_2O_3	1.00	2.06	1.27	1.53	0.85	1.75	1.52	1.77
FeO	0.72	0.88	0.52	0.42	0.36	2.48	0.78	1.24
MnO	0.03	0.03	0.03	0.02	0.02	0.03	0.03	0.06
MgO	0.26	0.44	0.24	0.37	0.49	1.77	0.58	1.15
CaO	0.76	0.40	0.42	0.25	0.49	0.22	0.22	0.26
Na_2O	0.97	1.40	3.45	1.79	2.17	2.12	1.63	2.40
K_2O	4.58	3.99	3.59	5.01	2.49	3.37	1.60	3.24
P_2O_5	0.16	0.16	0.14	0.15	0.13	0.16	0.14	0.16
H_2O^+	0.84	1.56	0.45	0.99	1.26	1.95	0.64	1.19
CO_2	-	0.13	-	0.07	-	0.03	0.05	0.07
L.O.I.	1.84	2.09	3.22	1.22	1.53	2.19	1.11	1.71
TOTAL	100.58		100.16	98.58	99.57	99.21	100.53	100.04
ppm								
Ba	1008	1305	818	1124	772	563	453	699
Rb	210	253	88	164	115	154	65	139
Sr	76	94	148	89	119	83	64	140
Y	49	68	52	55	37	62	49	59
Zr	212	248	194	211	177	250	185	226
Cu	28	-	44	-	-	-	-	-
Th	18	18	15	17	14	18	13	15
Nb	18	22	24	22	25	23	23	23
La	35	42	20	41	20	51	5	32
Ce	71	86	46	78	41	107	22	69
Nd	44	49	35	50	28	59	20	47
U	nd	4	nd	nd	nd	4	7	nd
Pb	127	7	125	nd	nd	nd	nd	nd
F	-	-	-	377	-	-	-	-
Cl	-	-	-	180	-	-	-	-
Zn	70	-	36	-	-	-	-	-

Table 8.1 (cont)

	Killeen Lava								
Wt%	7217	7218	9440	9461	9484	9502	9742	9743	9744
SiO_2	75.75	74.48	78.22	73.62	73.66	76.11	66.79	78.82	73.87
TiO_2	0.285	0.283	0.253	0.306	0.273	0.269	0.373	0.227	0.281
Al_2O_3	12.20	12.58	11.22	13.23	12.39	11.70	17.12	9.81	12.57
Fe_2O_3	0.90	1.35	0.53	0.77	1.31	1.90	1.59	1.01	1.06
FeO	0.62	0.49	0.37	1.18	0.74	0.18	0.90	0.46	0.81
MnO	0.03	0.03	0.02	0.02	0.03	0.03	0.04	0.08	0.04
MgO	0.32	0.24	0.28	0.31	0.54	nd	1.18	0.59	0.76
CaO	0.83	0.73	0.65	0.26	0.55	0.26	1.00	2.53	2.19
Na_2O	2.18	2.02	2.81	3.39	1.71	3.19	1.24	0.53	0.88
K_2O	4.99	5.62	3.94	4.98	6.51	4.68	5.64	2.90	3.54
P_2O_5	0.08	0.08	0.12	0.14	0.14	0.14	0.16	0.13	0.14
H_2O^+	0.80	0.53	0.80	0.58	0.66	0.44	1.77	1.17	1.39
CO_2	-	-	-	-	0.35	-	0.66	-	1.54
L.O.I.	1.58	1.47	1.12	0.88	1.32	0.60	3.13	2.28	3.69
TOTAL	99.76	99.36	99.71	99.09	99.17	99.06	99.17	99.37	99.83
ppm									
Ba	1252	756	945	722	1338	747	756	375	448
Rb	150	208	125	172	199	147	323	135	167
Sr	191	108	184	106	255	77	174	269	426
Y	53	58	45	49	54	44	70	46	55
Zr	230	229	191	240	224	207	324	161	226
Cu	-	-	-	-	-	-	-	-	-
Th	17	15	24	19	16	13	21	6	13
Nb	22	26	23	20	19	21	22	12	17
La	31	32	29	27	33	28	47	28	34
Ce	62	68	56	64	64	61	96	61	76
Nd	40	42	38	36	42	37	55	38	42
U	nd	4	nd	6	5	nd	4	nd	nd
Pb	15	21	6	11	13	nd	64	23	52
F	-	-	-	-	-	-	-	-	-
Cl	-	-	-	-	-	-	-	-	-
Zn	-	-	-	-	-	-	-	-	-

Table 8.1 (cont)

	Killeen Lava					
Wt%	7203	7205	8372	8375	9517	9586
SiO_2	74.35	75.19	73.22	76.12	75.37	68.44
TiO_2	0.271	0.271	0.279	0.290	0.278	0.341
Al_2O_3	11.68	12.54	12.47	12.66	12.42	15.59
Fe_2O_3	1.00	1.08	1.74	1.39	1.67	1.41
FeO	0.82	0.20	0.29	0.31	0.34	0.43
MnO	0.06	0.02	0.08	0.01	0.02	0.06
MgO	0.35	nd	0.48	0.25	0.45	0.52
CaO	2.47	0.23	1.08	0.34	0.86	2.54
Na_2O	0.52	3.31	2.42	2.47	1.32	3.41
K_2O	3.83	4.86	5.52	5.70	5.05	3.52
P_2O_5	0.07	0.07	0.14	0.14	0.14	0.15
H_2O^+	0.89	0.46	0.57	0.60	1.08	1.36
CO_2	-	-	-	-	-	2.10
L.O.I.	3.66	0.67	1.87	0.86	2.03	3.70
TOTAL	99.06	98.59	99.62	100.54	99.95	100.11
ppm						
Ba	489	739	935	1363	507	631
Rb	202	172	193	181	183	159
Sr	209	89	221	143	68	318
Y	56	64	44	60	52	68
Zr	205	221	225	231	221	291
Cu	-	-	33	26	-	-
Th	17	15	16	19	18	24
Nb	21	23	16	19	18	20
La	32	74	24	32	42	46
Ce	70	122	59	64	99	106
Nd	41	82	36	38	49	54
U	9	8	nd	5	nd	nd
Pb	8	nd	306	72	6	21
F	-	-	-	-	-	-
Cl	-	-	-	-	-	-
Zn	-	-	115	63	-	-

Table 8.1 (cont)

	Dykes		Agglomerates		Tuffaceous Sediments			
Wt%	8742A	8859	9148	9431	7200	7201	7209	7212
SiO_2	57.85	67.16	78.53	77.62	75.21	72.90	75.77	76.81
TiO_2	0.283	0.377	0.227	0.232	0.346	0.317	0.342	0.248
Al_2O_3	15.63	18.94	10.67	11.08	11.94	12.25	10.86	10.97
Fe_2O_3	2.29	0.15	1.05	1.23	1.73	1.51	1.33	0.90
FeO	9.36	0.29	0.38	0.41	0.58	1.40	1.19	0.92
MnO	0.17	0.04	0.04	0.08	0.05	0.08	0.07	0.08
MgO	5.88	nd	0.63	1.15	0.55	0.82	1.11	0.30
CaO	0.22	0.28	0.64	1.78	0.80	1.62	1.09	0.20
Na_2O	2.75	10.78	4.14	1.54	4.00	4.81	2.97	2.14
K_2O	1.14	0.24	1.38	2.60	2.04	1.06	1.85	5.59
P_2O_5	0.15	0.20	0.15	0.14	0.09	0.11	0.10	0.08
H_2O^+	4.20	0.58	0.58	0.91	0.68	0.82	1.02	0.82
CO_2	0.08	0.02	0.74	1.28	-	1.14	-	-
L.O.I.	4.61	0.29	1.62	2.89	1.42	2.19	2.09	1.94
TOTAL	100.35	99.06	99.45	100.75	98.76	99.35	98.76	100.18
ppm								
Ba	239	nd	199	449	582	240	540	455
Rb	57	3	61	115	76	51	76	68
Sr	63	176	158	111	181	211	195	167
Y	69	147	52	53	26	42	52	36
Zr	248	350	179	179	255	264	216	168
Cu	-	-	-	-	-	-	-	-
Th	14	34	18	19	14	15	14	7
Nb	15	32	26	20	26	26	25	20
La	10	95	38	41	37	28	37	27
Ce	49	188	85	84	82	72	77	59
Nd	37	99	48	50	44	41	44	41
U	4	nd	nd	nd	nd	4	9	4
Pb	nd	14	nd	14	10	45	nd	6
F	642	-	-	-	-	-	-	-
Cl	46	-	-	-	-	-	-	-
Zn	-	-	-	-	-	-	-	-

Table 8.1 (cont)

	Tuffaceous Sediments				Terrigenous Sediments		
Wt%	7216	8423	8435	8480	7758B	7759	9724
SiO_2	71.12	78.72	78.04	77.36	75.81	66.17	86.35
TiO_2	0.331	0.359	0.335	0.374	0.609	0.776	0.247
Al_2O_3	13.17	9.95	9.61	10.66	8.75	13.95	5.43
Fe_2O_3	1.91	0.75	1.39	0.87	1.75	1.04	0.74
FeO	1.12	1.68	1.07	1.53	1.93	4.48	0.42
MnO	0.09	0.08	0.08	0.05	0.11	0.07	0.06
MgO	1.24	0.77	1.21	1.17	2.64	3.87	0.59
CaO	1.66	1.17	1.91	1.20	2.06	0.84	1.73
Na_2O	1.53	2.29	0.57	1.91	1.44	1.40	1.47
K_2O	4.40	2.99	2.99	3.36	1.15	2.32	0.89
P_2O_5	0.10	0.16	0.15	0.16	0.16	0.16	0.14
H_2O^+	1.32	0.73	1.21	0.85	1.61	2.79	0.61
CO_2	1.09	-	1.21	-	-	0.42	1.36
L.O.I.	2.93	1.50	2.84	1.73	3.10	3.88	3.47
TOTAL	99.59	100.42	100.19	100.36	99.48	98.95	101.55
ppm							
Ba	962	1120	649	866	234	380	133
Rb	197	71	130	121	41	84	39
Sr	204	137	61	155	94	52	64
Y	53	48	28	37	21	44	8
Zr	260	208	141	176	300	253	82
Cu	-	-	-	-	-	-	-
Th	14	12	9	9	nd	8	nd
Nb	23	14	10	13	12	15	13
La	42	34	18	27	19	20	6
Ce	78	64	45	56	44	57	27
Nd	47	43	30	38	31	34	14
U	nd	nd	nd	nd	nd	nd	nd
Pb	8	51	37	21	14	nd	nd
F	-	-	-	-	-	-	-
Cl	-	-	-	-	-	-	-
Zn	-	-	-	-	-	-	-

technique was sought for distinguishing between secondary and primary variation. The petrographic observations made in Chapter 6 have shown that mineralogically and texturally the lavas are very similar and appear to have been originally rhyolites. The Bennaunmore lava provides by far the freshest specimens, and it was from this lava that a primary magmatic composition was sought.

8.2 Geochemistry of the Bennaunmore Rhyolite Lava

Inspection of table 8.1 reveals some major oxide and trace element variation among specimens from the Bennaunmore lava (e.g. Al_2O_3,10.07–13.43 wt.%;Na_2O,1.35–3.20 wt.%; Sr, 75–227 ppm.). Primary magmatic variations of such magnitude are very unlikely within this lava flow particularly because:

i) The phenocryst contents are low (see modal analyses, appendix E), and their modal variation too small to be responsible for the bulk chemical variations observed.

ii) No cumulate textures were encountered, and the lava possesses a remarkably uniform texture.

iii) The chemical variations were found to be randomly distributed throughout the flow.

Watkins *et al.* (1970) found no significant primary chemical variation in a lower viscosity basaltic lava flow unit in Iceland, except those due to uneven phenocryst distribution. No similar studies have been made on more acidic and viscous lavas which have not been altered. It is considered therefore that the bulk chemical variations are entirely due to secondary metasomatism.

In the Hughes (1973) alkali ratio diagram (fig. 8.1) the analyses of Bennaunmore rhyolite mostly plot near to the extreme right hand side of the field of the normal igneous spectrum (i.e. high K_2O : total

Fig. 8.1 Plot of total alkalis against alkali ratio (Hughes, 1973). Spectrum of normal igneous compositions is bounded by the solid lines.

Key to symbols used in figs. 8.1, 8.2, 8.3, 8.4, 8.9, 8.11, 8.12, 8.13, 8.18, and 8.19:

Solid circle = Bennaunmore rhyolite,

Solid triangle = ADRP,

Stars = Killeen rhyolite,

Solid square = Miscellaneous rhyolite analyses.

The dashed line delimits the field of Bennaunmore rhyolite compositions.

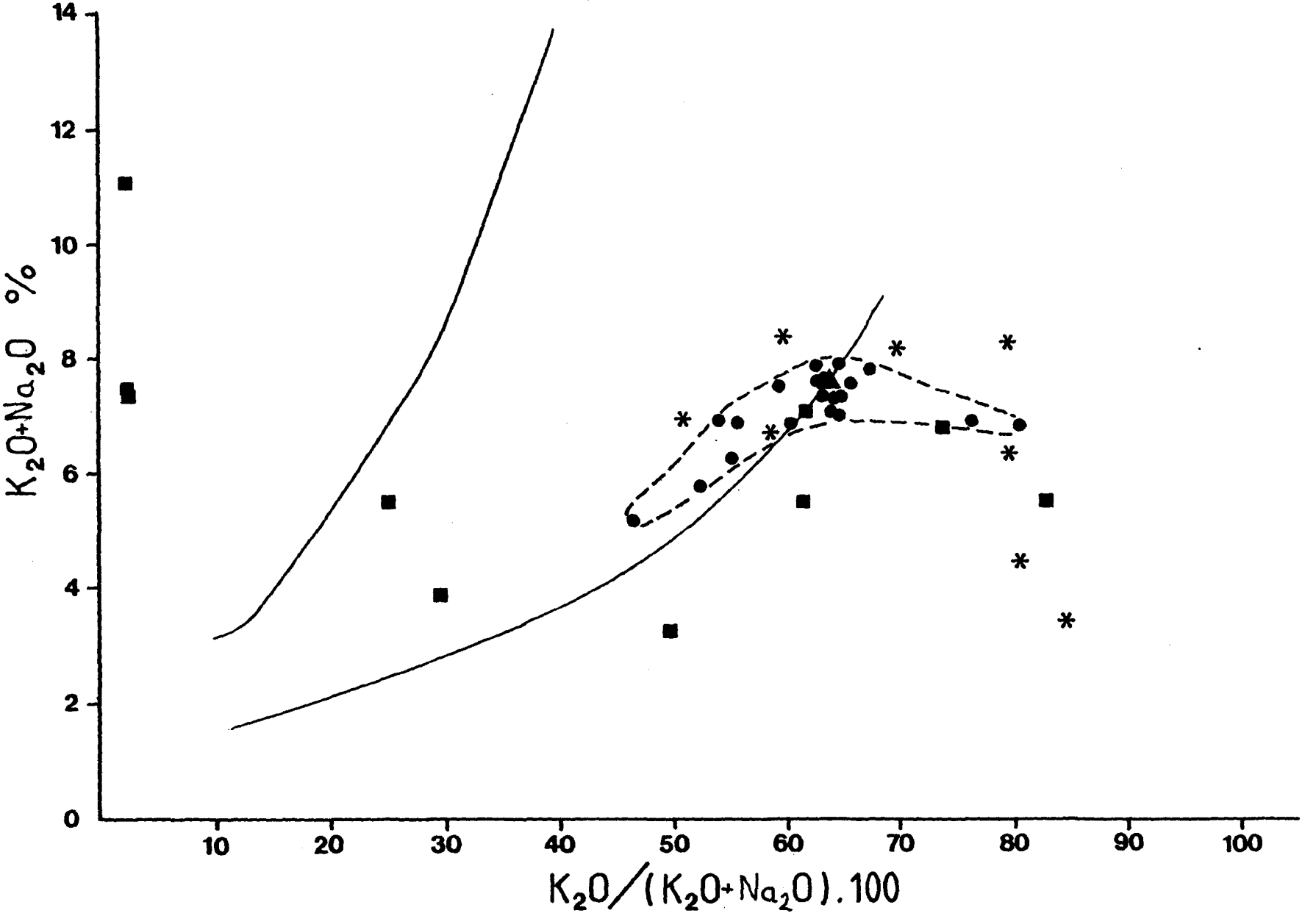
14
12
10
8
6
4
2
0
K_2O+Na_2O %
10
20
30
40
50
60
70
80
90
100
$K_2O/(K_2O+Na_2O).100$

alkalis ratio). There is a tendency for the least petrographically altered specimens to cluster tightly around a total alkali content of 7.5 weight percent with K_2O representing 63% of that total. Outside this tight cluster the field is extended by more altered rocks in which either Na_2O is depleted at near constant total alkalis, or K_2O is depleted with Na_2O constant.

Similar broad distributions are observed in an AFM diagram (fig. 8.2) and a diagram of Na_2O against K_2O and total Fe (fig. 8.3). The tight groupings represent the same set of specimens in each of these plots, and correspond to the most mineralogically fresh specimens. This suggests that these analyses are probably close to a common "parental" bulk composition from which more altered types were derived.

Six bulk analyses were selected for the invariability of the above chemical parameters they possessed, and also for the relative constancy of the levels of the more mobile trace elements, Ba, Rb and Sr. These analyses are presented in table 8.2 along with their averaged bulk analysis termed the Average Bennaunmore Rhyolitic Parent, or ABRP. At this stage no suggestion is made that the composition of ABRP is identical to that of the freshly erupted lava. Minor metasomatism has been observed during the conversion of obsidian to felsite (Zielinski *et al.*, 1977) and the ABRP is thought only to be close to the composition of the devitrified lava beforethe more extensive alteration related to the regional metamorphism took place. The word "parent" is thus synonymous with "pre-metamorphic composition".

Binary diagrams were plotted to investigate the relationships between all the elements determined in the Bennaunmore lava. Correlation coefficients were calculated, and those pairs of elements showing

Fig. 8.3 FeO_T-Na_2O-K_2O diagram of Lough Guitane rhyolite compositions.
Additional symbols used:
Open circle = Eskduff rhyolite,

Fig. 8.2 AFM diagram of Lough Guitane rhyolite compositions.
Additional symbols used:
Dotted line delimits the field of Killeen rhyolite compositions.

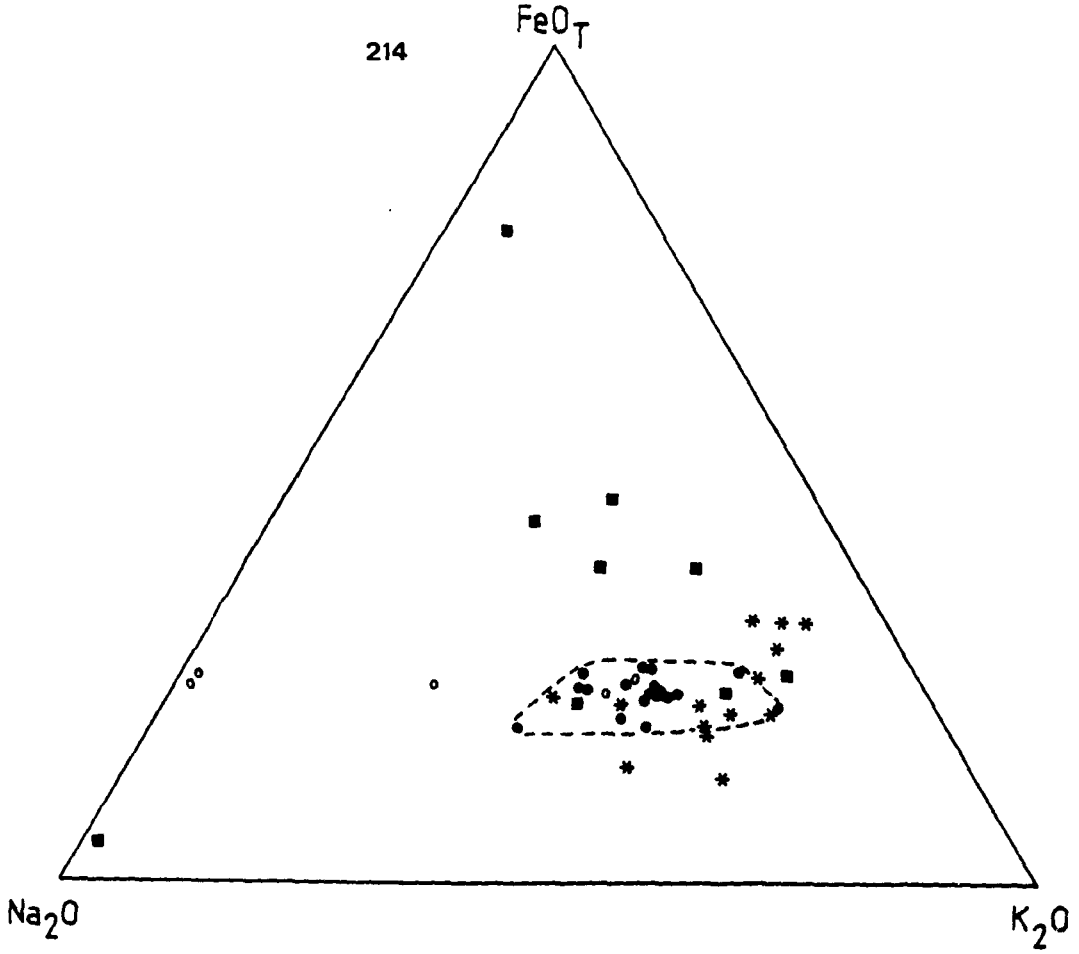
FeO$_T$
Na$_2$O
K$_2$O

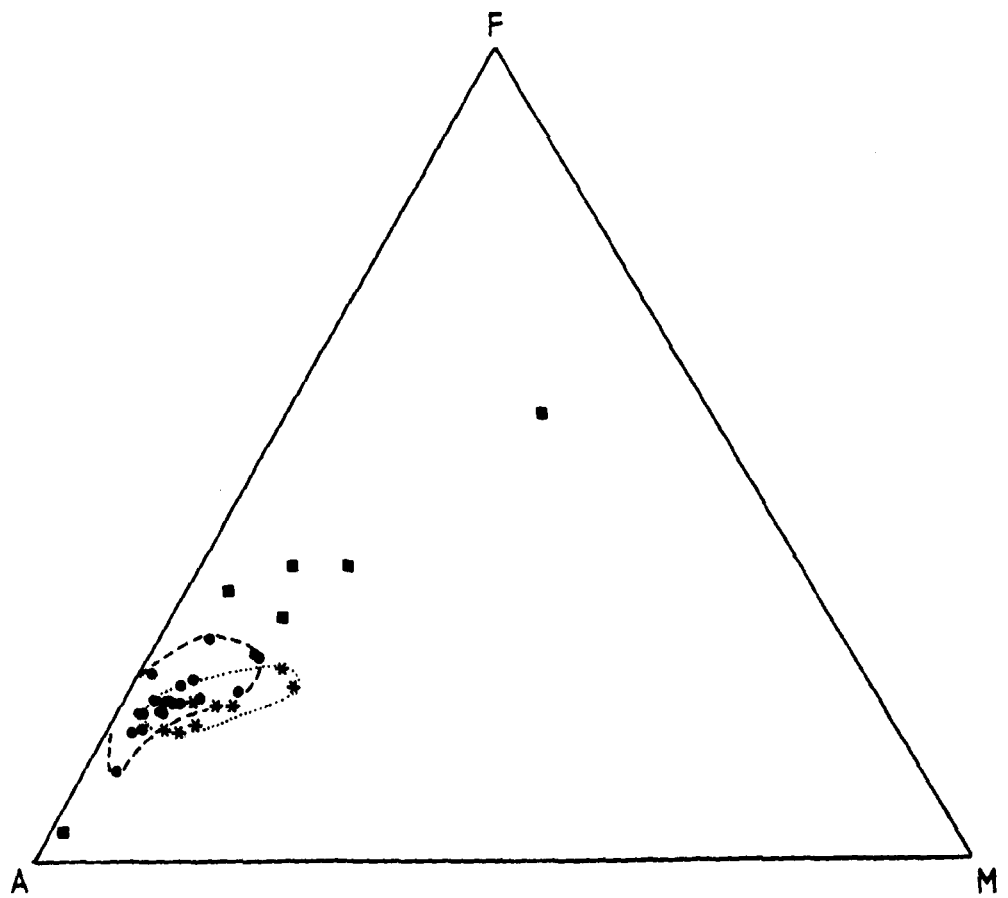
F
A
M

Table 8.2

Calculation of the Average Bennaunmore Rhyolitic Parent (ABRP)

Specimen Analysis (wt. %)	8392	7750	8418	8552	8755	8795	ABRP
SiO_2	75.26	75.51	75.69	75.54	75.77	75.50	75.55
TiO_2	0.258	0.264	0.267	0.269	0.265	0.270	0.2655
Al_2O_3	11.86	12.56	12.34	12.09	12.20	12.52	12.26
Fe_2O_3	0.49	0.63	0.55	0.58	0.71	0.62	0.60
FeO	1.43	1.35	1.76	1.47	1.50	1.43	1.49
MnO	0.07	0.05	0.07	0.03	0.04	0.05	0.05
P_2O_5	0.16	0.09	0.15	0.14	0.14	0.15	0.14
MgO	0.33	0.63	0.65	0.80	1.22	0.51	0.69
CaO	0.50	0.34	0.51	0.29	0.32	0.40	0.39
Na_2O	2.84	2.59	2.72	2.64	2.55	2.83	2.695
K_2O	4.73	4.96	4.64	4.66	4.51	4.83	4.72
H_2O	0.54	0.79	0.60	0.63	0.86	0.69	0.685
CO_2	nd	nd	0.19	nd	nd	nd	(0.19)
TOTAL	99.17	100.12	100.46	99.48	100.31	100.04	99.73
(ppm.)							
Ba	766	707	814	849	963	707	801
Rb	179	172	142	163	167	177	167
Sr	116	98	145	147	161	100	128
Y	62	63	68	56	64	56	61.5
Zr	224	231	228	226	219	218	224
Cu	54	nd	32	nd	nd	nd	nd
Th	19	13	15	16	18	16	16
Nb	20	25	21	21	21	21	21.5
La	36	45	41	38	39	40	40
Ce	80	91	87	79	83	88	85
Nd	48	55	50	44	48	50	49
Zn	128	nd	75	nd	nd	nd	nd
Density ($gm.cm^{-3}$)	2.641	2.648	2.649	2.653	2.653	2.646	2.648

nd = not determined

Table 8.3

Selection of Significant Correlation Coefficients

Elements		Correlation Coefficient	
		All Data	Bennaunmore Lava
SiO_2	TiO_2	-0.870	-0.885
SiO_2	Al_2O_3	-0.932	-0.917
SiO_2	Rb	-	-0.730
SiO_2	Zr	-0.855	-0.900
TiO_2	Al_2O_3	0.918	0.937
TiO_2	Zr	0.950	0.899
Al_2O_3	Zr	0.933	0.890
MgO	H_2O	-	0.803
Na_2O	Ba	-	-0.708
Na_2O	Y	0.756	-
Na_2O	Ce	0.701	-
K_2O	Rb	0.760	0.579
Y	La	0.753	-
Y	Ce	0.741	0.542
Y	Nd	0.658	0.546
Ce	La	0.956	0.931
Nd	La	0.937	0.940
Nd	Ce	0.966	0.907
CaO	CO_2	0.984	-

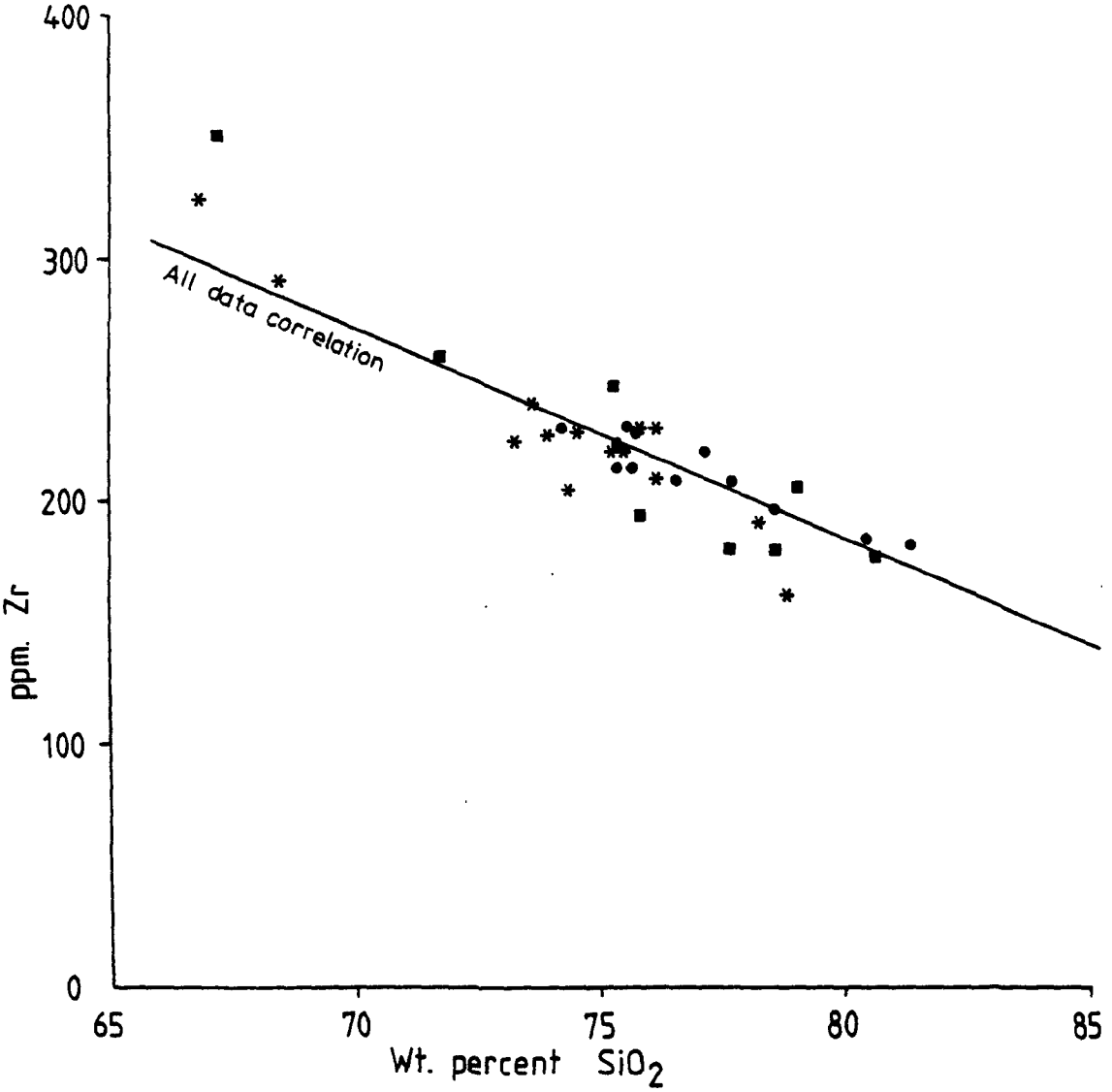

Fig. 8.4 Zr against SiO_2 plot of Lough Guitane rhyolite compositions.

significant[1] correlation are presented in table 8.3. Some of these variation diagrams are presented in figs. 8.4, 8.9-8.14, 8.18 and 8.20. However, they can only reveal compositional trends controlled by one or exceptionally two factors. For example, the plots of Zr against SiO_2 (fig. 8.4) and TiO_2 against SiO_2 show strong negative correlations with intercepts on the SiO_2 axes near 100% SiO_2. This confirms the relative immobility of Zr and TiO_2 and their dependence upon the addition or depletion of silica. However no significant correlations were observed between many pairs of elements, reflecting the complexity of the geochemical processes operating.

8.3 Mass Transfer Computations and Metasomatism in the Bennaunmore Lava

8.3.1 The Mass Transfer Computations

The geochemical relationship between the ABRP and other individual altered/metasomatised specimens from the Bennaunmore rhyolite lava can be studied using the mass-transfer computation techniques outlined by Gresens (1967), Babcock (1973), and Appleyard and Woolley (1978). These calculations have the advantage over binary diagrams as they are capable of comparing individual analyses in a metasomatic environment with a common parent. They also reveal the relationship between groups of elements and their relative mobilities.

A modified version of the mass transfer computation of Babcock (1973) used in this thesis is presented in Appendix G. All volume factors calculated for the bulk rock pairs are presented in table 8.4.

---

[1] Significant correlations were selected largely on qualitative appearance as well as on the correlation coefficient. It was generally found that those coefficients that fell below about 0.6 or 0.5 did not show any significant visual pattern. No statistical estimate of significance was undertaken. The complexity of the calculation of such estimates is prohibitive in "closed systems", i.e. those in which the components must add up to a fixed number (100.00 weight percent in this case).

They have been calculated in two forms:

1. The percentage rock volume required for component n (an element or oxide) to have been immobile between parent A and product B = K_v^n .

2. The chemical transfer of component n between rocks A and B, normalised to the content of n in the parent rock A = ΔF^n.

Theory predicts that two elements or groups of elements possessing markedly different values of K_v^n must have behaved in significantly different ways, and that both cannot have been immobile. This facilitates two powerful geochemical tests.

1. When two rocks are compared, it is possible to determine whether one can be derived metasomatically from the other if certain elements are assumed to be immobile.

2. Conversely, if one rock can confidently be said to be derived from the other, then any immobile elements will always have closely similar values of K_v^n related only to gross volume changes brought about by addition or depletion of major oxide components such as silica.

The geochemical relationship between the ABRP and the bulk analyses of the most chemically unusual specimens listed in table 8.4 can be considered.

8.3.2 Example of the Computations - Specimen 8396

Specimen 8396 possesses the most aberrant bulk analysis of all the 21 analyses of specimens from the Bennaunmore lava flow itself. The values of ΔF^n and K_v^n listed in table 8.4 are plotted on a modified composition - volume diagram derived from Babcock (1973), (fig. 8.5).

SiO_2 is the only component showing absolute enrichment. It is the only component with a positive value of ΔF^n at constant volume ($\Delta F^n > 0$, when $K_v^n = 100$) or a value of K_v^n less than 100 when $\Delta F^n = 0$. The widely varying values of K_v^n for the other components implies that

Key to specimens in table 8.4:

8396 Pale green, veined example from the Bennaunmore rhyolite.

9070 Pale green example of the Horses Glen rhyolite.

9746 Dark grey specimen from single large block in the North Stoompa rhyolite.

9484 Medium grey example of the Killeen rhyolite.

8859 Specimen of the 'Pale' Dyke (albitised).

8461 Pinkish grey example of the Eskduff rhyolite.

8674 Eskduff rhyolite.

8742A Specimen of the Green Dyke (chloritised).

9126 Greenish grey example of the Horses Glen rhyolite.

9742 Pale greenish grey example of the Killeen rhyolite.

9586 Pale patchily pink-green grey example of the Killeen rhyolite.

9743 Pale greenish grey, phenocryst-poor example of the Killeen rhyolite.

Table 8.4

Calculated values of K^n_v and ΔF^n

K^n_v / ΔF^n	8396	9070	9746	9484	8859	8461	8674	8742A	9126	9742	9586	9743
SiO_2	*92.9* 0.08	*93.7* 0.07	*87.7* 0.14	*102.3* −0.02	*113.6* −0.12	*97.0* 0.03	*97.1* 0.03	*124.2* −0.20	*103.4* −0.03	*111.0* −0.10	*108.5* −0.08	*93.5* 0.07
Al_2O_3	*121.6* −0.18	n.d.	*105.6* −0.05	*98.7* 0.01	*65.4* 0.53	*104.0* −0.04	*102.7* −0.03	*74.6* 0.34	*90.7* 0.10	*70.2* 0.42	*77.3* 0.29	*121.5* −0.18
FeO*	*195.3* −0.49	n.d.	*120.2* −0.17	*105.8* −0.06	n.d.	*∿100* ∿0	*97.1* 0.03	*16.9* 4.91	*49.1* 1.04	*85.4* 0.17	*119.5* −0.16	*148.4* −0.33
MnO	n.d.	n.d.	n.d.	n.d.	n.d.	*250* −0.6	n.d.	*27.9* 2.58	n.d.	n.d.	n.d.	*60.9* 0.64
P_2O_5	n.d.	n.d.	*∿100* ∿0	*∿100* ∿0	*70.7* 0.41	*∿100* ∿0	*77.8* 0.29	*88.8* 0.13	*85.8* 0.17	*85.8* 0.17	n.d.	*104.9* −0.05
MgO	*127.7* −0.22	n.d.	*118.3* −0.16	*127.4* −0.215	n.d.	*7143* −0.99	*344.8* −0.71	*11.2* 7.96	*38.2* 1.62	*57.3* 0.74	*130.4* −0.23	*88.5* 0.13
Na_2O	*104.5* −0.04	n.d.	*164.5* −0.39	*157.2* −0.36	*27.1* 2.69	*37.0* 1.71	*38.6* 1.59	*93.2* 0.07	*124.7* −0.20	*213* −0.53	*77.7* 0.29	*495* −0.80
K_2O	*195.7* −0.49	n.d.	*293.3* −0.66	*72.3* 0.38	*1695* −0.94	*2632* −0.96	*2500* −0.96	*393* −0.75	*137.4* −0.27	*82.1* 0.22	*131.8* −0.24	*158.7* −0.37
TiO_2	*118.0* −0.15	*115.9* −0.14	*113.4* −0.12	*96.5* 0.04	*71.1* 0.41	*102.5* −0.02	*102.1* −0.02	*89.3* 0.12	*91.7* 0.09	*69.8* 0.43	*76.9* 0.30	*114.0* −0.12
Zr	*123.2* −0.19	*126.6* −0.21	*120.5* −0.17	*∿100* ∿0	*64.6* 0.55	*99.1* 0.01	*101.8* −0.02	*85.9* 0.16	*87.9* 0.14	*68.0* 0.47	*75.6* 0.32	*135.7* −0.26
Nb	*107.5* −0.07	n.d.	*93.0* 0.08	*112.9* −0.11	*67.8* 0.47	*86.0* 0.16	*89.6* 0.12	*136.4* −0.28	*89.5* 0.12	*100* ∿0	*105.7* −0.05	*174.5* −0.43
Y	*136.6* −0.27	*166.2* −0.40	*124.9* −0.20	*113.0* −0.12	*42.3* 1.37	*54.9* 0.82	*80.9* 0.24	*84.8* 0.18	*97.3* 0.03	*86.2* 0.16	*89.3* 0.12	*130.3* −0.23
La	*129.0* −0.23	*200.0* −0.50	*793* −0.87	*120.9* −0.17	*42.5* 1.35	*58.8* 0.70	*47.6* 1.10	*380* −0.74	*76.9* 0.30	*83.5* 0.20	*85.5* 0.17	*139.3* −0.28
Ce	*121.5* −0.18	*207.5* −0.52	*384* −0.74	*132.5* −0.25	*45.7* 1.19	*57.8* 0.73	*39.5* 1.53	*165* −0.39	*77.9* 0.28	*86.8* 0.15	*78.8* 0.27	*135.9* −0.26
Nd	*111.4* −0.10	*175.1* −0.43	*244* −0.59	*116.4* −0.14	*50.0* 1.00	*70.0* 0.43	*37.4* 1.67	*125.9* −0.21	*81.4* 0.23	*87.3* 0.15	*89.2* 0.12	*125.6* −0.20
$K_D(\Delta_1)$	1.000	1.000	1.005	1.013	0.990	1.000	1.000	1.048	1.020	1.027	1.013	1.026

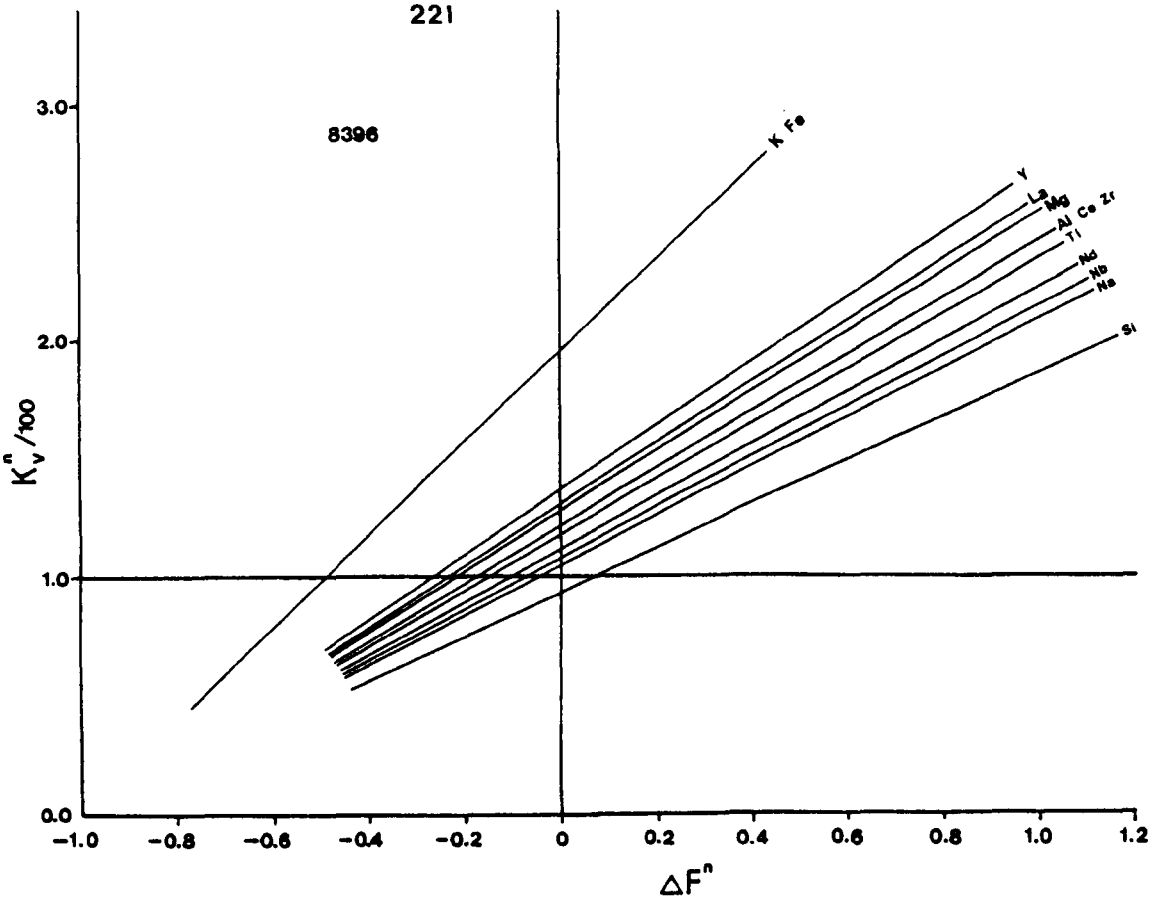

Fig. 8.5 Modified composition–volume diagram for spec. 8396.

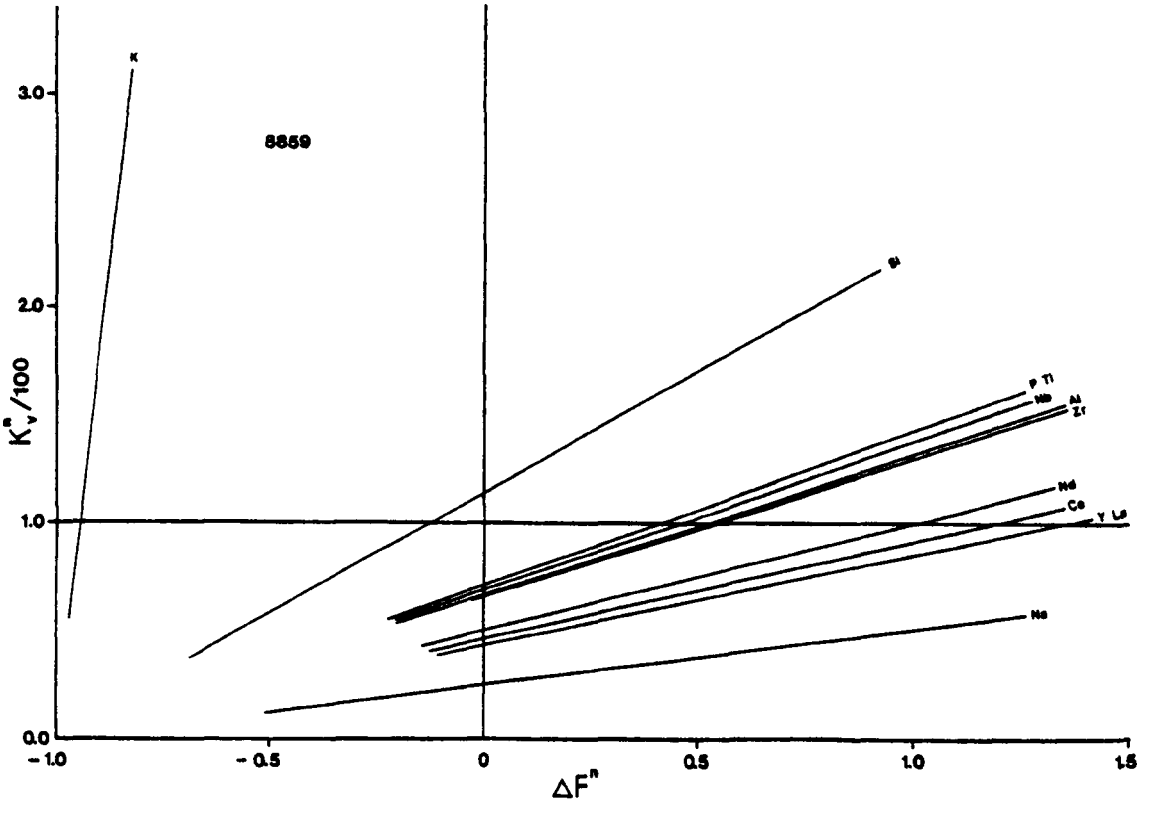

Fig. 8.6 Modified composition–volume diagram for spec. 8859.

they cannot all have been solely controlled by silica enrichment. Applying test (2) above, TiO_2, Zr, Al_2O_3 and Ce all possess comparable values of $\Delta F^n/K_v^n$. If these elements are assumed to have been immobile, then a volume increase of about 20% is implied ($K_v^n \simeq 118$ to 123). Clearly, the other elements cannot also have been immobile Na_2O, Nd and Nb have been enriched, and MgO, La, Y, K_2O and total Fe depleted relative to the immobile group.

Inverting the above argument, most of the elements which would have been assumed to be immobile under test (1), (Zr, TiO_2 and perhaps Al_2O_3) have closely comparable values of K_v^n . It is unlikely that such elements of differing geochemical properties, if all mobile, would have behaved in such a closely similar pattern. Thus, the application of both the geochemical tests has been vindicated.

8.4 Metasomatism and the Bennaunmore "Dykes"

On textural and mineralogical grounds it has been suggested (Chapter 6.6) that the Green Dyke, and the Pale "Dykes" observed intruding the Bennaunmore lava are strongly metasomatised bodies, whose original composition was identical to, or very close to that of the rhyolite lava flow.

8.4.1 The Pale "Dyke" - Specimen 8859

The composition of this rock is extremely unusual, and approaches that of pure albite (see table 8.5 for comparison). Such a rock, with the mineralogical and geochemical nature of an albitite, but with phenocrysts similar in morphology and modal proportions to those of the Bennaunmore lava cannot have been the product of primary magmatic processes alone. Strong sodium metasomatism must have played an important role.

Table 8.5

Comparison between pure albite and the bulk rock composition of the Pale "Dyke" (Deer *et al.*, 1966)

Specimen/Mineral (Wt. %)	8859	Albite (anal. 1, p. 324)
SiO_2	67.16	67.84
TiO_2	0.38	0.00
Al_2O_3	18.94	19.65
Fe_2O_3	0.15	0.03
FeO	0.29	0.02
MnO	0.04	0.00
P_2O_5	0.20	0.00
MgO	0.16	0.04
CaO	0.28	0.00
Na_2O	10.78	11.07
K_2O	0.24	0.29
H_2O	0.58	0.56
CO_2	0.02	-
Total	99.22	99.50

The composition volume diagram (fig. 8.6) derived from the data in table 8.4 emphasises the strong enrichment of Na_2O and depletion of K_2O relative to ABRP. Ba and Rb are also reduced to levels below instrumental detection limits (table 8.1). Among the remaining elements showing absolute enrichment, the similarity of K_v^n values for the supposedly immobile elements TiO_2, Al_2O_3, Zr, Nb and P_2O_5 is striking, although the light rare earth elements (LREE) and Y are all relatively enriched. This grouping of relatively immobile elements, using test (1) above, provides strong evidence for the derivation of the Pale "Dykes" by metasomatism of a rock of Bennaunmore lava composition.

8.4.2 The Green Dyke - Specimen 8742A

On textural and mineralogical grounds the Green Dyke has also been suggested as either

(a) a metasomatised dyke rock of primary composition close to the ABRP (Chapter 6.6), or

(b) a basaltic magma contaminated by rhyolitic magma of Bennaunmore lava composition.

In table 8.6 the major oxide composition of the Green Dyke is compared with the average basalt and andesite of Nockolds (1954). Total Fe, MgO and H_2O are seen to be high, and TiO_2 and CaO exceptionally low for an igneous rock of about 58% silica. The trace element contents and ratios displayed in table 8.7 confirm the unusual composition of the Green Dyke when compared with average basalt and andesite (Winchester & Floyd, 1977), while the similarities with the ABRP are striking.

The modal proportions of the phenocrysts renders the contamination model (b) unlikely without some special process to incorporate the phenocrysts preferentially from the acidic magma. Alternatively, many

Table 8.6

Comparison of bulk rock analyses of average Andesite and Basalt with the Green Dyke

(Wt. %)	Andesite[1]	Basalt[1]	Green Dyke
SiO_2	54.20	50.83	57.85
TiO_2	1.31	2.03	0.28
Al_2O_3	17.17	14.07	15.63
Fe_2O_3	3.48	2.88	2.29
FeO	5.49	9.05	9.36
MnO	0.15	0.18	0.17
MgO	4.36	6.34	5.88
CaO	7.92	10.42	0.22
Na_2O	3.67	2.23	2.75
K_2O	1.11	0.82	1.14
P_2O_5	0.28	0.23	0.15
H_2O	0.86	0.91	4.20
CO_2	-	-	0.08
Total	100.00	100.00	100.00

[1]Average composition (oxides wt. %) from Nockolds (1954)

Table 8.7

Comparison of bulk rock trace element contents of average basalt and andesite, with the Green Dyke

	Basalt[1] (High Al)	Andesite[1] (s.l.)	ABRP	Green Dyke
TiO_2	11000	8000	2700	2800
P_2O_5	0.21	0.20	0.14	0.15
Y	25	25	61.5	69
Zr	126	126	224	248
Nb	5.6	4.6	21.5	15
Ce	47	30	85	49
Zr/TiO_2	0.011	0.015	0.084	0.087
Nb/Y	0.22	0.18	0.35	0.22

[1] Average compositions from Winchester and Floyd (1977)

authors (e.g. Whitehead & Goodfellow, 1978; Hellman *et al.*, 1979; Chikhaoui *et al.*, 1980; Strong *et al.*, 1979) have shown Fe and Mg to be mobile under low grade alteration. The metasomatic model can be evaluated using mass transfer calculations.

Fig. 8.7 again illustrates the close correlation of K_v^n values between the supposedly immobile elements Zr, TiO_2, Y and P_2O_5, although Al_2O_3 appears to be slightly enriched. As would be expected MnO, MgO and total Fe have been strongly enriched, while SiO_2, K_2O and the LREE have been depleted.

8.4.3 Summary of Metasomatism in the Bennaunmore Rhyolite

Mass transfer computations and their application through the two approaches outlined in section 8.3.1 have been shown to be useful tools in quantifying metasomatic processes within the Bennaunmore lava flow when an initially uniform composition is assumed. The significant correlations between pairs of elements listed in table 8.3 can thus be explained as follows:

1. Correlations between the more immobile components, Al_2O_3, TiO_2 and Zr, and to a lesser extent Y and Rb can be explained by their dependence upon SiO_2 enrichment or depletion.

2. Those elements which indicate the degree of alteration, for example SiO_2, CaO (as calcite), FeO (oxidised to Fe_2O_3), MgO and H_2O.

3. Those elements which possess similar geochemical characteristics, e.g. Rb and K_2O, CaO and Sr, and the LREE and Y.

A closer examination of there relations, and the behaviour of individual elements is undertaken in section 8.6 when the bulk geochemistry of all the lavas has been described. Why particular dykes or rocks have been susceptible to a particular type of metasomatism is discussed in section 8.7.

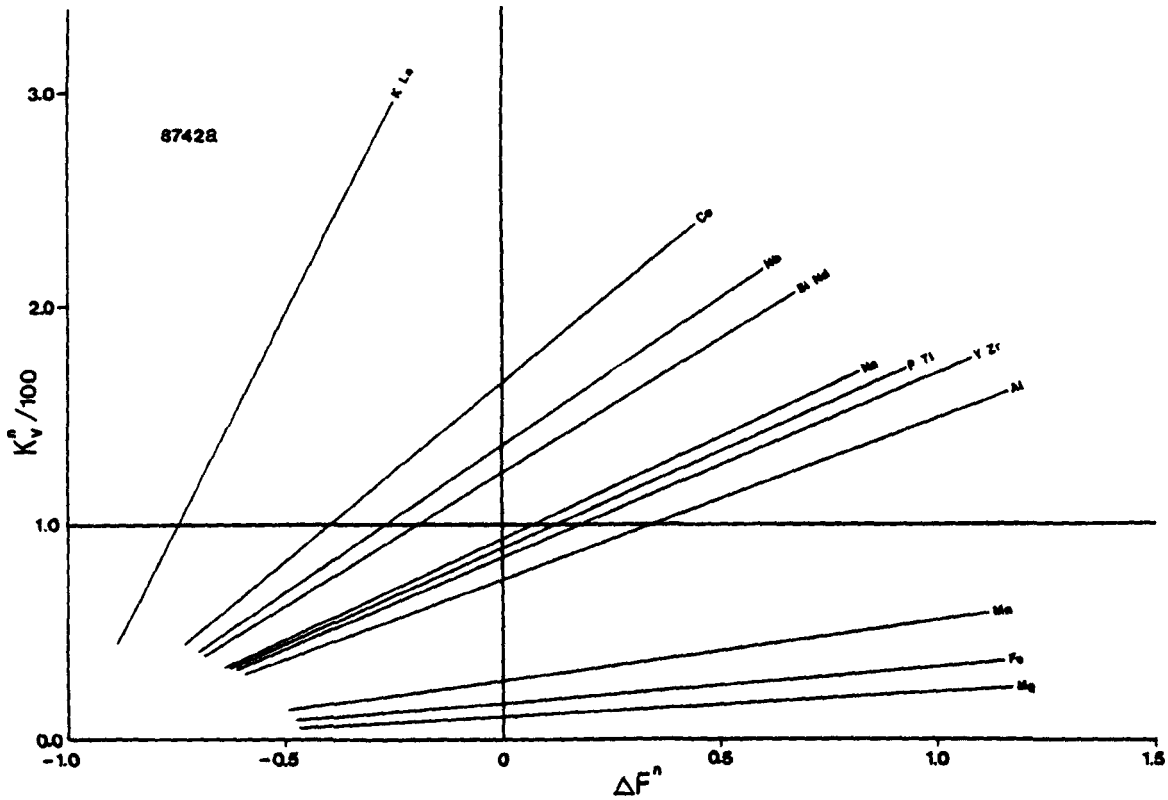

Fig. 8.7 Modified composition-volume diagram for spec. 8742a.

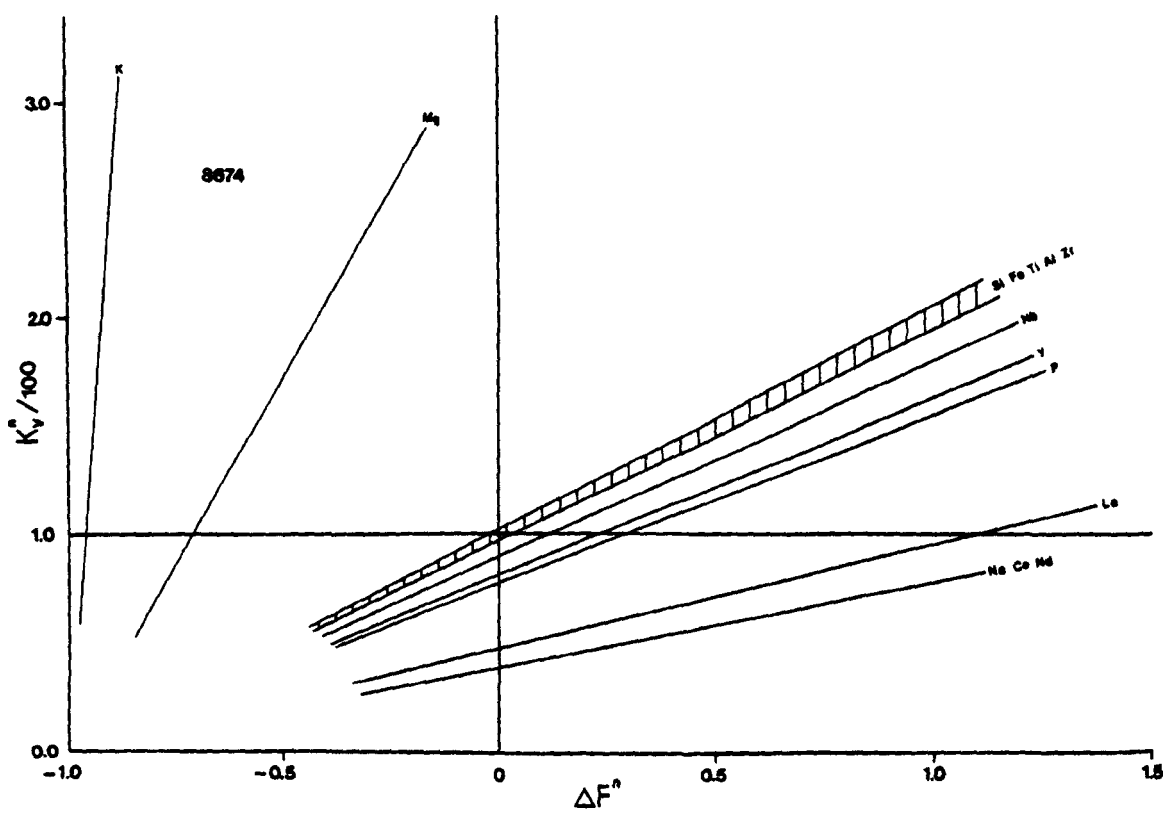

Fig. 8.8 Modified composition-volume diagram for spec. 8674.

8.5 Mass Transfer Computations and Metasomatism in the other lavas

8.5.1 Introduction

The strong mineralogical and textural similarities between the Bennaunmore rhyolite and the other lava flows of the Lough Guitane area have been noted in Chapter 6. An examination of the data in table 8.1 reveals a general similarity in the contents of the more mobile major and trace elements, although the broader spread of compositions probably reflects the generally more altered state of the specimens.

Alkalis are particularly variable (figs. 8.1 and 8.3) along with CaO, total Fe, SiO_2 and MgO, while Ba, Sr, Zn and Pb show wider variation than in the Bennaunmore lava. Immobile elements such as TiO_2, Al_2O_3, Zr and Nb are encountered at almost identical levels in all lava specimens with a few notable exceptions which will be dealt with below. Those elements which showed systematic covariance within the Bennaunmore lava alone appear to behave in the same way when the survey is extended to all the data (table 8.3).

These overall similarities indicate an opportunity to extend the use of mass transfer equations to the comparison between the ABRP and other distinctly separate rhyolitic lava flows, and in particular with those more aberrant bulk compositions thought possibly to represent primary magmatic variations.

8.5.2 The Eskduff lava

In specimen 8674 (see table 8.4) the immobile elements TiO_2, Al_2O_3 and Zr all possess very similar values of ΔF^n and K_v^n, near to zero and near 100 respectively thereby implying no significant volume changes during metasomatism (see also fig. 8.8). It is not surprising therefore that SiO_2, already suggested as a major controlling factor over immobile element levels, should also have a K_v^n near to 100. K_2O

and MgO are the only strongly depleted elements while Na_2O and the LREE are strongly enriched. Fe and Nb show little mobility.

In specimen 8461, SiO_2 again has been little altered along with Al_2O_3, total Fe, P_2O_5, TiO_2 and Zr. K_2O, MgO, MnO and CaO show strong depletion while Na_2O, LREE and Y show strong enrichment. This behaviour supports the hypothesis that these specimens have been metasomatised from a parental Eskduff lava composition very close to that of the ABRP.

8.5.3 Other Lava Flows

Mass transfer computations have been made on analyses from the Horses Glen lava (specs. 9126, 9070), the North Stoompa lava (spec. 9746) and the Killeen lava (specs. 9484, 9586, 9742, 9743). Their values of ΔF^n and K_v^n are presented in table 8.4. Of these, the Horses Glen lava specimens conform to a model of derivation from a parental composition close to that of the ABRP, as do specimens 9484, 9586 and 9742 from the Killeen lava, and the North Stoompa specimen. However, specimen 9743 exhibits a marked overdepletion of Zr relative to Al_2O_3 and TiO_2 outside the possible variation due to experimental error. It is possible therefore that specimen 9743 had an original parental magmatic composition significantly different from the ABRP, at least in the level of Zr.

8.6 Elemental Behaviour During Metasomatism

Leaving aside the petrogenetic implications of the composition of the ABRP, and the deviant composition of specimen 9743, the data described above facilitate a close study of the behaviour and mobility of the elements investigated.

SiO_2: The close relationship between the immobile element contents and the silica content has already been described above. The immobility

of Al_2O_3 suggests that a large proportion of the SiO_2 in these rocks is fixed in aluminosilicates, and that the SiO_2 variations are due entirely to the addition (e.g. spec. 8396) or removal (e.g. spec. 8859) of free silica in the form of quartz. The dominance of quartz as a vein mineral supports this hypothesis, as is the total absence of free quartz in the albitised Pale "Dyke" (spec. 8859).

Total Iron as FeO*: In binary diagrams total iron fails to correlate significantly with any other element or oxide. It is probable that total iron levels reflect the amount of chlorite, and to a lesser extent opaque ore minerals, present. Iron mobility is also indicated by the presence of chlorite as a common vein mineral. Neither the oxidation ratio, or the individual levels of FeO and Fe_2O_3 correlate with any other element or oxide confirming the independence of iron in this metasomatic system, and underlining the unreliability of its oxidation state as a general indicator of the degree of alteration.

MnO: Because of the very low manganese contents encountered, very little significance can be attached to the spread of data. Only in the Green dyke (spec. 8742A) a strongly iron enriched rock, is significant MnO enrichment observed. The high chlorite content of this rock probably controls this enrichment: Electron microprobe analyses (see Chapter 7) reveal chlorite in the dyke to contain up to 1.5 per cent MnO.

MgO: The high variation of MgO in the six analyses used to calculate the ABRP (table 8.2) renders assessment of its behaviour via mass-transfer calculations unreliable. Electron microprobe analyses (see Chapter 7) reveal a MgO content in chlorites from the Bennaunmore lava of about 5 per cent, and the rough positive correlation of MgO with FeO in highly iron enriched or depleted rocks probably indicates that most of the MgO is held in chlorite.

Na_2O: The only sodium phase in these lavas is albite. Modal contents of albite phenocrysts vary little (see appendix F) and the large variations in Na_2O content must therefore be dependent upon sodium feldspar in the groundmass. This probably reflects the higher susceptibility of sodium to redistribution either in the originally glassy groundmass or later in the very finely recrystallised state. The negative correlation between Na_2O and Ba probably relates to the removal of Ba during the progressive albitisation of some of the rocks, but the positive correlation with Y and Ce cannot be explained by any simple chemical process.

K_2O: K_2O also exhibits extreme mobility. In strongly sodium metasomatised rocks (specs. 8859, 8674 and 8461) K_2O is virtually absent. White mica, the only major K_2O phase in the lavas is very scarce in these specimens, but relatively abundant in the groundmass of rocks enriched in K_2O.

CaO and CO_2: The interdependence of these two components is illustrated in fig. 8.9. With two exceptions all the points lie roughly equidistant from, and below, a line representing the composition of calcite. Petrography confirms that calcite is the dominant carbonate mineral and the constant excess calcium causing the displacement of the points in fig. 8.9 from the calcite line is due to the stability of apatite. Using an acidified potassium ferricyanide staining technique (Hutchison, 1974) the carbonate mineral present in the least altered lavas was found to be ferroan calcite. This goes some way to explaining the deficiency in CaO encountered in many of the lavas, especially those with high carbonate contents, when executing mesonorm calculations (appendix D), and the position of some points in fig. 8.9 close to, or above the calcite curve.

H_2O^+: White mica of phengitic composition (Chapter 7) and chlorite

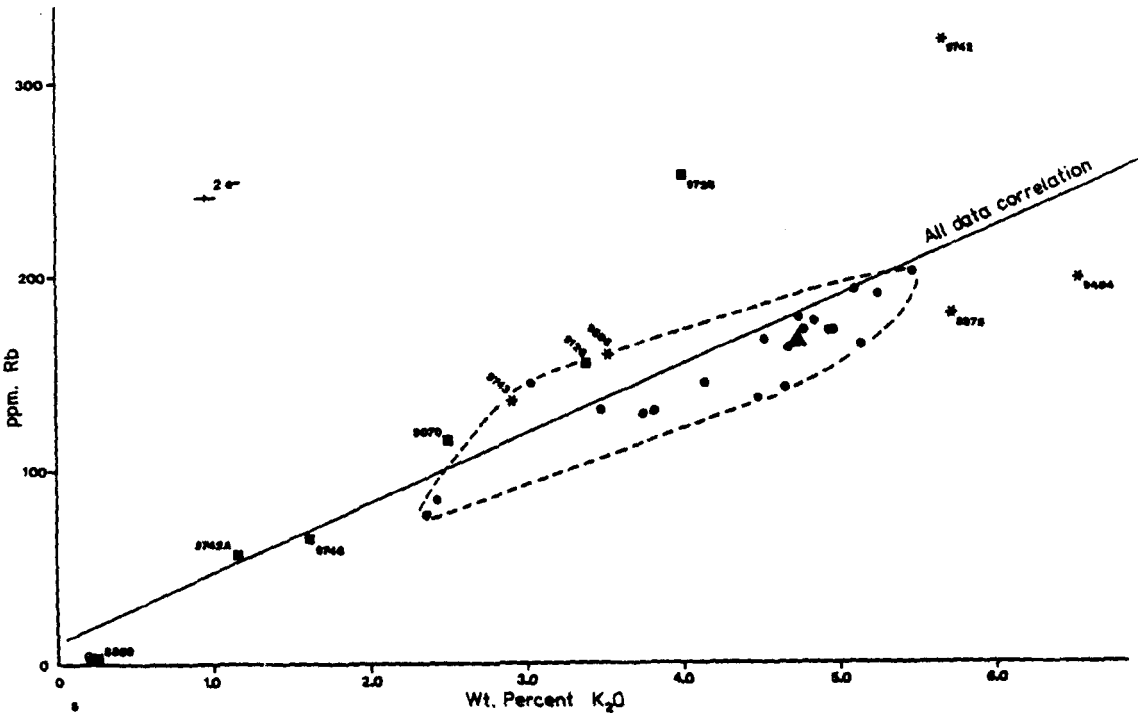

Fig. 8.10 Plot of Rb against K_2O for selected Lough Guitane Rhyolite compositions.

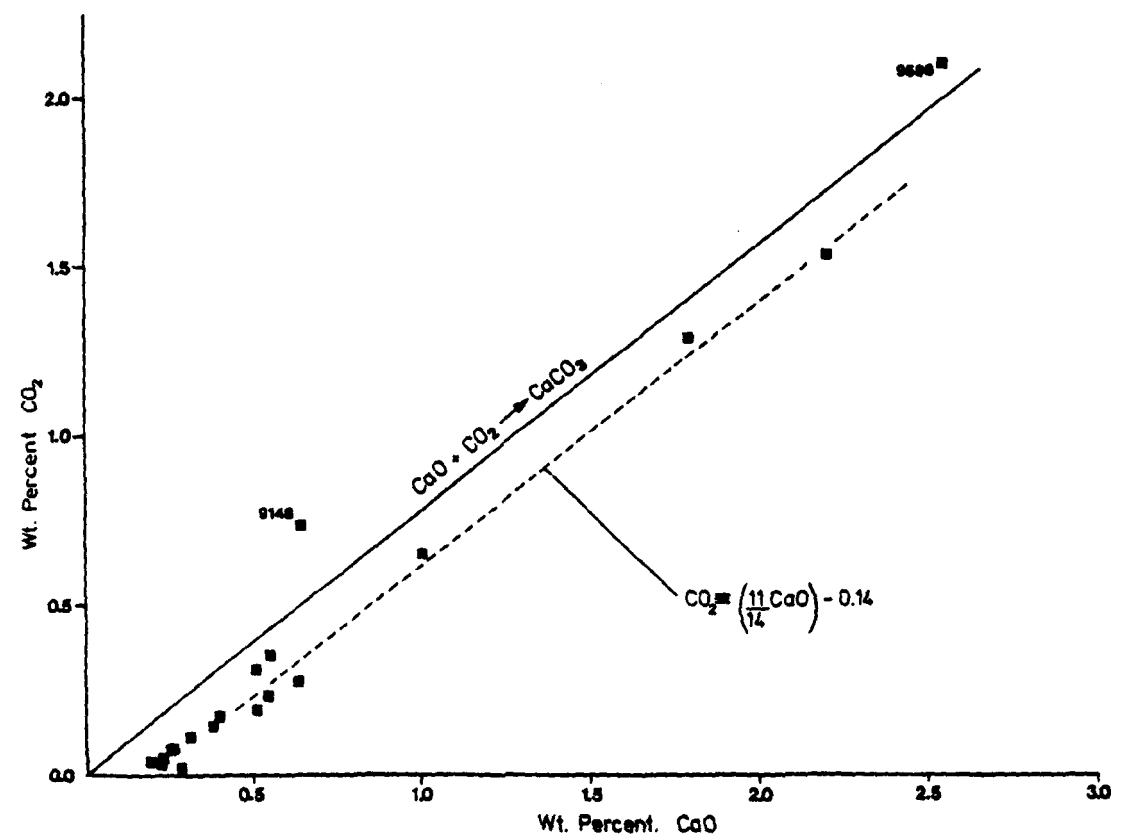

Fig. 8.9 Plot of CO_2 against CaO for selected Lough Guitane rhyolite compositions.

both possess significant water contents and probably exert the largest influence over the bulk rock water content. The correlation between H_2O^+ and MgO in the analyses of the Bennaunmore lava (table 8.3) reflect the dominant control of chlorite in specimens of a lava in which K_2O (and therefore white mica) is fairly constant.

P_2O_5: P_2O_5 appears to be relatively immobile. Marked deviations of ΔF^n and K_v^n from that of TiO_2 and Zr are absent although the very low P_2O_5 contents make a reliable quantitative assessment impossible. Apatite is a ubiquitous accessory mineral in the most altered and the freshest rocks, and appears stable under all prevailing metasomatic conditions.

Rubidium: Most Rb is held in potassium minerals (e.g. white mica) as reflected by the correlation between Rb and K_2O (fig. 8.10). In rocks almost completely leached of K_2O, Rb levels fall below the instrumental detection limit. Only two rocks showed significant Rb enrichment (specs. 9728, 9742) above the correlation curve.

Strontium: Like Rb, Sr contents are highly variable reflecting the mobility of this element. The correlation with CaO (table 8.3) suggests that most Sr was expelled from the plagioclase on albitisation, and that most is now present in calcite. Sr levels are high in specimens with high contents of secondary calcite.

Barium: In relatively fresh rocks Ba varies between 500 and 1305 ppm., although in specimens with exceptionally low K_2O, Ba levels fall below the instrumental detection limit. Apart from this, Ba shows no correlation with any other element or oxide and must be regarded as behaving independently.

Copper and Zinc: Some variation of these elements is observed (table 8.1), but none that can be correlated with any other element or oxide. Such variations may reflect very limited degrees of mineralisation.

Lead: Lead levels in the lavas suggests that some minor lead mineralisation has occurred, whole-rock contents reaching over 300 ppm in two instances, while background levels encountered in half of the analyses fall below the instrumental detection limit. The anomalous concentrations cannot be correlated with any other element or with any petrographic feature, and no geographical pattern emerges from the locations of samples with high lead.

Thorium and Uranium: Both these elements occur at levels near to, or below the instrumental detection limits. No anomalously high values were obtained, or any other significant variations observed.

Light Rare Earth Elements (LREE), La, Ce and Nd: Binary diagrams of one LREE plotted against another (figs. 8.11, 8.12, 8.13) reveal very close correlations between La, Ce and Nd (see also table 8.3). However such variation appears to be independent of silica and mass transfer computations (table 8.4) reveal that overall enrichment and depletion relative to the immobile elements are common phenomena, especially in the more altered rock specimens.

Each of the LREE appears to behave in a similar way. Their values of K_v^n are usually very similar with a few notable exceptions discussed below. These similarities are illustrated in fig. 8.14, a plot of Ce K_v^n against La K_v^n. In effect, if in fig. 8.14, each normalised analysis (K_v^n) plots on or near the line drawn, then the two elements have behaved in very similar ways independent of any gross rock volume changes. In fig. 8.15, the LREE are plotted against K_v^n Zr, an element known to be immobile, and the K_v^n of which is dependent only on gross rock volume changes. In contrast with the close correlation in fig. 8.14, the plots in fig. 8.15 show no correlation, illustrating the independent, but mutual behaviour of the LREE. The apparent over-depletion of La relative to Ce and Nd in specimens 8742A, 9746 and 9070

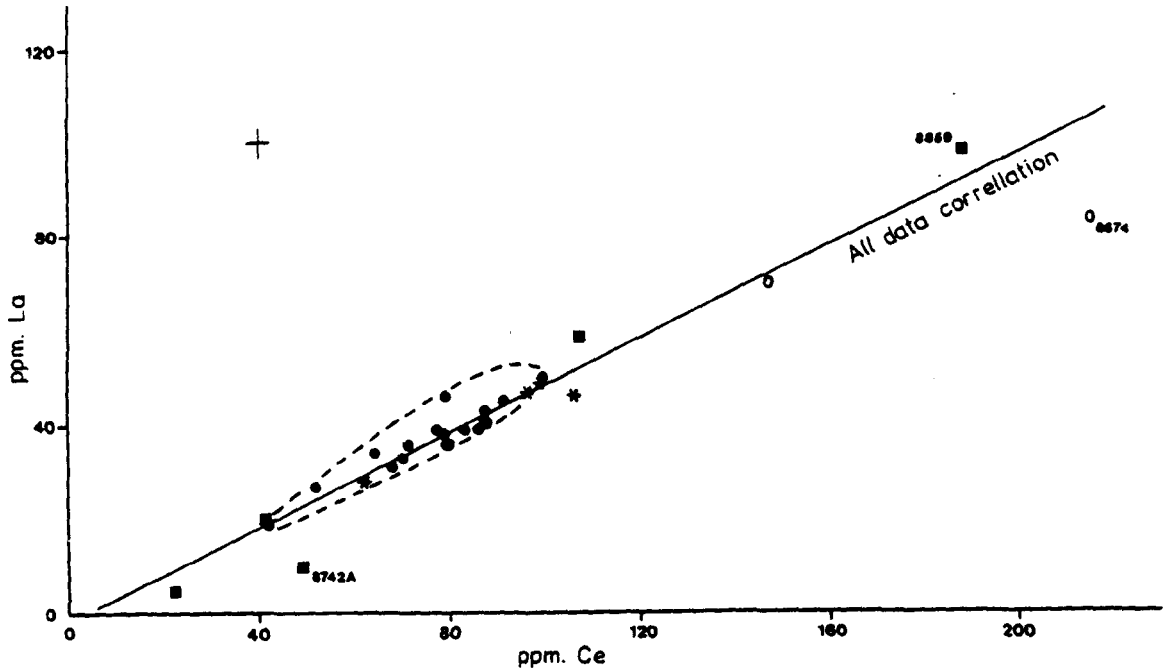

Fig. 8.11 Plot of La against Ce for selected Lough Guitane rhyolite compositions.

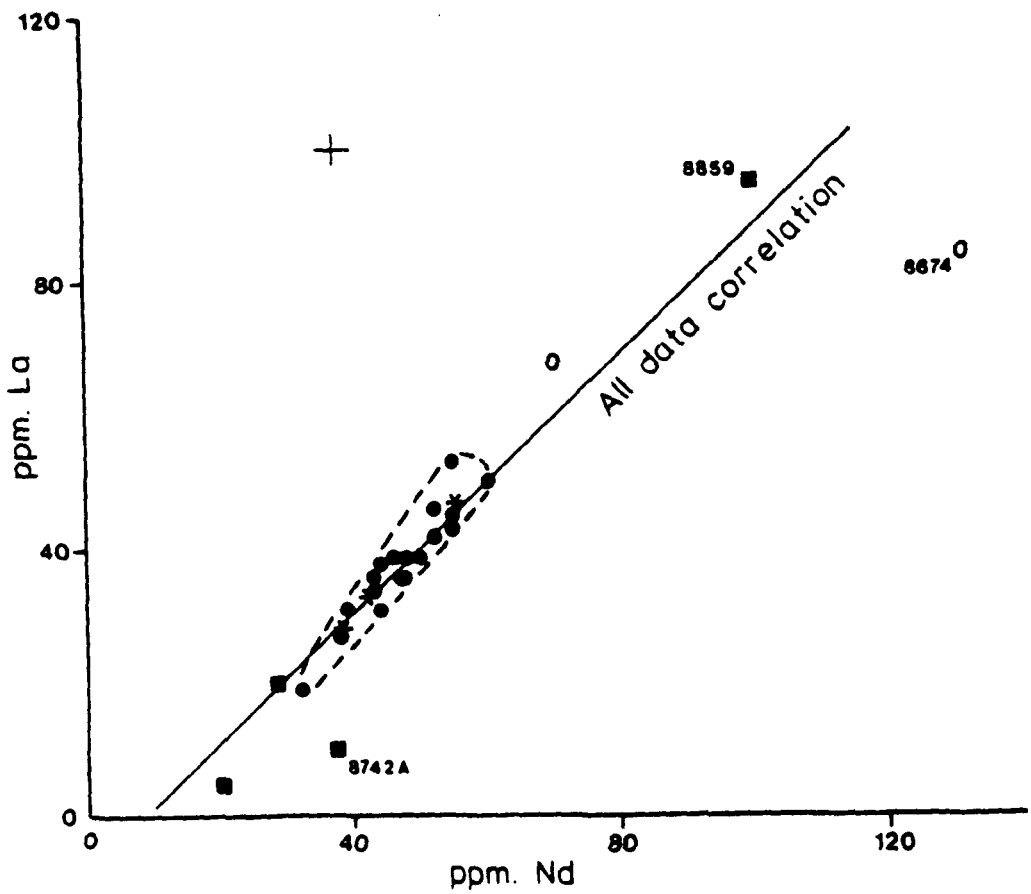

Fig. 8.12 Plot of La against Nd for selected Lough Guitane rhyolite compositions.

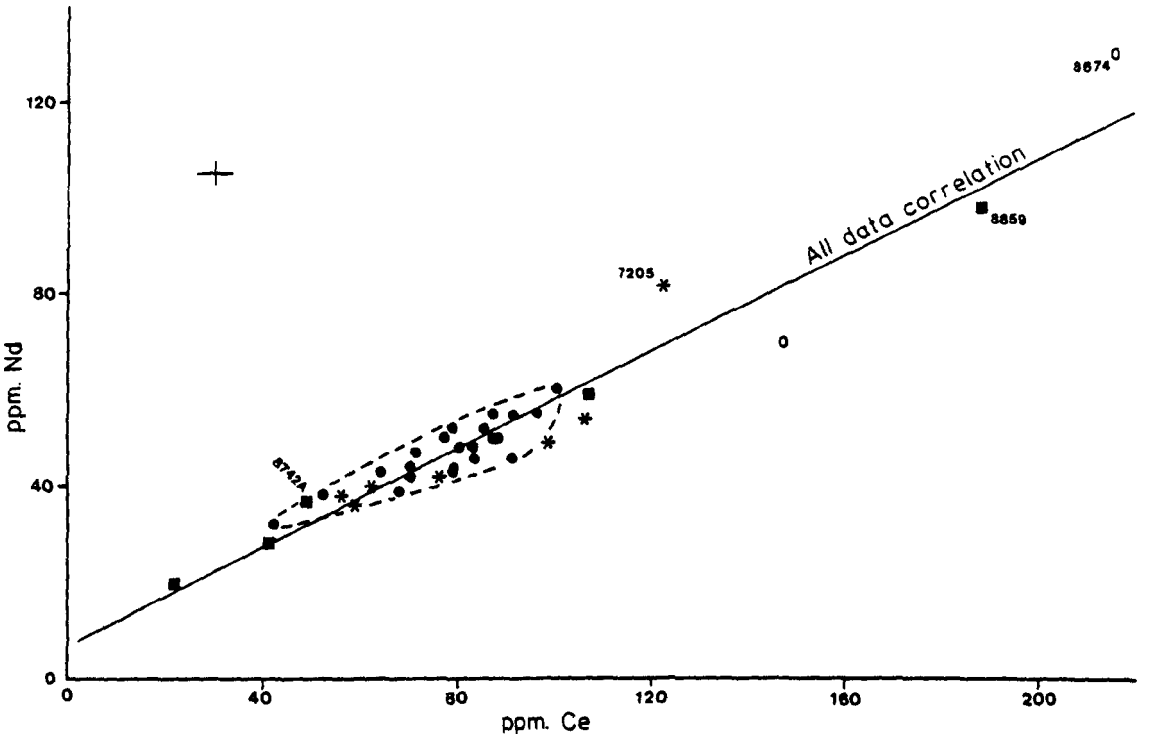

Fig. 8.13 Plot of Nd against Ce for selected Lough Guitane rhyolite compositions.

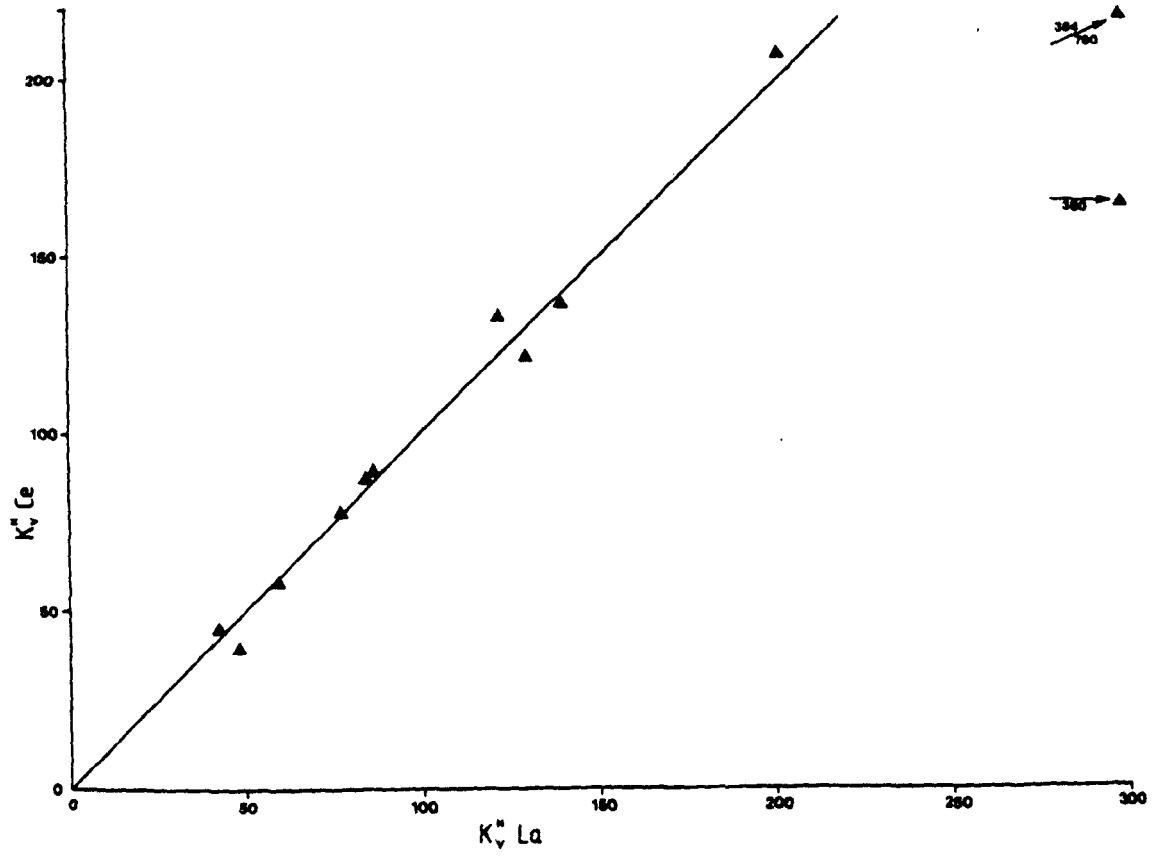

Fig. 8.14 Plot of K_v^n Ce against K_v^n La. (Values from table 8.4).

Fig. 8.15 Plots of K_v^n Zr against K_v^n La, Ce and Nd.

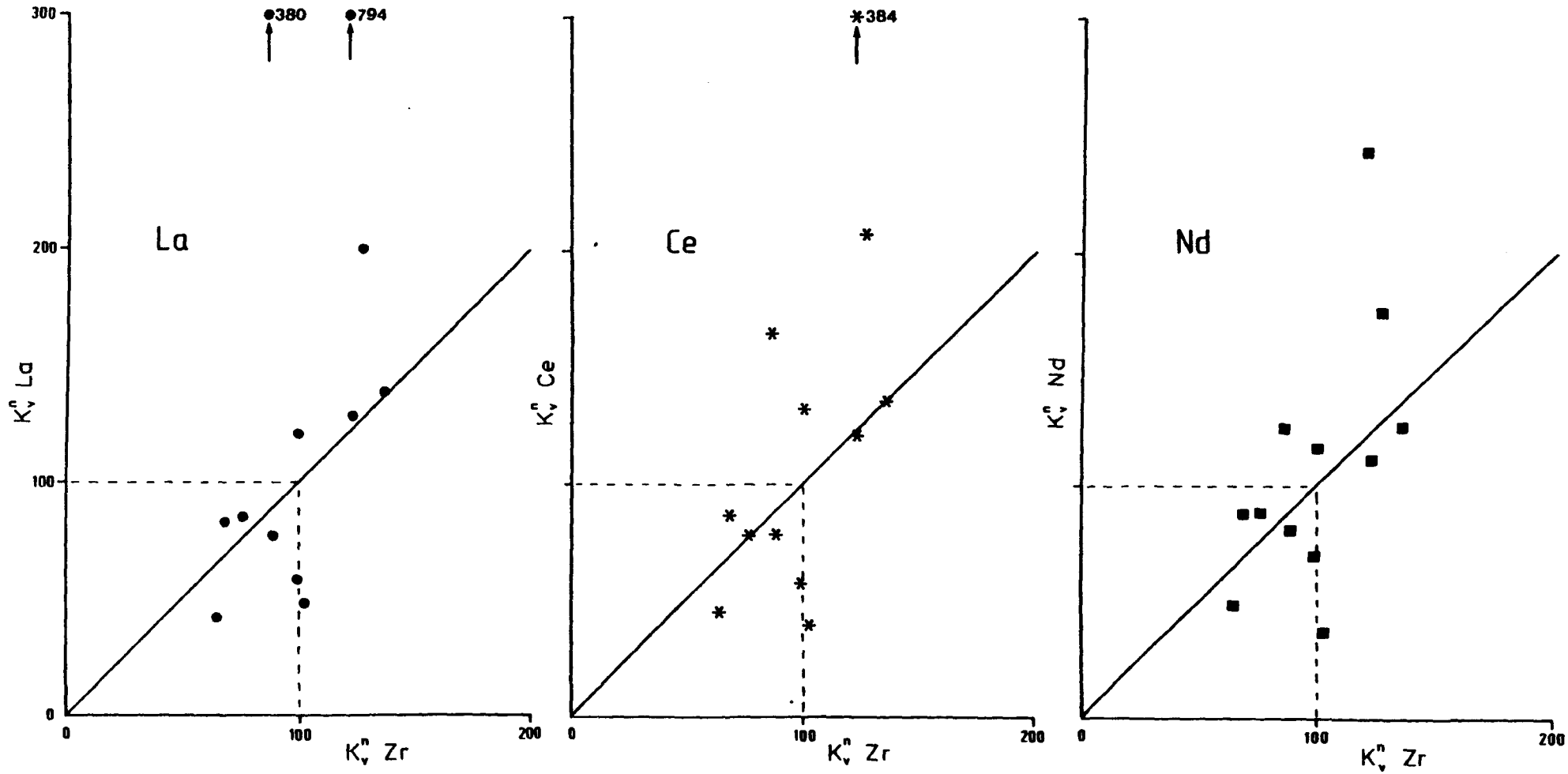

indicated by unequal values of $\Delta F^n/K_v^n$ reflects the failure of the regression lines in figs. 8.11, 8.12, 8.13 to pass through the origin. These discrepancies are difficult to explain by any geochemical phenomenon, and probably represent an instrumental defect. This problem is further discussed in Appendix B.

Allanite, observed in many thin sections, is the dominant LREE mineral (see mineral analyses Chapter 7). As a secondary mineral its presence in high modal proportions in the chloritised ferromagnesian phenocrysts (Appendix F) probably reflects mobility over distances of the order of a millimetre to iron-rich sites where crystallisation of a phase capable of accommodating LREE was occurring. Such short range mobility was important in the freshest specimens, but the presence of allanite as a vein mineral illustrates mobility over distances in excess of hand specimen size.

Total Rare Earth Elements: Fig. 8.16 shows two total REE plots normalised to an average chondrite, one from a specimen of the Bennaunmore rhyolite (8775) and the other from the Green dyke (8742A) (see also table 8.8). The rhyolite, whose bulk rock chemistry is very similar to that of the ABRP, exhibits limited LREE enrichment relative to the HREE, (Ce_N/Yb_N = 2.53) and a pronounced negative europium anomaly (Eu^*/Eu_N = 0.31). The Green dyke exhibits relatively depleted LREE and enriched HREE resulting in a flat pattern (Ce_N/Yb_N = 0.98) although the europium anomaly remains virtually unchanged (Eu^*/Eu_N = 0.34).

It is possible to make only general remarks on the metasomatic behaviour of the REE between these two rocks. However, the flattening of the chondrite normalised plot is similar to that described by Alderton *et al.* (1980) from a chloritised granite from southwest England, and possibly indicative of certain low-grade metamorphic terrains (Hellman *et al.*, 1979). It is not possible, given the limited

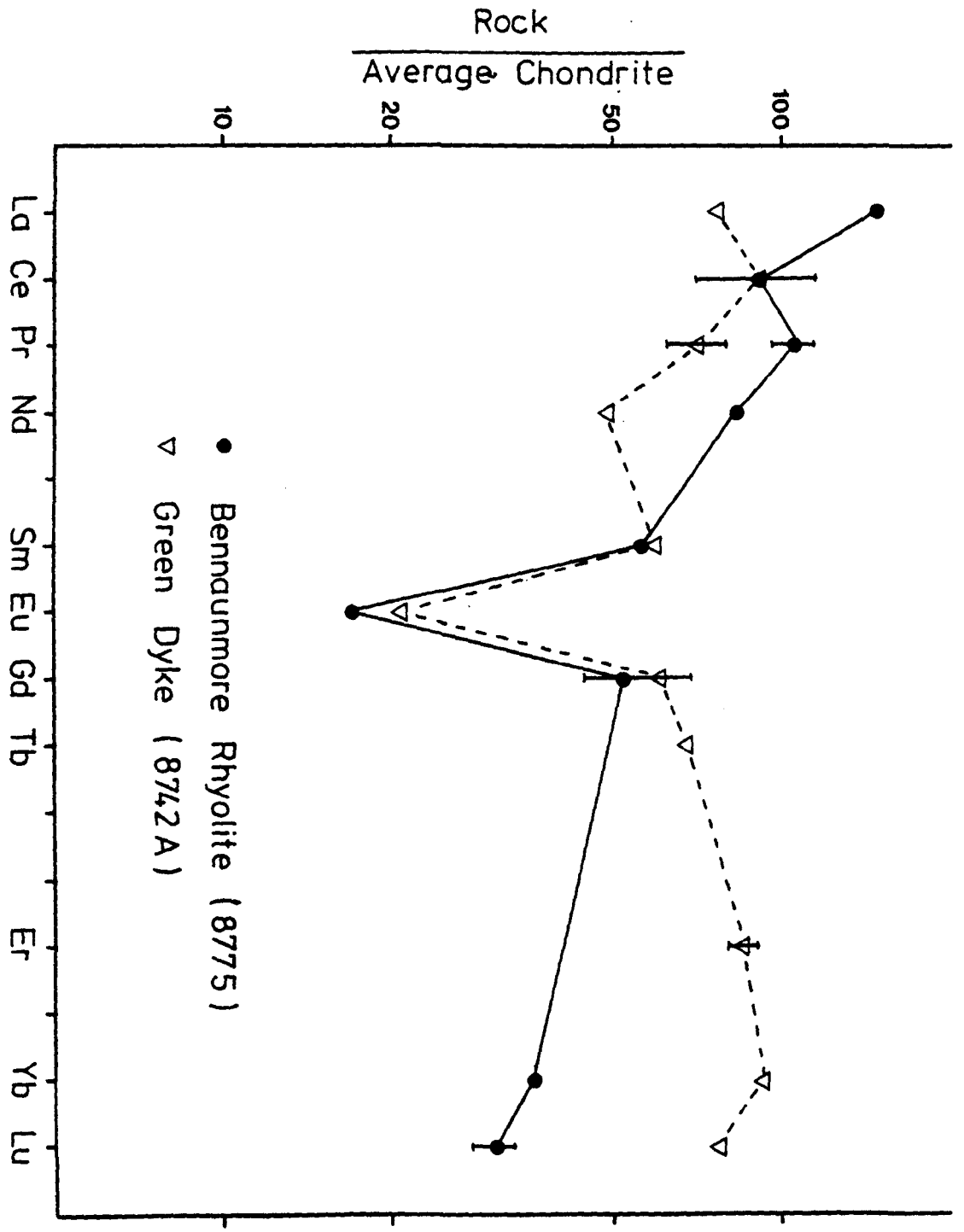

Fig. 8.16 Rare earth element contents from table 8.8, normalised to an average chondrite (Frey et.al., 1968).

Table 8.8

Rare Earth Element analyses of a sample of Bennaunmore rhyolite and the Green Dyke

Spec. No. (ppm)	8775		8742A	
La	49.1	(0.4)	25.4	(0.7)
Ce	80	(20)	80	(20)
Pr	12	(1)	8	(1)
Nd	50	(2)	29	(2)
Sm	10.2	(0.2)	10.7	(0.2)
Eu	1.17	(0.03)	1.42	(0.04)
Gd	13	(2)	15	(2)
Tb			3.18	(0.09)
Dy	14.8	(0.6)	22.7	(0.9)
Ho			5	(0.2)
Er			17	(1)
Yb	7.2	(0.2)	18.5	(0.8)
Lu	1.05	(0.02)	2.6	(0.2)

REE values and 2σ errors in brackets for a sample of Bennaunmore rhyolite (8775) and the Green Dyke (8742A)

data available, to assess conclusively whether the europium anomalies are of primary magmatic or metasomatic origin. The former is extensively documented from magmas which have undergone plagioclase fractionation, while europium mobility during alteration and weathering is variable, probably being dependent upon its oxidation state (Sun & Nesbitt, 1978). Europium behaved in parallel with the other REE in a study of a weathering profile (Duddy, 1980) while Alderton *et al.* (1980) found divalent europium, to behave differently from the other REE in both K-silicate and sericitic granite alteration. It is felt, simply because of the remarkable similarity between the normalised europium anomalies of the two specimens and despite the strong Fe-Mg metasomatism of one, that europium has not been mobile, and the anomaly is primary and petrogenetically significant.

Yttrium: Y is commonly assumed to behave in a fashion similar to the REE (Mason, 1966) and the HREE in particular (Balashov *et al.*, 1964) owing to its similar ionic potential. In the Lough Guitane lavas correlation coefficients between Y and the LREE are about 0.7 (table 8.3) supporting this view, although some limited correlation with silica and the other immobile elements has been noted (fig. 8.18). In those specimens on which mass transfer computations have been undertaken, values of ΔF^n and K_v^n for Y compare closely with those for the LREE in most cases, with little correlation with K_v^n Zr (fig. 8.19). The exceptions are specimens 8742A (Green Dyke), 9746 and 8674 where it appears to have been relatively immobile with the LREE either strongly enriched or depleted. No correlation between the mobility or immobility of Y and the type of metasomatism is apparent, 8742A being chloritised and 9746 and 8674 being silicified. Of the common minerals known to concentrate Y (Lambert & Holland, 1974), apatite and zircon appear stable in these rocks, while allanite is a secondary mineral, and probably

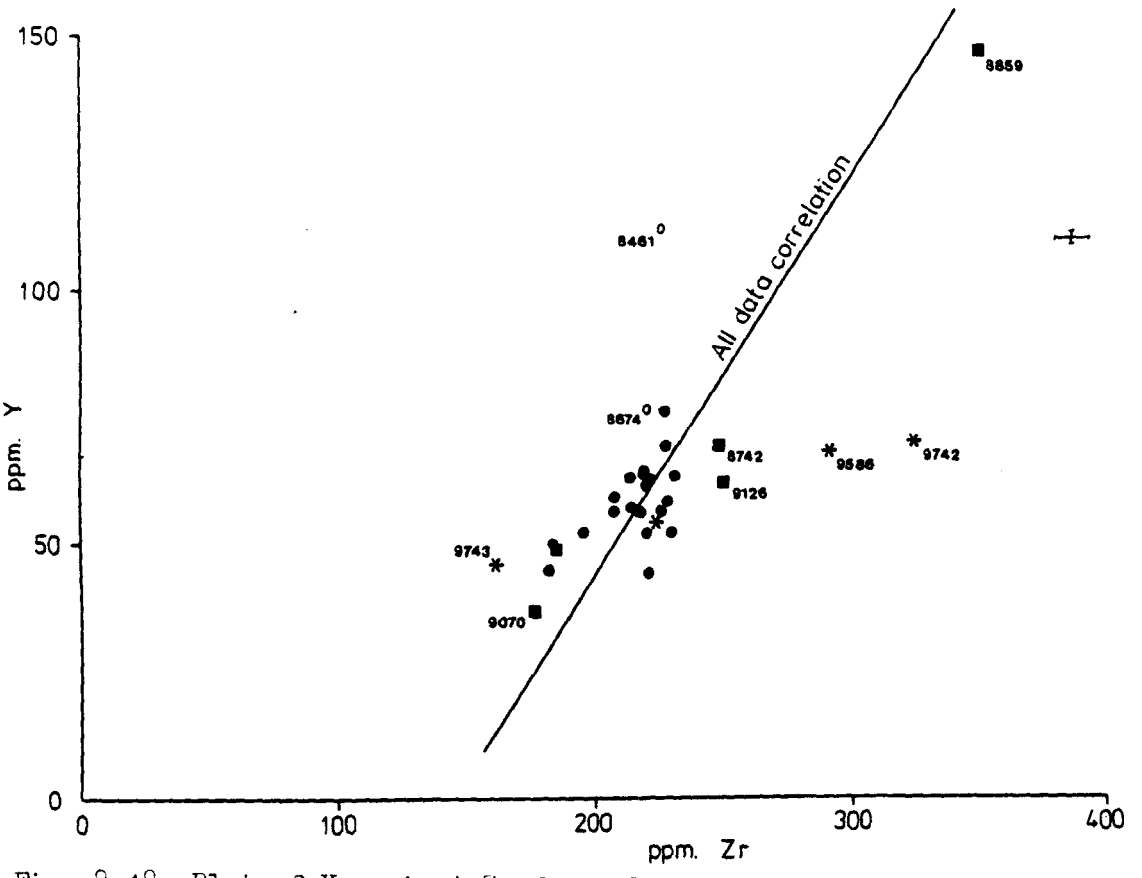

Fig. 8.18 Plot of Y against Zr for selected Lough Guitane rhyolite compositions.

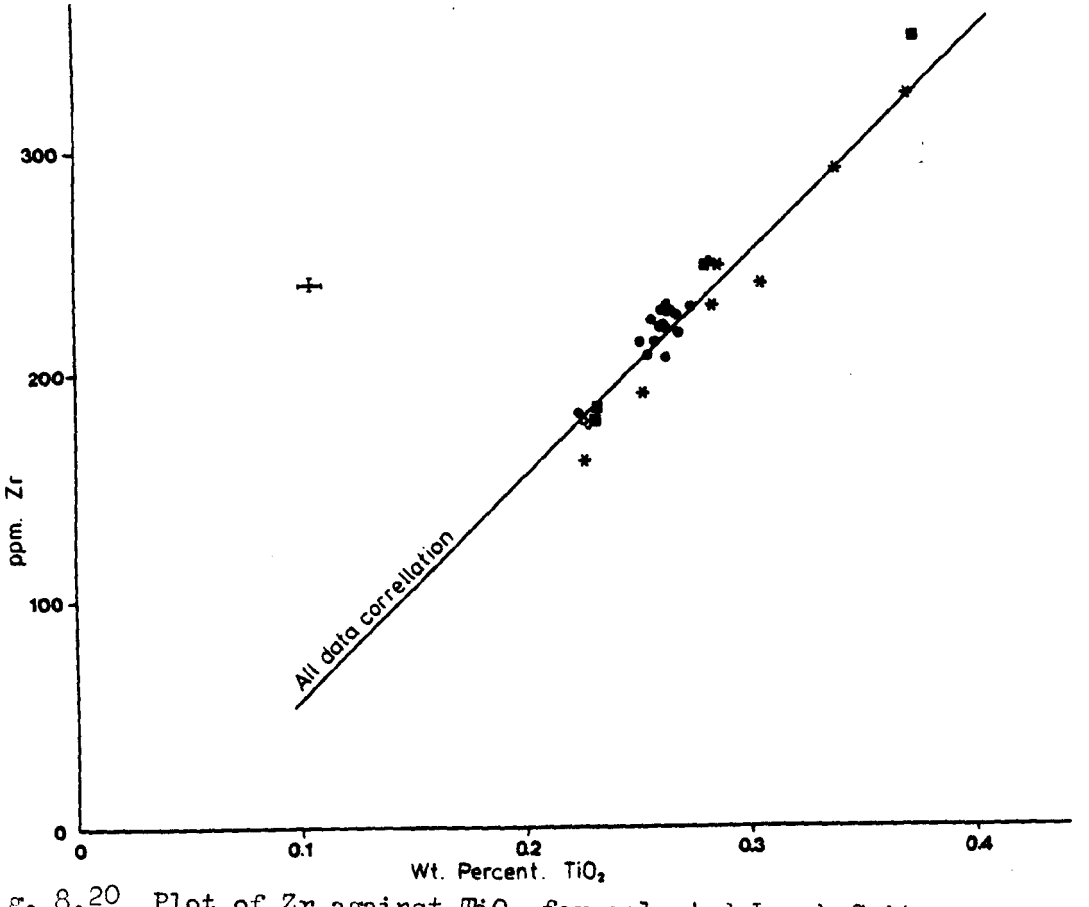

Fig. 8.20 Plot of Zr against TiO_2 for selected Lough Guitane rhyolite compositions.

contains a large proportion of the bulk rock Y.

Niobium: Despite the lack of correlation observed between K_v^n Zr and K_v^n Nb in fig. 8.19. Nb is considered to be relatively immobile. Small deviations of ΔF^n and K_v^n from those of Zr are probably due to experimental imprecision. Only the Green Dyke (spec. 8742A) possesses an anomalously low Nb content, and specimen 9743 is relatively depleted in Nb, but this rock may have had a parental magmatic composition different from that of the ABRP (see section 8.3 above). The relative immobility of Nb reflects its stability in most metasomatic environments (Heinrich, 1966), and its presence in stable titanium minerals such an anatase and sphene in these rocks.

TiO_2: In all but one rock values of K_v^n for TiO_2 are almost identical to Zr, the two values for each specimen plotting on a line of "mutual immobility" in fig. 8.19. Although petrographic evidence in the form of leucoxene overgrowths on anatase (see Chapter 6) suggest TiO_2 is mobile on a millimetre scale, it is obviously immobile over distances greater than about 1 cm. The inequality of K_v^n TiO_2 and K_v^n Zr in specimen 8743 probably reflects a parental composition different from ABRP.

Zirconium: Finally, mention must be made of Zr, which has been used as a standard by which the mobility of other elements and oxides is measured. Only in exceptional metamorphic or metasomatic environments has Zr been proved to be mobile (Dostal *et al.*, 1980; Clough & Field, 1980). The ubiquitous presence of primary unaltered zircon in all the specimens studied supports the contention that this element is immobile under these alteration/metasomatic conditions. Zr plotted against TiO_2 in a binary diagram (fig. 8.20) reveals the close correlation between these two components already outlined above (fig. 8.19).

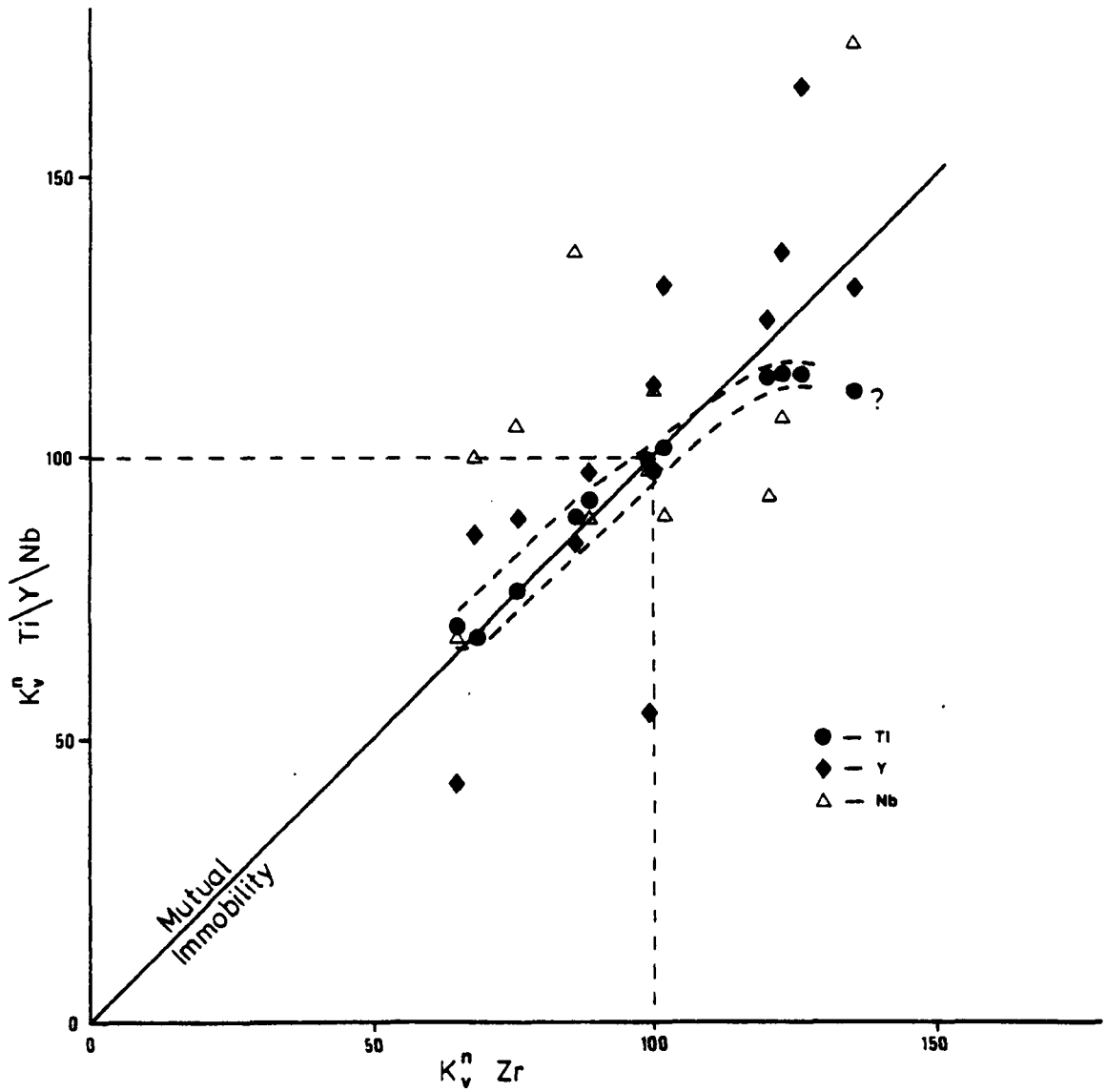

Fig. 8.19 Plot of K_v^n Zr against K_v^n Ti, K_v^n Y and K_v^n Nb. Values from table 8.4.

8.7 Metasomatism in the Lough Guitane Lavas - Discussion

Numerous geochemical studies have been made of metaigneous terrains using the premise that certain trace elements which successfully classify unaltered volcanic rocks, are immobile during post-consolidation metamorphic processes and can therefore be used to classify such metaigneous rocks (Pearce & Cann, 1973; Floyd & Winchester, 1975, 1978; Winchester & Floyd, 1975, 1977; Smith & Smith, 1976). Such schemes have often been applied to specific geochemical problems in metaigneous suites (Whitehead & Goodfellow, 1978; Strong *et al.*, 1979; Davies *et al.*, 1979, 1980; Chikhaoui *et al.*, 1980). In a study similar to the present project, involving coexisting calc-alkaline rhyolitic obsidians and felsites Zielinski *et al.* (1977) used the REE as indicators of primary bulk chemical variations which were interpreted as the result of *in situ* crystal-melt fractionation.

On the other hand an increasing number of studies imply that many of the "immobile" elements are mobile in certain circumstances (MacGechan, 1978; Hellman *et al.*, 1979; Duddy, 1980; Hynes, 1980; Alderton *et al.*, 1980). In the Bennaunmore lava, the evidence for the mobility of the LREE is unequivocal. In addition, the HREE appear to have been preferentially enriched in the chloritised Green Dyke (Alderton *et al.*, 1980). Likewise Y is also proven to be mobile. Only TiO_2, Zr and Al_2O_3 appear reliably immobile, with P_2O_5 and Nb showing only very limited mobility.

Table 8.9 presents a classification of alteration/metasomatism defined by a series of parameters including those commonly used as alteration parameters (Hart *et al.*, 1974). Silicification is characterised by the depletion, or more properly dilution, of most components except of course silica, and thus a metasomatising fluid rich in silica, but poor in most other components, is envisaged.

Table 8.9

Classification of Alteration/Metasomatism Types

	8396 9070 9746 Silicification	9484 Minor Sericitisation	8859 8461 8674 Albitisation	8742A 9126 Chloritisation	9742 9586 Desilicification/ Calcification
SiO_2	+	0	-	- -	-
$CaO/CO_2/Sr$	- or 0	0	- -	-	+
Fe ox ratio	high	high	unaffected or high	low or high	high
Total Fe	-	0	- -	+	0
$K_2O/Rb/Sr$	-	+	- -	-	+ or 0
Na_2O	- or 0	-	+	-	+ or 0
LREE	- or 0	0	+	-	+
HREE				+	
H_2O	+ or 0	0	-	+	+

+ = enriched
0 = unaffected
- = depleted
- - = strongly depleted (often completely removed)

Sericitisation is another common alteration type, occurring commonly in lava flow tops and bases. K_2O replaces Na_2O with no change in total alkalis or other parameters except for the oxidation of iron. The exchange of sodium for potassium illustrates the instability of albite in K_2O rich metasomatising fluids (Alderton *et al.*, 1980).

Albitisation is characterised by the depletion, often complete, of components except Na_2O and LREE as the bulk rock composition approaches that of pure albite (table 8.6). It is interesting to note the patchy development of fluorite in fresher specimens of the Bennaunmore lava (e.g. specs. 8418 and 8371) which has been interpreted as a late-stage mineralisation (Chapter 6). Such an early post-consolidation hydrothermal phase, most active along fractures in the newly solidified lava, might have been responsible for an initial LREE enrichment. The mineralogical and textural evidence for this may have been removed by the later albitication, also controlled by fractures in the rhyolite lava flow. Such fracture control has produced the dyke-like character of these rocks, and obliterated any positive evidence for the previous presence of a magmatic dyke *sensu stricto*. Values of K_v^n calculated from specimen 8859 also indicate that a volume loss of about 30 per cent has occurred with little petrographic evidence for such a loss.

Petrogenetic problems are even more acute when elucidating the chloritised Green Dyke (fig. 5.37). Chloritised specimens are depleted in all components except FeO, MgO, H_2O^* and the HREE. The enrichment of HREE relative to LREE (fig. 8.16) can be explained in terms of the ability of chlorite to accomodate the HREE relative to the LREE from the breakdown of the primary phases (Alderton *et al.*, 1980). However the mass-transfer computations indicate that additional HREE must have been introduced into the system.

The very sharply defined margins of the Green Dyke (fig. 5.37) are

difficult to reconcile with its highly metasomatised state. The original rhyolitic dyke must have possessed some property which the host lava did not have, and which rendered it particularly susceptible to chloritisation while leaving the adjacent rhyolite unaffected, (specimen 8742B was taken from within less than a metre of the dyke).

It is not possible to say whether the metasomatising fluids were juvenile or connate, or why particular parts of the Bennaunmore lava should be affected by one metasomatic event, but not by another. The obvious complexity of the processes operating, coupled with the relative paucity of data makes such problems impossible to resolve without further work.

On the premise that the composition of the ABRP is that of a rhyolite, only the most extremely metasomatised specimens (8859, 8674) fall significantly outside the fields defined by their REE content in the discrimination diagrams of Floyd and Winchester (1978). However, if such discriminatory diagrams are to be used successfully, great care must be taken over sampling metaigneous rocks, and over the choice of the relatively immobile elements.

8.8 The Terrigenous and Tuffaceous Sediments

The three analyses of terrigenous sandstones presented in table 8.1c illustrates the wide variation in the chemistry and mineralogy of these sediments. All three specimens were fresh and unaltered with no evidence for large scale metasomatism. On this basis they have been classified using the diagram of Pettijohn *et al.* (1972) (fig. 8.21). They plot within the lithic arenite and subarkose fields illustrating the immature character of these sediments typical of molasse deposits, and supporting the classification suggested in Chapter 6.6 by petrography.

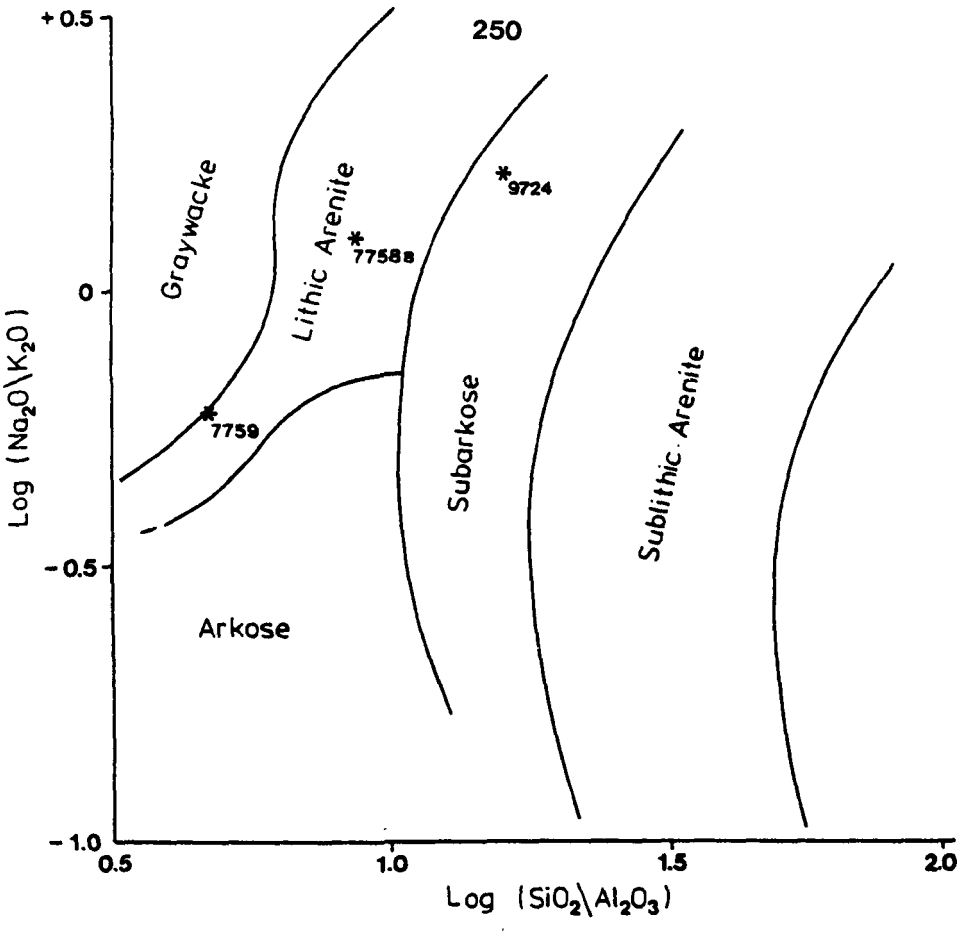

Fig. 8.21 Terrigenous sediment nomenclature (Pettijohn et.al., 1972).

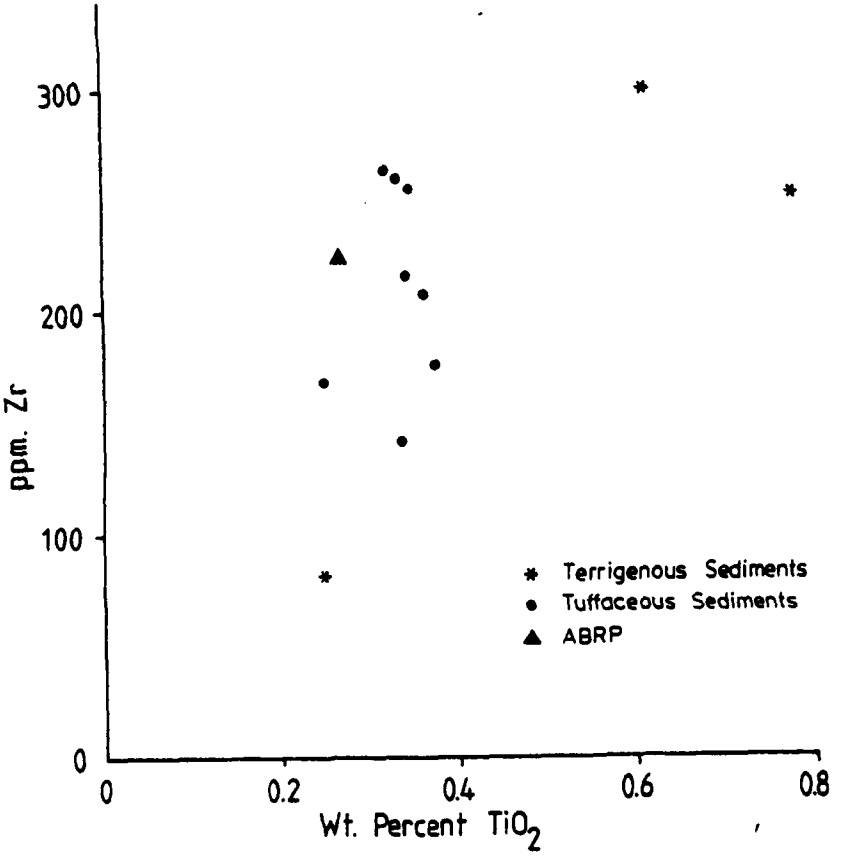

Fig. 8.22 Plot of Zr against TiO_2 for the Lough Guitane terrigenous and tuffaceous sediments.

The variation in the composition of the terrigenous sediments suggests that the analyses of the tuffaceous sandstones (mixed tuffs) must be assessed with great caution. Variables controlling the composition of these rocks include:

a) The relative proportions of volcanogenic and terrigenous sediments,

b) The composition of the volcanogenic component,

c) The composition of the terrigenous component,

d) Any secondary alteration/metamorphism.

The metasomatic alteration (d) can be assumed to be minimal, and the composition of the volcanogenic component (b) can be assumed to be constant, and near to that of the ABRP. However, the relative proportions of components (a) is virtually impossible to assess accurately (Chapter 6.5), and the composition of the terrigenous sediments (c) unknown, and demonstrably variable. A binary plot of TiO_2 against Zr of both the terrigenous and tuffaceous sediments (fig. 8.22) shows the latter spread evenly around the composition of the ABRP with no discernable pattern.

8.9 The Petrogenesis of the Lough Guitane Lavas

In an attempt to formulate a viable petrogenesis for the Lough Guitane rhyolites it is useful to consider the processes cited in recent discussion of the genesis of granitic magmas. They fall into four categories:

1. Partial fusion of crustal rocks (Brown & Fyfe, 1970; Ewart *et al.*, 1968; Fyfe, 1973; Brown, 1973).

2. Fractional crystallisation of basic magma (Osborn, 1959)

3. Partial melting of oceanic basaltic crust or upper mantle along a subduction zone inclined under a continental margin (Dickinson,

1968, & 1970), or melting of the associated ocean-floor sediments (Huang & Wyllie, 1973).

4. Combinations of the above processes, especially crustal contamination of a fractionally crystallised basic parent (Walsh *et al.*, 1979).

The best available estimate of the original magmatic composition of the bulk of the Lough Guitane lava flows is that of the ABRP. In table 8.10 it is compared with a variety of other rhyolitic-granitic rocks. Among the major oxides, the ABRP is only significantly different from the Pantellerite (analysis 8) which has higher TiO_2, Fe_2O_3, FeO, MnO and Na_2O and lower SiO_2 and Al_2O_3. The differentiated subalkaline rhyolite (Noble *et al.*, 1972; analysis 5) also possesses low TiO_2 and Iron. The ABRP can also be classified as subalkaline, plotting to the right of the bisectrix in fig. 8.24 i.e. Al_2O_3 > total alkalis, in contrast with the peralkaline pantellerite in which Al_2O_3 < total alkalis.

Trace element contents are however commonly used in addition to certain element ratios in an attempt to distinguish between the possible sources for rhyolites listed above. Taylor *et al.* (1968) used the elements Rb, Sr, Ba and Zr, and the ratios Ba/Rb and K/Rb to distinguish between rhyolites of crustal partial melt origin and leucogranites of fractional crystallisation origin (table 8.11). Taylor *et al.* (1968) considered that these trace element differences were consistent with large scale feldspar fractionation in the leucogranite parental magma. The composition of the ABRP, and the Sinclair Group felsic rocks (Watters, 1978) are closely comparable with the composition of the crustal-derived rhyolite.

However, Carmichael *et al.* (1974) point out that despite radically different origins for the various types of siliceous magmas in table 8.11, the ratio K/Rb is remarkably constant. In particular it is

Table 8.10

Published bulk analyses of rhyolitic-granitic rocks

	ABRP	1 (Ewart *et al.*) Average Taupo Rhyolite	2 (Turekian Wedepohl) Average Low Ca Granite	5 (Noble *et al.*) Differentiated Subalkaline-Rhyolite	3 (Fryer & Jenner) Ave. PAG high SiO_2 Rhyolite	4 (Watters) Rhyolite Lava Barby Form^{n}. S.W. Africa	Ave. Crust (Mason)	8 (C.T.V.) Pantellerite	6 (C.T.V.) Iceland Rhyolite	7 (Taylor *et al* Leucogranites
SiO_2	75.55	74.22	74.23	77.05	76.49	74.82		69.81	74.96	76.3
TiO_2	0.265	0.28	0.20	0.07	0.16	0.24		0.45	0.23	0.09
Al_2O_3	12.26	13.27	13.60	12.58	12.00	11.98		8.59	12.55	13.1
Fe_2O_3	0.60	0.88	1.83*	0.31	1.84*	1.97		2.28	1.72	1.19
FeO	1.49	0.92		0.45		0.97		5.76	0.71	
MnO	0.05	0.05	0.05	0.04	0.03	0.04		0.28	0.04	
MgO	0.69	0.28	0.27	0.03	1.14	0.05		0.10	0.02	0.20
CaO	0.39	1.59	0.71	0.44	1.23	0.48		0.42	0.90	0.71
Na_2O	2.695	4.24	3.48	3.96	2.10	3.94		6.46	4.41	3.64
K_2O	4.72	3.18	5.06	4.68	2.84	4.61		4.49	3.65	4.69
P_2O_5	0.14	0.05	0.14	0.01	0.00	0.02		0.13	0.04	
H_2O	0.68	0.80		0.17		0.02		0.05	0.34	
CO_2	(0.19)			0.02				0.76†		
TOTAL	99.72	99.99†	99.57	99.91				99.58	100.22*	99.92
Ba	801	870	840	<20	554	729	425	<10	1000	270
Rb	167	108	170		82	151	90	175	125	390
Sr	128	125	100	<20	48	59	375	<5	120	42
Y	61.5	27.5	40	38	56	98	33	145	45	26
Zr	224	160	175	100	284	542	165	1800	400	88
Cu	(43)	6		<2			55	3.6	9	2
Th	16	11					7			17
Nb	21.5	5.6	21	28		23	20	320	26	
La	40	26		56	44		30			
Ce	85	43			93		60			
Nd	49	18			40		28			
Zn	(101)			<50			70	440	125	
Ba/Rb	4.8	8.1	4.9	-	6.8	5.3	4.7	<0.05	8.3	0.69
K/Rb	283	150	298	-	346	240	287	256	252	120
Zr/TiO_2	0.085	0.057	0.088	0.143	0.178	0.151	-	0.40	0.174	0.098

† = Cl *includes H_2O^+ = 0.65

Table 8.11

	Rhyolites (Partial Melt) Taylor *et al.* 1968	Leucogranites (Fractional Crystallisation) Taylor *et al.*	Sinclair Group felsic rocks (Partial Melt)	ABRP
Rb	108	390	184	167
Sr	125	42	78	128
Ba	870	270	778	801
Zr	160	88	363	224
Ba/Rb	8.1	0.71	5.3	4.8
K/Rb	150	100	240	283

difficult to find any significant trace element differences between the Iceland rhyolite (Carmichael *et al.*, 1974) of fractional crystallisation origin, and the various acidic magmas supposedly of crustal melting origin (analyses 1, 2, 3 and 4).

Although the composition of the ABRP is the closest approximation to the original erupted composition of the Bennaunmore lava, some doubt must remain, especially when considering the normative felsic mineral values (appendix E) which are particularly dependent upon the mobile alkalis. However, some reasons for considering the alkali content of the ABRP reliable have already been outlined in section 2 of this chapter, and in addition it is unlikely that the geographically well separated specimens used to calculate the ABRP could have undergone such uniform alteration to produce the tight cluster of points observed in figs. 8.1 and 8.24. It is significant therefore that these rocks, and the ABRP plot very close to the quaternary minima in fig. 8.23 (Luth *et al.*, 1964; Tuttle & Bowen, 1958), although felsic magmas of this composition can be derived either by partial melting or fractional crystallisation of a parental basic magma.

The ABRP can also be considered to be peraluminous, because corundum is a ubiquitous normative mineral. The origin of corundum-normative magmas was discussed by Cawthorn *et al.* (1981). Of the models cited, two can be applied to the genesis of the Lough Guitane lavas - crustal remelting and amphibole fractionation. However the two most notable arguments in favour of a crustal remelting origin are:

1. The presence of a small quantity of restite in the lavas suggests that little if any crystal fractionation has occurred (see Chapter 6.7).

2. Felsic magmas of this composition, when derived by either partial melting or fractional crystallisation of a parental basic magma, occur in volcanic suites dominated by respectively intermediate and basic

Fig. 8.23 Normative Qz-Ab-Or diagram (experimentally determined field boundaries at 0.5, 2.0 and 5kb water pressure after Luth et.al., 1964, and Tuttle and Bowen, 1958). Data plotted correspond to Bennaunmore rhyolite analyses used to calculate the ABRP.

Fig. 8.24 Triangular Al_2O_3-(Na_2O+K_2O)-(CaO+MgO+FeO) diagram to discriminate between peralkaline and subalkaline igneous rocks. Data plotted correspond to Bennaunmore rhyolite analyses used to calculate the ABRP.

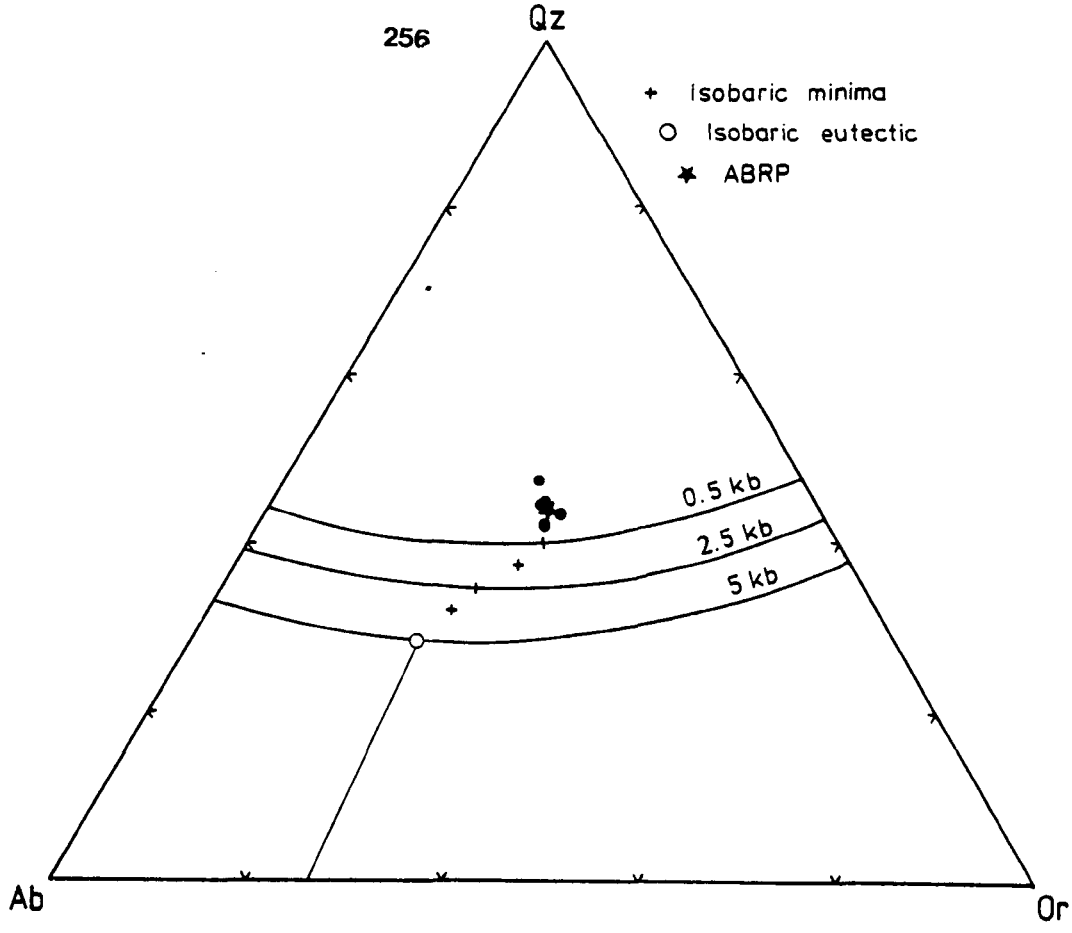
Qz
+ Isobaric minima
O Isobaric eutectic
ABRP
0.5 kb
2.5 kb
5 kb
Ab
Or

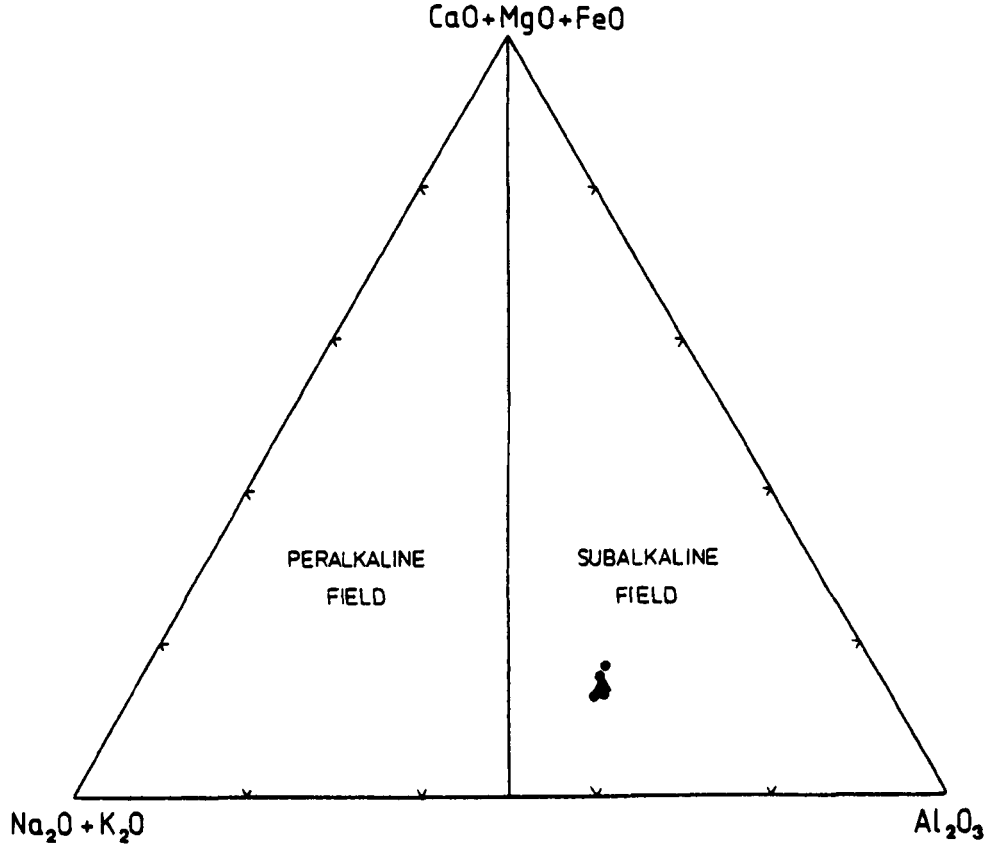
CaO+MgO+FeO
PERALKALINE FIELD
SUBALKALINE FIELD
$Na_2O + K_2O$
Al_2O_3

rocks (Carmichael *et al.*, 1974). In the Lough Guitane region, contemporary basic and intermediate volcanics are absent rendering such a derivation for these rhyolites very unlikely. On the same grounds, a basic magma contaminated with sialic crustal material could not have produced an exclusively acidic suite of rocks. Furthermore, the strong positive gravity anomaly which would be associated with basic rocks at depth is absent in the area, and indeed the whole of S. W. Ireland is characterised by a large negative gravity anomaly (Murphy, 1974).

Thus, the evidence seems to favour the derivation of the Lough Guitane rhyolites by crustal partial melting. The conditions under which the melting took place, the nature of the source rocks, the degree of melting and the subsequent modification which the magma may have undergone prior to eruption can now be considered.

The following discussion is based on a series of general assumptions listed below, which apply to the generation and emplacement of granitic magmas.

1. The source rocks lack interstitial water, but possess an assemblage containing hydrous minerals (Hyndman, 1981).

2. Melting in the continental crust begins when rocks are subjected to temperatures immediately above the stability field of muscovite, if assumption (1) is held to be true.

3. The temperature remains nearly constant, at approx. 700^{o}C, during the melting of a muscovite + quartz+ Na-rich plagioclase assemblage until all the muscovite has decomposed.

4. Further phases of melting of the same source rocks must occur when the temperature has risen above the temperature of dehydration of biotite at approx. 800-850^{o}C (Fyfe, 1973; Hyndman, 1981) and subsequently amphibole at approx. 900-950^{o}C (Brown & Fyfe, 1970).

5. Before further phases of melting can be initiated, the interstitial melt produced will be displaced from the source zone. Such a melt may begin to rise under the influence of the lower density of the magma, and the concurrent deformation ubiquitous under high-grade regional metamorphic conditions.

6. Discounting adiabatic cooling, and loss of heat to the surroundings, each pulse of magma will only rise to the depth represented by the pressure for the solidus at the given melting temperature (see fig. 8.25). Thus the earliest formed, lowest temperature melts will rise the shortest distance, and be emplaced at the greatest depths, while those melts initiated by biotite and amphibole decomposition will rise to the shallowest depths.

With specific reference to the Lough Guitane lavas, a number of important inferences should be emphasised.

i) The strong textural and chemical similarities between the lavas suggest that only one large magma chamber fed the Bennaunmore, Horses Glen and Devils Punch Bowl lavas while a separate high level chamber may have fed the Killeen lavas. The observed homogeneity in the former group also implies that convective mixing of originally inhomogenous 'acid' melts must have been active.

ii) The bulk composition of the melt is unlikely to have been modified by the previous tapping of the magma chamber because older volcanics have not been observed.

iii) The lavas are virtually devoid of vesiculation and evidence for highly explosive pyroclastic eruptions caused by high vapour pressure is absent.

iv) The homogeneity of the lavas, and the ubiquitous presence of restite fragments in the melts suggests that little, if any, crystal fractionation has occurred. If the magma had undergone a phase of

Fig. 8.25 P-T diagram (after Hyndman, 1981) showing the common granite solidus and approximate temperature ranges of mineral dehydration.

Fig. 8.26 P-T diagram (after Harris et.al., 1970) showing the relationship between liquidus temperature of granitic melts and their water content.

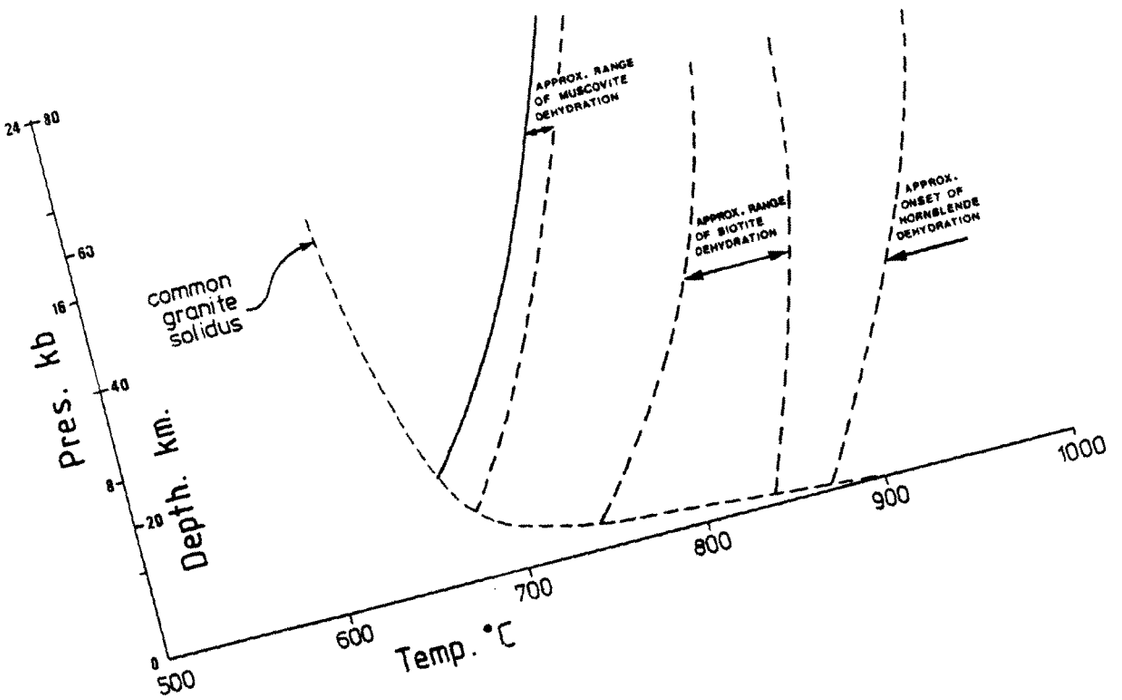
APPROX. RANGE OF MUSCOVITE DEHYDRATION
APPROX. RANGE OF BIOTITE DEHYDRATION
APPROX. ONSET OF HORNBLENDE DEHYDRATION
common granite solidus
Pres. kb
Depth. km.
Temp. °C
24
80
60
16
40
8
20
0
500
600
700
800
900
1000

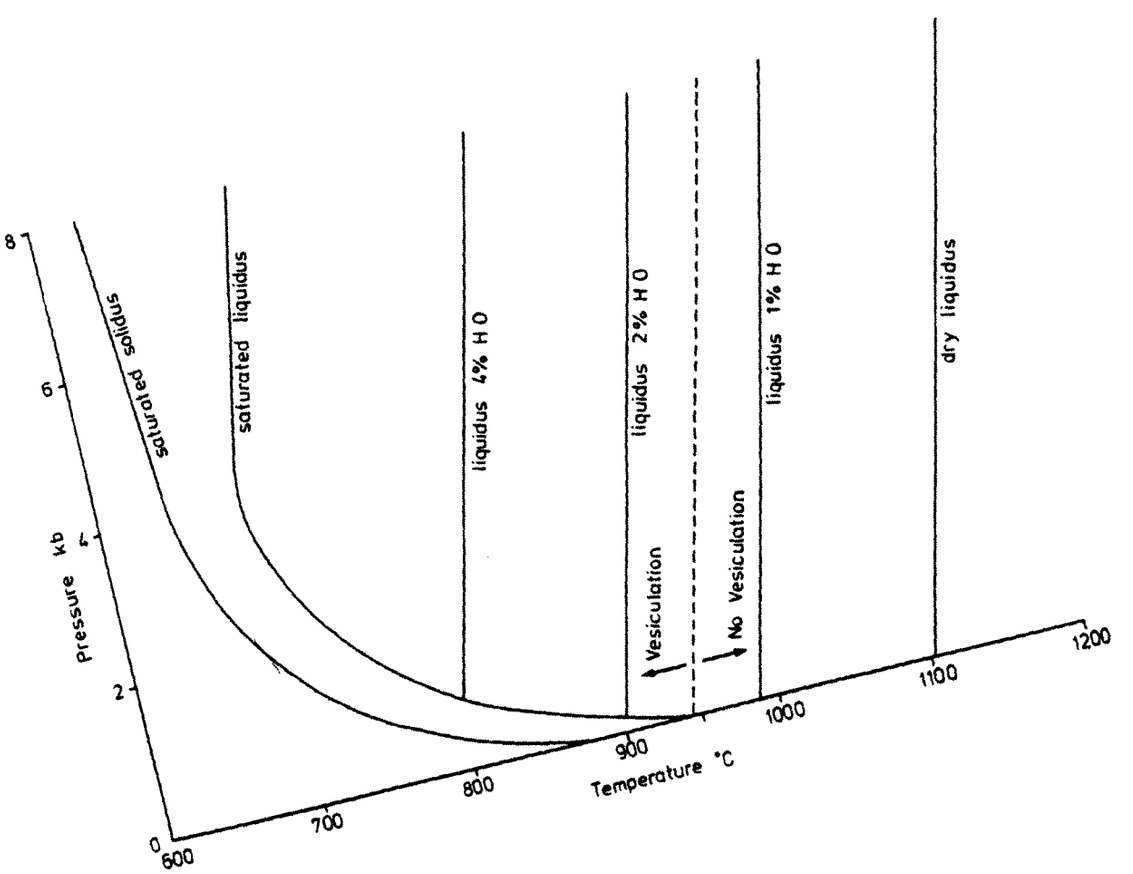
saturated solidus
saturated liquidus
liquidus 4% H O
liquidus 2% H O
liquidus 1% H O
dry liquidus
Vesiculation
No Vesiculation
Pressure kb
Temperature °C
8
6
4
2
0
600
700
800
900
1000
1100
1200

crystal separation, then the restite would also have separated under gravity.

Taking the above inferences and observations together, it is reasonable to add a further specific assumption to those listed above.

7. That the composition of the liquid plus precipitated crystals must have been close to the composition of the primary partial melt. The modification of whole rock trace element contents by the presence of a portion of restite crystals will be discussed later.

Inspection of fig. 8.26 (after Harris *et al.*, 1970) suggests that for the Bennaunmore rhyolite to have been erupted without vesiculation the water content cannot have exceeded 1.5 per cent, and the magma temperature cannot havebeen below approximately 950°C. Further experimental data (Carmichael, 1967) suggests that temperatures of this order are in accordance with those of approximately 900° conveyed by careful study of the phases present in glassy rocks. Original water contents of erupted rhyolitic melts of between 1 and 2 per cent are to be expected if the lower crust is essentially anhydrous as suggested by many authors (Wyllie, 1971; Presnall & Bateman, 1973; Fyfe, 1970, 1975).

Under the assumptions listed above, such erupted temperatures imply that amphibole may have been the phase controlling the melting of the source rocks. However, Brown & Fyfe (1970) point out that high temperature melts tend to be granodioritic, the high T and P conditions displacing the ternary minimum towards the Ab-Qz side of the Ab-Qz-Or triangle (fig. 8.23). This is at variance with the position plotted for the ABRP in fig. 8.21. It is possible in this case that the high degrees of partial melting suggested above have pushed the melt composition towards that of the bulk composition of the source rocks which may therefore have been granitic.

Formation of large volumes of granitic magma by high degrees of

partial melting may permit the retention of some residual or restite crystals (Presnall & Bateman, 1973; Hyndman, 1981), already suggested on textural grounds in the Lough Guitane lavas. However, the identification of crystal clusters as restite in a granitic melt, must be compatible with the derivation of that melt, and in particular its trace elements, from a source rock with a bulk composition equivalent to that melt plus some unknown proportion of restite.

Although significant plagioclase separation has been discounted, a chondrite normalised REE plot determined for specimen 8775 from the Bennaunmore lava (fig. 8.11) shows a pronounced negative europium anomaly. Emmerman *et al.* (1975) considered that such an anomaly in granitic rocks can also arise by the retention of plagioclase in the residual material. This hypothesis is particularly attractive in view of the dominance of plagioclase in the restite fragments present in the lavas.

However, central to the discussion is the primary mafic mineralogy of the restite, and its high content of incompatible element-rich accessory phases such as allanite and zircon. The LREE have previously been demonstrated to be mobile, and therefore the presence of allanite does not necessarily imply a high primary LREE content for the mafic phase, whereas the zircons can be assumed to be primary constituents of the restite.

Experimental data by Watson (1979) suggests that a maximum of 100 ppm Zr is soluble in sub-alkaline silicate liquids, and that higher concentrations must represent a composite value for melt plus zircon crystals derived from the source, in this case at Zr levels of about 220 ppm. Thus, some refractory zircons must be present in the Lough Guitane lavas. Similarly, although the total REE content of the ABRP (approx. 250 ppm) is almost identical to that of average granite (Herman,

1969), the HREE (Gd-Lu) in fig. 8.16 are enriched by a factor of about two relative to average granite.

Zircon preferentially incorporates the HREE (Nagasawa, 1970), and therefore to double both the whole rock Zr, and HREE contents from expected values, only approx. 0.5 modal per cent restite contaminant is required if it contains about 2 modal per cent zircon (see modal analyses, appendix E). These figures agree closely with the observed modal contents of chloritised mafics, which range between 0.0 and 0.9 per cent.

The primary restite mafic mineralogy is not known. If high degrees of partial melting took place, then little, if any, amphibole would remain intact. It is not possible, on bulk chemical or textural grounds to discriminate between the alternative mafic phases and consequently it is not possible to validate conclusively a genetic relationship between the supposed restite and the melt. However, the weight of evidence is still in favour of derivation of the Lough Guitane lavas from a granitic source-rock with amphibole the dominant mafic phase, by high degrees of partial melting at temperatures in excess of 950^{o}C.

The injection of basic or intermediate magma into the base of the crust has often been cited as responsible for crustal fusion (e.g. Presnall & Bateman, 1973) and seems a likely heat source for the Lough Guitane volcanics. Large volumes of intermediate magma are produced in close association with subduction zones at destructive plate margins (Dickinson, 1970, and others) through a variety of partial melting and fractionation processes involving subducted oceanic crust and the overlying mantle. However, there is no evidence for subduction near to southwest Ireland in the Upper Devonian. In common with southwest England, and northern central Europe, the area under study was subjected to a tensional regime leading to the development of a system of large sedimentary basins (Zwart & Dornsiepen, 1978; Ziegler, 1978). Bimodal

spilite-keratophyne volcanic suites have been identified from many regions within this tensional regime (Ziegler, 1978) and are characteristic of intracontinental rifts (Martin & Piwinski, 1972). Although contemporary basic volcanics are absent in the Lough Guitane area, they have been identified elsewhere in southwest Ireland.

Zwart and Dornsiepen (1978) have suggested that the lithosphere was abnormally hot during the Hercynian orogeny, and further suggested the presence of a mantle plume throughout the Palaeozoic under central and western Europe. Such a plume could have provided the impetus for both the development of a deep sedimentary basin in southwest Ireland, and the melting of the lower crust to produce the volcanics.

During the rise of the acid magma, or during brief storage prior to eruption, some crystallisation of quartz and feldspar occurred. Only the Killeen lava shows any significant textural or mineralogical variations from the Bennaunmore lava. The former possesses higher total phenocryst contents including the only examples of albitised alkali feldspars (Chapter 6, page 168) recorded in the Lough Guitane lavas. However, the restite fraction is not significantly different in texture or modal proportions from that of the Bennaunmore lava, again suggesting that despite a differing crystallisation history, no crystal settling has occurred. In this respect it is significant that the bulk rock chemistry of the Killeen lava is not unlike that of the ABRP.

It is further significant that the only whole rock specimen to show any trace element variance from the ABRP (spec. 9743) also possesses a much lower modal phenocryst and restite content. Thus the low Zr content of spec. 9743 can be explained by the removal of some of the zircon-rich restite fragments.

In summary, a granitic source rock with hornblende as the dominant mafic mineral, melted under near anhydrous conditions at a minimum

temperature of 950°C, probably in the lower crust. High degrees of partial melting are envisaged, pushing the melt composition towards that of its parent. Some small fraction of the parental rock was retained by the rising magma as restite fragments which enriched the levels of certain trace elements in the lavas. Only limited and localised crystal fractionation subsequently occurred before the magma was erupted as a dry, glassy, relatively crystal-poor sub-alkaline rhyolite.

CHAPTER 9

Conclusions and Suggestions for further work

9.1 Conclusions

The geology of the Lough Guitane area can be summarised as follows:

1. Initiation of the Munster Basin by the development of a system of large E-W aligned normal faults with downthrows to the S during the Middle Devonian. Rapid subsidence lead to the accumulation of at least 7 Km of clastic sediments, mostly derived from the N.

2. More localised faulting near the centre of the basin developed in the Lough Guitane area producing a locally bimodal palaeocurrent pattern indicative of an E-W oriented downwarp.

3. Volcanic activity was initiated in the region, characterised by;

a) An exclusively subalkaline and acidic geochemistry and virtually identical petrographic character of all the erupted rocks.

b) The preponderance of very thick (up to 300 m) rhyolite lava flows with a low phenocryst content, including 1-2% of restite, and very little evidence for vesiculation.

c) The ubiquitous presence of terrigenous clastic sediment mixed with the locally derived volcaniclastics.

d) The control exerted by large faults contemporaneous with the volcanism in the Bennaunmore volcanic centre over the pattern of deposition of the volcanic rocks. These faults included an E-W set which produced a graben-like feature, and a subcircular set, within the graben, which surround a central subsided area.

e) The E-W alignment of the 3 major volcanic centres, in coincidence with the orientation of the contemporaneous graben in the Bennaunmore volcanic centre described above.

f) The association with some of the contemporaneous faults of

laterally discontinuous sandstone boulder agglomerates (boulder tuffs), and which are thought to have been the product of slumping along exposed fault escarpments during eruption of the volcaniclastics.

g) The relatively subdued nature of the volcaniclastic eruptions.

h) Geochemical evidence for the derivation of the magma by high degrees of partial melting of acidic crustal material controlled by the decomposition of amphibole at temperatures in excess of 950°C.

These features lead to the conclusion that the local bimodal palaeocurrent pattern, the geometry of the Munster Basin, the alignment of the Lough Guitane volcanic centres, and the orientation of the Bennaunmore graben faults are all probably related to the same system of deep crustal fractures. In the Lough Guitane area these fractures may have been used as conduits for the deep crustal melts.

The absence of highly explosive volcanicity probably related to the considerable thickness of partially lithified or unconsolidated clastic sediments through which the magma had to rise, and which also probably ensured the incorporation of at least some of this terrigenous sediment in all the volcaniclastics. This thickness would have produced an overburden pressure exceeding the critical water vapour pressure.

4. The volcanic pile was subjected to little erosion or redistribution before rapid burial by exclusively terrigenous clastic sediments.

5. After subsidence in the Munster Basin ceased, the whole area was subjected to a N-S compressive stress related to the Sudetic-Asturian phases of the Hercynian orogeny. In the Lough Guitane area this led to major reversed faulting along an E-W strike, the Muckross-Millstreet fault, and a complementary parallel anticlinorium, the steeply southward dipping axis of which lies 3 Km to the south. The structural elevation of the crest of the anticlinorium relative to the ground to the north of the fault probably exceeds 4 Km.

The course of the fault is displaced southwards by 2 Km on the eastern side of a major dextral transverse fault at a point 1 Km north of Bennaunmore. This is probably related to the influence of a shallow intrusive body related to the vent which fed the Bennaunmore rhyolite lava, and which behaved differently from the clastic sediments under the N-S compressive stresses.

6. During the burial of the volcanics, and the subsequent greenschist-facies metamorphism related to the tectonic events described above, the lavas were subjected to moderate to severe metasomatism of widely varying character, leading to the development of albitised, chloritised, sericitised and silicified rocks. Under these conditions, of the elements analysed, only Zr, Ti, P and Al appear to have remained geochemically immobile.

9.2 Suggestions for further work

9.2.1 The Lough Guitane area

1. Closer examination of the ground covered for further evidence of faulting contemporaneous with the volcanism might lead to a better understanding of the field relationships of some of the volcanic units. This might also reveal whether slumping occurred along exposed fault escarpments prior to eruption of the volcanics.

2. An exhaustive geochemical survey of the Bennaunmore rhyolite lava, in particular the more altered lithofacies, using mass-transfer computations might lead to a better understanding of the metasomatic processes operating, and the behaviour of individual elements.

3. On the assumption that at least some of the zircon is inherited from the source rocks of the rhyolites, a study of zircon U-Pb systematics might indicate the age of the basement rocks concerned.

4. Further electron-microprobe studies would expand the knowledge

of the geochemical relationships between the phases present, in particular the anatase-sphene-leucoxene system, and the rare-earth content of allanite.

9.2.2 South West Ireland

Detailed studies of the clastic sediments of the Munster Basin, including

a) an extensive program of palaeocurrent measurements

b) detailed mapping of grain-sizevariations under improved stratigraphic control

c) the logging of a large number of sections - are essential if a proper understanding of the development of the basin is to be obtained.

APPENDIX A

Geochemical Analysis Programme

A.1 Specimen Preparation for Analysis

A.1.1 Crushing Programme

Specimens selected for geochemical analysis were stripped of any unwanted weathered or altered portions, and split into small fragments up to 3 cm in size using a Tavishelm hydraulic rock splitter. The sample was then weighed. Weights averaged 1.0 Kg, ranging from 500 gm (the minimum sample size for dominantly fine grained rocks) to 2.0 Kg.

The whole sample was then passed through a Sturtevant jaw crusher to reduce the maximum particle size to about 0.5 cm. The entire sample was then subdivided using a cone and quartering technique to provide a representative subsample of about 100 gm, which was placed in a Tema ring mill containing tungsten carbide rings and a central cylinder. The sample was crushed for 60 seconds, producing a rock powder of which 99 percent passed through a 120 mesh sieve. About 10 gm of the powder was then ground in a ball mill for 20 minutes so that it would pass freely through a 200 mesh sieve.

A.1.2 Preparation of Fused Disks for X-Ray Fluorescence Spectrometry (XRFS)

About 1.0 gm of rock powder was weighed out accurately and placed in a furnace at 1000^{o}C for 30 minutes. The crucible plus ignited rock powder were then reweighed when cool, and the loss of weight on ignition calculated.

Exactly 0.5 gm of this ignited powder was accurately weighed, and 2.5 gm of lithium metaborate flux was added. The powder and the flux were thoroughly mixed before being placed in a platinum crucible

and fused over a meker burner until a quiescent melt was formed. When fusion was complete the fluid was poured into a circular cast which had been heated to 240°C and rimmed with a loose thick copper wire to give strength to the disc on removal from the cast. When cool the glass discs were stored in sealed polythene bags and stored ready for major element oxide analysis.

A.1.3 Preparation of Pressed Powder Pellets for XRF analysis of Trace Elements

About 6 gm of rock powder were roughly weighed out and placed in an agate mortar. It was then thoroughly mixed with approximately ten drops of 2 percent Moviol solution with the agate pestle until homogenous. The mixture was then placed in a hydraulic piston press operating at 25 tons using polished tungsten carbide coated plattens to produce smooth surfaces on each face of the circular pressed pellet. On removal from the press after 5 minutes the pellet was dried at 110°C and then labelled and stored.

A.1.4 Sources of Contamination during sample Preparation

It was noted that tiny slivers ($\sim$ 1 mm) of metallic iron appeared in the sample after passing through the jaw crusher. To estimate the level of such contamination all magnetic material was removed from a representative portion of fourof the samples ranging from the hardest, highly silicified rhyolite to softer unaltered specimens using a strong bar magnet. Despite the fact that some natural magnetic minerals were also removed along with the metallic iron, the total amount of material removed only corresponded to between 0.03 and 0.05 weight percent of the whole rock. Such low levels of contamination are not significant when dealing with whole rock total iron contents commonly of about 1.0 percent.

It was feared that the Tema ring mill grinding might induce

oxidation of the ferrous iron portion of the sample due to frictional heating. To discover whether such oxidation was occurring, 50 gm portions of rock chips from each of 5 specimens were ground in the Tema mill for only 15 seconds, i.e. before appreciable frictional heating could occur. However, FeO levels in these samples were not significantly different from FeO levels in the corresponding samples ground for 60 seconds.

No other sources of contamination are thought to be significant.

A.2.1 X-Ray Fluorescence Spectrometry

Major and trace element data were determined at Keele in two Phillips X-ray fluorescence spectrometers, an automatic model PW 1212, and a semi-automatic model PW 1220. Instrumental drift was monitored by sequential analysis of a standard rock, resident in the machine (as a glass disc or powder pellet, as appropriate) for the entire period of analysis. Operating conditions are presented in tables A.1 and A.2.

Major element calibrations were made by analysing between seven and fifteen well characterised international standards, prepared by the same methods as described for the unknowns. The data of Flanagan (1973) was used for calibration after recalculation on an oxidised volatile-free basis. Thus iron was determined as Fe_2O_3. The calibrations were then obtained by least squares linear regression (assuming zero error in concentration).

Empirical corrections for matrix effects in the samples were derived by G. J. Lees following the method of Norrish and Hutton (1969), using a series of multicomponent mixtures of the ten oxides except Na_2O which was determined on the pressed powder pellets.

The twelve trace elements (table A.2) were determined using calibrations obtained by a spiking technique similar to that of Leake

Table A.1

XRFS Operating Conditions for Major Elements

Element	K	Ti	Si	Ca	Al	Mg	Na	P	Fe	Mn
Radiation Line Used	Kα	Kα	Kα	Kα	Kα	Kα	Kα	Kα	Kα	Kα
Tube	Cr	Cr	Cr	Cr	Cr	Cr	Cr	Cr	Cr	W
Kv	40	40	40	40	40	60	40	60	60	60
mA	8	8	16	8	24	32	32	24	8	32
Crystal	PE	LiF200	PE	LiF200	PE	KAP	TRAP	GE	LiF220	LiF220
Collimator	Coarse	Fine	Coarse	Fine	Coarse	Coarse	Coarse	Coarse	Fine	Fine
Counter	Fl	Fl	Fl	Fl	Fl	Fl	Fl	Fl	Fl	Fl
Vacuum/air path	Vac	Vac	Vac	Vac	Vac	Vac	Vac	Vac	Vac	Vac
Method	AR	AR	AR	AR	AR	AR	AR	AR	AR	Abs
Time	FC	FC	FC	FC	FC	FC	FC	FC	FC	40 secs
Counts	10^4	10^4	10^4	10^4	10^4	10^4	10^4	10^4	10^4	FT

Table A.2

XRFS Operating Conditions for Trace Elements

Element	Ba	Rb	Sr	Y	Zr	Pb	Th	U	La	Ce	Nd	Nb
Radiation line used	$L\beta_2$	Kα	Kα	Kα	Kα	Kα	Kα	Kα	Lα	$L\beta_1$	$L\beta_{1,4}$	Kα
Tube	W	Mo	Mo	Mo	Mo	Mo	Mo	Mo	W	W	W	W
Ku	60	60	60	60	60	60	60	60	60	60	60	60
mA	30	30	30	30	30	28	28	28	30	30	30	30
Crystal	LiF220	LiF220	LiF220	LiF220	LiF220	LiF220	LiF220	LiF220	LiF220	LiF220	LiF220	LiF220
Collimator	Coarse	Fine	Fine	Fine	Fine	Fine	Fine	Fine	Coarse	Coarse	Coarse	Fine
Counter	Fl+Sc	Sc	Sc	Sc	Sc	Sc	Sc	Sc	Fl	Fl	Fl	Sc
Vacuum/air path	Vac	Vac	Vac	Vac	Vac	Vac	Vac	Vac	Vac	Vac	Vac	Vac
Method	Abs	Abs	Abs	Abs	Abs	Abs	Abs	Abs	Abs	Abs	Abs	Abs
Time	40	40	40	40	40	40	40	40	40	40	40	40

et al. (1969). The spiking matrix used was a homogenised composite of the rhyolite lavas and volcaniclastics found in the Lough Guitane area. Differences in mass absorption between the spiking matrix and the unknowns was not found to be significant. However, the ($MoK\alpha_c$) method of Reynolds (1963) was used for Rb, Sr, Y and Zr to correct for such differences.

Trace and major element data were processed on a Digico M16E mini-computer using programs written by G. J. Lees and D. Emley.

A.3 Wet Chemical and other Analytical Techniques

A.3.1 Determination of FeO

0.25 gm of rock powder from the tema mill was placed in a polythene bottle, and with 10 mls of 1:1 conc. HF/conc. H_2SO_4 mixture, placed on a steam bath for 15 minutes. 200 ml of saturated boric acid solution was then added and the decanted mixture titrated against a standardised solution of potassium dichromate using diphenylamine indicator.

A.3.2 Determination of CO_2

Carbon dioxide was liberated from the carbonate in the 0.5 - 2.0 gm of rock powder by heating with concentrated orthophosphoric acid. The evolved gas was carried by nitrogen through absorbents to remove water and hydrogen sulphide and was then absorbed into a 5 percent solution of monoethanolamine in dimethylformamide containing thymolphthalein as indicator. The CO_2 is finally titrated directly with a solution of 0.1N tetra n-butyl ammonium hydroxide in toluene.

A.3.3 Determination of H_2O^+

Water was driven from an accurately weighed 1.0 gm sample of rock powder by heating in a pyrex tube using 2.0 gm of lead chromate as a flux. The water is condensed onto a piece of dried and preweighed filter paper in the upper part of the tube which is cooled in an ice

bath. The wet filter paper is then reweighed inside a weighing phial to prevent loss by evaporation.

A.4 The Cambridge Energy Dispersive Electron Microprobe (EDS)

The electron microprobe used to obtain the mineral analyses in Chapter 7 was designed and constructed in the Department of Earth Sciences, Cambridge, with a Si(Li) detector and Harwell Highspec pulse processor system 3073 (Kandiah *et al.*, 1975) interfaced to a Data General Nova 1220 minicomputer with 20K core storage. Peaks were processed and measured by iterative peak stripping (Statham, 1976), with correction methods after Sweatman and Long (1969).

Analytical conditions are presented in table A.3.

A.5 REE Analyses

The REE analyses presented in table 8.8 were obtained as a commercial basis from the Universities Research Reactor, Risley. The analytical technique is a modification of the method of Graber *et al.* (1970) and involves radiochemical group separation and thermal-neutron activation.

Table A.3

EDS Analytical Conditions

Accelerating potential	20 kV
Nominal beam current	50 nA
Beam current at specimen surface	$\sim$ 35 nA
Counting time	80 live seconds
Take off angle	40^{o}
Specimen-Detector distance	270 mm
Detector resolution at MnKα (5.89 keV)	$\sim$ 156 eV FWHM

APPENDIX B

Accuracy and Precision

B.1 Calculation of Data Presented in Table B.1

Column 1. Detection limit is calculated as 2σ of the background XRF counts.

Column 2. Pooled sampling precision is calculated from the pooled standard deviation of ten specimens for which two fused discs and two pellets were prepared and analysed.

Column 3. Relative sampling precision is calculated by the division of the average oxide/element level in the ten duplicated samples by their corresponding values of pooled sampling precision and expressed as percent.

Column 4. Instrumental Precision is derived from the pooled variance of the XRF peak counts.

Column 5. Instrumental precision expressed as percent of the average of all the analyses obtained.

Note 1. FeO, H_2O and CO_2 were measured by methods other than XRF, and detection limits were not calculated.

Note 2. Cu, Zn, U, Pb and Th were not determined in the ten duplicated samples.

Note 3. In all cases the pooled sampling precision is considerably less than the instrumental precision or at worst approximately equal to it, i.e. imprecision due to the instrument will always mask the error due to unrepresentative sampling of the rock powder.

B.2 Light Rare Earth Element Determination

It was noted in Chapter 8 section 6 that although correlation coefficients of over 0.9 existed between La, Ce and Nd, the regression

lines did not all pass through the origin of their respective inter element plots. However, La and Ce (fig. 8.11) regression line passes very close to the origin, while the regression lines derived from Nd against both La and Ce, both pass through the Nd axis at about 10 - 20 ppm. It is very unlikely that any natural geochemical process could produce this effect and it must be concluded that either Nd has been overestimated by about 15 ppm or La and Ce have been underestimated by 15 ppm in all analyses.

Such a systematic error is almost certainly instrumental. However, the powder used to produce the spiked series for calibration was a composite mixed from a selection of Lough Guitane lavas and tuffs and should therefore have eliminated any mineralogical matrix effects.

It is interesting to note the discrepancies between LREE values obtained via thermal-neutron activation (table 8.7) and those derived by XRF (table 8.1). Neutron activation is not a reliable method for determining Cerium, but is for La and Nd. La levels are between 15 and 20 ppm lower in XRF analyses, while Nd shows no consistent relationship between the two methods. It is suggested therefore that both La and Ce have been underestimated in the XRF analyses by a systematic instrumental error of unknown origin.

Table B.1

XRFS Analytical Accuracy and Precision

Element/ Oxide	Detection Limit (% of p.p.m.)	Pooled Sampling Precision	Relative Sampling Precision (percent)	Instrumental Precision	Relative Instrumental Precision (percent)
SiO_2	0.06	± 0.59	± 0.87	± 1.00	± 1.35
TiO_2	0.003	0.003	0.65	0.01	3.7
Al_2O_3	0.004	0.10	0.68	0.24	2.0
Fe_2O_3	0.04	0.08	5.16	0.08	10.4
MnO	0.001	0.001	1.43	0.0005	1.14
P_2O_5	0.006	0.005	2.9	0.006	4.0
MgO	0.16	0.12	4.8	0.09	12.2
CaO	0.006	0.05	3.1	0.07	4.7
Na_2O	0.08	0.02	0.7	0.11	4.2
K_2O	0.002	0.01	0.3	0.06	1.4
FeO	-	0.05	2.9	-	-
H_2O	-	0.07	11.6	-	-
CO_2	-	0.08	7.2	-	-
Ba	35	± 11.5	± 2.3	± 22.7	± 2.9
Rb	3	1.6	1.0	1.6	1.0
Sr	3	3.0	1.9	2.2	1.5
Y	2	1.5	2.2	1.5	2.6
Zr	7	7.7	3.1	6.3	2.9
Cu	4	-	-	2.2	6.9
Zn	3	-	-	1.9	2.8
Nb	2	1.25	6.3	1.2	5.7
La	3	1.0	2.4	2.5	6.6
Ce	6	2.0	2.1	3.6	4.6
Nd	5	2.4	5.1	2.5	5.3
U	4	-	-	2.0	57.1
Pb	6	-	-	3.2	6.3
Th	5	-	-	3.4	21.3

Table B.2

Energy Dispersive Microprobe Instrumental Data

Element	Detection limit (percent) (3σ)	Relative Accuracy* (percent)
Na	0.25	2.0
Mg	0.15	2.0
Al	0.10	2.0
Si	0.10	2.0
K-Zn	0.05	2.0

*If more than 5 percent of the element is present

APPENDIX C

Hand Specimen Descriptions

The Lavas

All the lavas are microcrystalline and porphyritic, containing between 2 and 10 percent phenocrysts of plagioclase, quartz and chloritised ferromagnesian mineral. Significant variations are essentially of matrix tint and the staining and alteration of the plagioclase phenocrysts. Table C.1 presents a classification of all the lavas according to these criteria. The quartz phenocrysts are rarely larger than 1 mm in size, rounded and glassy.

The Volcaniclastic Sediments

7200 Dark pinkish grey poorly sorted tuffaceous coarse sandstone.

7201 Dark greenish grey poorly sorted tuffaceous coarse sandstone with pink stained volcanogenic feldspars particularly common.

7209 Dark greenish grey poorly sorted tuffaceous coarse sandstone with common large (1-2 cm) mudflakes. The volcanogenic feldspars are common and colourless.

7212 Mid greenish grey well cleaved tuffaceous sandstone. Volcanogenic feldspars are yellowish and rare while small mudflakes (2-5 mm) are very common.

7216 Very poorly sorted tuffaceous sandstone, mid green grey in colour with dark green volcanogenic clasts up to 5 cm in size.

8423 Mid-dark green grey unsorted tuffaceous sandstone with yellow volcanogenic feldspars, pinkish grey volcaniclasts up to 1 cm in size and small dark green-grey mudflakes (2-5 mm).

8435 Mid green grey medium grained sandstone with very rare colourless volcanogenic feldspars.

Table C.1

Lava Hand Specimen Descriptions

	Matrix colour		Phenocryst colour	Specimen numbers	Comments
	Depth	Tint			
Bennaunmore Lava	~~Grey~~ dark	blue-green	White	8365, 8366, 8392, 8418, 8552, 8555, 8742B, 8755, 8756, 8850, 8775, 8795, 7750, 7751	
	pale	green	colourless	8396, 8396W	8396W includes some weathered and badly veined material
	mid	mauve-pink	pink-brown	7215	
	pale	yellow	yellow	8824	
	dark	blue	white	8909	Possesses fracture cleavage
	pale	pink	yellow	9281	
	mid-dark	purple and yellow patches	yellow	9386	

Table C.1

Lava Hand Specimen Descriptions (cont)

	Matrix colour		Phenocryst colour	Specimen numbers	Comments
	Depth	Tint			
Killeen Lava	~~Grey~~				
	mid	pink	colourless	7205	
	mid	pink	white and pink (flesh coloured)	8372, 8375	two generations of feldspar phenocryst distinguished by colour
	mid	pale green	white and colourless	9440	two generations of feldspar phenocryst
	mid	pink patches	pink and colourless	9502	two generations of feldspar phenocryst
	mid	pink	pink	9461	
	mid-dark	untinted	slightly white	9484	plus < 1 mm quartz micro-veining

8480 Dark green grey medium grained sandstone with very rare colourless volcanogenic feldspars.

The Terrigenous Sediments

7758B Mid green grey medium grained micaceous sandstone.

7759 Mid green grey fine grained micaceous sandstone.

9724 Mid grey medium grained sandstone.

APPENDIX D

Calculation of Normative Mineral Compositions

Owing to the highly altered nature of many of the rocks analysed, the CIPW norm was not used. Instead the Barth (1959) Mesonorm was calculated with one small modification. It was found that some analyses possessed insufficient CaO to calculate apatite after the reduction of CaO in the calculation of calcite (see Chapter 8.6).

In view of the identification of ferroan calcite (Chapter 8.6) it was felt that if apatite was calculated first, and then calcite, any excess CO_2 could be accommodated by calculating siderite.

The steps 5-7 (Hutchinson, 1974 page 420) now become:

5. a) If $PO_{2\frac{1}{2}} < 3 \times F$, make apatite = $3 \times PO_{2\frac{1}{2}}$. Reduce CaO by an amount = 1.667 of $PO_{2\frac{1}{2}}$. Reduce F by 0.33 of $PO_{2\frac{1}{2}}$.

b) If $PO_{2\frac{1}{2}} \geq 3 \times F$, make apatite = $(2.667 \times PO_{2\frac{1}{2}}) + F$. Reduce CaO by 1.667 of $PO_{2\frac{1}{2}}$; F becomes zero.

6. Make cassiterite = SnO_2 (Not Calculated).

7. a) If $CO_2 > CaO$, make calcite = $2 \times CaO$, reduce CO_2 by amount = CaO. Make siderite = $2 \times CO_2$, reduce FeO by amount = CO_2, CO_2 becomes zero.

b) If $CO_2 \leq CaO$, make calcite = $2 \times CO_2$, reduce CaO by amount = CO_2.

The calculated mesonorms are presented in tables E1 - E4.

Table E1 Bennaunmore Lava

Specimen number	8365	8366	8392	8396	8396W	7750	8418	8552	8555	8742B	8755	8756	8850	7751	7215	8775	8795	8824	8909	9281	9386
Q	40.10	41.47	37.33	50.19	48.55	37.52	38.38	38.85	39.31	42.84	39.20	39.71	38.95	34.46	59.37	39.43	36.67	34.48	34.56	38.74	45.15
C	3.36	3.93	2.05	3.03	2.10	3.13	3.06	2.93	3.88	4.64	3.32	2.84	2.91	2.64	4.66	2.78	2.80	2.35	3.45	2.12	3.72
or	25.85	16.54	25.83	11.87	11.20	25.78	23.79	23.98	19.54	12.39	21.56	19.30	24.71	28.53	7.59	19.08	25.36	24.66	25.97	24.31	30.23
ab	14.44	25.12	25.56	24.59	24.68	22.76	24.08	23.54	23.86	23.86	22.26	27.46	22.90	23.05	15.34	28.09	24.95	23.98	26.18	27.50	12.10
an	1.33		0.53		2.46												0.06	0.25			
bi	6.80	5.73	3.49	3.21	3.64	4.62	5.19	5.38	6.47	7.55	6.95	4.88	4.60	4.02	5.38	4.03	4.25	6.45	4.11	3.11	3.27
mt	0.63	0.59	0.59	0.32	0.35	0.58	0.69	0.62	0.57	0.65	0.65	0.57	0.59	0.63	0.67	0.57	0.61	0.62	0.49	0.51	0.51
sp	0.51	0.42	0.55	0.22	0.49	0.16	0.20	0.31	0.49	0.03	0.39	0.21	0.28	0.16	0.63	0.14	0.55	0.52	0.10	0.17	0.12
ap	0.30	0.31	0.34	0.31	0.31	0.18	0.31	0.29	0.32	0.32	0.29	0.31	0.33	0.19	0.20	0.31	0.31	0.34	0.35	0.33	0.33
cc	0.87	0.28	0.57	0.69	1.30	0.32	0.47	0.21	0.32	0.02	0.26	0.14	0.19	0.81	2.62	0.57	0.39	0.45	0.07	0.12	0.08
sid	0.04	0.05	0.06	0.06	0.03	0.03	0.03	0.02	0.02	0.06	0.01	0.03	0.08	0.08	0.08	0.08	0.03	0.09	0.08	0.06	0.07
H_2O	6.16	5.64	3.34	5.48	5.54	4.62	3.65	3.86	5.31	7.55	5.17	4.48	4.42	4.02	5.38	4.03	4.25	6.45	4.49	2.95	4.32
TOTAL	100.12	100.07	100.23	99.96	100.62	99.86	99.85	100.00	100.08	99.82	100.06	99.94	99.97	99.90	100.06	99.91	100.15	100.20	99.86	99.93	99.89

Table E2 Killeen Lava

Specimen number	7217	7218	9440	9461	9484	9502	9742	9743	9744	7203	7205	8372	8375	9517	9586
Q	40.03	38.30	42.56	31.95	35.34	36.87	31.94	54.06	49.42	52.70	34.66	33.54	36.17	42.67	26.36
C	3.45	3.48	2.50	2.45	2.41	1.52	8.26	1.93	7.70	7.73	2.01	1.36	2.60	4.18	2.41
or	27.19	31.47	21.58	27.04	35.79	26.34	27.17	14.35	17.20	20.56	27.61	29.97	31.73	26.75	17.61
ab	19.28	18.23	24.79	30.21	15.33	28.83	10.49	4.65	7.64	4.70	29.87	21.67	21.78	11.59	28.69
an					0.87		2.44	10.63				3.45		2.32	9.76
bi	2.94	3.05	2.06	3.46	4.18	2.38	6.77	3.82	4.85	3.51	2.00	4.08	2.14	3.86	3.00
mt	0.44	0.54	0.26	0.58	0.61	0.59	0.70	0.42	0.54	0.55	0.37	0.58	0.48	0.57	0.51
sp	0.21	0.23	0.06	0.22	0.56	0.23	0.75	0.47	0.11	0.24	0.26	0.58	0.45	0.57	0.67
ap	0.17	0.17	0.25	0.29	0.29	0.30	0.32	0.27	0.28	0.15	0.15	0.29	0.29	0.29	0.29
cc	1.27	1.09	0.92	0.15	0.72	0.15	1.47	4.56	3.77	4.58	0.10	1.77	0.30	1.31	4.35
sid	0.19	0.19	0.19		0.16		0.10	0.01	0.01	0.01	0.01	0.02	0.52	0.03	0.63
H_2O	4.87	3.29	4.86	3.56	4.07	2.74	10.30	7.06	8.31	5.53	2.86	3.51	3.64	6.52	7.87
TOTAL	100.04	100.04	100.03	99.92	100.33	99.94	100.70	102.22	99.84	99.86	99.89	100.82	100.10	100.64	102.13

Table E3 Other Lavas

Specimen number	8390	9728	81108	81120	9070	9126	9746	9747	8461	8464	8613	8660	8674
Q	49.85	45.66	39.28	42.17	52.08	40.25	65.70	43.97	30.86	37.45	44.77	38.91	32.86
C	4.67	7.20	1.71	3.89	3.87	6.24	2.79	5.12		2.82	1.79	2.48	0.25
or	25.00	19.42	19.67	27.15	12.32	11.94	6.56	13.87	0.18	23.46	8.92	22.90	
ab	8.63	11.97	31.51	15.93	18.91	17.82	14.81	20.85	61.40	28.34	30.29	23.93	61.98
an	1.83		0.75							0.16	3.67	0.60	
bi	2.91	4.85	3.04	3.50	3.13	10.72	4.81	7.45	1.40	3.07	2.69	4.08	1.77
hy													0.95
mt	0.51	0.82	0.54	0.56	0.35	1.17	0.68	0.86		0.61	0.45	0.63	0.64
sp	0.52	0.07	0.51	0.15	0.47	0.03	0.11	0.14		0.54	0.49	0.56	
ap	0.33	0.32	0.30	0.31	0.26	0.31	0.30	0.32	0.33	0.29	0.43	0.31	0.37
cc	1.08	0.31	0.47	0.10	0.61	0.02	0.07	0.09		0.43	1.79	0.61	
sid	0.05	0.05	0.01	0.07		0.05	0.06	0.08			0.19	0.16	0.10
ri									3.08				
H_2O	5.14	9.18	2.83	6.06	7.55	11.28	4.00	7.11	2.64	3.02	5.39	5.10	0.91
TOTAL	100.52	99.86	100.21	99.90	100.29	99.82	99.89	99.86	99.89	100.20	100.85	100.26	99.83

Table E4 Miscellaneous

Specimen number	8742A	8859	9148	9431	ABRP
Q	20.83	3.03	44.46	50.39	37.90
C	8.91	0.96	2.01	3.35	2.88
or		0.73	6.44	11.34	24.41
ab	20.42	90.14	36.87	13.56	23.88
an			1.38	6.96	0.08
bi	8.91	0.94	2.63	5.96	4.89
hy	15.73				
mt	3.03	0.13	0.40	0.47	0.62
sp	0.05	0.05	0.48	0.47	0.56
ap	0.26	0.39	0.31	0.29	0.29
cc	0.04	0.03	0.87	3.10	0.40
sid	0.13	0.02	0.99	0.08	0.07
H_2O	21.45	3.34	3.55	5.51	4.20
TOTAL +	99.76	99.76	100.40	101.49	100.16

APPENDIX F

Modal Analyses

General Notes

1. Undifferentiated groundmass includes quartz, feldspar, white mica, and chlorite.

2. No distinction is made between the plagioclase phenocrysts which form part of the restite fragments and the euhedral plagioclase phenocrysts thought to have crystallised from the magma.

Other Notes Referring to Tables F2 and F4

*[1] Mafic phenocryst replaced by opaque ore minerals.

*[2] Includes 22.3 percent recorded as spherulite.

Modal Analyses of Pseudomorphed Ferromagnesian Phenocrysts (Table F3)

In each of five specimens from the Bennaunmore Lava, all the chloritised/sericitised mafic restite fragments were analysed for their modal mineral contents. Tabulated are the number of crystal aggregates measured, the number of points counted, the average content of all the crystal aggregates within each specimen, and the range of modal contents encountered from individual crystal aggregates.

Table F1 Killeen Lava

Specimen number	7202	7218	9742	7764	7203	7205	8372	8375	9517	9559	9502	9484	9446	7217	9547	9456	9743
Number of points	1162	1093	1067	1144	1160	1103	986	1086	1074	1099	954	804	924	1147	1215	1221	611
Undifferentiated Groundmass	88.3	89.8	91.1	90.0	66.3	88.7	87.3	90.3	89.5	90.9	89.3	90.9	89.3	91.2	90.2	89.4	85.4
Plagioclase laths	6.0	4.1	3.3	4.0	4.4	5.3	4.8	4.8	4.9	4.9	5.1	4.2	1.3	2.4	4.0	5.3	1.6
Plagioclase rounded	3.1	4.5	2.1	3.0	6.0	3.3	3.7	3.9	2.2	1.8	3.3	3.4	1.0	3.7	3.9	3.4	0.3
Quartz	0.9	0.8	1.4	0.8	1.0	1.8	0.7	0.8	1.7	1.3	1.1	0.9	2.1	1.3	0.9	1.3	1.2
Chlorite			0.7										3.8	0.6			2.0
White Mica	0.6	0.6		1.7		0.8	0.4		1.0	0.9	0.9	0.5		0.4	0.7		
Calcite	1.0	0.2	1.3	0.2	22.2		3.0		0.3				2.6	0.4		0.7	8.7
Opaque Ore	0.1		0.2	0.4	0.3	0.2	0.1	0.2	0.4	0.2	0.3	0.1		0.1	0.4		0.8
TOTAL	100.0	100.0	100.1	100.1	100.2	100.1	100.0	100.0	100.0	100.0	100.0	100.0	100.1	100.1	100.1	100.1	100.0

Table F2 Other Lavas

Specimen number	9126	81120	81108	9011	9096	810801B	8633	9746	9747	810802	810804	8388	8390	9728
Number of points	1375	1140	1160	1143	1078	1144	1291	1075	1016	1336	1137	1237	1006	1116
Undiff. Groundmass	96.7	96.9	96.4	96.6	95.9	98.0	96.1	98.1	95.3	96.7	96.8	97.8	96.2	95.7
Plagioclase	2.3	2.1	2.1	2.8	2.6	1.6	2.5	1.6	4.6	2.0	2.2	1.5	3.0	2.9
Quartz	0.8	0.8	0.3	0.4	0.6	0.3	1.1	0.4		0.9	0.5	0.3	0.3	1.2
Chlorite			0.1						0.1					
White Mica	0.2	0.1	0.3										0.2	0.2
Zircon				0.1							0.1			
Allanite							0.2					0.1		0.1
Calcite		0.1	0.7										0.3	
Opaque Ore	0.1		0.3	0.1	0.6	0.2 *1	0.2 *1			0.5 *1	0.5 *1	0.3 *1		
Feldspar Xenocryst				0.1	0.4									
TOTAL	100.1	100.0	100.2	100.1	100.1	100.1	100.1	100.0	100.0	100.1	100.1	100.0	100.0	100.1

Table F3 Bennaunmore Lava

Specimen number	8552						8392					8418					8371				8555
Thin section number	1	2	3	4	5	ave.	1	2	3	4	ave.	1	2	3	4	ave.	1	2	3	ave.	
Number of points	1246	1047	1107	1199	1188		1147	1034	1046	1168		1217	1202	1088	1217		1279	1217	1267		2317
Undiff. Groundmass	95.8	95.6	96.0	96.1	97.0	96.1	93.2	96.7	96.1	92.5	94.5	96.3	97.8	94.8	95.1	96.0	95.9	93.7	97.4	95.7	96.3
Plagioclase	2.7	2.9	2.8	2.8	2.3	2.7	5.6	1.6	2.7	5.7	4.0	3.1	1.5	4.1	3.4	3.0	3.4	5.2	1.7	3.4	2.7
Quartz	0.2	0.4	0.4	0.7	0.3	0.4	0.8	0.6	0.5	0.4	0.6	0.2	0.4	0.6	0.8	0.5	0.4	0.7	0.6	0.5	0.5
Chlorite	0.6	0.4	0.3	0.2	0.1	0.3	0.2	0.5	0.2	0.5	0.3							0.3	0.1	0.1	0.1
White Mica	0.2	0.3		0.1	0.3	0.2	0.2			0.1	0.1				0.3	0.1	0.2		0.1	0.1	0.1
Zircon		0.1				<0.1						0.1				<0.1					
Allanite							0.5	0.1	0.2	0.2								0.1	0.1	0.1	
Anatase		0.1		0.2		<0.1	0.1			0.1	<0.1							0.1	0.1	0.1	
Leucoxene	0.1					<0.1															
Calcite	0.4	0.2	0.5	0.1	0.2	0.3			0.5	0.2	0.2	0.2	0.3	0.5	0.3	0.3					0.2
Opaque Ore		0.1				<0.1															0.1
Fluorite												0.2		0.1	0.3	0.1					
TOTAL	100.2	100.1	100.0	100.2	100.2	100.0	100.1	100.1	100.1	99.7	99.9	100.1	100.0	100.1	100.2	100.0	99.9	100.1	100.1	100.0	100.0

Table F4 Miscellaneous

Specimen number	8742A	8787	8859	8867
Number of points	2928	886	1163	1133
Undiff. Groundmass	96.5	95.8	95.8	97.1
Plagioclase	2.3	3.2	3.8	2.3
Quartz	1.0			
Chlorite	0.2			0.4
Anatase	0.1		0.1	
Leucoxene				0.3
Apatite		0.1	0.1	
Opaque Ore			0.2 *1	
Xenocrysts		0.8	0.2	
TOTAL	100.1	100.0	100.1	100.1

Table F5 Mafic clots in the Bennaunmore Lava

Specimen	8552	range	8392	range	8371	range	8555	range	8775
Number of phenocrysts	8		8		5		4		1
Number of points	675		770		448		295		210
Chlorite	51.6	61-41	61.8	77-49	30.8	62-10	61.0	69-57	49.5
White Mica	24.9	36-15	13.9	33-2	34.4	48-14	25.1	28-17	20.5
Zircon	3.9	10-1	2.5	6-0	2.7	7-1	3.1	6-0	1.4
Allanite			8.9	11-2	8.5	15-4			1.9
Anatase	5.4	14-1	2.1	5-0	4.9	7-1	2.7	4-0	9.1
Leucoxene			3.7	12-0	13.6	17-2	3.7	11-0	15.2
Apatite	3.4	5-2	2.1	6-0	4.5	7-0			1.0
Opaque Ore	6.8	14-2	2.6	7-0	0.7	3-0	4.4	7-0	1.4
Stilpnomelane* Sphene†	4.2*	13-2	2.4†	5-0					
TOTAL	100.2		100.0		100.1		100.0		100.0

APPENDIX G

Mass-transfer computations

Derivation of the composition-volume equation (adapted from Babcock, 1973).

The process of chemical transfer within any rock system can be described by the following notation:

$$aA \pm X \rightarrow bB$$

where:

a = grams of parent rock A

b = grams of product rock B

X = grams of material added or removed

When studying two rocks containing n components, A and B can be considered as two separate "phases" such that:

$$A = x_1^{\alpha} + x_2^{\alpha} + \ldots\ldots x_n^{\alpha}$$

$$B = x_1^{\beta} + x_2^{\beta} + \ldots\ldots x_n^{\beta}$$

where:

x_n^{α} = the weight fraction of chemical component n in rock A

x_n^{β} = the weight fraction of chemical component n in rock B.

The magnitude of chemical transfer for any given component in this system can be expressed as:

$$\Delta x_n = b(x_n^{\beta}) - a(x_n^{\alpha})$$

where:

Δx_n = the chemical transfer (in grams) of component n between rocks A and B.

If K_v = ratio between final and initial volume of the rock mass and,

ρ^{α} and ρ^{β} are the specific gravities of the parent (A) and product (B) rocks respectively,

then:

$$\Delta X_n = a \left| (K_v x_n^{\beta} \frac{\rho^{\beta}}{\rho^{\alpha}}) - X_n^{\alpha} \right|$$

If a is taken to be 100 grams, then ΔX_n becomes grams per 100 grams or weight percent.

Alternatively a becomes unity if X_n^{β} and X_n^{α} are taken initially as weight percent.

So:

$$\Delta X_n = (K_v X_n^{\beta} K_D) - X_n^{\alpha}$$

where $K_D = \frac{\rho^{\beta}}{\rho^{\alpha}}$

Information required to use this equation is

1. The chemical composition of the parent and product rocks.

2. The density of the parent and product rocks.

3. Either the volume change of the rock mass, or the magnitude of chemical transfer of any chemical component i.e. if K_v is assumed to equal unity then

$$\Delta X_n = X_n^{\beta} K_D - X_n^{\alpha}$$

or, if ΔX_n is assumed to equal zero then

$$K_v = \frac{X_n^{\alpha}}{X_n^{\beta} . K_D}$$

If K_v the volume change is plotted against ΔX_n for each of the n components a family of lines is obtained (see fig. G.1).

This diagram can be clarified if the values of ΔX_n are normalised relative to the original parent rock content of component n, X_n^{α}, so that

$$\Delta F^n = \frac{\Delta X_n}{X_n^{\alpha}}$$

ΔF^n is therefore a factor describing how component n has behaved independent of the numerical effect of the original content. If K_v is

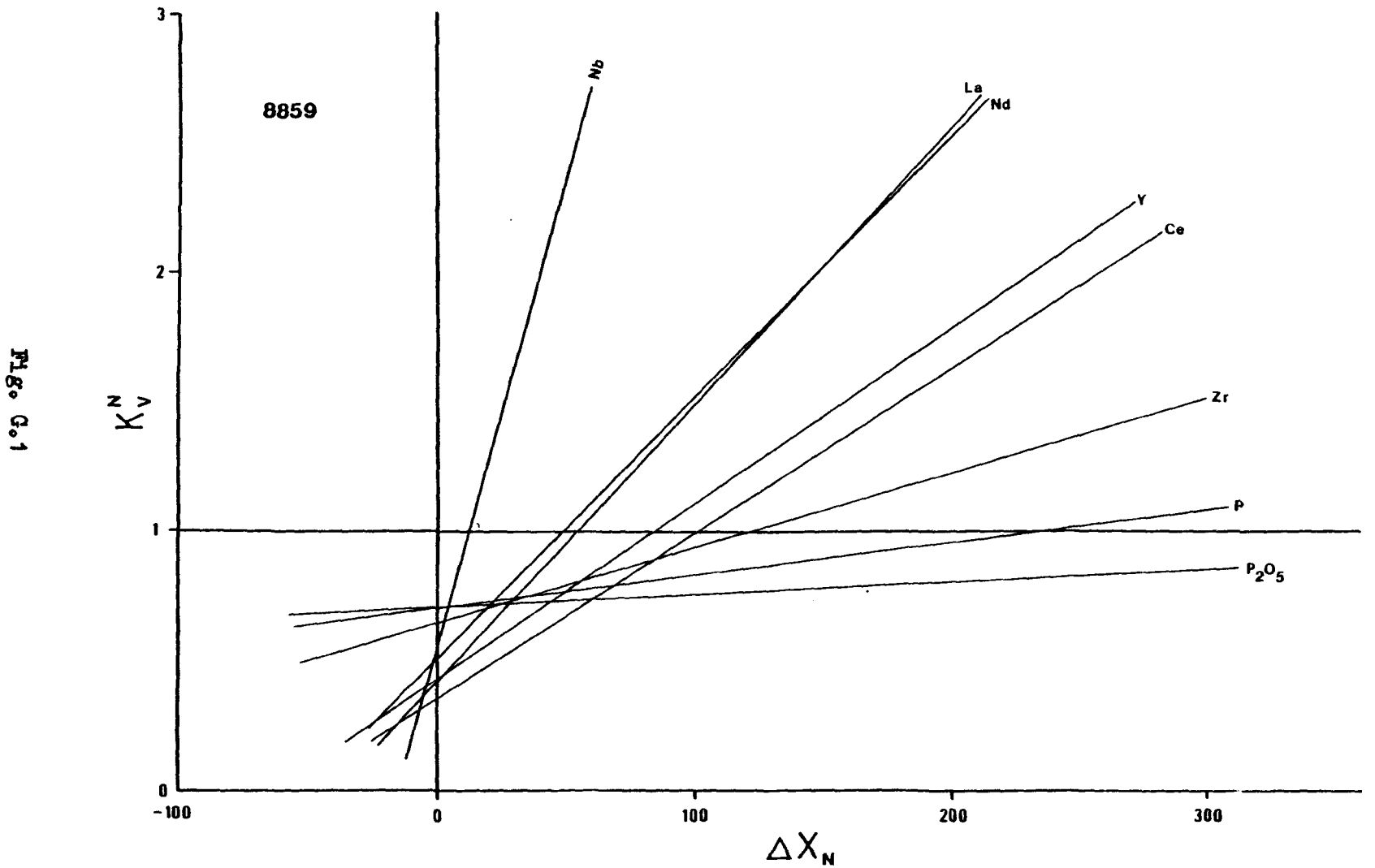

Fig. 6.1

plotted against ΔX_n, then the lines representing each component do not cross, and the diagram become visually easier to understand (compare fig. 8.6).

If the negative values of ΔF^n are removed by adding one to each, then

$$K_v^n = \frac{100}{(\Delta F^n + 1)}$$

where K_v^n = the percentage volume change required for no exchange of component n to have occurred between parent and product rocks.

References

ALDERTON, D. H. M., PEARCE, J. A. and POTTS, P. J. 1980. Rare earth element mobility during granite alteration: Evidence from southwest England. Earth planet. Sci. Lett., 49, p. 149-165.

ALLEN, J. R. L. 1963. The classification of cross-stratified units with notes on their origin. Sedimentology, 2, p. 93-114.

APPLEYARD, E. C. and WOOLLEY, A. R. 1979. Fenitisation: An example of the problems of characterising mass transfer and volume changes. Chem. Geol., 26, p. 1-15.

BABCOCK, R. S. 1973. Computational models of metasomatic processes. Lithos, 6, p. 279-290.

BALASHOV, Yu. A. 1963. Regularities in the distribution of the rare earths in the Earth's crust. Geochemistry (USSR), English Translation, p. 107-124.

BARTH, T. F. W. 1962. Theoretical Petrology, 2nd Ed., Wiley, New York.

BATTEY, M. H. 1955. Alkali metasomatism and the petrology of some keratophyres. Geol. Mag., 92, p. 104-126.

BROWN, E. H. 1967. The greenschist facies of part of eastern Otago. Contrib. Mineral. Petrol., 14, p. 259-292.

BROWN, E. H. 1968. The Si^{4+} content of natural phengites: A discussion. Contrib. Mineral. Petrol., 17, p. 78-81.

BROWN, G. C. 1973. Evolution of granite magmas at destructive plate margins. Nature, 241, p. 26-28.

BROWN, G. C. and FYFE, W. S. 1970. The production of granitic melts during ultrametamorphism. Contrib. Mineral. Petrol., 28, p. 310-318.

CAPEWELL, J. G. 1951. The Old Red Sandstone of the Inch and Annascaul district, Co. Kerry. Proc. R. Ir. Acad., 54B, p. 141-167.

CAPEWELL, J. G. 1957. The stratigraphy and structure of the country around Sneem, Co. Kerry. Proc. R. Ir. Acad., 58B, p. 167-183.

CAPEWELL, J. G. 1965. The Old Red Sandstone of Sleive Mish, Co. Kerry. Proc. R. Ir. Acad., 64B, p. 165-174.

CAPEWELL, J. G. 1975. The Old Red Sandstone Group of Iveragh, Co. Kerry. Proc. R. Ir. Acad., 75B, p. 155-171.

CARMICHAEL, I. S. E. 1967. The iron/titanium oxides of salic volcanic rocks and their associated ferromagnesian silicates. Contrib. Mineral. Petrol., 14, p. 36-64.

CARMICHAEL, I. S. E., TURNER, F. J. and VERHOOGEN, J. 1974. Igneous Petrology. McGraw-Hill, New York.

CAWTHORN, R. G., STRONG, D. F. and BROWN, P. A. 1981. Origin of corundum - normative intrusive and extrusive magmas. Nature, 259, p. 102-104.

CHIKHAOUI, M., DUPUY, C. and DOSTAL, J. 1980. Geochemistry and petrogenesis of late Proterozoic volcanic rocks from north-western Africa. Contrib. Mineral. Petrol., 73, p. 375-388.

CHRISTIANSEN, R. L. and LIPMAN, P. W. 1966. Emplacement and thermal history of a rhyolite lava flow near Fortymile Canyon, S. Nevada. Geol. Soc. America Bull., 77, p. 671-684.

CLAYTON, G. , GRAHAM., J. R., HIGGS, K., HOLLAND, C. H. and NAYLOR, D. 1980. Devonian rocks in Ireland: a review. J. Earth Sci. R. Dublin Soc., 2, p. 161-183.

CLOUGH, P. W. L. and FIELD, D. 1980. Chemical variation in metabasites from a Proterozoic amphibolite - granulite transition zone, S. Norway. Contrib. Mineral. Petrol., 73, p. 277-286.

COE, K. 1966. Intrusive tuffs of west Cork, Ireland. Q. J. geol. Soc. Lond., 122, p. 1-28.

COE, K. and SELWOOD, E. B. 1963. The stratigraphy and structure of part of the Beara Peninsula, Co. Cork. Proc. R. Ir. Acad., 63B, p. 33-59.

COE, K. and SELWOOD, E. B. 1968. The Upper Palaeozoic stratigraphy of West Cork and parts of South Kerry. Proc. R. Ir. Acad., 66B, p. 113-131.

COLLINSON, J. D. 1978. Alluvial Sediments. Chapter 3, In: Sedimentary Environments and Facies, Ed. H. G. Reading, p. 15-60.

COOPER, M. A. 1977. Bristol University Palaeocurrent Analysis System. Unpublished computer program, Dept. of Geology, University of Bristol.

DAVIES, J. F., GRANT, R. W. E. and WHITEHEAD, R. E. S. 1979. Immobile trace elements and Archaean volcanic stratigraphy in the Timmins mining area, Ontario. Can. J. Earth Sci., 16, p. 305-311.

DAVIES, J. F. and WHITEHEAD, R. E. S. 1980. Further immobile element data from altered volcanic rocks, Timmins mining area, Ontario. Can. J. Earth Sci., 17, p. 419-423.

DEER, W., HOWIE, R. A. and ZUSSMAN, J. 1962/1963. Rock Forming Minerals. Vol. 1, Ortho- and Ring Silicates (1962), Vol. 2, Chain Silicates (1962), Vol. 3, Sheet Silicates (1962), Vol. 4, Framework Silicates (1963), Vol. 5, Non-Silicates (1963), Longman, London.

DICKINSON, W. R. 1968. Circum-Pacific andesite types. J. Geophys. Research, 73, p. 2261-2269.

DICKINSON, W. R. 1970. Relations of andesites, granites and derivative sandstones to arc-trench tectonics. Rev. Geophysics Space Phys., 8, p. 813-860.

DONNELLY, T. W. 1963. Genesis of albite in early orogenic volcanic rocks. Am. J. Sci., 261, p. 957-972.

DORAN, R. J. P., HOLLAND, C. H. and JACKSON, A. A. 1973. The sub-Old Red Sandstone surface in southern Ireland. Proc. R. Ir. Acad., 73B, p. 109-128.

DOSTAL, J., STRONG, D. F. and JAMIESON, R. A. 1980. Trace element mobility in the mylonite zone within the ophiolite aureole, St. Anthony Complex, Newfoundland. Earth Planet. Sci. Lett., 49, p. 188-192.

DOWTY, E. 1980. Synneusis reconsidered. Contrib. Mineral. Petrol., 74, p. 75-84.

DUDDY, I. R. 1980. Redistribution and fractionation of rare earth and other elements in a weathering profile. Chem. Geol., 30, p. 363-382.

EMMERMAN, R., DAIEVA, L. and SCHNEIDER, J. 1975. Petrologic significance of rare-earths distribution in granites. Contrib. Mineral. Petrol., 52, p. 267-283.

EUGSTER, H. P. 1956. Stability of hydrous iron silicates. Carnegie Inst. Washington. Ann. Rep. Dir. Geophys. Lab., 1955-1956, 55, p. 158.

EWART, A., TAYLOR, S. R. and CAPP, A. C. 1968. Trace and minor element geochemistry of the rhyolitic volcanic rocks, central N. Island, New Zealand. Total rock and residual liquid data. Contrib. Mineral. Petrol., 18, p. 76-104.

FLOOD, R. H., VERNON, R. H., SHAW, S. E. and CHAPPELL, B. W. 1977. Origin of pyroxene - plagioclase aggregates in a rhyodacite. Contrib. Mineral. Petrol., 60, p. 299-309.

FLOYD, P. A. and WINCHESTER, J. A. 1975. Magma type and tectonic setting discrimination using immobile elements. Earth Planet. Sci. Lett., 27, p. 211-218.

FLOYD, P. A. and WINCHESTER, J. A. 1978. Identification and discrimination of altered and metamorphosed volcanic rocks using immobile elements. Chem. Geol., 21, 291-306.

FOSTER, M. D. 1962. Interpretation of the composition, and a classification of the chlorites. U.S.G.S. Prof. Paper No. 414-A, p. 1-33.

FRANCIS, P. 1976. Volcanoes. Penguin, New York.

FRIEND, P. F. 1978. Distinctive features of some ancient river systems. In: Fluvial Sedimentology, Ed. A. D. Miall, p. 531-542.

FRIEND, P. F. and MOODY-STUART, M. 1972. Sedimentation of the Wood Bay Formation (Devonian) of Spitzbergen: regional analysis of a late orogenic basin. Norsk Polarinstitutt Skrifter, 157.

FYFE, W. S. 1970. Some thoughts on granite magmas. In: Mechanism of igneous intrusion, Eds. G. Newall and N. Rast. J. Geol. Spec. Issue, 2, p. 201-216.

FYFE, W. S. 1973. The generation of batholiths. Tectonophysics, 17, p. 273-283.

GARCIA, M. O. and JACOBSON, S. S. 1979. Crystal clots, amphibole fractionation and the evolution of calcalkaline magmas. Contrib. Mineral. Petrol., 69, p. 319-327.

GARDINER, P. R. R. 1975. Tectonic controls of Devonian and Lower Carboniferous sedimentation in the south of Ireland. Proc. 9th Cong. Internat. Sedimentol., 4, p. 141-146.

GARDINER, P. R. R. 1978. Is the Hercynian Front in Ireland a local feature? Nature, 271, p. 538-539.

GARDINER, P. R. R. and HORNE, R. R. 1972. The Devonian and Lower Carboniferous clastic correlatives of S. Ireland. Bull. geol. Surv. Ireland, 1, p. 335-366.

GARDINER, P. R. R. and HORNE, R. R. 1976. Devonian and Lower Carboniferous clastic correlatives of S. Ireland - some modifications. Bull. geol. Surv. Ireland, 2, p. 79-84.

GILL, W. D. 1962. The Variscan fold-belt in Ireland. In: Some aspects of the Variscan fold-belt, Ed. K. Coe, p.

GRABER, F. M., LUKENS, H. R. and MacKENZIE, J. K. 1970. Neutron activation analysis determination of all 14 stable rare-earth elements with group separation and Ge(Li) spectrometry. J. Radioanal. Chem., 4, p. 229-239.

GRESENS, R. L. 1967. Composition-volume relationships of metasomatism. Chem. Geol., 2, p. 47-65.

HARLAND, W. B. 1980. Comment and reply on 'A palaeomagnetic pole position from the folded Upper Devonian Catskill red beds, and its implications'. Geology, 8, p. 258-260.

HARMS, J. C. and FAHNESTOCK, R. K. 1965. Stratification bed forms and flow phenomena (with an example from the Rio Grande). In: Primary sedimentary structures and their hydrodynamic interpretation, Ed. G. V. Middleton. Soc. Econ. Paleontologists and Mineralogists Spec. Pub. 12, p. 84-115.

HARMS, J. C., SOUTHARD, J. B., SPEARING, D. R. and WALKER, R. G. 1975. Depositional environments as interpreted from primary sedimentary structures and stratification sequences. Soc. Econ. Paleontol. Mineral., Short course No. 2, Dallas. Chapters 3 and 4, p. 45-79.

HARRIS, P. G., KENNEDY, W. Q. and SCARFE, C. M. 1970. Volcanism versus plutonism - the effect of chemical composition. In: Mechanism of igneous intrusion, Eds. G. Newall and N. Rast. J. Geol. Spec. Issue, 2, p. 187-200.

HART, S. R., ERLANK, A. J. and KABLE, E. J. D. 1974. Sea floor basalt alteration: some chemical and Sr isotopic effects. Contrib. Mineral. Petrol., 44, p. 219-230.

HEINRICH, E. W. 1966. The geology of carbonatites. Rand McNally.

HELLMAN, P. L., SMITH, R. E. and HENDERSON, P. 1979. The mobility of the R.E.E.s: evidence and implications from selected terrains affected by burial metamorphism. Contrib. Mineral. Petrol., 71, p. 23-44.

HERRMANN, A. G. 1974. Yttrium and lanthanides. In: Handbook of Geochemistry, Ed. K. H. Wedepohl. II - 5, p. 57-71. Springer, Berlin, Heidelberg, New York.

HEY, M. H. 1967. A new review of the chlorites. Min. Mag., 30, p. 277-301

HORNE, R. R. 1970. A preliminary re-interpretation of the Devonian palaeogeography of western Co. Kerry. Bull. geol. Surv. Ireland, 1, p. 53-60.

HOWARD, J. D. 1966. Sedimentation of the Panther Sandstone Tongue. Utah geol. miner. Surv. Bull., 80, p. 23-33.

HUANG, W. L. and WYLLIE, J. P. 1973. Muscovite dehydration and melting in deep crust and subducted oceanic sediments. Earth Planet. Sci. Lett., 18, p. 133-136.

HUGHES, C. J. 1973. Spilites , keratophyres and the igneous spectrum. Geol. Mag., 109, p. 513-527.

HULL, E. 1879. On the geological age of the rocks forming the southern highlands of Ireland, generally known as "The Dingle Beds" and "Glengarriff Grits and Slates" (Jukes). Q. J. geol. Soc. Lond., 35, p. 699-723.

HURLBUT, C. S. 1956. Muscovite from Methuen Township, Ontario. Am. Miner., 41, p. 892-

HUSAIN, S. M. 1957. The geology of the Kenmare Syncline, Co. Kerry, Ireland. Unpublished Ph.D. thesis of the University of London.

HYNDMAN, D. W. 1981. Controls on source and depth of emplacement of granitic magma. Geology, 9, p. 244-249.

HYNES, A. 1980. Carbonatization and mobility of Ti, Y and Zr in the Ascot Formation metabasalts, S. E. Quebec. Contrib. Mineral. Petrol., 75, p. 79-87.

INAMDAR, D. D. 1974. A total field magnetic survey of Co. Kerry. Geol. Surv. of Ireland Report Series RS 74/1 (Geophysics).

JUKES, J. B. and DU NOYER, G. V. 1859. Explanation to accompany Sheet 184. Mem. geol. Surv. Ir.

JUKES, J. B. and DU NOYER, G. V. 1861. Explanation to accompany Sheets 185 and 186. Mem. geol. Surv. Ir.

KANDIAH, K., SMITH, A. J. and WHITE, G. 1975. A pulse processor for X-ray spectrometry with Si(Li) detectors. Paper 2.9 In: the 2nd ISPRA nuclear electronics symposium, Stresa, Italy.

KINAHAN, G. H. 1879. The Dingle and Glengarriff grits. Geol. Mag., 6, p. 348-353.

LAMBERT, R. St. J. and HOLLAND, J. G. 1974. Y geochemistry applied to petrogenesis utilising Ca-Y relationships in minerals and rocks. Geochim. Cosmochim. Acta, 38, p. 1393-1414.

LE BAS, M. J. and SABINE, P. A. 1980. Progress in 1979 in the nomenclature of pyroclastic materials. Geol. Mag., 117, p. 389-391.

LEAKE, B. E., HENDRY, G. L., KEMP, A., PLANT, A. G., HARVEY, P. K., WILSON, J. R., COATS, J. S., AUCOTT, J. W., LUNEL, T. and HOWARTH, R. J. 1969. The chemical analysis of rock powders by automatic X-ray fluorescence. Chem. Geol., 5, p. 7-86.

LEOPOLD, L. B. and WOLMAN, M. G. 1957. River channel patterns: braided, meandering and straight. U.S.G.S. Prof. Paper No. 282B, p. 39-85.

LONG, D. G. F. 1978. Proterozoic stream deposits: some problems of recognition and interpretation of ancient sandy fluvial systems. In: Fluvial Sedimentology, Ed. A. D. Miall, p. 313-341.

LUTH, W. C., JAHNS, R. H. and TUTTLE, O. F. 1964. The granite system at pressures of 4 to 19 kilobars. J. Geophys. Research, 69, p. 759-773.

MACDERMOT, C. V. and SEVASTOPULO, G. D. 1972. Upper Devonian and Carboniferous stratigraphical setting of Irish mineralisation. Bull. geol. Surv. Ireland, 1, p. 267-280.

MACDONALD, G. A. 1972. Volcanoes. Prentice-Hall, New Jersey.

MACGEEHAN, P. J. 1978. The geochemistry of altered volcanic rocks at Matagami, Quebec: a geothermal model for massive sulphide genesis. Can. J. Earth Sci., 15, p. 551-570.

MARTIN, R. F. and PIWINSKI, A. J. 1972. Magmatism and tectonic settings. J. Geophys. Research, 77, p. 4966-4975.

MASON, B. 1966. Principles of Geochemistry. (3rd Ed.). Wiley, New York and London.

McCABE, P. J. and JONES, C. M. 1977. Formation of reactivation surfaces within superimposed deltas and bedforms. J. Sed. Petrol., 47, p. 707-715.

McKEE, E. D., CROSBY, E. J. and BERRYHILL, H. L. 1967. Flood deposits in Bijou Creek, Colorado, June 1965. J. Sed. Petrol., 37, p. 829-851.

MIALL, A. D. 1974. Palaeocurrent analysis of alluvial sediments: a discussion of directional variance and vector magnitude. J. Sed. Petrol., 44, p. 1174-1185.

MIALL, A. D. 1977. A review of the braided-river depositional environment. Earth-Sci. Rev., 13, p. 1-62.

MIALL, A. D. 1978. Lithofacies types and vertical profile models in braided river deposits: a summary. In: Fluvial Sedimentology, Ed. A. D. Miall, p. 597-604.

MURPHY, T. 1960. Gravity anomaly map of Ireland, Sheet 5 - South West. Dublin Inst. Adv. Stud. Geophys. Bull., 18.

MURPHY, T. 1974. Gravity anomaly map of Ireland - Scale 1:750000. Dublin Inst. Adv. Stud., Series D, Geophys. Bull., 32.

NAGASAWA, H. 1970. Rare earth concentrations in zircons and apatites and their host dacites and granites. Earth Plan. Sci. Lett., 9, p. 359-364.

NAYLOR, D. 1978. A structural section across the Variscan fold belt, S. W. Ireland. J. Earth Sci. R. Dublin Soc., 1, p. 63-70.

NAYLOR, D. and JONES, P. C. 1967. Sedimentation and tectonic setting of the Old Red Sandstone of southwest Ireland. In: International symposium on the Devonian system, Ed. D. Oswald. Calgary, Alberta. Vol. 2, p. 1089-1099.

NAYLOR, D., JONES, P. C. and MATTHEWS, S. C. 1974. Facies relationships in the Upper Devonian-Lower Carboniferous of southwest Ireland and adjacent regions. Geol. J., 9, p. 77-96.

NAYLOR, D. and SEVASTOPULO, G. D. 1979. The Hercynian "Front" in Ireland. Krystalinikum, 14, p. 77-90.

NOBLE, D. C., KORRINGA, M. K., HEDGE, C. E. and RIDDLE, G. O. 1972. Highly differentiated subalkaline rhyolite from Glass Mt., Mono County, California. Geol. Soc. America Bull., 83, p. 1179-1184.

NOCKOLDS, S. R. 1954. Average chemical compositions of some igneous rocks. Geol. Soc. America Bull., 65, p. 1007-1032.

NORRISH, K. and HUTTON, J. T. 1969. An accurate X-ray spectrographic method for the analysis of a wide range of geological samples. Geochim. Cosmochim. Acta., 33, p. 431-453.

OSBORN, E. F. 1957. Role of oxygen pressure in the crystallisation and differentiation of basaltic magma. Am. J. Sci., 259, p. 609-647.

PEARCE, J. A. and CANN, J. R. 1973. Tectonic setting of basic volcanic rocks determined using trace element analyses. Earth Plan. Sci. Lett., 19, p. 290-300.

PENNEY, S. R. 1978. Devonian lavas from the Comeragh mountains, Co. Waterford. J. Earth Sci. R. Dublin Soc., 1, p. 71-76.

PETTIJOHN, F. J. 1975. Sedimentary Rocks. Harper and Row, New York.

PETTIJOHN, F. J., POTTER, P. E. and SIEVER, R. 1972. Sand and Sandstone. Springer-Verlag, Berlin, Heidelberg, New York.

POTTER, P. E. and PETTIJOHN, F. J. 1977. Palaeocurrents and Basin Analysis. Springer-Verlag, Berlin, Heidelberg, New York.

PRESNALL, D. C. and BATEMAN, P. C. 1973. Fusion relations in the system $NaAlSi_3O_8$ - $CaAl_2Si_2O_8$ - $KAlSi_3O_8$ - SiO_2 - H_2O and generation of granitic magmas in the Sierra Nevada Batholith. Geol. Soc. America Bull., 84, p. 3181-3202.

REYNOLDS, R. C. Jr. 1963. Matrix corrections in trace-element analysis by X-ray fluorescence: estimation of the mass absorption coefficient by compton scattering. Am. Mineral., 48, p. 1133-1143.

RUSSEL, K. J. 1978. Vertebrate fossils from the Iveragh Peninsula and the age of the Old Red Sandstone. J. Earth Sci. R. Dublin Soc., 1, p. 151-162.

RUST, B. R. 1978. Depositional models for braided alluvium. In: Fluvial Sedimentology, Ed. A. D. Miall, p. 605-625.

SCHALLER, W. T. 1950. An interpretation of the composition of high silica sericites. Min. Mag., 29, p. 406-

SCHWARTZ, G. M. 1958. Alteration of biotite under mesothermal conditions. Econ. Geol., 53, p. 164-

SHACKLETON, R. M. 1940. The succession of rocks in the Dingle Peninsula, Co. Kerry. Proc. R. Ir. Acad., 46B, p. 1-12.

SHAH, S. H. A. 1958. The rocks and structure of the country south-east of Killarney, Co. Kerry, Ireland. Unpublished Ph.D. thesis of the University of London.

SMITH, J. V. 1974. Feldspar Minerals. Vol. 2, Chemical and Textural Properties. Springer-Verlag, Berlin, Heidelberg, New York.

SMITH, R. E. and SMITH, S. E. 1976. Comments on the use of Ti, Zr, Y, Sr, K, P and Nb in classification of basaltic magmas. Earth Plan. Sci. Lett., 32, p. 114-120.

SPRY, A. 1969. Metamorphic Textures. Pergamon, Oxford.

STATHAM, P. J. 1976. A comparative study of techniques for quantitative analysis of X-ray spectra obtained with a Si(Li) detector. X-ray Spectrometry, 5, p. 16-28.

STEWART, D. C. 1975. Crystal clots in calc-alkaline andesites as breakdown products of high-Al amphiboles. Contrib. Mineral. Petrol., 53, p. 195-204.

STRONG, D. F., DICKSON, W. L. and PICKERILL, R. K. 1979. Chemistry and prehnite-pumpellyite facies metamorphism of calc-alkaline Carboniferous volcanic rocks of southeastern New Brunswick. Can. J. Earth Sci., 16, p. 1071-1085.

SUN, S. S. and NESBITT, R. W. 1978. Petrogenesis of Archaean ultrabasic and basic volcanics: evidence from rare earth elements. Contrib. Mineral. Petrol., 65, p. 301-325.

SWEATMAN, T. R. and LONG, J. V. P. 1969. Quantitative electron-microanalysis of rock-forming minerals. J. Petrol., 10, p. 332-379.

TAYLOR, S. R., EWART, A. and CAPP, A. C. 1968. Leucogranites and rhyolites: trace element evidence for fractional crystallisation and partial melting. Lithos, 1, p. 179-186.

TUTTLE, O. F. and BOWEN, N. L. 1958. Origin of granite in the light of experimental studies in the system $NaAlSi_3O_8$ - $KAlSi_3O_8$ - SiO_2 - H_2O. Geol. Soc. America Mem., 74, p. 153-

VANCE, J. A. and GILREATH, J. P. 1967. The effect of synneusis on phenocryst distribution patterns in some prophyritic igneous rocks. Am. Mineral., 52, p. 529-536.

VAN der VOO, R., BRIDEN, J. C. and DUFF, B. A. 1980. Late Precambrian and Palaeozoic palaeomagnetism of the Atlantic - bordering continents. Proc. 26th Intern. Geol. Congr., Paris.

VAN der VOO, R., FRENCH, A. N. and FRENCH, R. B. 1979. A palaeomagnetic pole position from the folded Upper Devonian Catskill red beds and its tectonic implications. Geology, 7, p. 345-348.

VELDE, B. 1967. Si^{4+} content of natural phengites. Contrib. Mineral. Petrol., 14, p. 250-258.

WALKER, R. G. 1976. Facies models 3: sandy fluvial systems. Geoscience Canada, 3, p. 101-109.

WALSH, J. N., BECKINSALE, R. D., SKELHORN, R. R. and THORPE, R. S. 1979. Geochemistry and petrogenesis of Tertiary granitic rocks from the island of Mull, northwest Scotland. Contrib. Mineral. Petrol., 71, p. 99-116.

WALSH, P. T. 1968. The Old Red Sandstone west of Killarney, Co. Kerry, Ireland. Proc. R. Ir. Acad., 66B, p. 9-26.

WATKINS, N. D., GUNN, B. M. and COY-YLL, R. 1970. Major and trace element variations during the initial cooling of an icelandic lava. Am. J. Sci., 268, p. 24-49.

WATSON, E. B. 1979. Zircon saturation in felsic liquids: experimental results and applications to trace element geochemistry. Contrib. Mineral. Petrol., 70, p. 407-419.

WATTERS, B. R. 1978. Petrogenesis of the felsic rocks of the late-Precambrian Sinclair Group, South West Africa. Geol. Rundschau, 67, p. 743-774.

WHITEHEAD, R. E. S. and GOODFELLOW, W. D. 1977. Geochemistry of volcanic rocks from the Tetagouche Group, Bathurst, New Brunswick, Canada. Can. J. Earth Sci., 15, p. 207-219.

WILLIAMS, H. and McBIRNEY, A. R. 1979. Volcanology. Freeman, Cooper and Co., San Francisco.

WINCHESTER, J. A. and FLOYD, P. A. 1976. Geochemical magma type discrimination: application to altered and meta-morphosed basic igneous rocks. Earth Plan. Sci. Lett., 28, 459-469.

WINCHESTER, J. A. and FLOYD, P. A. 1977. Geochemical discrimination of different magma series and their differentiation products using immobile elements. Chem. Geol., 20, p. 325-343.

WINGFIELD, R. T. R. 1968. The geology of Kenmare and Killarney. Unpublished Ph.D. thesis of the University of Dublin.

WRIGHT, W. B. 1927. The geology of Killarney and Kenmare. Mem. geol. Surv. Ireland.

WYLLIE, P. J. 1971. The Dynamic Earth. Wiley, New York.

ZIEGLER, P. A. 1978. North-western Europe: tectonics and basin development. Geol. Mijnbouw, 57, p. 589-626.

ZIELINSKI, R. A., LIPMAN, P. W. and MILLART, H. T. Jr. 1977. Minor element abundances in obsidian, perlite and felsite of calc-alkaline rhyolites. Am. Mineral., 62, p. 426-437.

ZWART, H. J. and DORNSIEPEN, V. F. 1978. The tectonic framework of central and western Europe. Geol. Mijnbouw, 57, p. 627-654.